TAMING THE AUTOGYRO: WILL THE AUTOGYRO EVER BE TRULY DOMESTICATED?

Thesis submitted in accordance with the requirements of the University of Liverpool for the degree of Doctor in Philosophy

by

Sophie Robinson

July 2014

ABSTRACT

Aviation is a pastime enjoyed by many amateur pilots. Of the 21 000 aircraft registered in the UK [1], 96% are engaged in general aviation activities (non-commercial flying). The UK Civil Aviation Authority (UK CAA) classifies microlights, gliders and autogyros as recreational sports aircraft. Of the 21 000 UK-registered general aviation aircraft, only 306 are autogyros, compared to over 4300 microlights and almost 2600 gliders. Despite this fact, the autogyro has been seen to exhibit a fatal accident rate up to 100 times higher than those of the microlight or glider.

In response to the identification of this high accident rate amongst autogyro type vehicles, the CAA commissioned a programme of research intended to understand the cause. This research, undertaken in the UK by the University of Glasgow, consisted of analytical, wind tunnel and flight test activities. These studies concluded that the autogyro displayed "conventional lateral and directional dynamic stability characteristics", and that both the static and dynamic stability (in particular, a lightly damped phugoid mode) was highly sensitive to the vertical position of the centre of gravity (c.g.) relative to the propeller thrust line. The lack of provision within the autogyro community to collect meaningful data in relation to the airworthiness requirements was also highlighted. Outside of the work performed as part of the research programme that generated this report, there is still considered to be "little indication that rigorous scientific or engineering investigation of airworthiness has occurred". Therefore, there remains significant scope for further research into just what makes autogyros so unsafe to fly and how to improve their airworthiness.

Prior research into the autogyro and its aerodynamic characteristics can be broadly divided into two phases, the first being from its inception in 1923 to the beginning of World War II and the period between 1996 and the present day, when a resurgence of interest in the autogyro began to occur. Much of the early works concentrate on characterising the autogyro's aerodynamic characteristics, relying heavily upon wind tunnel testing, flight testing and analytical investigation to establish an understanding of the fundamental flight dynamics of the autogyro. With the first flight of the first functional helicopter, the outbreak of World War II and the death of the inventor of the autogyro, research interest in this aircraft type was critically diminished. Only three papers on the subject of autogyros were published between 1939 and 1996.

The Air Accident Investigation Branch (AAIB) review of the airworthiness of the grounded Air Command autogyro, conducted after the occurrence of 5 fatal accidents between 1989 and 1991, recommended the commissioning of a programme of research into both the airworthiness and aerodynamic characteristics of light autogyros. As a result of this recommendation, the autogyro experienced a resurgence in research interest, culminating in the publication of a CAA Paper which presented 4 recommendations intended to improve the airworthiness of the autogyro:

1. It is recommended that the vertical location of the centre of gravity (c.g.) should lie within a ± 2 inch envelope of the propeller thrust line.

2. Horizontal tailplanes are largely ineffective in improving the long term pitch dynamic stability (phugoid mode).

3. Extreme manoeuvring can lead to excessive rotor teeter angles during certain phases of flight, potentially resulting in the rotor blades striking the prop or empennage.

4. The chordwise centre of gravity of the rotor blades should always lie at or ahead of the 25% chord position to prevent rotor blade instability.

One of the primary aims of this Thesis was to assess the validity and applicability of these recommendations; in order to do so, a simulation model of an autogyro was created. The model was based on the G-UNIV research autogyro owned by Glasgow University and validated against flight test data in order to ensure the required level of fidelity was achieved.

Upon re-assessing the recommendations, in some cases, different conclusions were drawn. The first recommendation, while accepted as a sensible design aim, was found to be overly restrictive. BCAR Section T, the airworthiness specification for autogyros, specifies requirements on the period and time to half amplitude of any longitudinal oscillations present in the aircraft. Limiting the vertical position of the centre of gravity to within ±2 inches of the propeller thrustline resulted in forcing a design which is compliant with the requirements of BCAR Section T outside the specified range, to become non-compliant when the centre of gravity lies within the range.

Recommendation 2 suggests that the removal of the tailplane of the aircraft has little impact on the longitudinal trim control positions and the characteristics of the phugoid mode. It was found that the results from the simulation model disagreed with this conclusion; the removal of the tailplane changed the characteristics of the phugoid model and the trimmed control positions significantly.

The third recommendation highlighted the potential for a rotor blade to strike the propeller or the empennage under extreme manoeuvring. The simulation environment provided a safe environment in which to test this recommendation; it was found under the loading of an extreme manoeuvre it was possible for the main rotor to strike the tail, supporting the conclusion drawn in CAA Report 2009/02.

It was not possible to assess the fourth and final recommendation, relating the positioning of the chord-wise position of the blade centre of gravity, due to the limitations of the simulation model developed.

Another focus of the recent work surrounding the autogyro has been on quantifying and assessing the handling qualities of such vehicles. This presents many challenges, including the fact that no autogyro-specific handling qualities specifications currently exist. One of the main themes of this Thesis was to progress towards the creation of such a specification, either through development of a new methodology or development of existing specifications, such as ADS-33E-PRF.

The first steps in this field have been taken by Glasgow University using ADS-33; the primary specification used in the assessment of military rotorcraft. Assessment of the autogyro was previously carried out in a real-world flight trial using existing Mission Task Elements (MTEs) taken from ADS-33, the Slalom and the Acceleration-Deceleration. The results from this trial were then used to derive proposed Level 1, 2 and 3 boundaries for quickness and pilot attack. This Thesis replicated this trial using real-time piloted simulation, and the method described in the work carried out by Glasgow University was also utilised to derive a set of predicted handling qualities Levels for both quickness and pilot attack. It was found that the predicted Level boundaries generated from the simulation trial did not agree well with those predicted in the original flight trial. There were several reasons for this; in the original flight trial the pilot used a non-standard technique to fly the Slalom manoeuvre, using sideslip to

complete the test course. Additionally, both the original flight trial and the simulated flight trial used data from several different course geometries. This resulted in the ordering of the Level boundaries being reversed for the Levels predicted by the simulated flight trial, as those test points carried out on the more aggressive course geometries received lower handling qualities ratings, whilst using the most aggressive control inputs, compared to those on easier courses which used lower magnitude and aggression inputs, and thus a lower quickness, while receiving better handling qualities. Recommendations were made to address these issues in future iterations of this work.

This Thesis also sought to establish whether the MTEs specified in ADS-33 highlighted the deficiencies within the autogyro in the same manner as they do in the helicopter, as well as identifying the fundamental differences between the autogyro and helicopter. For the most part, the MTEs chosen did highlight the deficiencies in the same manner for both autogyro and helicopter, with the exception of the Acceleration-Deceleration. When assessing the helicopter, the Acceleration-Deceleration is intended to highlight the presence of any undesirable roll due to pitch cross couplings present in the aircraft. As the autogyro uses throttle setting to accelerate, and not pitch attitude, the Acceleration-Deceleration cannot be used to assess the impact of this cross coupling in the autogyro. The Acceleration-Deceleration also revealed the presence of a roll due to throttle coupling in the autogyro which had not previously been reported.

Alongside the repetition of this original flight trial, new MTEs were analysed. The Heave Hop and the Roll Step are MTEs originally intended to assess tilt rotor type aircraft; however, they have shown some utility in assessing the autogyro. The Heave Hop in particular highlighted another of the fundamental differences between the autogyro and the helicopter. The Heave Hop is intended to test the ability of the aircraft to sustain a positive load factor, before transitioning to a negative load factor. Much of the effect of this changing load factor is mitigated for the helicopter by the presence of a rotor speed governor, which maintains the rotor speed at a constant value for irrespective of the rotor loading. However, the autogyro rotor is unpowered, meaning that changes in the rotor loading also change the rotor speed. This results in potentially problematic changes in the autogyro handling qualities; reducing or increasing the available control power or quickness available to the pilot.

The completion of the work described herein has raised many possible avenues for further work; although it has been shown that ADS-33 style predicted handling qualities represent a good baseline for development of autogyro specific handling qualities, there remains scope for redefinition of the Level 1/2 and Level 2/3 boundaries for the predicted handling qualities parameters, such as quickness and control power, as well as for the re-definition of MTEs to make them autogyro-specific. In order to draw absolute conclusions, these manoeuvres must also be reassessed using different autogyro types and configurations – often the work presented herein is only the second time such an assessment has taken place. The development of the easily reconfigurable autogyro model developed as part of this Thesis presents an ideal tool to achieve this goal.

In summary, through development of existing work and introduction of new ideas, some progress has been made in the progression towards an autogyro-specific handling qualities specification. Whilst there is still a long way to go in thoroughly domesticating the autogyro, this Thesis represents a step in the right direction.

ACKNOWLEDGEMENTS

There are many individuals to whom I owe thanks for their support and guidance throughout my doctoral studies. First and foremost, thanks must go to Dr Mike Jump, my supervisor and mentor, for his invaluable support both inside the academic arena and beyond. Thank you for sticking with me, and for guiding me through the rollercoaster that is a PhD.

Thanks also go to Dr Mark White, Dr Neil Cameron and Dr Philip Perfect for sharing their wealth of experience in the simulation field; without the combined force of their problem solving skills this Thesis would not have been possible. I must also thank Professor Gareth Padfield for his support during my undergraduate and postgraduate research.

Thanks also go to Dr Douglas Thomson of Glasgow University for providing us with access to their research autogyro, and the UK Civil Aviation Authority for allowing us to use their flight test data to validate our model; invaluable contributions.

Test Pilots Martin Mayer, Andy Berryman and Alistair Riches are also deserving of thanks. Their willingness to share their expertise and their hard work and enthusiasm for my project did not go unnoticed.

I would also like to thank fellow members of the Flight Science and Technology research group at the University of Liverpool and the members of our surrounding support system; Linghai Lu, Mike Jones, Emma Timson, Denise Stewart, Maria White and Steven Bode. You have been my sounding board, my friends and my support system.

Thanks go to my partner Dr Garnet Ridgway. You have been one of the few constants throughout this project; my biggest cheerleader and my best friend. Without exaggeration, I could not have done this without you.

Finally, I'd like to take this opportunity to thank my parents and sister, Peter, Laura and Penny, for their unwavering support and encouragement of all my goals in life. And yes, Mum, I have backed this up.

Sophie Robinson, July 2014

This research was funded by the Engineering and Physical Sciences Research Council, UK.

LIST OF ACRONYMS & ABBREVIATIONS

AAIB	*Air Accident Investigation Branch*
ADS-33	*Aeronautical Design Standard Performance Specification: Handling Qualities Requirements For Military Rotorcraft [2]*
AR	*Aspect Ratio*
ART	*Advanced Rotorcraft Technology*
BAES	*BAE Systems*
c.g.	*Centre of Gravity*
CAP	*Civil Aviation Publication*
CFD	*Computational Fluid Dynamics*
CSGE	*Control Systems Graphical Editor*
FLME	*FLIGHTLAB Model Editor*
FST	*Flight Science and Technology*
GVE	*Good Visual Environment*
HQR	*Handling Qualities Rating*
MTE	*Mission Task Element*
NACA	*National Advisory Committee for Aeronautics (now known as NASA)*
PPO	*Power Push Over*
UCE	*Useable Cue Environment*
UK CAA or CAA	*United Kingdom Civil Aviation Authority*
UoL	*University of Liverpool*
VSTOL	*Vertical and Short Take-Off and Landing*

NOMENCLATURE

C_D	*Drag coefficient [nd]*	P_{act}	*corrected power [hp]*
C_L	*Lift coefficient [nd]*	P_{nom}	*Nominal engine power [hp]*
C_M	*Moment coefficient [nd]*	q	*Pitch rate [deg.sec^{-1}]*
CF_X	*Axial Force Coefficient [nd]*	Q_{roll}, Q_{pitch}, Q_{yaw}	*Roll, pitch and yaw quickness [sec^{-1}]*
CF_Y	*Side Force Coefficient [nd]*	r	*Yaw rate [deg.sec^{-1}]*
CF_Z	*Normal Force Coefficient [nd]*	rpm	*Rotor speed*
CM_X	*Pitching Moment Coefficient [nd]*	S	*Area of surfaces [ft^2]*
CM_Y	*Rolling Moment Coefficient [nd]*	S_f	*Flap area [ft^2]*
CM_Z	*Yaw Moment Coefficient [nd]*	T	*Torque [Nm]*
c	*Chord length [ft]*	T_{amb}	*Ambient Temperature [°C]*
CF	*Correction factor [nd]*	$throt_{actual}$	*Throttle position [%]*
c_f	*flap chord [ft]*	T_{DIFF}	*Temperature difference [°C]*
$C_{l\alpha}$	*lift curve slope of the surface with flap un-deflected [nd]*	T_{ISA}	*International Standard Atmosphere (ISA) temperature [°C]*
p	*Roll rate [deg.sec^{-1}]*		
α	*Angle of attack [°]*	δ_f	*Flap deflection [°]*
β	*Sideslip angle [°]*	ζ	*Damping ratio [nd]*

η	*Viscosity correction factor [nd] or lateral stick displacement [%]*	$\Delta\varphi 2\ \omega_{180}$	*Phase lag change between the neutral stability frequency and twice the neutral stability point [°]*
ϑ	*Pitch attitude [°]*	ψ	*Yaw/Heading Angle [°]*
μ	*Tip Speed Ratio [nd]*	Ω	*Rotorspeed [rpm]*
τ	*Flap Effectiveness [nd]*	Ω_{eng}	*Engine Speed [rpm]*
τ_p	*Phase Delay [°]*	ω_n	*Natural Frequency [Hz]*
φ	*Roll Attitude [°]*	ω_{180}	*Neutral Stability Frequency [Hz]*

CONTENTS

Chapter 1

INTRODUCTION

This Chapter defines the context, scope and motivation for the research presented in this Thesis.

1.1 RESEARCH BACKGROUND AND AUTOGYRO AVIATION SAFETY REVIEW

The first controlled autogyro flight occurred in January 1923, pre-dating the first flight of the helicopter by more than 15 years [3].

Existing published research on the subject of the autogyro can be broadly divided into two time periods; the period before the first flight of the helicopter, leading up to World War II, and the current period of renewed research interest from 1996 onwards. Early research into the autogyro during the 1930s was diverse in its focus, with extensive wind tunnel testing and flight testing being carried out, alongside analytical investigations, all investigating the fundamental flight mechanics of the autogyro.

The death of the inventor and main champion of the autogyro, Juan de la Cierva, in 1936, the outbreak of World War II in 1939, and the maiden flight of Igor Sikorsky's VS-300 helicopter in 1940 all contributed to the decline in interest in the autogyro. After World War II, the majority of rotary wing research focussed on the helicopter, and interest in the autogyro was critically diminished and the autogyro has become the preserve of sports aviation enthusiasts.

In the early 1990s, resurgence in research interest in the autogyro began to occur, owing to the identification by the UK Civil Aviation Authority (UK CAA) of the comparatively high occurrence of accidents amongst autogyro type vehicles. This is illustrated in Figure 1. The autogyro is classified by the CAA in the same category as microlights and gliders, and as such, the accident statistics for these aircraft types are also presented in Figure 1 for comparison. The data is presented as a three-year moving average.

It can clearly be seen that the autogyro displays a considerably higher rate of accidents per million hours flown than the microlight or glider.

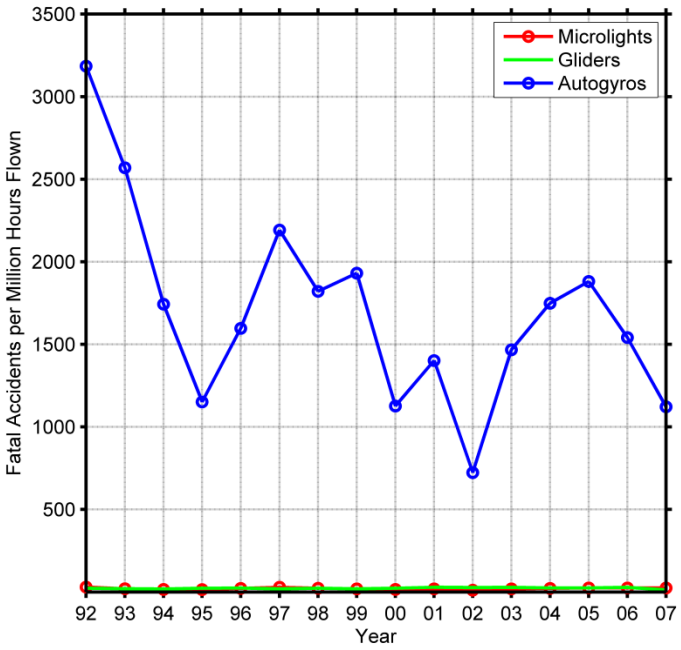

Figure 1: Autogyro historical accident rates, compared to gliders and microlights (data source: CAA)

Prompted by this fact, and the occurrence of 5 fatal accidents in the 2 years between April 1989 and March 1991 involving the Air Command autogyro, the Air Accident Investigation Branch (AAIB) recommended the commissioning of a programme of research into the airworthiness and aerodynamics of autogyro-type vehicles in 1991. The majority of research has been carried out by Glasgow University under CAA funding. The outcomes of this research programme were published in August 2010 as CAA Paper 2009/02 [4].

Paper 2009/02 [4] presented 4 main findings/recommendations:

1) It is recommended that the vertical location of the centre of gravity (c.g.) should lie within a ±2 inch envelope of the propeller thrust line. Ref. 4 accepts this as a "sensible design aim to achieve pitch dynamic stability (phugoid mode)" but accepts there are autogyros which achieve good stability with a c.g. location well outside this envelope, and that other factors can impact upon the phugoid stability (such as the drag damping from the rotor and fuselage, the pod and tailplane effectiveness and the airspeed).

This recommendation was included in the revision of CAP 643 British Civil Aviation Requirements Section T: Light Gyroplanes [5] (referred to as BCAR Section T), the CAA's autogyro airworthiness and design standard.

2) Horizontal tailplanes are largely ineffective in improving the long term pitch dynamic stability (phugoid mode).

3) Extreme manoeuvring can lead to excessive rotor teeter angles during certain phases of flight, potentially resulting in the rotor blades striking the prop or empennage.

A recommendation to ensure satisfactory control margin and rotor clearance up to 1.1 V_{NE} (the never exceed speed) was included in the revision of Ref. 5 as a result of this recommendation.

4) The chordwise centre of gravity of the rotor blades should always lie at or ahead of the 25% chord position to prevent rotor blade instability. A sudden reduction in main rotor speed due to aeroelastic instability has often been a feature of autogyro accidents, and it is a phenomenon which is not well understood. Work carried out as part of the research programme prescribed in Ref. 66 noted that a key parameter in aeroelastic instability is the blade torsional dynamic behaviour. Placing the blade chordwise centre of gravity at or ahead of the 25% chord position will, in the worst case scenario, result in a blade with zero torsional stiffness.

BCAR Section T (659) [5] requires the rotor blades to position the chordwise c.g. at or forward of 25% chord, however, Paper 2009/02 [4] states that "the technical ability of the gyroplane community and the test and analysis facilities available to them, may severely compromise or inhibit the collection of meaningful, or even correct data with which to demonstrate compliance. Any recommendations that might be made in respect of Section T, therefore, may be *only of academic consequence, and do little to enhance Section T and therefore airworthiness*" [4].

Paper 2009/02 represents the culmination of the most significant body of work surrounding the autogyro in recent years and serves as an illustration of the growing body of knowledge surrounding the autogyro configuration; however, it concludes that

"*there remains little indication that rigorous scientific or engineering investigation of airworthiness has occurred*" [4] due to the limited number of configurations used in the research.

Outside of the research carried out by Glasgow University, work has been carried out at The University of Liverpool (UoL) on behalf of BAE Systems (BAES) [6], through the development and validation of a simulation model of a Rotorsport UK MT-03 autogyro. Jump et al. [6] highlight the lack of engineering data and practical design experience associated with the autogyro (in comparison to more established fixed- and rotary wing aircraft). This is attributed to the lack of serious interest in the autogyro concept over an extended period of time, as discussed previously.

Both the University of Liverpool and Glasgow University introduced the concept of handling qualities assessment of the autogyro as a method of identifying deficiencies in the autogyro which may be responsible for the high accident rate observed in Figure 1. As no autogyro-specific handling qualities specification exists, ADS-33 [2] is suggested as an appropriate starting point for development of metrics against which the autogyro can be assessed. ADS-33 is a military specification which contains the requirements for the flying and ground handling qualities of rotorcraft. It is intended to cover rotorcraft which have primary missions ranging from scout and attack to utility and cargo.

1.2 RESEARCH AIMS AND OBJECTIVES

In light of an assessment of the body of research carried out to date, several research themes and questions became apparent. It is these themes that will be pursued in this Thesis.

1. CAA Paper 2009/02 represents the most significant body of work surrounding the autogyro in recent years; however, it presents 4 main findings [4]. The report itself concludes that little rigorous scientific or engineering investigation has occurred, and therefore there may remain scope to improve and develop the recommendations within Ref. 4. The present nature of the recommendations makes them difficult to apply in practice and unlikely to be implemented by the autogyro community at large; for these recommendations to provide any improvement to autogyro airworthiness or safety, they must be able to be utilised.

2. The use of existing rotary wing specifications, such as ADS-33 [2], has been shown to have some utility in assessment of the autogyro [7], however, a limited number of aircraft configurations have been assessed, and there remains scope to broaden the number of configurations in order to advance towards being able to create a specification specifically for the assessment of the autogyro.
3. It also still remains unclear if the metrics as defined in ADS-33 will highlight the deficiencies in the handling and performance of the autogyro; further flight testing is required to provide a clear illustration of whether ADS-33 is able to identify the deficiencies of the autogyro in the same manner it does for the helicopter. Some work has already been carried out in this field, with Bagiev and Thomson analysing selected Mission Task Elements (MTEs), namely the Slalom and Acceleration-Deceleration manoeuvres, and predicted handling qualities metrics, such as quickness and pilot attack in Ref. 7.
4. If existing specifications such as ADS-33 are not applicable to the autogyro, new metrics to assess the handling qualities of the autogyro must be developed.
5. The fundamental differences between the autogyro and the helicopter have never been comprehensively assessed; no like-for-like comparison has ever been conducted. The underlying fundamental differences, such as the unpowered rotor, or the separation of the control of thrust and the control inceptors in the autogyro may account for the high accident rate.

As a result of these emergent themes, the following objectives were defined for the project.

1. Creation of a simulation model of an autogyro, which will be validated through the use of flight test data. This model will be used in the completion of the remaining objectives.
2. An assessment of the recommendations made in Paper 2009/02 [4] should be carried out. These recommendations were defined using 2 different simulation models; it is the intention of this Thesis to re-assess the

recommendations presented in [4] and to build upon them using a different simulation model.

3. A comprehensive analysis of the autogyro model against the predicted handling qualities metrics defined in ADS-33 will be carried out. This is intended to develop the work detailed in Ref. 7, which features analysis of some of the parameters defined in ADS-33.
4. A select analysis of the assigned handling qualities of the autogyro against ADS-33 will be performed. Bagiev and Thomson have already carried out some work in this area [7], assessing the research aircraft designated G-UNIV against the Slalom and Acceleration-Deceleration manoeuvre (defined in ADS-33). It is the intention of this Thesis to re-assess these manoeuvres using real-time piloted simulation. Alongside these ADS-33 manoeuvres, the autogyro will also be assessed against the Heave Hop and Roll Step manoeuvres (both initially designed for tilt rotor aircraft). This is intended to broaden the range of manoeuvres the autogyro has been assessed against, as well as contribute new knowledge to the field.
5. Alongside the creation of an autogyro model, a geometrically equivalent (i.e. same mass, rotor geometry etc.) model of a helicopter will be created. This model will be evaluated using the same techniques as describe in points 3 and 4, allowing for the direct comparison of the helicopter and autogyro; something which has not previously been undertaken.

1.3 THESIS SCOPE, STRUCTURE & CONTENT

It should be noted that this Thesis relies heavily upon flight simulation, as opposed to the testing of real aircraft. Aside from the obvious benefits of using simulation (decreased costs, increased availability and non-reliance on ambient weather conditions), simulation also offered an environment in which the aircraft models could be pushed to the limits of their respective flight envelopes in relative safety. The facilities described in Chapter 2 have been used for a significant number of previous flight trial activities [8], and as such is considered representative enough of the aircraft environment to be an appropriate test bed for the experimental work contained herein.

The scope of this Thesis is limited by financial and temporal constraints; the volume and number of flight hours required to draw firm conclusions relating to airworthiness

recommendations for the autogyro, and their associated cost, is simply beyond the scope of a single doctoral Thesis. As such, this Thesis is intended to somewhat broaden and deepen existing work in the field of autogyro airworthiness [9 & 10] and highlight avenues with potential for further work. Where avenues which may prove fruitful for further work are identified, they will be clearly highlighted within the text and conclusions of each Chapter.

This Thesis is divided in 7 distinct Chapters, each addressing one or more of the research aims and objectives described in Section 1.2.

Chapter 2 describes the history of the autogyro and traces the progression of relevant research already conducted in this field. Chapter 2 also presents a review of autogyro safety statistics, which illustrates the extent of the issues surrounding autogyro safety. Chapter 3 demonstrates and documents the development, construction and validation of an autogyro simulation model in FLIGHTLAB, which is then used throughout the remaining Chapters of this Thesis. Chapter 3 also describes the development of a helicopter model which is geometrically similar to that of the autogyro, which is used in Chapters 5 and 6. Chapter 4 assesses the existing recommendations generated by CAA Report 2009 [4]. Chapters 5 and 6 describe each describe the assessment of the autogyro and helicopter models' handling qualities against the established rotary wing test and evaluation specification, ADS-33 [2].

The concluding chapter, Chapter 7, draws together the conclusions from Chapters 3 to 6, and assesses the implications of the results with respect to the research questions posited in Chapter 2.

1.4 ORIGINALITY AND NOVELTY

The work described in this study must constitute an original contribution to learning. This can be achieved by satisfying one or more of the following criteria [11]:

1. The discovery of entirely new knowledge

2. The expansion of knowledge in an existing field

3. The explanation or connection of previously observed results

4. Revision of established views

The aspects of the research detailed in this Thesis which satisfy these criteria are highlighted throughout the body of their respective Chapters, and are also stated explicitly here for clarity:

1. The modelling, validation and real-time simulation of an autogyro presented in Chapter 3 is novel in the sense that little similar work has been carried out previously. Specifically, the use of assigned handling qualities ratings to validate the fidelity of the autogyro model has not been previously reported. Additionally, the use of real-time simulation in both Chapter 3 and throughout this Thesis, and the comparison of data from both simulated real-time and real-world flight test are entirely new. As such, this contributes to both the expansion of existing knowledge and the discovery of new knowledge.

2. Chapter 4 evaluates the existing recommendations made in "*CAA Paper 2009/02: The Aerodynamics of Gyroplanes"* [4]. Re-evaluating the recommendations made using a different method of aircraft modelling and a new aircraft geometry both contributes new knowledge and expands upon the existing knowledge generated in the initial development of the recommendations. Analysis of the recommendations relating to tailplane effectiveness and vertical centre of gravity location relative to the propeller thrustline also generated new knowledge. It was previously concluded in Ref. 4 that the tailplane is largely ineffective in improving the long-term characteristics of the phugoid mode; research presented in Chapter 4 has demonstrated that the tailplane is influential in shaping the key aerodynamic derivatives which determine the phugoid mode characteristics. The recommendation that the vertical centre of gravity lie within a ±2 inch envelope of the propeller thrustline in order to ensure compliance with BCAR Section T was also investigated; for the geometry of aircraft used, this was shown to be overly restrictive. Whilst these conclusions alone may not be enough to force a wholesale revision of established views, they do represent a significant contribution and expansion to knowledge in an existing field and

provide a basis for further work. They are also significant when considered in the context of the relative paucity of other research carried out in this field.

3. Within Chapter 4, the investigation of tailplane effectiveness represents both expansion of knowledge and the discovery of entirely new knowledge. It is the first time that the contributions from individual aircraft components and their effects on aerodynamic derivatives, as shown in Figure 70– Figure 75, have been considered in the context of autogyro type vehicles. This may also result in the revision of the established view (after further work has been carried out) that the tailplane has no significant effect on the longitudinal stability characteristics of the autogyro.

4. Chapter 5 presents a comprehensive analysis of predicted autogyro handling qualities. These results are also compared to predicted handling qualities for a geometrically similar helicopter model. It is the first time a comparison of the differences in predicted handling qualities between autogyro- and helicopter-type aircraft has been performed, and as such this constitutes the discovery of entirely new knowledge in the field. The expansion of the number of metrics used to assess the predicted handling qualities of the autogyro also expands upon the investigations carried out in Ref. 7.

5. Similarly to Chapter 5, Chapter 6 presents a comparison of assigned handling qualities for both helicopter and autogyro. It is the first time the autogyro has been assessed using the Heave Hop and Roll Step manoeuvres, and as such this constitutes new knowledge. The evaluation of the Acceleration-Deceleration and Slalom manoeuvres also extend upon work carried out in Ref. 7.

6. The extensive use of real-time simulation in all aspects of this Thesis is also novel; previous research has focussed on real-world flight test or non-piloted simulation.

Chapter 2

LITERATURE REVIEW

The objective of this Chapter is to present a summary of the current status of the area of research and a comprehensive review of work already performed within this area. It also serves to identify potential knowledge gaps, and thus to provide a number of research questions that form the basis of the work reported in subsequent Chapters.

2.1 BACKGROUND

In 1923, the autogyro became the first rotary wing aircraft to achieve sustained powered flight, pre-dating the first practical helicopter by more than 15 years [3]. Cierva intended to design an air vehicle which ensured "stability, uplift and control should remain independent from forward speed" [12], while being flown by a pilot of average skill. In order to satisfy this condition, Cierva concluded that the rotor system "must be independent of the engine. It was thus necessary that the rotary wings were free-spinning and unpowered" [12]. The autogyro was born; a revolutionary aircraft with an unpowered rotor.

Existing published research on the subject of the autogyro can be broadly divided into two time periods; the period before the first flight of the helicopter, leading up to World War II, and the current period of renewed research interest from 1996 onwards. These are described in Sections 2.2 and 2.4 respectively.

2.2 EARLY WORKS (1926 – 1939)

Intense interest in the autogyro led to over a decade of research into all aspects of its operation. Early literature is diverse in its focus, with extensive wind tunnel testing, flight tests and analytical investigations being performed throughout the 1930s. Therefore, it should be noted that a significant proportion of this research carried out during this period was dedicated to fundamental flight dynamics, rather than to piloted handling qualities.

In 1926, Glauert published a paper entitled "A General Theory of the Autogyro", which sought to establish "a theory which will explain the behaviour of an autogyro" and

"provide a method of estimating the effect of changes in the fundamental parameters of the system" [13]. This was the first theoretical exploration of the relationship between rotor inflow (the dynamic behaviour of air entering the rotor) and rotor performance. Glauert quantified rotor behaviour in climbing, descending, and horizontal flight regimes, and formulating fundamental equations that could be utilised to relate rotor performance to rotor design parameters. However, Glauert's theory was found to be inaccurate when applied to autorotation or descent; Cierva showed that descent rates achieved in flight tests were half that predicted by Glauert's theory [14]. These inaccuracies arose due to the fact Glauert's theory was unable to accurately describe the rotor inflow because he was unable to accurately predict the induced velocities that occur on the rotating rotor. Since the publication of Glauert's 1926 paper, the fact remains that there is no theory, derived from first principles, which can fully describe the aerodynamic behaviour of a rotor in the autorotative state.

Lock's paper, "Further Development of Autogyro Theory – Parts I and II", was written with the intention "to carry the theory a stage further" [15] by removing some of the approximations and simplifications implemented in Glauert's work; taking into account the flapping motion of the rotor blades (thus removing the assumption of infinitely heavy blades). Glauert also developed a method to more accurately predict the aerodynamic forces acting on the blades by accounting for the higher order harmonics of the tip speed ratio (designated 'μ', defined as the ratio of the horizontal component of velocity in the plane of rotation of the tip speed) – a factor which becomes increasingly important with airspeed in the prediction of the lift to drag ratio. The removal of these assumptions is further discussed in Ref. 16.

Alongside the early analytical works of Glauert and Lock, extensive wind tunnel tests were also undertaken [17–19], with the objective of characterising the aerodynamic performance of the autogyro. The first full-scale flight tests were undertaken in 1933 [20 & 21], both of which focussed on classifying the aerodynamic properties of the autogyro. After further wind tunnel testing [22] and formulation of "an extension of the autogyro theory of Glauert and Lock" [23], Wheatley sought to establish the validity of Glauert and Lock's treatises on the autogyro so that the theory could be applied to the autogyro design process. In order to do this, Wheatley developed Lock's analysis to include the influence of linear variation of blade pitch with rotor radius and incorporated the

influence of several factors which Lock had neglected [23]. A method for accounting for the effect of reversed flow over the retreating blade was developed and an approximation of the tip losses in calculation of thrust was introduced. Wheatley also formulated a method of calculating drag at extreme angles of attack. Wheatley concluded that two different methods must be employed in the calculation of drag; one for low incidence and one for high incidence [23]. After adapting Lock's theory, Wheatley applied his adaptation to the rotor head of the Pitcairn PCA-2 autogyro; these calculated results were then compared to wind tunnel test data for the PCA-2. Wheatley concluded that "the aerodynamic analysis of the autogyro as developed by Glauert and Lock is quantitatively usable except for the blade motion" due to the inability of the method to predict the distribution of the variation of induced velocities along the rotor radius. This limitation introduces increasingly large errors in the prediction of rotor inflow velocity as tip speed ratio (μ) increases, and is the same problem encountered by Glauert in Ref. 13. Wheatley also recognised the importance of parasitic drag in the prediction of rotor performance; however, he was not able to compare the calculated results for drag to wind tunnel data as it was not available.

Wheatley's work on the aerodynamics of the autogyro continued, more wind tunnel and flight tests were carried out [24 & 25], and further efforts made to reconcile the differences between theoretical calculations and experimental observations. Wheatley also carried out a study of one of the autogyro's unique features; the jump take-off [26]. Equations of motion to describe a vertical jump take-off were formulated, with suitable approximations, and the resulting predictions compared with the results of model wind tunnel tests. Relatively good agreement between the two was found.

Wheatley also focused attention on classifying the influence on rotor characteristics of the periodic blade twist which occurs as the rotor spins [27 & 28]. He was able to illustrate the pronounced effect blade twist has on flapping dynamics - the aerodynamic forces acting on the blade causing the blade to twist, resulting in a change of blade pitch attitude, producing a flapping motion. The effects on torque and thrust characteristics of the rotor were also demonstrated. These analytical results were again compared to wind tunnel test data, and found to be in "satisfactory" agreement [28].

Bailey's paper, "A study of the torque equilibrium of an autogiro rotor" [29] aimed to develop the work of Wheatley described in Ref. 23 by creating a method to estimate the rotor inflow in a more computationally efficient manner. Bailey also eliminated the large errors in rotor inflow velocity prediction at high tip-speed ratios through the use of charts based on graphical integration. Again, he compared the results of his analytical methods to wind tunnel test results, referring back the data collected by Wheatley in Ref 23. His new methodology was found to give accurate predictions of rotor inflow velocity across the tip-speed ratio range.

Bailey carried out further wind tunnel testing, which is described in "Observations in flight of the region of stalled flow over the blades of an autogiro rotor" [30]. By attaching silk streamers to the upper surfaces of the blades of the rotor head of a Kellett YG-1B autogyro and recording their motion while in a wind tunnel, Bailey was able to determine the regions in which stall was occurring. The size and position of these regions was compared to theoretical predictions; the experimental data showed the stalled regions to be much larger, and growing at a faster rate as the tip-speed ratio increased, than the theory predicted. Bailey recognised that the control of these stalled areas plays an important role in determining the lift-to-drag ratio of the rotor assembly and the blade flapping motion at higher tip-speed ratios.

In 1937, (aircraft builder and aviation pioneer) Louis Breguet published "The Gyroplane – its principles and its possibilities" [31]. This paper fully describes the autogyro, its operation, and its potential as an aircraft – the absence of a conventional stall, the ease of maintenance and small overall dimensions (ideal for storage), its vertical ascent and descent capabilities and its "inappreciable military qualities" as a potential scout vehicle or as a replacement for the naval deckplane. Breguet concludes that "the gyroplane problem should not be given up but, on the contrary, attacked in all seriousness".

The first paper concerning the stability and control of an autogyro was published in 1938. Schrenk's paper "Static longitudinal stability and longitudinal control of autogiro rotors" [32] describes three different systems of elevator control:

a) the standard ailerons and elevators used at the time;
b) Cierva's method of blade control (fixing the tail surfaces and allowing the rotor hub to move);

c) 'Gravity control', where the rotor and tail surface are allowed to move simultaneously.

Schrenk found that the control sensitivity ($^{dv}/_{d\beta}$) to be strongly dependent on airspeed for the standard aileron/elevator system, but "becoming substantially more uniform" in system b) and "practically constant" throughout the speed range in system c). Blade and gravity control enable the aircraft to recover smoothly and "with little stress" from high speed dives and prevent the aircraft controls becoming too sensitive at high speeds. They also allow the aircraft to land without large control deflections being required.

Despite Wheatley, Bailey and Schrenk's academic efforts, and Breguet's passions, interest in the autogyro began to wane in the early 1940s, with several factors contributing to the decline. The passing of the 1938 Dorsey Bill in the United States allocated the US Army $2 million "for the purpose of rotary wing and other aircraft research, development, procurement, experimentation, and operation for flight testing" [3], and resulted in the 1938 Rotating-Wing Aircraft Conference at the Franklin Institute. This conference brought together all of the pioneers and technical specialists in the rotary wing field, including Igor Sikorsky. The combination of funding from the Dorsey Bill and the technological advances generated from wartime efforts resulted in the successful development of the first helicopter, Sikorsky's VS-300. Combining this with the death in 1936 of the autogyro's strongest advocate, Cierva, and the outbreak of World War II in 1939 (which saw a moratorium declared on all rotary wing research), interest in the autogyro was critically diminished.

Research into rotary wing vehicles resumed towards the end of World War II, with the first conventional helicopter (the Sikorsky R-4) entering service in 1942 [33]. From a military perspective, the vertical flight capabilities and notionally greater useful payload offered by the helicopter made this configuration more immediately attractive than the autogyro. For this reason, rotary wing research since the end of World War II has focused almost entirely on the helicopter, and the autogyro has become the preserve of sports aviation enthusiasts.

2.3 REVIEW OF SAFETY STATISTICS

Anecdotal evidence suggests that autogyro safety statistics display a relatively high accident rate; it is the intention of this review of safety statistics to quantify and illustrate this.

Data has been gathered from Civil Aviation Authority (CAA) reports (CAP reports number 701 [34], 735 [35], 763 [36] and 780 [37]) dating from 1990 to 2007 (the widest range of data available at the time of writing). Each of the four reports span a period of 10 years and the periods overlap across reports. A summary of the data from these reports is shown in Table 1.

There are some discrepancies within the data reported in Refs. 34 - 37; often, the estimated number of hours flown for a given year varies. For example, CAP701 [34] states that in 1998 autogyros flew 5977 hours; for the same year, CAP780 [37] gives the number of hours flown as 1432. As a result of this, the data for number of fatal accidents per million hours of flight time (the metric by which accident rates are best compared), is skewed. In general, the oldest two reports (CAP 701 and CAP 735) show a higher number of predicted hours flown, and reasonable agreement between the figures during the years that they both cover. Similarly, the two most recent reports (CAP 763 and CAP 780) show a lower number of predicted hours, and again show good agreement within the years covered. Table 1 and Table 2 illustrate this. Numbers have been rounded to the nearest whole number for clarity in both cases.

In order to address the inconsistencies within the data, clarification was sought from the CAA during the course of this study. In response, up-to-date statistics (presented in Table 3) were provided which account for the discrepancies, identifying several factors as possible causes. One of the possible reasons for the discrepancies in the data is that flight time data is generally collected at the renewal of the Certificate of Airworthiness or validity period, and as such, the data for the previous three calendar years from the current year is likely to change with the addition of more information. It is also worthy of note that the most significant changes will appear in the data for the preceding three calendar years; for example, in 1999, data appearing for 1996, 1997 and 1998 will be most likely to change. This will also change the estimate of the number of hours flown, which are extrapolated from the records available at the time.

	Estimated hours flown by year								
	1990	**1991**	**1992**	**1993**	**1994**	**1995**	**1996**	**1997**	**1998**
CAP701	6112	2752	3953	4325	5237	5637	5315	5485	5977
CAP735			2840	3799	5428	4834	4663	4833	4738
CAP763						1800	1500	1500	1400
CAP780									1432

	1999	**2000**	**2001**	**2002**	**2003**	**2004**	**2005**	**2006**	**2007**
CAP701	5588								
CAP735	4463	4635							
CAP763	1400	1300	1600	2500	2100	1900			
CAP780	1445	1266	1596	2535	2315	1872	1960	2046	2188

Table 1: Autogyro estimated hours flown per year across CAP reports [34 – 37]

	Fatal accidents by year, per million hours flown								
	1990	**1991**	**1992**	**1993**	**1994**	**1995**	**1996**	**1997**	**1998**
CAP701	164	727	0	231	0	0	188	0	167
CAP735			0	263	0	0	214	0	211
CAP763						0	667	0	714
CAP780									698

	1999	**2000**	**2001**	**2002**	**2003**	**2004**	**2005**	**2006**	**2007**
CAP701	0								
CAP735	0	216							
CAP763	0	769	625	800	476	526			
CAP780	0	790	627	789	432	534	0	489	0

Table 2: Autogyro fatal accidents per million hours flown per year across CAP reports [34- 37]

Due to a change in the way the hours flown are recorded (the CAA was unable give details of what this change was), the hours attributed to a given year may be actual hours flown or an averaged number of hours, determined by various methods of calculation (no detail was provided as to what these methods were). As previously mentioned, not all flown hours are captured, and as such the data is extrapolated to provide an average number of hours flown. During the period 1990 – 2007, an average of 37% of aircraft on

record returned their hours flown, and the remaining aircraft are accounted for through extrapolation. This gives an approximation for the whole fleet.

	Estimated hours flown by year								
	1990	**1991**	**1992**	**1993**	**1994**	**1995**	**1996**	**1997**	**1998**
CAA Data	1085	643	815	1090	1589	1573	1331	1242	1261

	1999	**2000**	**2001**	**2002**	**2003**	**2004**	**2005**	**2006**	**2007**
CAA Data	1161	1030	1234	1825	1344	1621	2117	2475	3308

	Fatal accidents per year								
	1990	**1991**	**1992**	**1993**	**1994**	**1995**	**1996**	**1997**	**1998**
CAA Data	3	2	3	1	1	3	3	3	1

	1999	**2000**	**2001**	**2002**	**2003**	**2004**	**2005**	**2006**	**2007**
CAA Data	3	0	2	1	3	4	2	3	4

	Fatal accidents per million hours flown								
	1990	**1991**	**1992**	**1993**	**1994**	**1995**	**1996**	**1997**	**1998**
CAA Data	2765	3110	3681	917	629	1907	2254	2415	793

	1999	**2000**	**2001**	**2002**	**2003**	**2004**	**2005**	**2006**	**2007**
CAA Data	2584	0	1621	548	2232	2468	945	1212	1209

	3 year moving average - fatal accidents per million hours flown								
	1990	**1991**	**1992**	**1993**	**1994**	**1995**	**1996**	**1997**	**1998**
CAA Data	N/A	N/A	3185	2570	1743	1151	1597	2192	1821

	1999	**2000**	**2001**	**2002**	**2003**	**2004**	**2005**	**2006**	**2007**
CAA Data	1931	1126	1402	723	1467	1749	1881	1541	1122

Table 3: Accident and flight time statistic for autogyros, 1990 – 2007 (Source: CAA data)

Within the CAP reports, accident data is commonly presented as a three-year moving average. Where not available within the reports, the three year moving average is calculated using the accident rate per million hours for a given year and the two preceding years. The resulting analyses, including the accident statistics from the CAA, are shown in Figure 2. The CAA classifies autogyros in the same sub-category as

microlights and gliders, and as such Figure 2 shows the accident rate statistics for all three types of aircraft. The microlight and glider accident statistics are also gathered from Refs. 34 – 37, but they did not display the same level of variance as the autogyro statistics.

The revised data provided by the CAA is summarised in Figure 2, and clearly shows that the autogyro exhibits a significantly greater fatal accident rate per million hours flown than the microlight or glider.

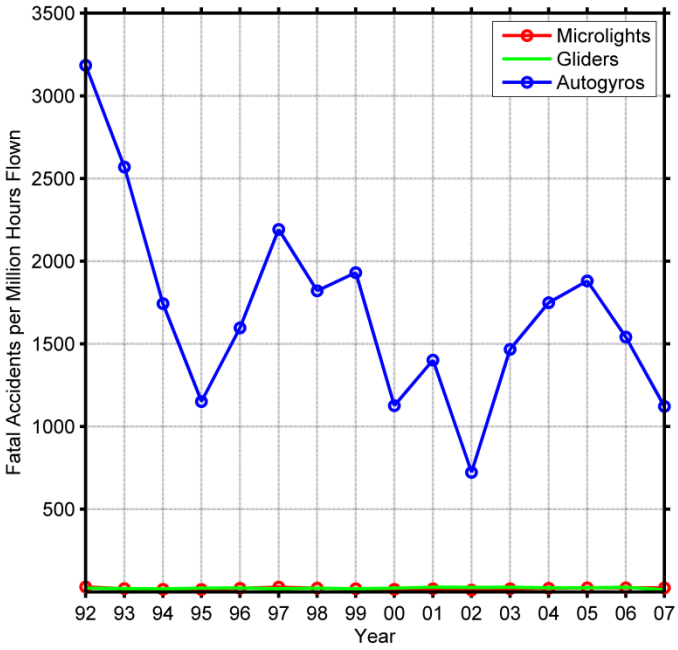

Figure 2: Autogyro historical accident rates, compared to gliders and microlights (data source: CAA)

2.4 RECENT WORKS (1996 – PRESENT)

This literature review found that, between 1939 and 1996, only three papers on subject of the autogyro were published. These papers were published in the 1960s and describe the history [38], the design and construction [39] and the performance of the autogyro [40]. There is also a letter to the Medical Journal of Australia [41] highlighting the six fatal accidents and four serious injuries over an 11 year period from 1975 to 1986.

2.4.1 CAA Paper 2009/02: The Aerodynamics of Gyroplanes

The excessively high accident rate amongst autogyros, illustrated in Figure 2, has led to a resurgence of interest in research into their flight dynamics and handling qualities, as well as in the physics and modelling of the autorotative state. The majority of recent research has been carried out by Glasgow University with CAA funding.

Published in August 2010, CAA Paper 2009/02 [4] presents the culmination of the most substantial body of recent work in the autogyro field. This report arose from recommendations of the Air Accident Investigation Branch (AAIB) review of the airworthiness of the grounded Air Command autogyro [42], conducted after the occurrence of 5 fatal accidents between 1989 and 1991. One of the key recommendations of this review was the commissioning of a programme of research into both the airworthiness and aerodynamic characteristics of light autogyros. Glasgow University were tasked with undertaking this research, and the results were published in Ref. 4. Research activities consisted of the creation and validation of simulation models, flight test and wind tunnel activities. The outcomes of these activities were published independently of Paper 2009/02, and are discussed in detail individually later in this Chapter.

Paper 2009/02 [4] presented 4 main findings/recommendations:

1) It is recommended that the vertical location of the centre of gravity (c.g.) should lie within a ± 2 inch envelope of the propeller thrust line. Ref. 4 accepts this as a "sensible design aim to achieve pitch dynamic stability (phugoid mode)" but accepts there are autogyros which achieve good stability with a c.g. location well outside this envelope, and that other factors can impact upon the phugoid stability (such as the drag damping from the rotor and fuselage, the pod and tailplane effectiveness and the airspeed).

This recommendation was included in the revision of CAP643 British Civil Aviation Requirements Section T: Light Gyroplanes [5] (referred to as BCAR Section T), the CAA's autogyro airworthiness and design standard.

2) Horizontal tailplanes are largely ineffective in improving the long term pitch dynamic stability (phugoid mode).

3) Extreme manoeuvring can lead to excessive rotor teeter angles during certain phases of flight, potentially resulting in the rotor blades striking the prop or empennage.

A recommendation to ensure satisfactory control margin and rotor clearance up to 1.1 V_{NE} was included in the revision of Ref. 5 as a result of this recommendation.

4) The chordwise centre of gravity of the rotor blades should always lie at or ahead of the 25% chord position to prevent rotor blade instability. A sudden reduction in main rotor speed due to aeroelastic instability has often been a feature of autogyro accidents, and it is a phenomenon which is not well understood. Work carried out as part of the research programme prescribed in Ref. 66 noted that a key parameter in aeroelastic instability is the blade torsional dynamic behaviour. Placing the blade chordwise centre of gravity at or ahead of the 25% chord position will, in the worst case scenario, result in a blade with zero torsional stiffness.

BCAR Section T (659) [5] requires the rotor blades to position the chordwise c.g. at or forward of 25% chord, however, Paper 2009/02 [4] states that "the technical ability of the gyroplane community and the test and analysis facilities available to them, may severely compromise or inhibit the collection of meaningful, or even correct data with which to demonstrate compliance. Any recommendations that might be made in respect of Section T, therefore, may be *only of academic consequence, and do little to enhance Section T and therefore airworthiness*" [5].

Paper 2009/02 serves as an illustration of the growing body of knowledge surrounding, and the resurgence of research interest in, the autogyro configuration; however, it concludes that "*there remains little indication that rigorous scientific or engineering investigation of airworthiness has occurred*" [4] due to the limited number of configurations used in the research.

2.4.2 Recent Works

The first papers published as a part of the resurgence of interest in the autogyro focussed on the identification of its stability characteristics. Houston's paper "Longitudinal stability of gyroplanes" [43] presents an analysis of autogyro longitudinal stability, taking into consideration the basic forces and moments in context with the rotor behaviour, to

assess the fundamental nature of autogyro stability. Houston highlighted the importance of the rotorspeed degree of freedom derivative, M_Ω, in autogyro stability. Unlike a helicopter, the autogyro's rotorspeed is free to vary in flight. This means that, for a given increase in rotorspeed, the rotor thrust will increase; if the aircraft were then to pitch down, the reduced rotor inflow would tend to reduce the rotorspeed. As such, it is desirable for stability that $M_\Omega < 0$. Houston was also able to illustrate the strong coupling between the rotorspeed degree of freedom and the "classical" rigid-body modes, in particular the phugoid, and highlights a specific safety concern – for configurations where the main rotor thrust line passes close to the centre of mass, changes in the phugoid stability (and therefore rotorspeed stability) will occur as the main rotor thrust line passes through the centre of mass as the rotor disc flaps. This can result in a potentially dangerous change in the aircraft's handling characteristics – the phugoid mode, and consequently the rotorspeed mode, has the potential to become unstable. Houston also highlights the significance of the positioning of the vertical location of the centre of gravity relative to the propeller thrust line. For example, if the propeller thrust line is placed below the centre of gravity, the nose up pitching moment generated by the propeller needs to be balanced by placing the main rotor thrust line aft of the centre of gravity. This was the genesis for recommendation 1) of Ref. 4. While this is a sensible design aim, there is no corresponding recommendation for positioning of the main rotor thrust line relative to the centre of gravity.

Houston's work in Ref. 43 was further developed in "Identification of autogyro longitudinal stability and control characteristics" [44]. A programme of flight tests using a VPM M16 autogyro were carried out and an in-flight investigation of autogyro stability and control was performed; at the time, this was unique in the literature. Houston was able to conclude that, unusually, the autogyro displays conventional fixed wing dynamic stability characteristics in the longitudinal axis and was stable throughout the speed range. The strong coupling between the phugoid mode and the rotorspeed mode reported in Ref. 43 was also observed. The flight test detailed in Ref. 44 lead to the introduction of the recommendation in BCAR Section T [5] that the propeller thrust line should lie within a ± 2 inch envelope of the vertical position of the centre of gravity; this relationship is identified as being key to conferring positive angle of attack stability which is important in stabilising the phugoid mode.

Houston also investigated the lateral/directional stability and control characteristics of the autogyro [45], concluding that the VPM M16 displayed "conventional lateral and directional dynamic stability characteristics", and states that the results for this particular aircraft can be interpreted more generally, as most contemporary autogyros display similar geometric configurations. Houston also states that this basic configuration "does not compromise lateral/directional characteristics, although a greater dihedral effect is possibly desirable" to improve spiral mode stability.

Alongside these analytical works and flight test programmes, wind tunnel tests were also resumed. Coton and Smrek's paper "Aerodynamic characteristics of a gyroplane configuration" [46] describes a programme of tests using a one-third scale model of a VPM M14 autogyro. The purpose of the tests was to collect basic aerodynamic data on the effects of configurational characteristics of the autogyro, with a view to assessing the degree to which specific design features (such as the cowling or tailplane) are beneficial to autogyro performance. The secondary aim of these tests was to provide aerodynamic data for input to mathematical models in order to be able to validate parametric studies that would be carried out as part of Glasgow University's CAA commissioned research programme. Ref. 46 concludes that the aerodynamic characteristics of the autogyro are "generally benign", but that the presence of a large cowling can have a detrimental effect on stability, increasing the wetted area presented to onset flow in sideslip which acts to oppose the stabilising effect of the tailplane.

In "Validation of a rotorcraft mathematical model for autogyro simulation" [47], Houston describes the creation and validation of an autogyro simulation using a rotorcraft mathematical model, configured as an autogyro. This autogyro model provided "satisfactory" estimation of the key stability derivatives without any modification of the original helicopter governing equations of motion. However, Houston concludes that in order to make a "definitive statement" that a rotary wing model can adequately simulate autogyro flight dynamics, further investigations using different autogyro configurations are required.

Using the model created in Ref. 47, Houston was able to further demonstrate coupling between the phugoid mode and the rotor speed degree of freedom [48]. "Analysis of Rotorcraft Flight Dynamics in Autorotation" [48] also provides a discussion of the

important stability derivatives which affect the rotor speed and phugoid modes, namely vertical force and pitching moment derivatives.

A second series of flight tests were performed using a fully instrumented Montgomerie-Parsons research gyroplane, registered G-UNIV. The result of these flight tests is reported in Ref. 49. It was concluded that the flight dynamic response of this particular autogyro is dominated by a "fast, neutrally stable mode, affecting all states" [49]. This mode results in significant cross-coupling between the longitudinal and lateral-directional dynamics, and was induced by almost any type of pilot control deflection. It is stressed that as the Montgomerie-Parsons research autogyro (designation G-UNIV) possesses a unique configuration due to its instrumentation, so this mode may not be present in other models of gyroplane, however, this does "provide impetus" for similar testing to be performed on other light autogyros with poor safety records.

One of the most important observations from Ref. 49 is the fact the autogyro does not comply with BCAR Section T [5]. The period of the dominant mode of motion described above was found to be 7.4 seconds; BCAR Section T states that "any oscillation having a period between five and ten seconds should damp to one half amplitude in not more than two cycles" [5]. BCAR Section T also prescribes a requirement that the oscillation should have "no tendency to persist". The 60 mph test case in Ref. 49 clearly indicates the Montgomerie-Parsons does not conform to this requirement. Similarly, the lower speed cases (40 and 50 mph) exhibit this characteristic to a lesser extent. Ref. 49 identifies this as posing "significant airworthiness and handling qualities implications" and warranting further investigation.

This non-compliance and presence of undesirable characteristics were further investigated in "Experiments in Autogiro Airworthiness for Improved Handling Qualities" [50]. Thomson et al. evaluated the VPM M16, the Montgomerie-Parsons and the grounded Air Command autogyros against BCAR Section T [5] to assess their compliance, using both flight tests and mathematical modelling. This served to question the validity of the requirements laid out in BCAR Section T. Similarly to Ref. 43, it was concluded that the vertical location of the centre of gravity in relation to the propeller thrust line was key in terms of autogyro stability (raising the c.g. increases pitch stability), although the actual stability characteristics remain dependant on the airframe aerodynamics and

ambient conditions (namely, dynamic pressure). Thomson et al. were able to suggest a potential design modification to the Air Command autogyro to "render a more favourable vertical c.g. and propeller thrust line relationship" – raising the c.g. (potentially by inverting the engine gearbox) or inclining the engine downwards, raising the fuel tank and seat; thus potentially making the Air Command autogyro airworthy again.

2.5 AUTOGYRO HANDLING QUALITIES

A combination of the poor safety record of autogyros and the in-depth identification of the source of airworthiness deficiencies [50] in autogyros led to consideration of autogyro handling qualities. There is an assumption that improving the airworthiness of the autogyro will improve its handling qualities. However, as no criteria for the assessment of the autogyro handling qualities exist, it remains impossible to quantify the level of improvement achieved (if any).

To begin the process of addressing the lack of handling qualities requirements for autogyros, Bagiev and Thomson [51] evaluated the Montgomerie-Parsons autogyro (G-UNIV) against existing ADS-33 [2], AGARD-R-577-70 [52], and MIL-HDBK-1797 [53] documents. These documents specify handling qualities requirements for rotary wing, fixed-wing and VSTOL (vertical and short take-off and landing) aircraft respectively by defining quantitative criteria that provide objective assessment of the aircraft performance, without the influence of the pilot's qualitative opinion.

ADS-33 differs from this description as it uses both objective and subjective methodologies for evaluating the handling qualities of the aircraft under consideration, using the subjective Cooper-Harper handling qualities rating scale [54] alongside objective mission task elements (MTEs). This approach is described by Mitchell et al. [55] as "a second revolution in handling qualities."

ADS-33 was intended to replace the helicopter specification MIL-H-8501A [56] and was to be used for the evaluation of the experimental LHX helicopter (now known as the RAH-66 Comanche). It became the first military rotorcraft specification to include frequency-domain requirements, visual cueing requirements and mission task elements (MTEs).

MTEs were introduced to address the lack of completeness within any given specification; the deficiencies in an aircraft's handling qualities may not be fully exposed by the quantitative criteria within the specification (for example PIOs), and the advancement of technological inceptors will always outpace the advances in handling qualities criteria.

Additionally, most of the previous requirements focussed solely on the single axis response, eliminating the evaluation of the cross-couplings between axes. In order to negate these problems, MTEs were introduced within ADS-33, and were intended to be "catch-all tasks" [55], however, they proved useful in both simulation and the flight test environment. ADS-33 features a comprehensive "menu" of MTEs, with stringent desired and adequate performance requirements, designed for different aircraft types (scout, utility, attack etc.), which are intended to reflect manoeuvres to be performed by the aircraft within its role, in order to expose any deficiencies in handling qualities.

Alongside the quantitative MTE metrics, ADS-33 also uses the qualitative Cooper-Harper scale. Cooper and Harper define handing qualities as "those qualities or characteristics of an aircraft that govern the ease and precision with which a pilot is able to perform the tasks required in support of an aircraft role" [54] - they recognised that handling qualities rely upon more than the stability and control characteristics of the aircraft under scrutiny alone. As a result of this, Cooper and Harper developed the Cooper-Harper Handling Qualities Rating (HQR) Scale, as shown in Figure 3. The scale is modelled as a flow chart, the pilot choosing 'yes' or 'no' answers at each stage in order to arrive at a HQR on a scale of 1 to 10; 1 being the best, 10 being the worst. As stated in Mitchell et al. [55], "the Cooper-Harper scale has "some shortcomings, but its strengths far outweigh any weaknesses".

Bagiev and Thomson [51] were able to predict the handling qualities of the autogyro using the existing methodologies in Refs. 2, 52 & 53, noting that ADS-33 [2] does not make distinctions based on aircraft size, which "makes this document universal and gives the possibility of developing future autogiro handling qualities requirements in a similar way".

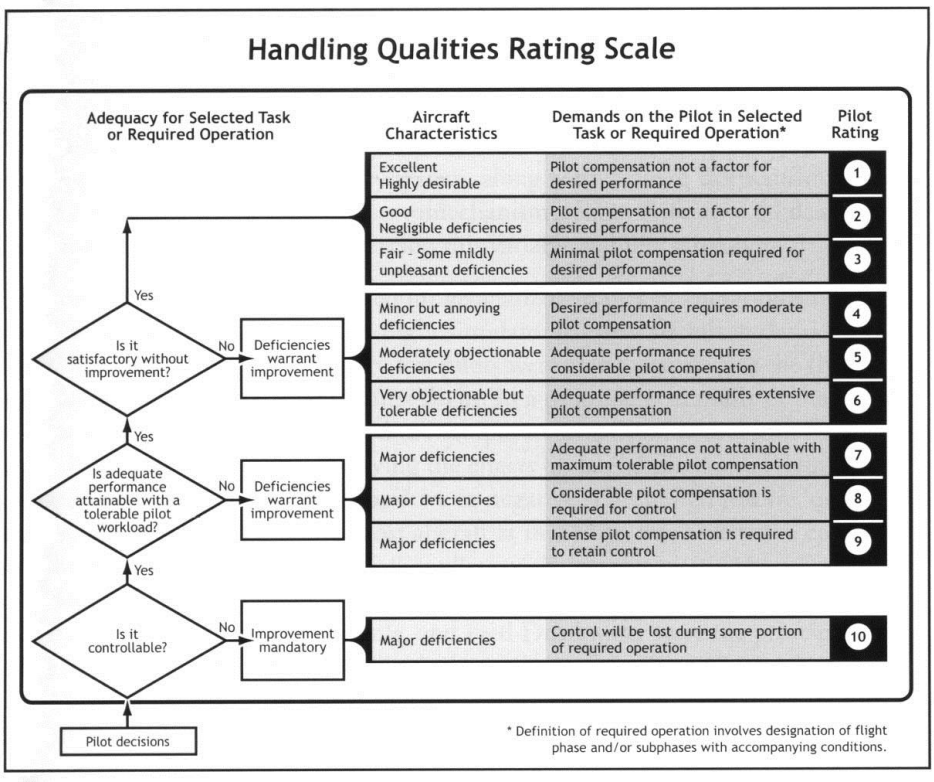

Figure 3: The Cooper-Harper Handling Qualities Rating Scale [2]

Having established ADS-33 as an appropriate basis for developing a handling qualities specification for autogyros, Bagiev and Thomson [7] proposed using inverse simulation as a preliminary tool to design test manoeuvres. In order to do this, a high fidelity individual blade/blade element coupled rotor-fuselage mathematical model of the G-UNIV autogyro was developed and coupled with a generic inverse simulation algorithm. An inverse simulation algorithm calculates the pilot control inputs that are required for the vehicle to fly a specified manoeuvre. One way to do this is to use a numerical integration technique, as first proposed by Hess et al. [57]. The algorithm used by Bagiev and Thomson is a modified version of the "GENISA" algorithm described in Rutherford and Thomson [58]; GENISA segments the initial flight trajectory into small periods and integrates the nonlinear equations of motion in order to generate a flight path. This flight path is then compared to the desired trajectory, with the difference between the two forming an error function. A Newton-Raphson iterative scheme is applied to minimise this error function.

Ref. 7 focusses on two manoeuvres taken from MTEs prescribed by ADS-33 – the acceleration/deceleration and the Slalom. Inverse simulation enables key parameters to be varied in order to ensure appropriate performance levels will be met by the real aircraft; this allows the aggressiveness of the manoeuvres to be varied and suitable performance standards created. For example, within the Slalom manoeuvre (shown in Figure 4), a key metric which defines the aggressiveness of the manoeuvre is the aspect ratio (AR). Aspect ratio is defined by Padfield [59] as:

$$AR = \frac{Width}{Length}$$

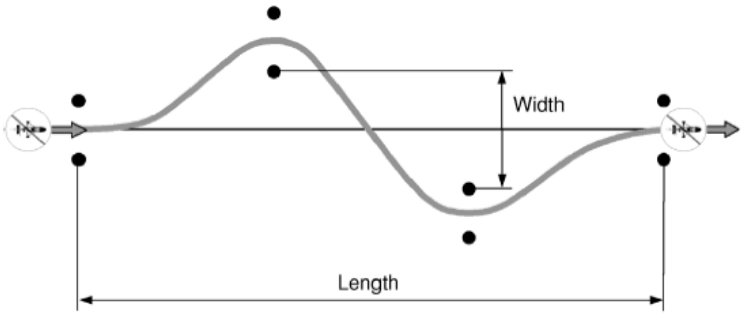

Figure 4: The autogyro Slalom manoeuvre [2]

Using the inverse simulation technique, Bagiev and Thomson showed that during the Slalom manoeuvre at 50mph for increasing values of aspect ratio, increasing lateral control inputs are required, which in turn increases pilot workload and the aggression required to complete the course. It was predicted by the simulation that somewhere between AR = 0.13 and AR = 0.15 the rotor shaft travel limit would be reached.

The effect of airspeed was also investigated. It was found that this had a similar effect on aggressiveness of the manoeuvre as aspect ratio; increasing airspeed increased the required level of aggressiveness, due to the fact that the time available to complete the manoeuvre had decreased. From these parametric investigations, Bagiev and Thomson were able to estimate the boundaries of the flight envelope of the G-UNIV gyroplane during the Slalom manoeuvre.

To validate the predictions of the inverse simulation, flight tests were performed and the aircraft assessed using both the requirements defined in ADS-33, the Cooper-Harper

scale, and the Bedford workload rating (WR) scale. As predicted by the simulation, increasing the airspeed and the aspect ratio resulted in degradation in both HQR and workload rating for the Slalom manoeuvre; the higher the aggressiveness required to complete the manoeuvre, the lower the HQRs and WRs awarded by the pilot.

The acceleration/deceleration manoeuvre, as described in ADS-33, requires the aircraft to accelerate to a target airspeed from a stabilised hover, before decelerating aggressively back to hover. As the autogyro cannot hover, some modification to the way the manoeuvre is performed is required. Instead of starting the manoeuvre from hover, the manoeuvre would instead be initiated from a stabilised airspeed (in this case 40mph) before accelerating to the target airspeed, attempting to achieve maximum acceleration.

As the autogyro does not use pitch attitude to accelerate and decelerate, the requirements for a maximum nose-up attitude of at least 30 degrees shortly before returning to hover and a maximum nose-down attitude of at least 12 degrees below the hover attitude during acceleration as prescribed by ADS-33 were also removed for the autogyro case.

As with the Slalom, the manoeuvre was assessed using the Cooper-Harper scale and the Bedford workload rating scale alongside ADS-33. It was found that "subjective pilot assessment of handling qualities and workload show that the G-UNIV autogiro meets Level 1 and Level 2 handling qualities, and a low level of workload for the proposed acceleration–deceleration manoeuvre" – however, the vehicle failed to meet the lateral deviation requirements.

The results of these flight tests were compiled to form the beginnings of a database for use in developing handling qualities criteria for the autogyro. The first parameters investigated were roll attitude quickness and pilot attack.

Roll attitude quickness was calculated from the Slalom manoeuvre. Roll attitude quickness is defined as the ratio of peak roll rate to change in roll attitude:

$$Roll\ attitude\ quickness\ (sec^{-1}) = \frac{p_{pk}}{\Delta\varphi}$$

As every calculation point also shares a corresponding subjective pilot HQR (from 1 to 10), handling qualities levels could be assigned, Level 1 corresponding to HQRs 1 – 3, Level 2 corresponding HQRs 4 – 6 and Level 3 corresponding HQRs 7 - 10. It was found that the distinction between levels was not as clear as could be desirable, and it was proposed that this was due to the pilot using considerable amounts of sideslip to make turns during the Slalom manoeuvre. The sample data set was also relatively small.

"Pilot attack" is defined by Padfield [59] as:

$$Pilot\ attack = \frac{\dot{\eta}_{pk}}{\Delta\eta}$$

where $\dot{\eta}_{pk}$ is "the peak value in the rate of change of lateral stick displacement and $\Delta\eta$ is the corresponding change in net stick displacement". As for roll quickness, each data point for pilot attack corresponds to a HQR rating, and handling qualities levels were assigned in the same way.

It was concluded that the methods outlined by Bagiev and Thomson [7] were appropriate for creation of handling qualities requirements, and provide "good grounds" for the design of MTEs for light autogyros. The determination of comprehensive handling qualities requirements could not be completed due to insufficient quantity of data and the use of only one pilot. Due to the requirements of type currency and experience, the pilot used was also not a test pilot, but a highly experienced autogyro pilot. This may have had an impact on the validity of the results obtained, as the pilot had not received any training in handling qualities assessment or the use of the Cooper-Harper rating scale prior to the trial. Additionally this pilot's extensive experience of the autogyro introduces the potential for deficiencies in the aircraft to be unconsciously neglected.

In spite of these issues it should be noted that, given the relative paucity of the research in this area during the preceding 50 years, Ref. 7 does provide an appropriate basis for further investigation of autogyro handling qualities.

2.6 PREVIOUS WORK AT THE UNIVERSITY OF LIVERPOOL

Alongside the work carried out by Glasgow University, work has been carried out at The University of Liverpool on behalf of BAE Systems (BAES) [6], through the development and validation of a simulation model of a Rotorsport UK MT-03 autogyro.

The autogyro concept has remained an attractive proposition since its inception in the 1920's – mechanically much simpler than a helicopter due to the lack of a requirement to counter the driven rotor torque, possessing the capability to perform vertical take-offs, short landings and very low speed flight. As a consequence, there has been a revival of interest in the autogyro as an alternative to more conventional types of air vehicle. Jump et al. [6] highlight the lack of engineering data and practical design experience associated with the autogyro (in comparison to more established fixed- and rotary wing aircraft). This is attributed to the lack of serious interest in the autogyro concept over an extended period of time, the reasons for which have been previously discussed.

In order to assist BAES with research into the capabilities of the autogyro configuration Jump et al. [6] created a dynamic simulation model of the MT-03 utilising the rotorcraft/dynamic systems modelling software FLIGHTLAB (described in Ref. 61). The model dynamics were validated using data collected from a fully instrumented MT-03 autogyro, owned by BAES.

Jump et al. [6] also introduced the concept of handling qualities requirements for the autogyro. Similarly to the work of Bagiev and Thomson [10], ADS-33 is suggested as an appropriate specification. Jump et al. [6] proposes to use this specification as an alternative method to judge the performance of both the real vehicle and the simulation model, alongside the more traditional metrics of performance previously discussed.

2.7 CONCLUSIONS AND RESEARCH QUESTIONS

Considerable amounts of research were carried out in the early stages of development of the autogyro, between 1926 and 1939, before research focus was diverted to the helicopter. The recent high rate of fatal accidents observed amongst the autogyro configuration, particularly when compared to other recreational sport aircraft such as microlights or gliders, proved to be a catalyst for resurgence in research interest in the autogyro.

Much of the recent research has been carried out by the University of Glasgow (with funding from the UK CAA) and the University of Liverpool. This lead to the generation of CAA Report 2009 [4], which presented 4 finding and recommendations, intended to improve autogyro airworthiness and safety. Whilst this report serves as an illustration of the growing body of knowledge surrounding, and the resurgence of research interest in,

the autogyro configuration, it also concludes that "*there remains little indication that rigorous scientific or engineering investigation of airworthiness has occurred*" [4] due to the limited number of configurations used in the research.

Work at both the University of Glasgow and the University of Liverpool also focussed on using modelling and simulation to explore the flight envelope of the autogyro, as well as positing that the development of autogyro-specific handling qualities requirements may go some way to improving the airworthiness of this type of vehicle.

Having established the outcomes of research to date, several research questions have arisen.

1. How valid are the 4 findings and recommendations made in CAA Paper 2009 [4]? The report itself concludes that little rigorous scientific or engineering investigation has occurred, and therefore there may remain scope to improve and develop the recommendations within Ref. 4. The present nature of the recommendations makes them difficult to apply in practice and unlikely to be implemented by the autogyro community at large; for these recommendations to provide any improvement to autogyro airworthiness or safety, they must be able to be utilised.
2. Can existing rotary wing specifications, such as ADS-33 [2], be used to analyse the handling qualities of the autogyro? The intention of any such specification is to highlight deficiencies in the handling and performance of the aircraft under test; do existing requirements provide a clear illustration of the deficiencies of the autogyro in the same manner they do for the helicopter? Some work has already been carried out in this field, with Bagiev and Thomson analysing selected Mission Task Elements (MTEs), namely the Slalom and Acceleration-Deceleration manoeuvres, and predicted handling qualities metrics, such as quickness and pilot attack in Ref. 7. This Thesis intends to expand upon these parameters, investigating both new MTEs and expanding the range of predicted handling qualities assessed.
3. What are the fundamental differences between the autogyro and the helicopter? Can these differences account for the high accident rate

observed in autogyros? No previous attempts have been made to directly compare geometrically-similar autogyro and helicopter models in order to assess the fundamental differences between the two aircraft types; this Thesis will aim to achieve this through use of modelling and simulation.

4. If existing specifications such as ADS-33 are not applicable to the autogyro, new metrics to assess the handling qualities of the autogyro must be developed. What are the requirements of these metrics and what methodology should be used to develop them? Some work has already been undertaken in this regard; in Ref. 7 Bagiev and Thomson propose a methodology for ascertaining handling qualities Levels for both quickness and pilot attack, as well as suggesting proposed Level boundaries for these parameters. These proposed boundaries will be assessed using data gathered during simulated flight trials.

These are the themes which are pursued in the subsequent Chapters of this Thesis.

Chapter 3

EXPERIMENTAL SETUP, MODEL DEVELOPMENT AND MODEL VERIFICATION

In order to address the research questions posited in Chapter 2, a simulation model of an autogyro was created using the FLIGHTLAB vehicle modelling and analysis tool. The model is based on the 'G-UNIV ', the autogyro operated by Glasgow University, which was used to undertake the flight tests described in Ref. 7. This aircraft was selected for a number of reasons:

1. There is a full set of the required inertial and geometric data available to create the model in FLIGHTLAB.
2. There is a limited amount of flight test data available for validation of the model dynamic response.
3. This aircraft configuration has been previously used in flight trials and for handling qualities assessments, providing baseline handling qualities ratings for comparison and further validation of the simulation model.

This model was then analysed during both real-time flight trials in the University of Liverpool's HELIFLIGHT simulator, and using offline simulation methods.

A model of a helicopter of similar weight and geometry to the G-UNIV autogyro was also created, in order to compare the fundamental differences between the two vehicle types.

The process by which these models were created, the software and the facilities used for the simulated flight trials are described in this Chapter.

3.1 SIMULATION FACILITIES

3.1.1 The HELIFLIGHT Simulator

The Flight Science & Technology Research Group (FST) operates two six degrees-of-freedom flight simulators [62], HELIFLIGHT and HELIFLIGHT-R. The HELIFLIGHT simulator, shown in Figure 5, was used for the purpose of flight trials described within this Thesis.

Figure 5: The HELIFLIGHT simulator

HELIFLIGHT has a single-seat cockpit with six visual and two audio channels [63]. Three of these visual channels are used to create a 140° lateral field of view, as shown in Figure 6, with the remaining three being used to provide cockpit instrumentation and a left and right chin window. The cockpit is equipped with a central control column (with several programmable buttons and switches), interlinked rudder pedals, a single throttle lever, a right-hand mounted sidestick and a left-hand mounted collective lever. HELIFLIGHT features a hexapod (6-legged) motion base which provides motion cues in 6 degrees of freedom.

Figure 6: Inside the HELIFLIGHT simulator

3.1.2 FLIGHTLAB Software

The modelling software used by the HELIFLIGHT simulator is FLIGHTLAB. FLIGHTLAB is a vehicle modelling and analysis tool developed by ART (Advanced Rotorcraft Technology Inc.) which enables users to produced vehicle models using a library of modelling components which can then be interconnected to form a custom architecture. Aircraft-specific data can then be assigned to these components to produce high-fidelity simulation models [61].

FLIGHTLAB also provides functionality for real-time simulation through the use of the PILOTSTATION interface, allowing the physical elements of the HELIFLIGHT simulator to connect with the FLIGHTLAB model. PILOTSTATION drives the motion base, handles the signals from the cockpit controls and defines the simulated physical environment in which the real-time tests are conducted, providing simulated solid surfaces with which the aircraft models can interact). FLIGHTLAB also enables data logging; the user is able to define which variables to record (accelerations, positions, control inputs and inputs to switches for example), as well as defining the start and end points of the recording. Data was captured in this manner throughout the flight trials described in this Thesis in order to assess if the performance requirements laid out in the MTEs used had been met and to illustrate levels of pilot compensation through analysis of control input histories.

FLIGHTLAB also allows the user to control the degrees of freedom in both offline and real-time simulation modes, allowing selected states to be “locked out” in order to remove any dynamic behaviour from the simulation. This feature was used when estimating the predicted handling qualities of the autogyro model, allowing the yaw dynamics to be disabled when estimating roll-due-to-pitch and pitch-due-to-roll cross couplings so that the requirement that yaw attitude be held constant could be met.

The level of customisation available in FLIGHTLAB makes it ideal for developing a high-fidelity autogyro model. The process of doing so will be described in detail later in this Chapter.

3.1.3 Visual Environment

Both the outside world visuals and the instrument panel used in HELIFLIGHT are generated by BAE Systems’ Landscape software [64]. Landscape allows for the

generation and display of custom visual environments. This capability was utilised in the process of validating the model. The Slalom and Acceleration-Deceleration manoeuvre courses described in Ref. 7 were recreated as part of the validation process, and the interface between Landscape and FLIGHTLAB allows the dimensions of the course to be altered during real-time simulation.

3.2 G-UNIV OVERVIEW

The Glasgow University autogyro, a two-seat autogyro manufactured by Montgomerie-Parsons and registered G-UNIV, is shown in Figure 7. The passenger seat has been removed in order to provide space for flight test instrumentation. It has a teetering rotor with two blades (7.62 m in diameter), attached to the hub without flap or lag hinges. The rotor head mechanism is actuated by a centre stick through connecting rods, giving control in pitch and roll. An 85hp Rotax 618 engine connected to a 3-bladed, 62 inch diameter fixed-pitch propeller powers the aircraft. The aircraft has an integrated horizontal stabiliser with two small winglets and a conventional rudder. The rudder is actuated via foot pedals connected to control cables. The aircraft is equipped with a tricycle undercarriage arrangement and has a mass of approximately 355kg in this test configuration (including pilot).

Figure 7: The Montgomerie-Parsons autogyro, registered G-UNIV [66]

3.3 FLIGHTLAB MODEL CREATION

3.3.1 Baseline FLIGHTLAB Model

FLIGHTLAB provides templates for fixed- and rotary-wing models, making the creation and assembly of such models much simpler by removing the need to manually connect

all components [61]. For example, it is possible to use a fixed-wing or helicopter model populated generic data as a baseline for further model development. However, the commercially available version of FLIGHTLAB does not have a standard autogyro template. The starting point for the creation of this model was therefore the model created in Ref. 6 (due to commercial restrictions, this model could not be used as part of this project in its original form). The model described in Ref. 6 has the requisite architecture and was used as a template to create a new model of the G-UNIV aircraft. This Section describes the modelling of each major component of the autogyro (Figure 8), and explains the source of the data used in creation of this model.

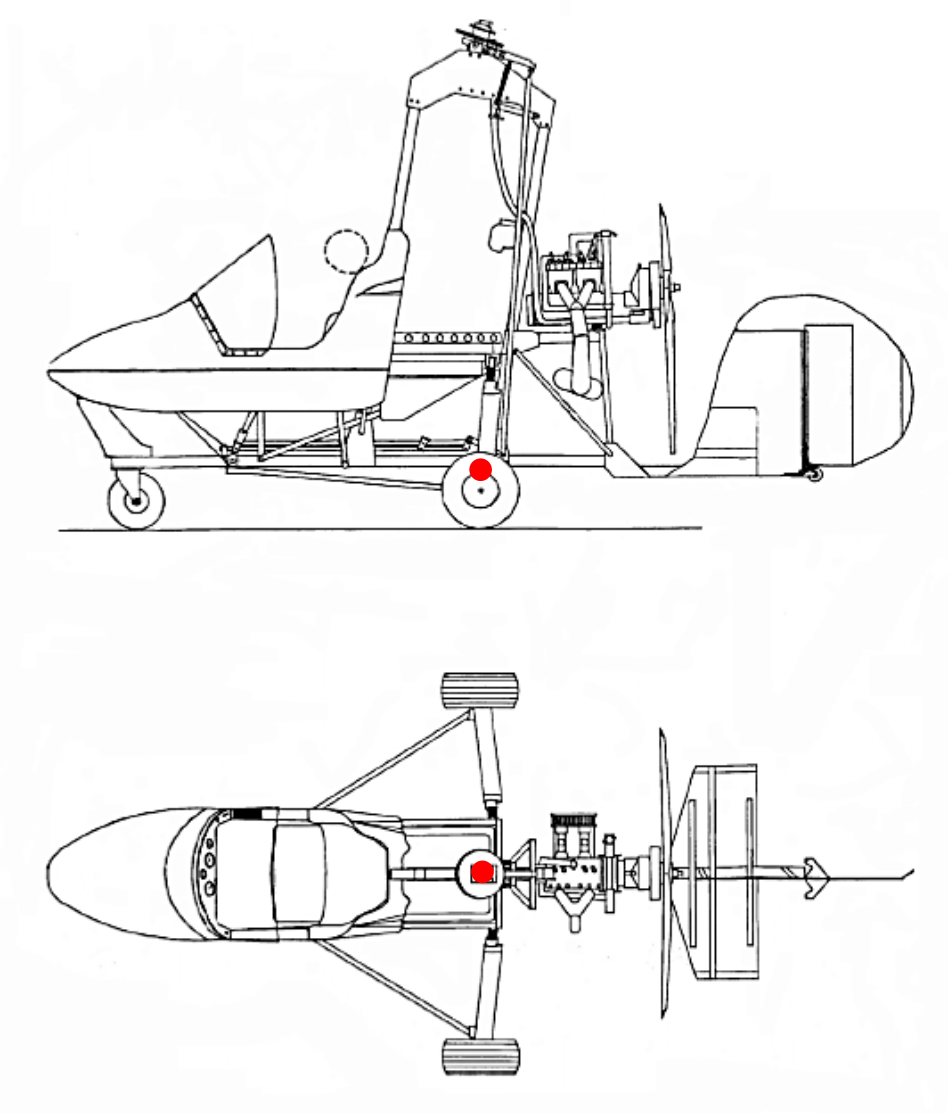

Figure 8: The Montgomerie-Parsons autogyro, with airframe reference point [Appendix A]

Each component requires a combination of geometric (size, shape, dimension), inertial (mass and mass distribution) and aerodynamic (lift, drag and pitching moment coefficients) data. The model also requires a reference point to be specified, and the location of all the remaining components are positioned relative to this point. In this case, the airframe reference point was taken as the intersection of the projection of the mast centreline and the keel centreline with the x-body axis aligned with the keel, consistent with the reference point defined in Appendix A. This is shown as a red dot in Figure 8. The major components of the model of G-UNIV are shown in Figure 9.

When all of the individual components of a model are connected, the resulting model takes the form of a hierarchy. The component connected 'below' a given component is referred to as the 'child'. The component to which the 'child' is connected is referred to as the 'parent'. The calculated motion for a given time step is passed from parent to child and the resulting forces are passed from child to parent. To solve for the selected model states at the given time step a generalised force imbalance between the states and the differential equations which describe the system is generated from these exchanges. This imbalance is driven to zero by an iterative Newton-Raphson method. The simulation then proceeds to the next time step [65].

FLIGHTLAB also allows for the easy removal or addition of components without having to reconfigure this hierarchy of components. This feature was found to be particularly useful when investigating the effect of removing the horizontal stabiliser on stability.

Each of the major components required populating with aerodynamic properties which interact with the international standard atmosphere model provided within FLIGHTLAB. For each simulation time step, the local forces and moments are calculated based on the current control positions for each of the model components. If the line of action of the force is not coincident with the vehicle centre of gravity, additional moments arising from the offset are calculated about the c.g. The main rotor and propeller are assigned mass distributions and their inertial properties are calculated by FLIGHTLAB. The remaining mass and inertial properties of the other components of the vehicle are accounted for within the total vehicle mass and inertia properties defined by the user in the fuselage modelling options.

With known external forces acting on a body of known mass distributions and inertia, the dynamic response of the vehicle can be calculated and propagated to the next time step in the simulation.

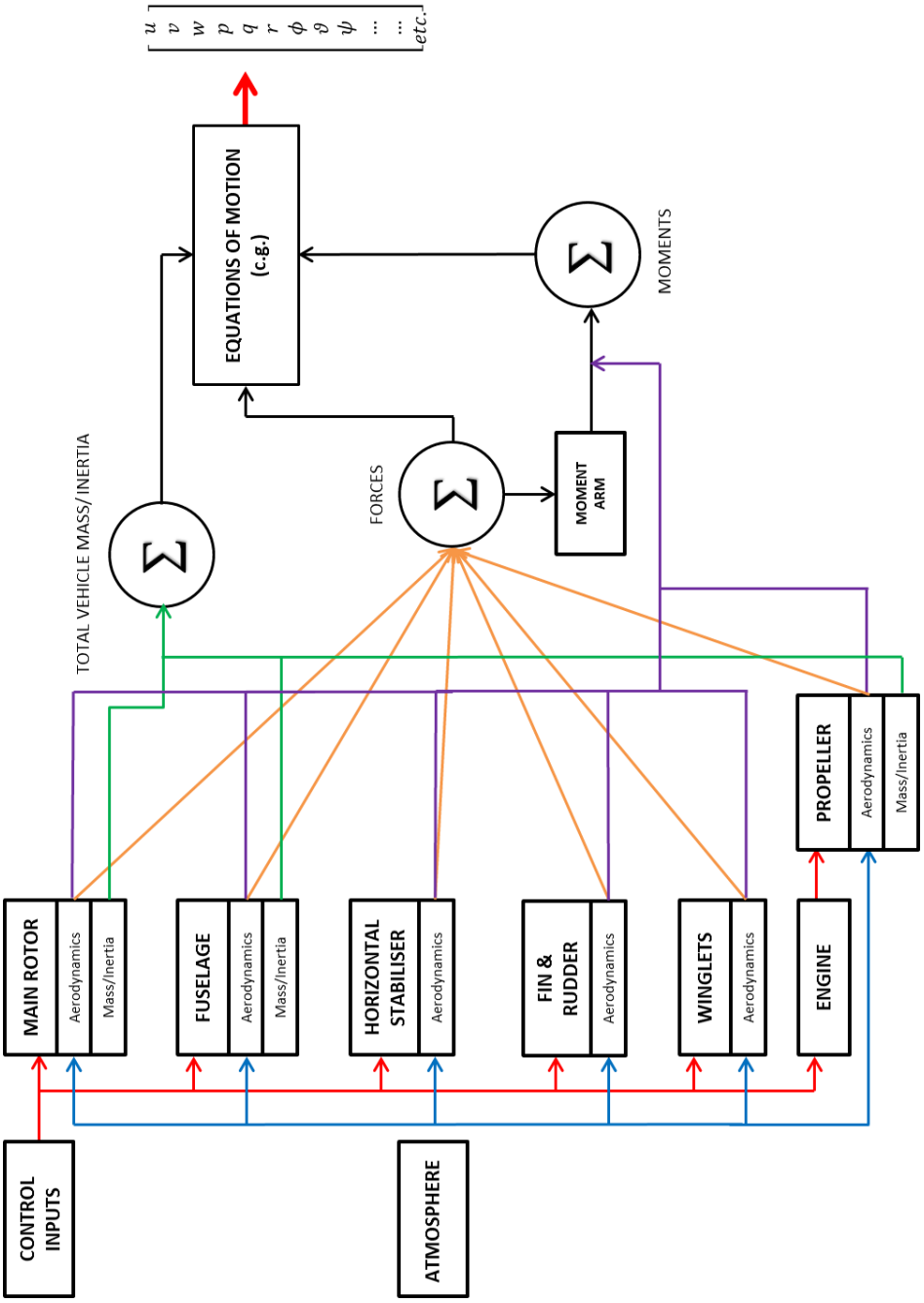

Figure 9: G-UNIV FLIGHTLAB model schematic

3.3.2 Flight Physics Model

The co-ordinate system used by the model is defined as follows:

a) For the definition of component locations,

X: positive downstream of the reference point (referred to as the fuselage station or station-line position in FLIGHTLAB);
Y: positive to port/left (referred to as the buttline station);
Z: positive upwards (referred to as the waterline station);

b) For outputs from the model,

X: positive forwards (or upstream);
Y: positive to starboard/right;
Z: positive downwards;

Positive angular quantities are taken as the clockwise direction when looking along the positive direction of a given axis.

c) FLIGHTLAB wind axes are defined as shown in Figure 10.

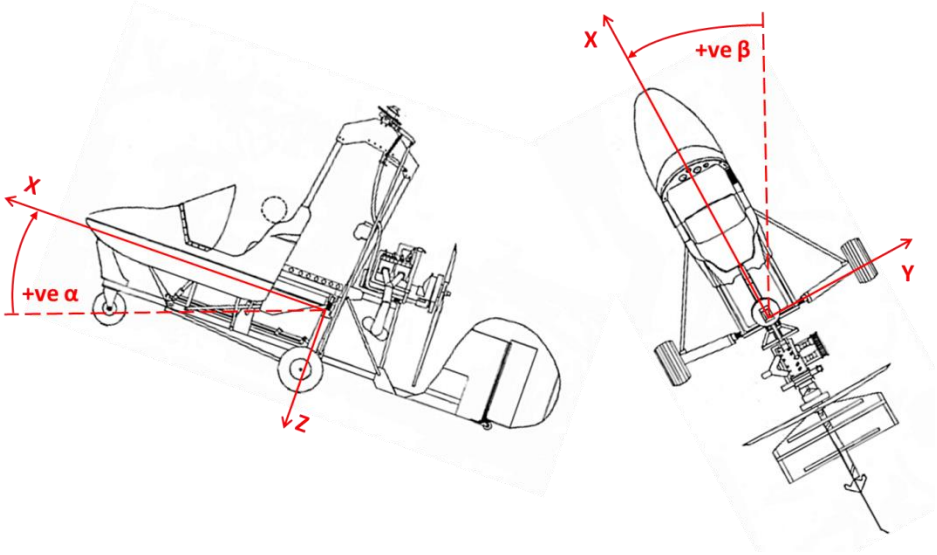

Figure 10: FLIGHTLAB body and wind axes definitions [Appendix A]

d) Control interceptor co-ordinates:

Centre stick back	→ positive pitch angle, pitch rate and rotorhead pitch angle;
Centre stick left	→ positive roll angle, roll rate and rotorhead roll angle;
Right pedal	→ positive yaw angle, yaw rate and rudder angle;
Open throttle	→ positive throttle position.

3.3.3 Model Composition and Tuning

The process of creating a FLIGHTLAB model to represent the dynamic response of an aircraft is complex and involves many compromises; it is not possible to simply populate the model template and generate a perfectly matching dynamic response to that of the real aircraft.

As such, the model described in this Chapter has undergone some tuning in order to optimise both the magnitude and trends within the dynamic response, the trimmed flight control positions and the aerodynamic derivatives. The tuning process followed that described in [6]:

- Initial tuning in order to bring the trimmed flight control positions of the model closer to those obtained in flight test. Trimmed flight control positions were assessed across the flight envelope (35 – 70mph).
- Dynamic response tuning using an example of a dynamic manoeuvre in each axis

Additionally, due to the small amount of flight test data available for the G-UNIV aircraft, consideration was also given to the magnitude and trend of the aerodynamic derivatives across the flight envelope, important in producing an accurate representation of the aircraft dynamics.

Due to financial constraints, it was not possible to characterise the aerodynamics of the G-UNIV aircraft itself, thus the model had to be populated with data which, whilst not totally unrepresentative, is not ideal. This meant a significant amount of tuning had to be undertaken in order to create a model which is dynamically representative of G-UNIV. Both the nature of the data used to populate the model and the extent of the tuning applied are discussed within each component's respective subsection, along with

justification of the tuning method chosen and demonstration of the effect of the tuning applied. For brevity, only the final 'tuned' configuration is shown against the original data for most of the model components; there were often simply too many different configurations tested to present them all here in a meaningful way.

3.3.4 G-UNIV Model Description

3.3.4.1 Main Rotor (Rotor 1)

The key difference between an autogyro and a helicopter is the mechanism which drives the rotor blades. The helicopter rotor is driven directly by an engine (the so-called 'power state'), whereas the autogyro rotor is unpowered and turns due to the action of the air passing over the rotor blades (the 'windmill state').

Modelling the main rotor in FLIGHTLAB requires the engine and related drive shaft to be permanently disconnected from the main rotor in order that the model is able to simulate autorotation. This was done in such a way that the normal solution process was not disrupted.

3.3.4.1.1 Geometric Data

The main rotor is modelled as a teetering rotor (also referred to as a semi-articulated, semi-rigid or see-saw rotor) in which the rotor blades are rigidly attached to the hub without flap or lag hinges. The blades themselves are modelled using a blade element model; the blades are broken down into smaller segments and the loads acting on each segment are evaluated. These loads are then integrated over the entire blade, and for each blade, for each revolution, determining the total force acting on the rotor. The main features of the rotor geometry are given in Table 4.

Description	Value	Reference	Comment
Rotor direction	Counter-clockwise	Appendix A	Viewed from above
Number of blades	2	Appendix A	
Rotor location	[0.038 0.0 1.968] m	Appendix A	
Rotor radius	3.81 m	Appendix A	
Rotor chord	0.197 m	Appendix A	
Rotor nominal speed	340 rpm	Appendix A	
Rotor underslung	0 m		Teeter bolt and rotor blades are coincident
Underslung mass	0 kg		

Table 4: Main rotor geometric data

3.3.4.1.2 Inertial Properties

The inertial properties of the main rotor are given in Table 5.

Description	Value	Reference	Comment
Rotor blade mass	8.6 kg	[66]	
Chord-wise c.g. offset	0.064 m	[66]	
Underslung mass	0 kg		Teeter bolt and rotor blades are coincident

Table 5: Main rotor inertial properties

The main rotor blade mass distribution is shown in Figure 11. The increase in the mass at the root and tip portions of the blade can be attributed to internal structural reinforcement.

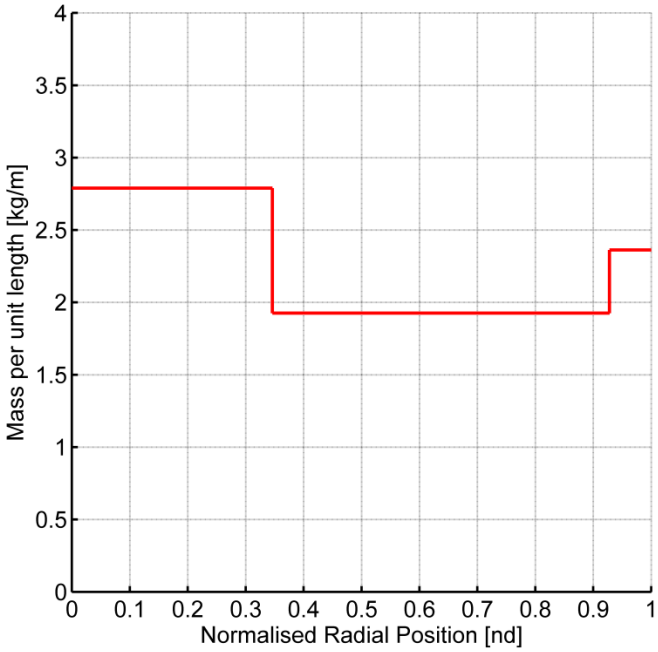

Figure 11: Main rotor normalised radial mass distribution

Taking the rotor radius to be 3.81m (Table 4), the total mass of the individual rotor blade is calculated as follows:

$$(2.79 \times 0.346 \times 3.81\ ) + (1.926 \times (0.9281 - 0.346) \times 3.81) + (2.362 \times (1 - 0.9281) \times 3.84) = \boldsymbol{8.6kg}$$

Appendix A gives the rotor blade mass as 17.255kg, while the mass distribution presented in Figure 4.1 of Ref. 66 gives a total mass of 11.25kg when calculated from the mass distribution. The rotor blade mass is also given as 11.25kg in Ref. 67. In order to account for these discrepancies, and to obtain a suitable total mass for the G-UNIV model, a method of trial and error was implemented. Initially, the distribution described in Figure 4.1 of Ref. 66 was compared to a distribution scaled to give a total blade mass of 17.255kg (as reported in Appendix A).

The total mass of the blade strongly affects the value of the pitch damping aerodynamic derivative, M_q, often referred to as pitch stiffness or pitching moment due to pitch rate. Both the 17.255kg and 11.25kg total mass rotor blade models produced M_q values of significantly greater magnitude than the values derived from flight data. This variation is

shown in Figure 12. M_q becomes increasingly negative (restorative) as the total mass of the main rotor increases. This is due to the fact that as blade mass increases so does blade inertia, which reduces the gyroscopic precession moment generated by the flapping hinge. This moment is generated about the roll axis, but due to the nature of the teetering rotor used there is a 90° phase lag, meaning the effect of this reduction is seen in the pitch axis. The flapping equation [59] of a centrally hinged blade (equivalent to that of a teetering rotor) illustrates this effect:

$$\ddot{\beta} + \beta = \gamma M_{\beta}$$

Where γ represents the Lock number, $\gamma = \frac{\rho C_{L\alpha} c R^4}{I_{\beta}}$, I_β represents the blade flapping inertia and M_β is the total flapping moment about the hinge.

As a result, the total mass of the main rotor was reduced to 8.6kg (approximately equal to half of 17.255kg), using the same distribution pattern as shown in Figure 11.

Setting the total mass of the rotor blade to 8.6kg also makes the rotor blade mass comparable to the rotor blades of other autogyros; for example, the MT 03 has a rotor blade mass of 10.75kg, and a radius of 4.2m. G-UNIV has a rotor radius of 3.81m, approximately 90% of that of the MT 03, and mass of 8.6 kg corresponds to 80% of the main rotor mass.

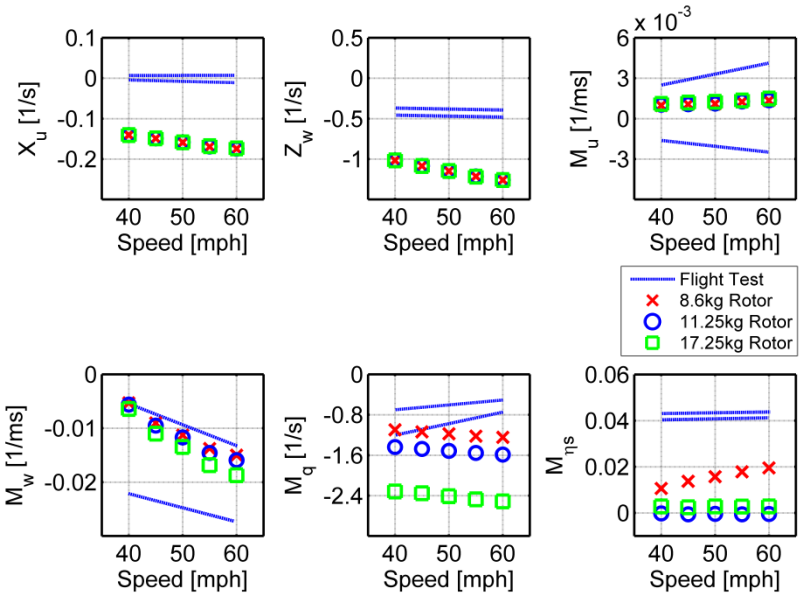

Figure 12: Variation in aerodynamic derivatives with variation in main rotor mass

3.3.4.1.3 Aerodynamic Properties

Information relating to the aerofoil section used for the main rotor of G-UNIV was unavailable. Therefore, the aerofoil used in the modelling of the MT 03 [6], the NACA 8H12, was selected for use in the G-UNIV model; this approximation was deemed appropriate based on the similarity between the two aircraft. FLIGHTLAB requires two-dimensional C_L, C_M and C_D values for angle of attack (α) in the range ±180°. The data for the NACA 8H12 aerofoil was taken from Ref. 68. However, Ref. 68 only provides coefficient data for $-8° \leq \alpha \leq 16°$. Outside this range, the FLIGHTLAB supplied data for the NACA 0012 is used in order to provide an approximation of data across the required ±180° range. This is shown in Figure 13. Figure 14 shows the data over the range, ±30°. Figure 13 and Figure 14 also show the data smoothing undertaken in order to smoothly blend the NACA 0012 data with the NACA 8H12.

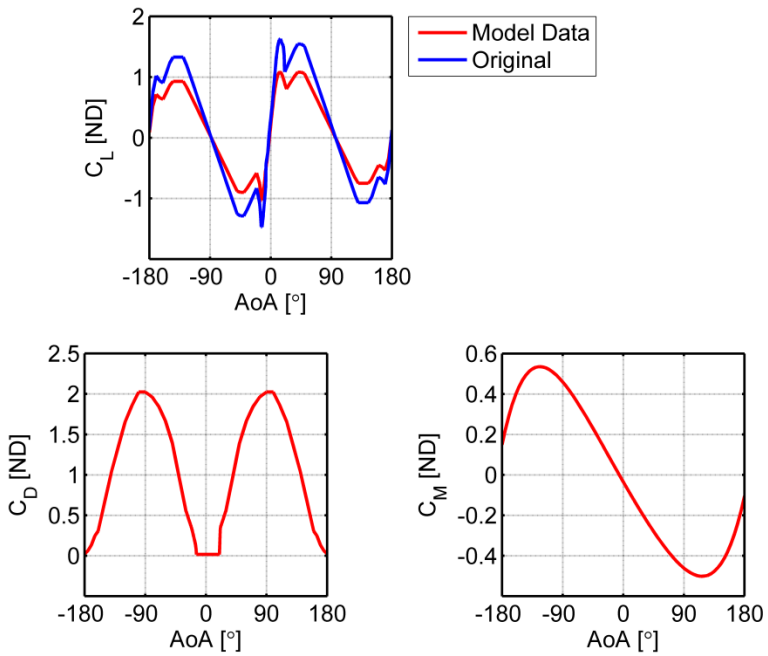

Figure 13: Main rotor two dimensional aerodynamic data for ±180° range

Some tuning of the data used for the main rotor was undertaken. In the initial version of the model, the main rotor speed was consistently too high. This can be accounted for by the fact that the aerodynamic properties (mainly C_L in this case) of the actual rotor blade are unknown, and therefore likely to be different to those of the NACA 8H12 which has been used in this model. The original NACA report which describes the properties of the NACA 8H12 aerofoil [68] comments upon the blade's sensitivity to surface roughness, and it is likely that the rotor blades used on the aircraft under consideration during the flight test have increased surface roughness compared to that of the rotor blade used in the laboratory environment to ascertain the lift, drag and moment characteristics of the aerofoil section. This may be due to environmental contamination or damage to the blades. This will lead to the rotor blades of the real aircraft producing less lift compared to those modelled in the original version of the FLIGHTLAB model, which manifests itself as the increased rotor speed seen in the original model. To correct this, the values of the lift coefficient were decreased by 30% in order to provide better agreement with the flight test data; this is shown in Figure 14.

The effect of this tuning process can be seen in Figure 15. Although the rotor lift coefficient was changed significantly using method of tuning, it was deemed appropriate due to the level of uncertainty in the source data for the main rotor aerofoil geometry.

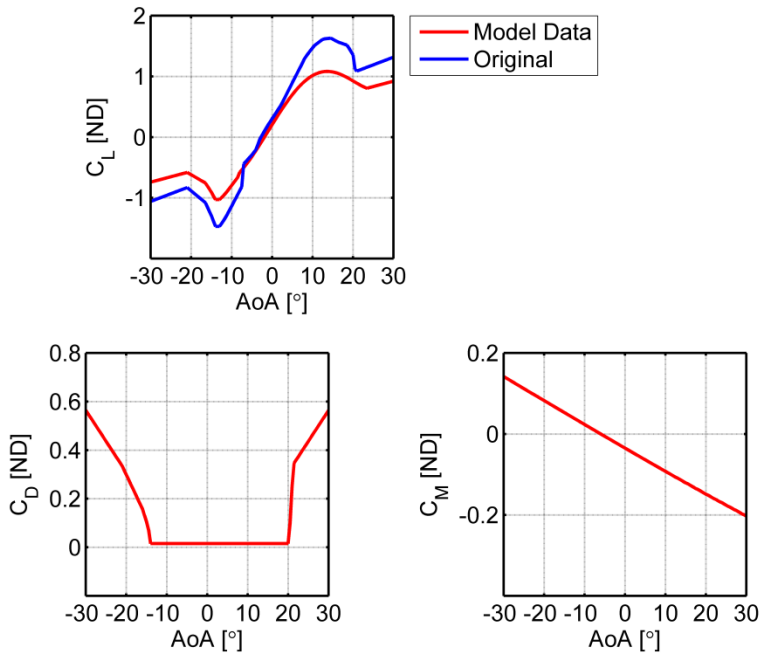

Figure 14: Main rotor two dimensional aerodynamic data for working range (±30°)

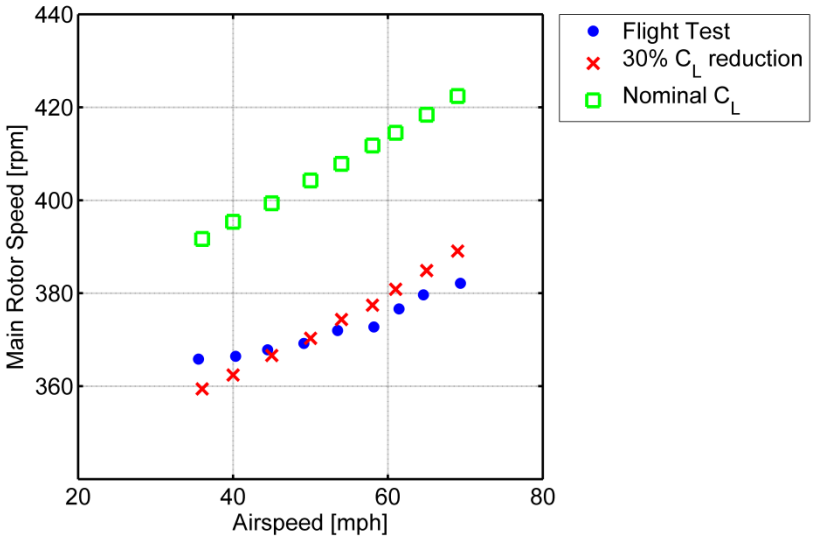

Figure 15: Effect of tuning main rotor C_L values on main rotor trim speed

3.3.4.1.4 Aerodynamic Inflow

FLIGHTLAB offers a range of rotor inflow modelling options, ranging from uniform to a fully defined, time-accurate vortex wake model. For this model, the flow around the main rotor is modified from its two-dimensional, steady-flow ideal using the Peters-He six state inflow dynamic wake model based on the model described in Ref. 7.

3.3.4.1.5 Aerodynamic Interference

FLIGHTLAB also has the capability to model the interference effect of the aerodynamic wake of one component impinging upon another component. In this model, two sets of 6-state interference were included; the effect of interference from the main rotor wake on both the fuselage and the horizontal stabiliser. Attempts were made to include the interference from the main rotor on the propeller, but this resulted in the trim process becoming computationally inefficient and significantly extending the solution time.

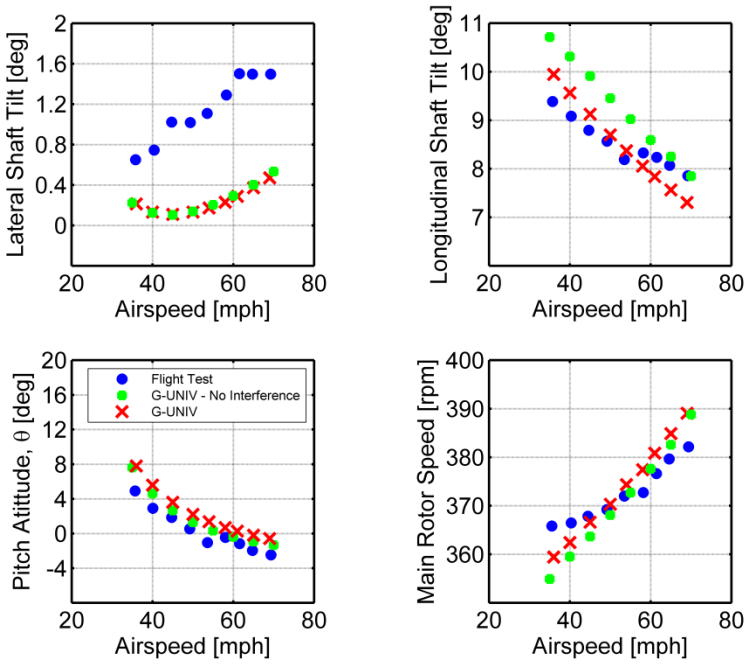

Figure 16: Effect of selection of main rotor interference on trim attitudes and rotor RPM

Alongside increased computational efficiency, altering the main rotor interference settings allows for further subtle tuning of the trimmed flight control positions as demonstrated in Figure 16. Turning on the interference modelling primarily effects the

longitudinal shaft tilt; this is due to the fact that a portion of the wake from the main rotor is now interfering with the fuselage, consequently reducing the incidence of the fuselage, meaning less drag is produced and the main rotor is not required to flap back to such a great angle.

3.3.4.2 Propeller (Rotor 2)

The FLIGHTLAB template provides provision for two rotors – Rotor 1 is usually the main rotor and Rotor 2 is the tail rotor. It is possible to orient and position the rotors in any direction and location. This enables the user to model non-conventional rotor configurations, such as a co-axial rotor or tilt rotor configuration, or as is the case for the autogyro, to model a propeller. In this model the propeller is modelled as an articulated rotor with very stiff and well damped hinges. In reality, the propeller is not articulated. The data requirements for the propeller are identical to those for the main rotor.

The propeller is an IVOPROP Ultralight model propeller; the input data for the FLIGHTLAB model was therefore taken from IVOPROP's website [69].

3.3.4.2.1 Geometric Data

The geometric properties of the propeller blades were established both through data provided in Appendix A and through direct measurement of the propeller blade in-situ. The recorded geometric properties are show in Table 6.

To establish the propeller twist distribution, photographs of the propeller were taken at a number of evenly distributed radial positions; this process is shown in Figure 17. The blade chord was also measured at these stations. The chord and twist distributions are presented in Table 7.

Description	Value	Reference	Comment
Rotor direction	Counter-clockwise		Viewed from above
Number of blades	3	Appendix A	
Rotor location	[0.91 0.0 0.795] m	Appendix A	
Rotor radius	0.787 m	Appendix A	
Rotor nominal speed	1800 rpm	Appendix A	

Table 6: Propeller blade inertial properties

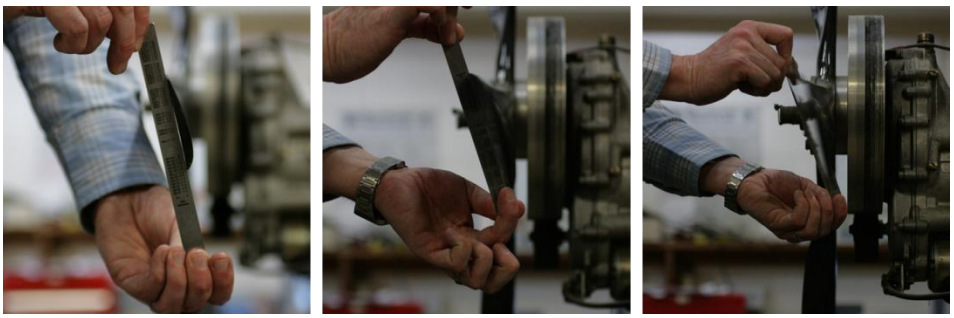

Figure 17: Establishing the radial twist distribution of the propeller

Normalised Radial Station	Blade chord (ft)	Blade twist (°)
0.0000	0.2789	-3.5
0.2345	0.2789	19.5
0.3622	0.3150	25.0
0.4898	0.3051	22.5
0.6173	0.2887	17.5
0.7449	0.2690	14.0
0.8724	0.2461	13.5
1.000	0.2100	12.0

Table 7: Propeller blade chord and twist radial distribution

3.3.4.2.2 Inertial Properties

The mass distribution of the propeller was unavailable, and as such was approximated using the assumption that the mass is proportional to the volume of the blade segment. The resulting mass distribution is shown in Figure 18. The remaining required inertial properties are listed in Table 8.

Description	Value	Reference	Comment
Rotor blade mass	3.63 kg	[69]	

Table 8: Propeller inertial properties

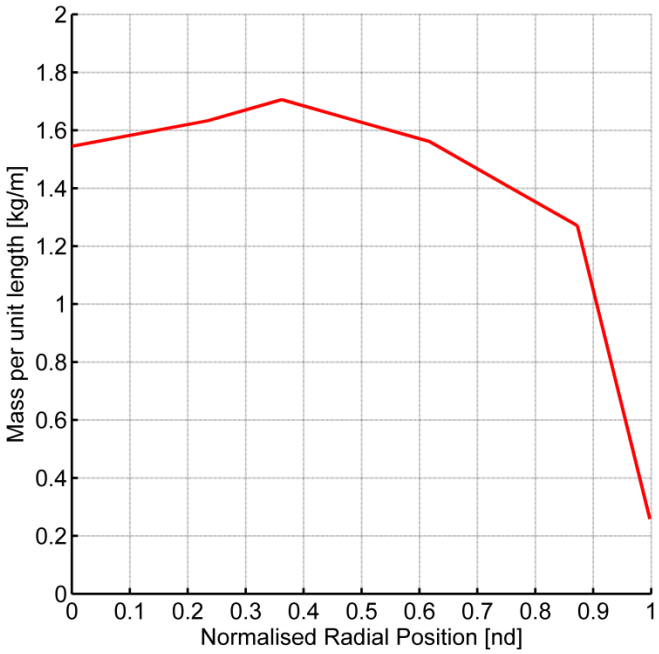

Figure 18: Propeller mass distribution

3.3.4.2.3 Aerodynamic Properties

The propeller blade aerofoil is an IVOPROP custom aerofoil, and as such data about its geometry and aerodynamic properties was unavailable. A Clark-Y hybrid aerofoil was used as a compromise as it displays similar geometric properties. Its geometry can be seen in Figure 19.

The aerodynamic coefficient data for this aerofoil was obtained from Ref. 70. As per the main rotor aerodynamic data set, the data outside the $-14° \leq \alpha \leq 21°$ normal operating range specified in Ref. 70 was populated using FLIGHTLAB-supplied data for the NACA0012 to provide data over the required ±180° range. This is shown in Figure 20 and Figure 21.

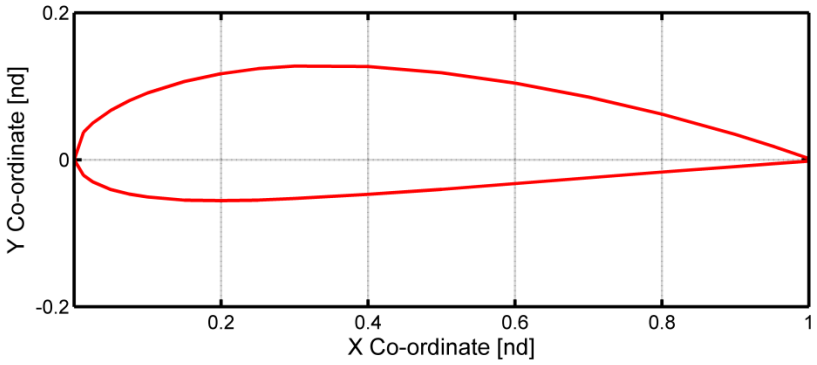

Figure 19: Clark Y hybrid aerofoil used for propeller

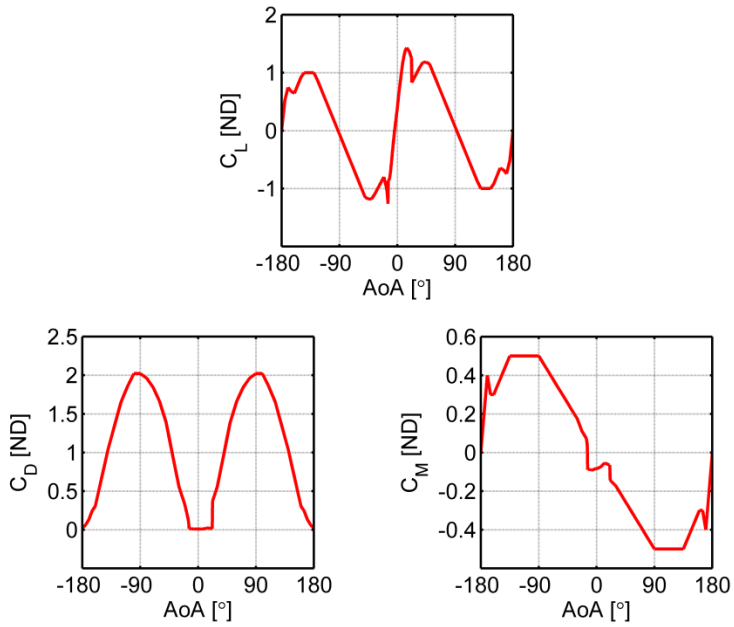

Figure 20: Propeller two dimensional aerodynamic data for ±180° range

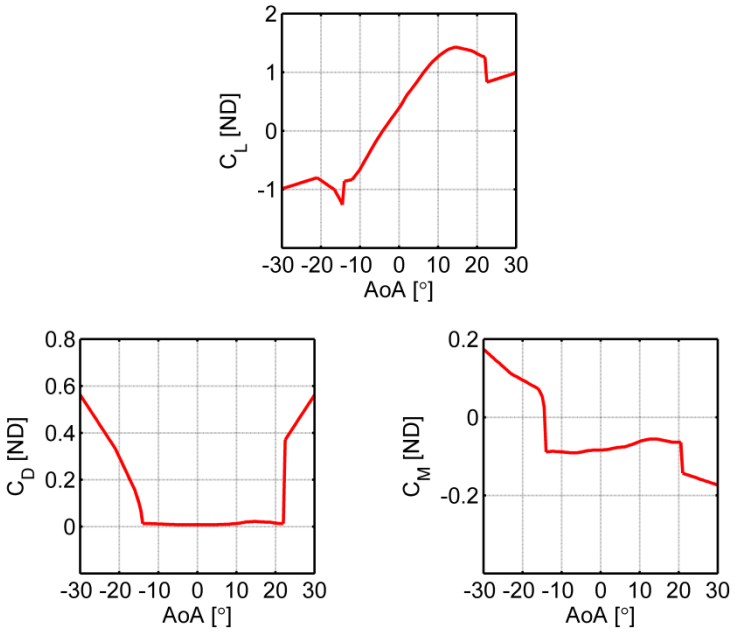

Figure 21: Propeller two dimensional aerodynamic data for ±30° range

3.3.4.2.4 Aerodynamic Inflow

As for the main rotor, FLIGHTLAB offer a number of standard inflow models. The inflow model selected for the propeller was the Peters-He 3-state dynamic wake model (based upon Ref. 71). It was considered that this model offered the best balance between computational complexity (allowing the model to run quickly in real time) and simulation fidelity.

3.3.4.2.5 Aerodynamic Interference

As a result of the configuration of the aircraft, the wake from the propeller would be expected to interfere with the empennage (horizontal tail surface, winglets and vertical fin/rudder). This was found to have a significant effect on the trimmed control positions of the aircraft model across the speed range, as shown in Figure 22. The interference modelling can be seen to have a considerable effect on the longitudinal shaft tilt, effecting both magnitude and trend of the trimmed flight control positions. The addition of interference effects over the horizontal tail surface reduce the amount of lift, and thus restoring force, that the tailplane is able to provide, and in the absence of this restoring force the main rotor is required to further tilt backwards in order to compensate for this. The trend in the longitudinal shaft tilt now becomes analogous to the drag curve of the

aircraft, as the longitudinal shaft tilt changes to counteract the drag generated by the fuselage.

It was therefore decided that, in order to provide a more consistent correlation with the flight test trim data, modelling of interference from the propeller onto the empennage should be disabled. Interference on other components, such as the fuselage and main rotor, was not modelled as the propeller is positioned aft of these components, where the effect of the propeller slipstream is negligible.

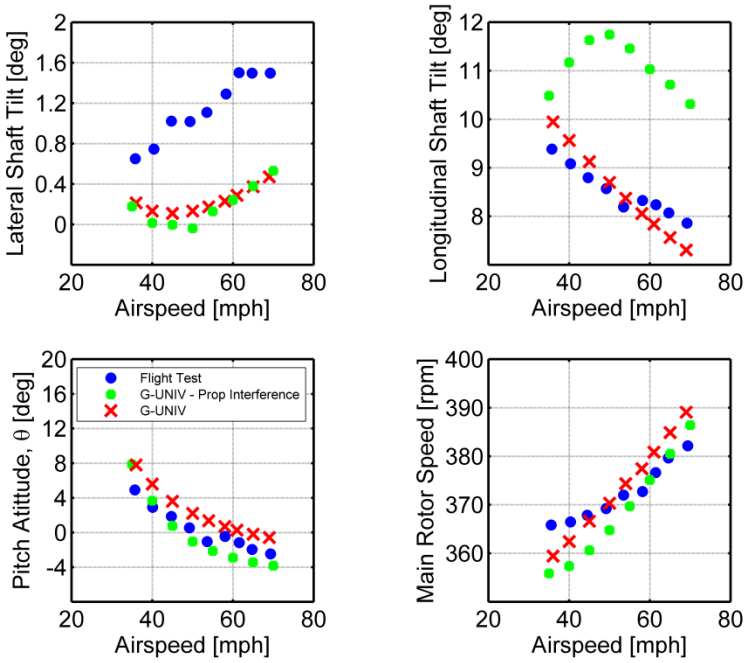

Figure 22: Effect of enabling/disabling propeller interference on trimmed flight control positions

3.3.4.3 Fuselage

FLIGHTLAB provides two options for fuselage structural modelling: rigid body or elastic. The rigid body option models the fuselage as an entity which can move with six degrees-of-freedom as a result of aerodynamic forces, but which cannot deform. Conversely, the elastic option allows for fuselage flexure by modal deformation modelling. Given the amount of data required to populate an elastic fuselage model and the computational expense required for real-time simulation, the rigid body option was selected for the G-UNIV model. This requires populating with basic geometric, inertial (total aircraft mass

and c.g. location) and aerodynamic data; the generation of which is described in this Section.

3.3.4.3.1 Geometric Properties

The fuselage geometric properties are given in Table 9. The c.g. location is taken from Appendix A; however, an offset of approximately 1 - 2° in the longitudinal shaft tilt was observed when the model's trimmed control positions were compared to those in the flight test data. This was remedied by moving the longitudinal position of the centre of gravity forward by 3cm from the nominal position, the effect of which is shown in Figure 23. This was considered acceptable given the inherent uncertainty in the location of the c.g. during the flight tests as a result of fuel state and pilot mass being unknown. Moving the centre of gravity forward considerably reduces the shaft tilt, particularly at low speed, which in turn reduces the rotor incidence, resulting in a slight reduction in the rotor speed.

Description	Value	Reference	Comment
Vehicle c.g. location	[-0.16 -0.04 0.7] m	Appendix A	

Table 9: Fuselage geometric properties

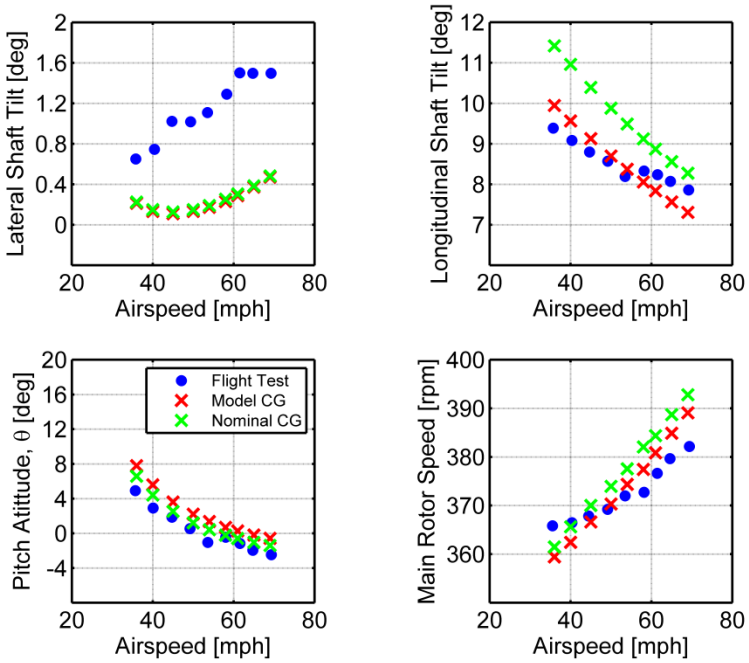

Figure 23: The effect of longitudinal c.g. positioning on trimmed control positions

3.3.4.3.2 Inertial Properties

The inertial properties of the fuselage model are given in Table 10. The values were initially taken from those quoted in Appendix A; however, these were found to be significantly smaller than those of vehicles of similar size and configuration. The mass and inertia quantities quoted were therefore tuned from those quoted in Appendix A in order to improve correlation between the dynamic response of the simulation model and the recorded flight data. The mass and inertia figures quoted account for the gross take-off mass of the vehicle.

Description	Value	Reference	Comment
Total vehicle mass	355.0 kg	Appendix A	
Total roll moment of inertia (I_{XX})	145.92 kg.m^2	Appendix A	
Total pitch moment of inertia (I_{YY})	594.42 kg.m^2	Appendix A	
Total yaw moment of inertia (I_{ZZ})	488.5 kg.m^2	Appendix A	

Table 10: Fuselage inertial properties

3.3.4.3.3 Aerodynamic Properties

No aerodynamic data for the G-UNIV fuselage or cowling was available, and wind tunnel testing or CFD analysis were beyond both the budget and the scope of this project. As an alternative solution, data from a CAA-funded investigation into the aerodynamic characteristics of the gyroplane configuration, as detailed in Ref. 46, were used. This provides body-referenced aerodynamic coefficient data for a VPM-M14 gyroplane, the geometry of which is shown in Figure 24.

The VPM-M14 shares many geometric characteristics with G-UNIV; namely, it is a dual-seat tandem vehicle with a large vertical fin, a large horizontal stabiliser with vertical winglets and a similarly positioned engine. Both aircraft also have a large cowling, which are similar but not identical. The use of the VPM-M14 data was considered an appropriate starting point to modelling the fuselage aerodynamics of G-UNIV.

Ref. 46 provides aerodynamic coefficient data for various configurations of the VPM-M14. The data presented in Ref. 46 was presented for various configurations (for example, power on or off, cowling on or off or tail on or off).

In order to create an approximation of the G-UNIV fuselage the data for the 'cowling on, tail off, power off' configuration was deemed most useful (in this context, 'tail off' refers to the horizontal tail only) as the aerodynamic loading from the tail and propeller are calculated individually by FLIGHTLAB.

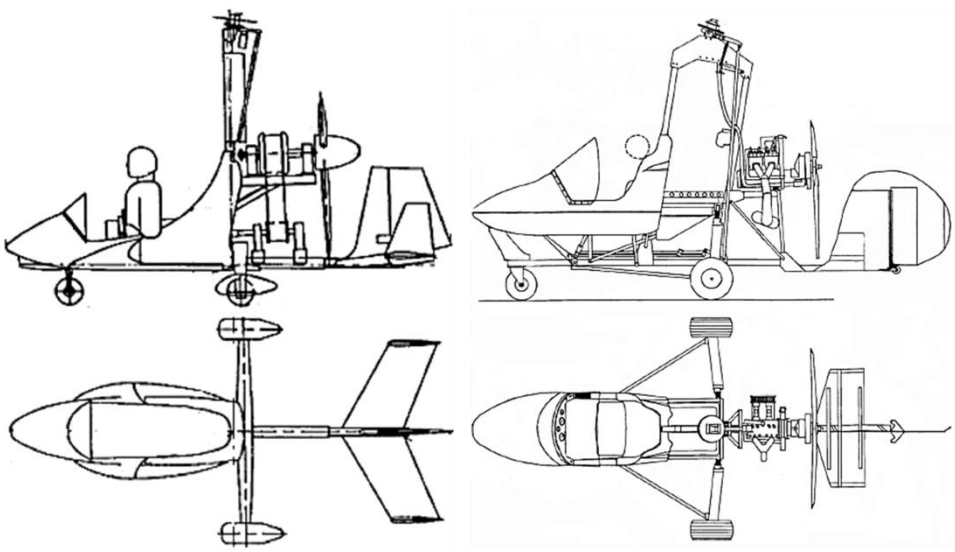

Figure 24: VPM-M14 (left) [46] and G-UNIV (right) [Appendix A] gyroplane configurations (to scale)

In some instances, data for this configuration was not available; to overcome this, various methodologies were used. Where data is presented for the axial force coefficient (C_X) with 'power on', the increment in C_X is 0.0516 compared to the 'power off' case. In order to remove the effect of power on C_X from the 'cowling off, tail off, power on' configuration data, this increment can simply be subtracted to create a reasonable approximation.

In the case of pitching moment coefficient, CM_Y, data were presented in Ref. 46 for the 'cowling on, tail on, power on' and 'cowling off, tail on, and power on' configurations. It

was deemed acceptable to subtract the two data sets in order to approximate a data set for the 'cowling on, tail off, power off' configuration.

It was also necessary to define each of the six force and moment coefficients for variations in both angle of attack, α, and sideslip angle, β. CF_Y and CM_Z were assumed not to vary with α. CF_Z and CM_Y were assumed to remain constant with β, as they are dominated by the effect of the tail and propeller – the effects of which are calculated separately in the FLIGHTLAB model. CF_X and CM_X vary with both α and β.

FLIGHTLAB requires the data to be specified a range of angles of attack (α), and a range of sideslip angles (β), in this case, $-40° < \alpha < 40°$ and $-40° < \beta < 40°$. In some instances, the data presented in Ref. 46 does not extend to fill this range. In this instance, if the data shows a strong gradient correlation (for example, in the case of rolling moment coefficient, CM_X, and CM_Y, the pitching moment coefficient) the data was extrapolated across the remaining, empty part of the range. If the data could not be extrapolated in this way, for example in the case of approximating the variation of axial force coefficient (CF_x) with sideslip angle, the increment in the coefficient between two given angles was calculated and this increment applied to populate the remaining values in the required range. The resulting data produced is shown in Figure 25.

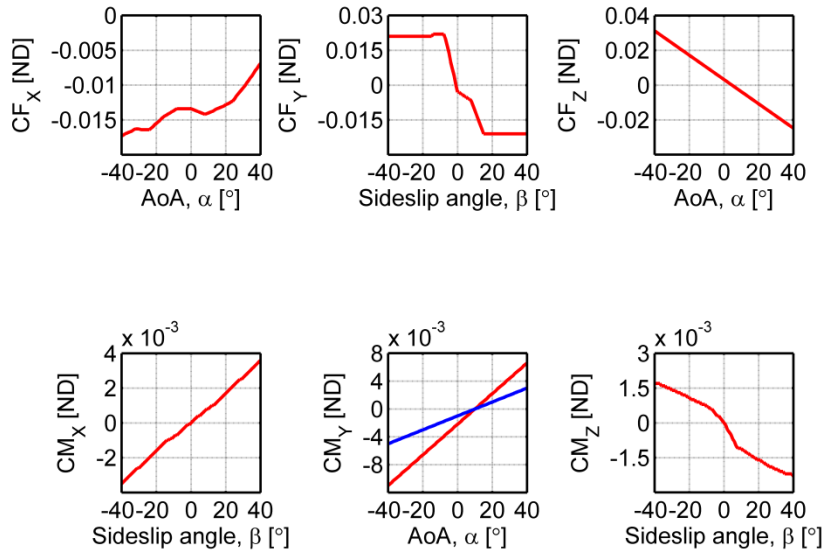

Figure 25: Body referenced fuselage aerodynamic coefficient data – red representing the model data and blue representing the orginal, unmodified aerodynamic data

Following initial integration of these values into the model, some tuning of the data was required in order to improve the correlation between the model response and the flight test data. The data has also been smoothed in order to reduce the amount of time the model takes to trim. The values of CM_Y were increased by a factor of 2.2 in order to influence the results of the trimmed rotor head pitch angle data, and provide a better match to the flight test data. The original values of M_Y are shown in Figure 25 in blue, with the modified data used in the model shown in red. An illustration of the improvement in trimmed rotor head pitch angles is shown in Figure 26.

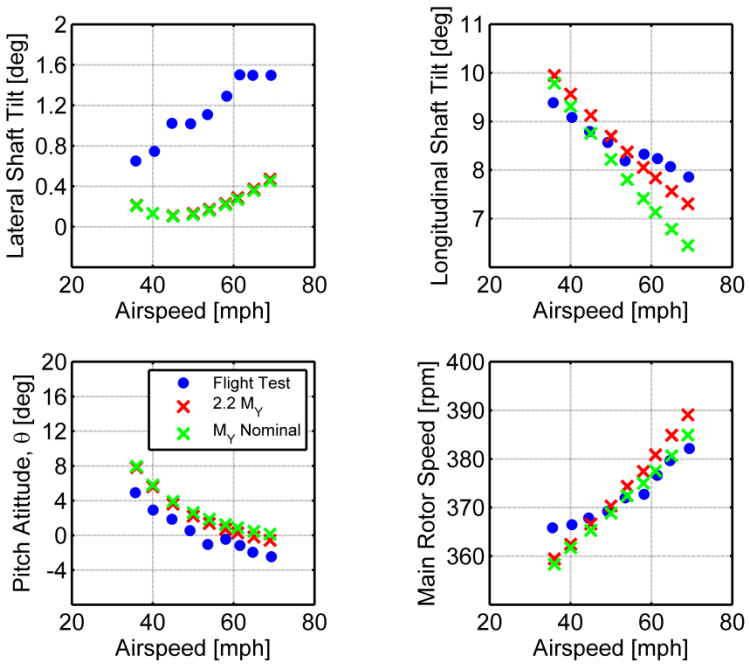

Figure 26: Effect of varying fuselage MY on trimmed control positions and rotor speed

Modifying M_Y also had a positive effect on the dynamic response of the model, as illustrated in Figure 27, with the overall angle of attack of the aircraft agreeing more closely with the flight test data. Modifying the data in this way was found to have no detrimental effect on the pitch rate response.

There are also a number of parameters associated with the fuselage aerodynamic data; these are shown in Table 11. Ref. 46 presents the data about the c.g., the same approach

has been used in creation of this model, and the 'airloads measurement point' is defined as being coincident with the c.g. of the aircraft.

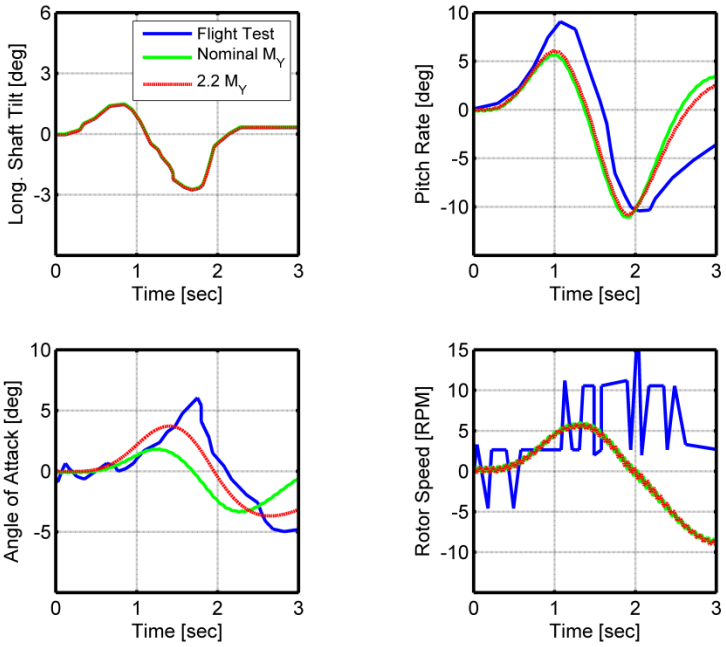

Figure 27: Longitudinal dynamic response showing the effect of modifying fuselage M_Y, plotted as perturbation from trim position

Description	Value	Reference	Comment
Airloads measurement point	[-0.16 -0.04 0.7] m	Appendix A	The point about which all fuselage airloads and moments are transmitted to the model.
Reference area	45.6168 m^2	Calculated	πR^2 is reference area
Reference length	3.81 m	Appendix A	Rotor radius (R) is reference area

Table 11: Fuselage aerodynamic parameters

3.3.4.4 Horizontal Stabiliser

The horizontal stabiliser was modelled using the "wing" element in FLIGHTLAB. The wing component requires only aerodynamic and geometric parameters to be defined as the

inertial properties are accounted for within the total vehicle inertial definition contained within the fuselage element.

3.3.4.4.1 Geometric Properties

The horizontal stabiliser was modelled as a rigid wing, the key geometric properties of which are shown in Table 12.

Description	Value	Reference	Comment
Wing location	[0.91 0.0 -0.0636] m	Appendix A	
Wing sweep angle	13.0°	Appendix A	
Wing dihedral angle	4.0°	Appendix A	
Wing span	0.95 m	Appendix A	
Semi-wing area	0.178 m^2	Appendix A	

Table 12: Horizontal stabiliser geometric properties

3.3.4.4.2 Aerodynamic Properties

The horizontal tail aerodynamics are modelled using a lifting-line model, with the profile of a flat plate. Two-dimensional C_L, C_D and C_M aerodynamic data was obtained from Ref. 11. Similarly to the main rotor aerodynamic data, the data for incidences beyond those provided in Ref. 72 (±30°) are taken from the FLIGHTLAB-supplied NACA0012 data. This data is shown in Figure 28 and Figure 29. The data has undergone some smoothing in order to reduce the time taken to reach the trim solution, and in order to blend the two data sets used.

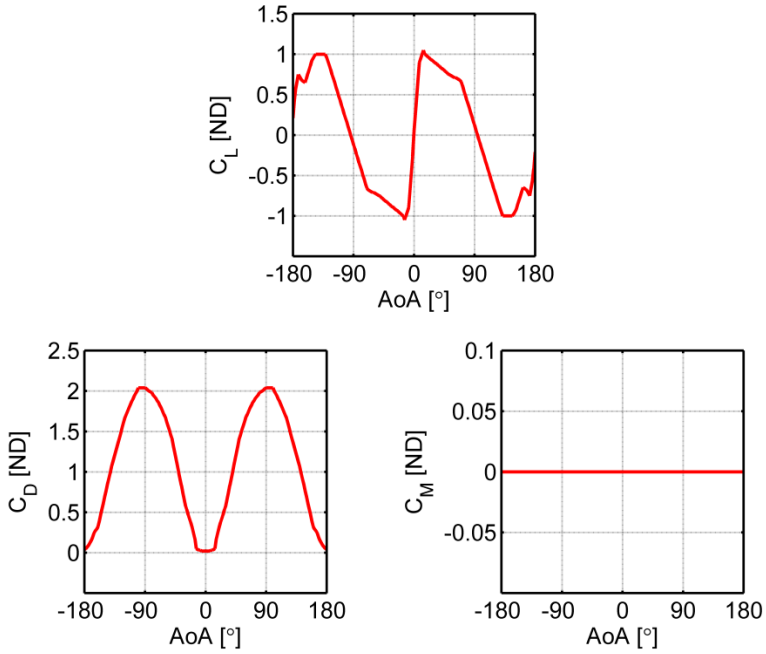

Figure 28: Horizontal stabiliser 2-dimensional aerodynamic data for ±180° range

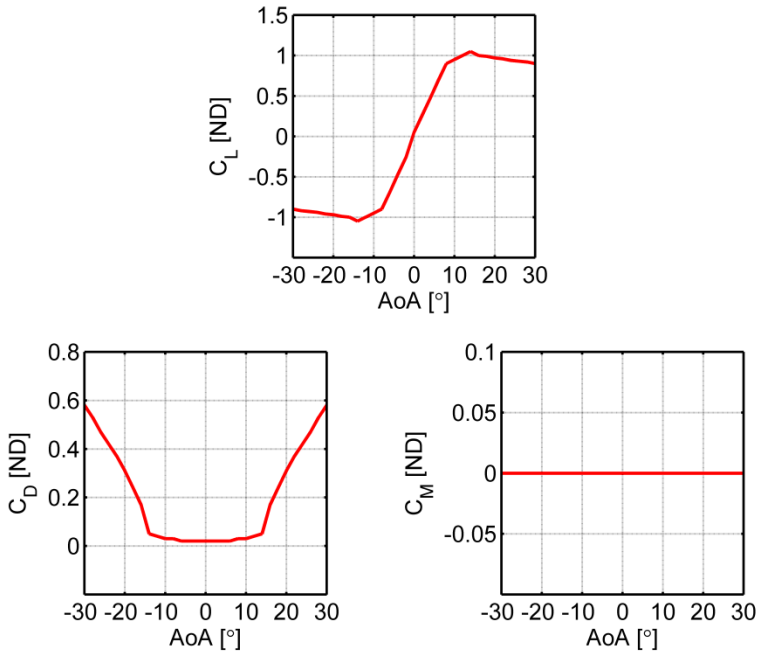

Figure 29: Horizontal stabiliser 2-dimensional aerodynamic data for ±30° range

The lift curve slope of the C_L data shown in Figure 29 is approximately 5.73/rad, which may seem high for an aerodynamic surface of very low aspect ratio such as the horizontal tailplane (AR = 2.54). FLIGHTLAB applies corrections for aspect ratio effects and induced drag to the aerodynamic data inputted into the model. FLIGHTLAB also applies a lift deficiency factor to the lifting surface, discussed in Section 3.3.4.4.3.

In a similar manner to other components in the model, attempts were made to tune the aerodynamic data used to model the tailplane. The data was modified to reduce the lift coefficient by 50%, in order to make the lift curve slope 2.86/rad. The results of this on the trimmed flight control positions and derivatives are shown in Figure 30 and Figure 31 respectively. Upon initial inspection of Figure 30, it would appear that reducing the lift coefficient of the horizontal stabiliser drastically improves the magnitude and trend of the longitudinal shaft tilt trimmed flight control positions, with the model data more closely matching that of the flight test data.

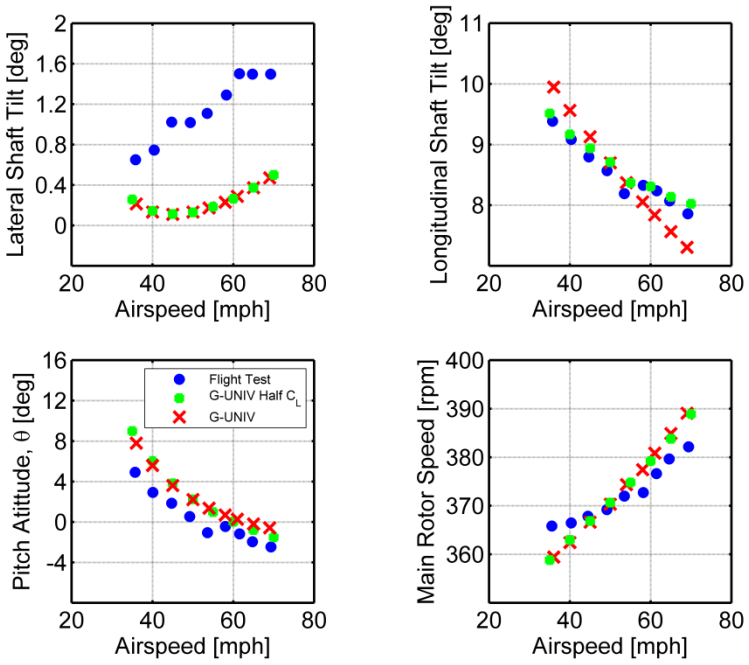

Figure 30: Impact of reducing lift curve slope of the horizontal stabiliser by 50% on trimmed flight control positions

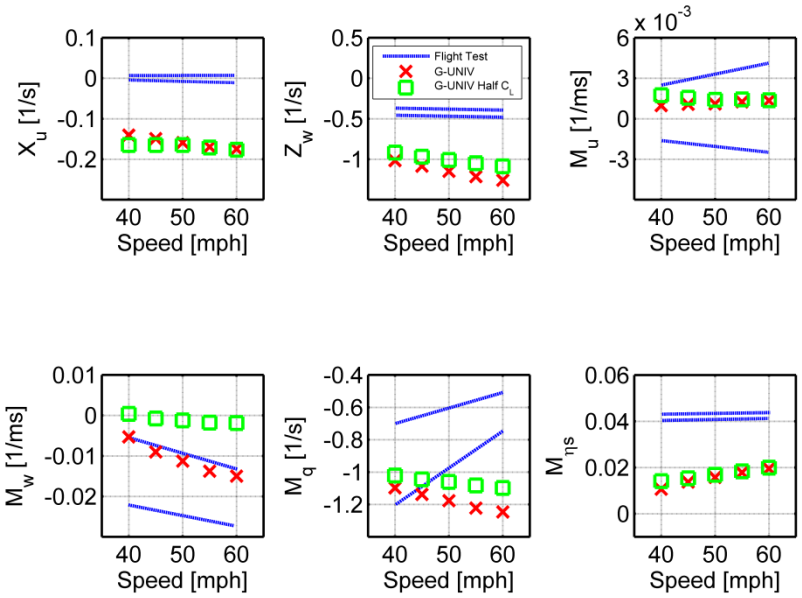

Figure 31: Impact of reducing lift curve slope of tail plane by 50% on aerodynamic derivatives

Whilst improving the longitudinal shaft tilt trend within the trimmed flight control positions, Figure 31 shows that reducing the lift curve slope of the horizontal stabiliser has a significant effect on the aerodynamic derivatives of the model. Whilst the value of M_q and Z_w are slightly reduced by decreasing the lift curve slope of the horizontal stabiliser, moving their value closer to those estimated from flight test, other derivatives such as X_u, M_u and particularly M_w are negatively affected, moving from within the bounds predicted by flight test.

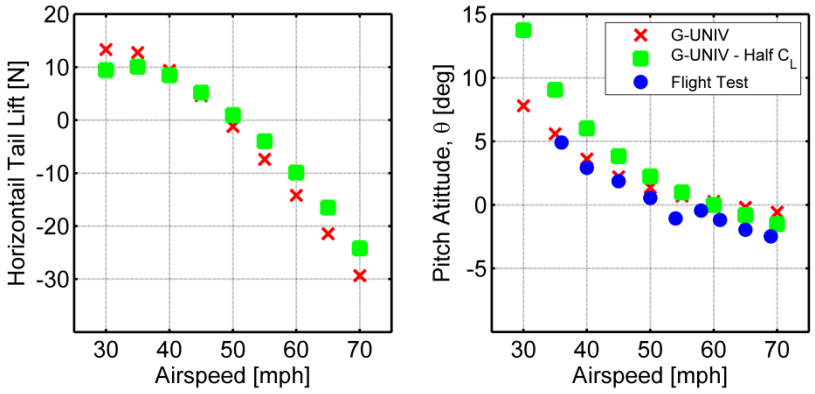

Figure 32: Impact of reducing the curve slope of the horizontal stabiliser by 50% on lift produced and aircraft trimmed pitch attitude across airspeed range

As a final comparison between the two horizontal stabiliser models, Figure 32 shows the absolute value of the lift force produced by the horizontal stabiliser across the flight envelope, and the pitch attitude of the aircraft (and thus the incidence of the horizontal stabiliser). It can be seen that the two models produce similar amounts of lift (due to the corrections applied by FLIGHTLAB) across the mid part of the flight envelope, and the main differences occur at the higher and lower ends of the speed range, with the model with the lift coefficient halved producing less force in both these regions. The maximum difference between the two modelling methods is approximately 7N at 70mph. When this is compared to the lift produced by the main rotor (in the region of 3500N at this condition), this small variation between the two models becomes insignificant.

Figure 32 also illustrates that whilst the prediction of pitch attitude for the reduced lift curve slope model is generally equivalent to or better than that of the original model at airspeeds of 55mph and above, predictions below that speed (the majority of the flight envelope) are not as closely matched to the flight test data, with prediction of pitch attitude becoming worse as airspeed decreases. It is not possible to predict accurately the correlation between flight test data and the two versions of the model at 30mph, as flight test data for this condition was not recorded; however, trends within the data suggest that the model with the reduced lift coefficient would considerably over predict the pitch attitude at this condition.

Due to the negative effect of reducing the lift curve slope on the values of the aerodynamic derivatives (which are strongly correlated to the aircraft's dynamic response) and the poor prediction of the aircraft's pitch attitude with this modification, it was concluded that retaining the original aerodynamic data used to model the horizontal stabiliser was the best course of action, despite the improvement in the trend of the longitudinal shaft tilt trimmed flight control positions that this modification would have offered.

Each half of the horizontal stabiliser is divided into three segments for the purposes of aerodynamic calculations. The plan form of one half of the stabiliser is shown in Figure 33. This is then mirrored about the aircraft's x-axis in order to create a model of the whole stabiliser.

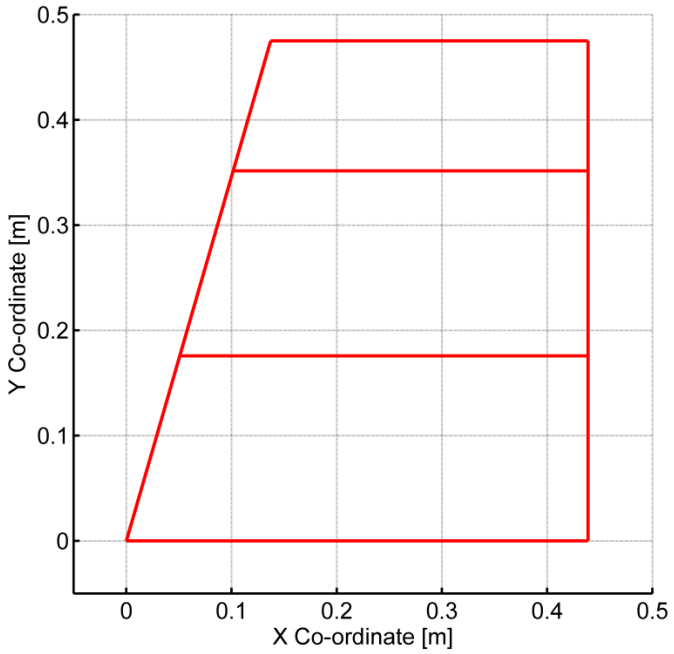

Figure 33: Horizontal stabiliser semi-span plan view

3.3.4.4.3 Aerodynamic Downwash

A lift deficiency factor was used in the place of a more sophisticated method. This method does not compute a wake flow field but instead decrements the lift produced by each aerodynamic segment by a single deficiency factor. This was found to be significantly more computationally efficient, and provides a means by which the longitudinal dynamic and trimmed response of the whole vehicle could be tuned. The lift deficiency factor in the G-UNIV model is set to 0.75; a value which was considered acceptable given the low aspect ratio (AR = 2.54) of the horizontal stabiliser.

3.3.4.5 Aerodynamic Surfaces

FLIGHTLAB allows for the modelling of generic aerodynamic surfaces, with or without control surface actuation. The term 'aerodynamic surfaces' refers to the winglets, vertical fin and rudder.

3.3.4.5.1 Geometric Properties

The fin and rudder assembly were modelled as 'controlled' surfaces, and the winglets were modelled as 'non-controlled' surfaces. The key geometric parameters of these surfaces are shown in Table 13 and Table 14.

Description	Value	Reference	Comment
Winglet location	[1.055 ±0.475 -0.063] m	Appendix A	
Sweep angle	14°	Appendix A	
Span	0.25 m	Appendix A	

Table 13: Winglet geometric properties

Description	Value	Reference	Comment
Fin location	[0.91 0.0 -0.0677] m	Appendix A	
Sweep angle	16.9°	Appendix A	
Span	0.82 m	Appendix A	

Table 14: Rudder & tail fin geometric properties

3.3.4.5.2 Aerodynamic Properties

As was the case for the horizontal stabiliser, the vertical fin and winglets were modelled using a flat plate profile, and use the same aerodynamic source data Ref. 72. The required data beyond the range presented in Ref. 72 was again populated with FLIGHTLAB-supplied NACA0012 data. The aerodynamic data used to model the non-controlled winglets is shown in Figure 34 and Figure 35. The winglet plan form is shown in Figure 36.

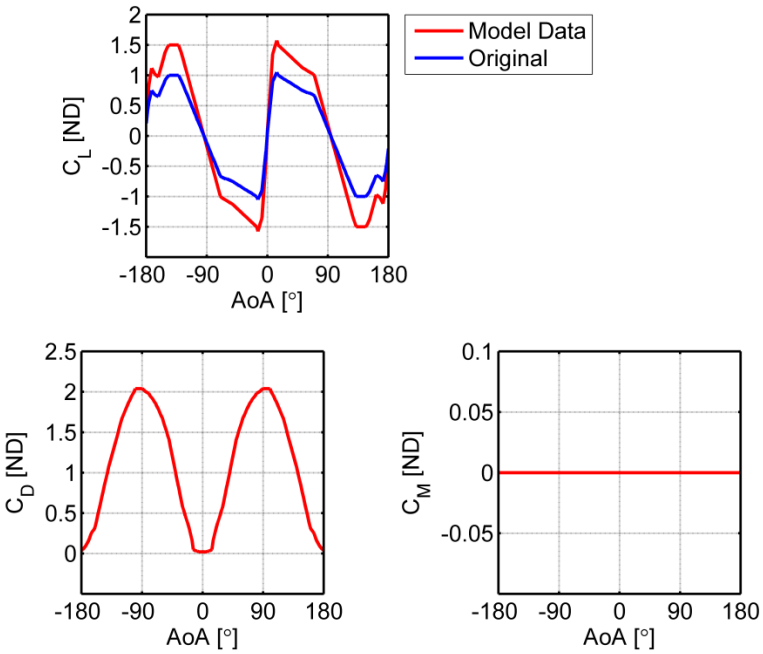

Figure 34: Winglet 2-dimensional aerodynamic data for ±180° range

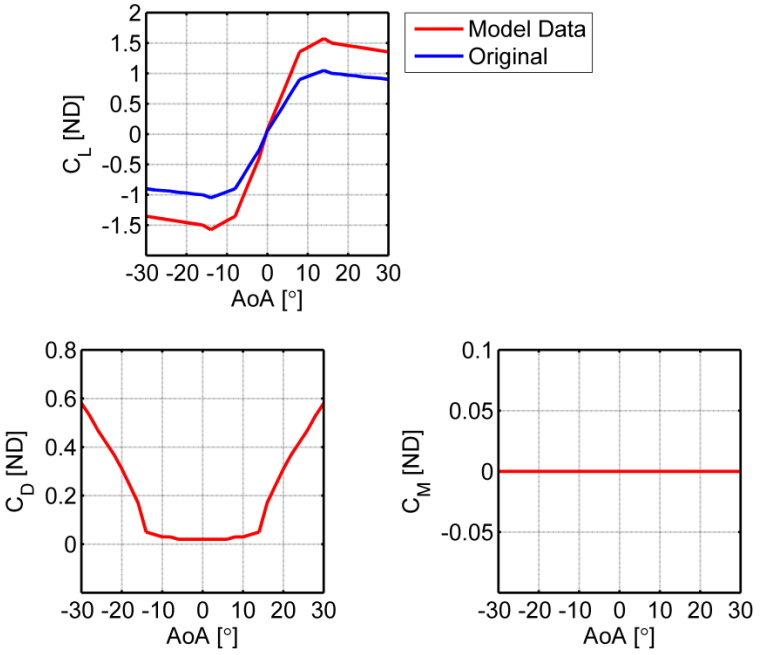

Figure 35: Winglet 2-dimensional aerodynamic data for ±30° range

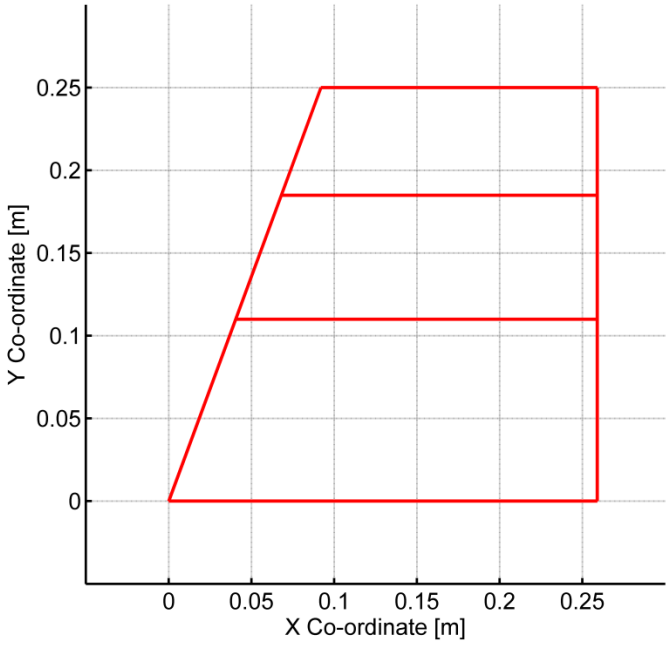

Figure 36: Winglet plan form

Following a preliminary validation exercise, the aerodynamic data used was tuned by increasing the lift coefficient by 50% in order to increase the yaw damping. This was found to result in a closer match to the dynamic responses within the flight test data.

For the controlled surfaces, FLIGHTLAB requires that the aerodynamic data used must be three-dimensional. Therefore, the two-dimensional data used for the horizontal stabiliser must be corrected to account for the increment of lift, drag and pitching moment with control surface deflection. The empirical method used is detailed in Ref. 72 and is reproduced here.

The increment in lift (ΔC_L) of the vertical fin for a given rudder deflection was estimated using the technique for plain flaps described in Ref. 73. The estimate of the increment of lift is given by:

$$\Delta C_L = C_{l\alpha} \tau \eta \delta_f$$

where $C_{l\alpha}$ is the lift curve slope of the surface with flap un-deflected, τ is the flap effectiveness (0.85 is a typical value for flat plate data), η is the empirical correction

factor added in to account for effects of viscosity (0.8 is a standard value), and δ_f is the flap deflection.

Similarly, the increment in drag is given by:

$$\Delta C_D = 1.7\left(c_f/c\right)^{1.38}\left(S_f/S\right)\sin^2\delta_f$$

where c_f is the flap chord, c is the chord of the surface, S_f is the flap area, S is the area of the surfaces and δ_f is the flap deflection.

The resulting data generated using this method is shown in Figure 37 and Figure 38, the red lines representing the un-deflected properties and the blue lines representing the maximum deflection properties (in this case ±40°). FLIGHTLAB linearly interpolates between these values to produce lift, drag and moment coefficients for any given deflection.

As no appropriate manoeuvre was able to be identified within the available flight test data for validating the yaw response, the aerodynamic data used for the rudder was tuned during piloted evaluation. This resulted in the lift coefficient data being increased by a factor of 2.5 in order to give an appropriate level of control power and an appropriate dynamic response. The data has also been smoothed.

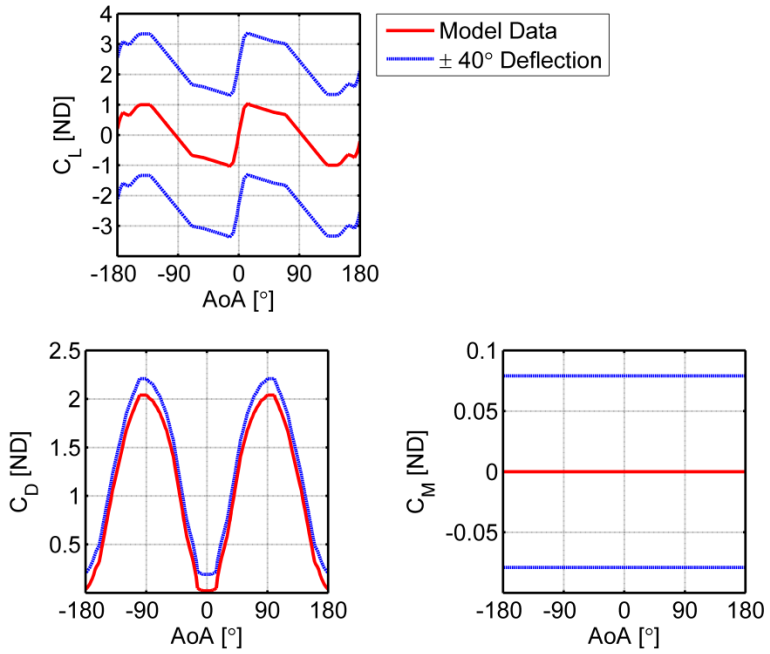

Figure 37: Rudder aerodynamic data for ±180° range

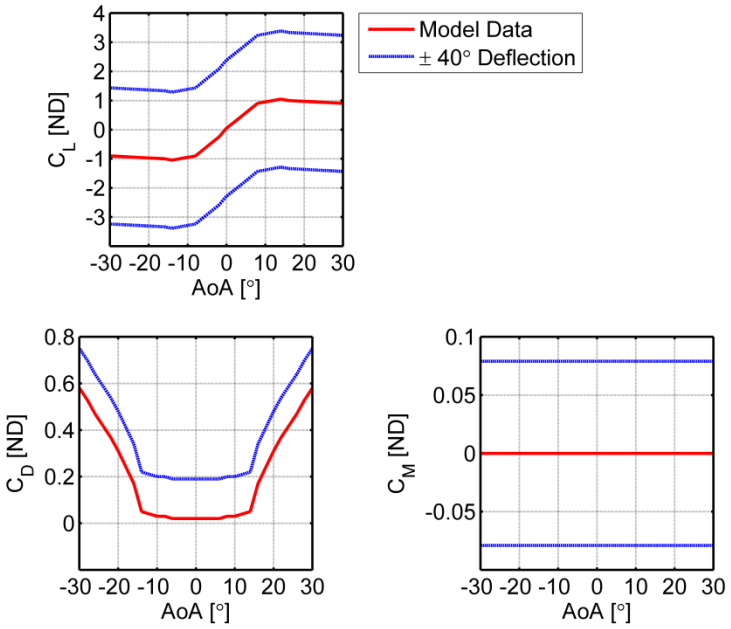

Figure 38: Rudder aerodynamic data for ±30° range

G-UNIV's rudder is shown in Figure 39, the moving segment of which is highlighted in red. It was not possible to model a moving segment of such complex geometry in FLIGHTLAB.

As a compromise, the moving segment of the FLIGHTLAB model was designed to be of the same percentage of the total vertical surface area as occupied by the real rudder geometry. The FLIGHTLAB rudder geometry is shown in Figure 40, with the articulated portion shown in red. As for the winglet, for the purposes of aerodynamic calculations, the rudder surface is divided into four segments, which can be seen in Figure 40.

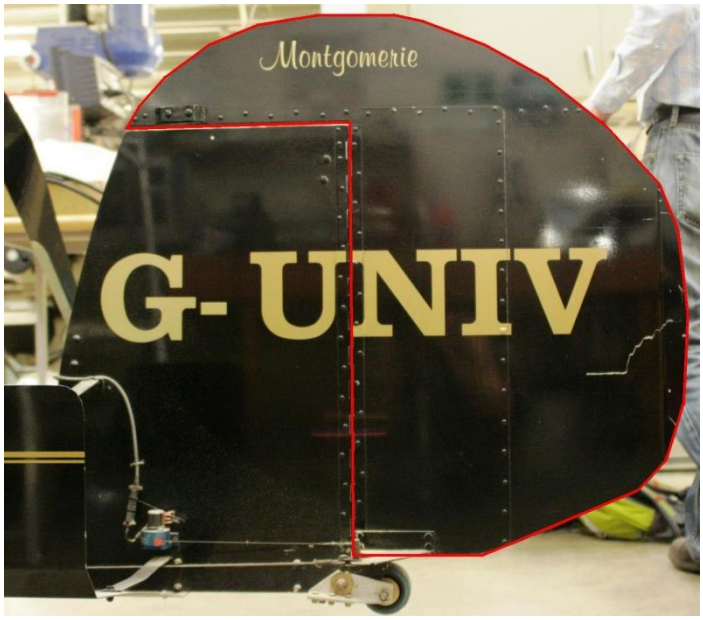

Figure 39: G-UNIV vertical tail surfaces, with moving rudder section outlined in red

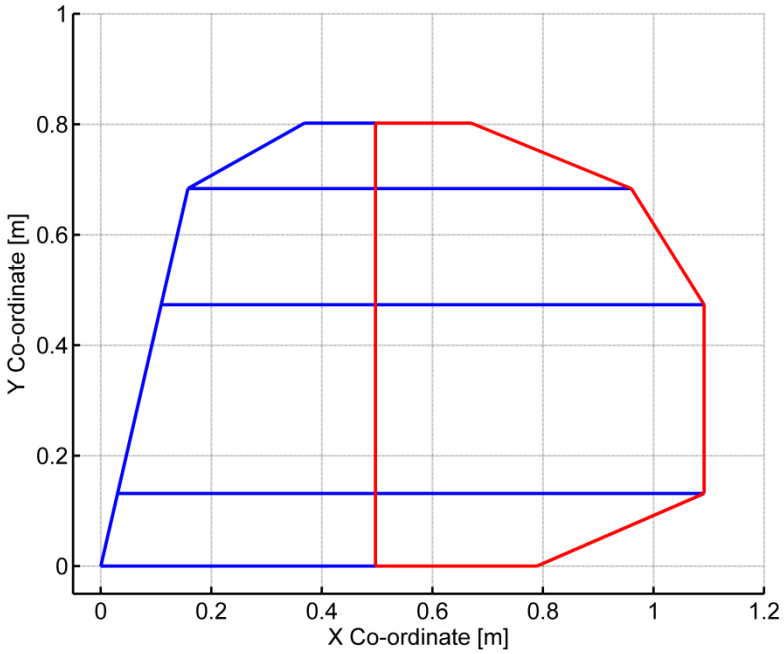

Figure 40: FLIGHTLAB rudder geometry, with moving segment highlighted in red

3.3.4.5.3 Aerodynamic Downwash

FLIGHTLAB does not have provision for downwash models to be applied to "aerodynamic surfaces" (i.e. non-lifting surfaces). A lift deficiency factor can be applied; however, in this case it was set to 1.0 as all tuning of the aerodynamic data was achieved through direct remodelling of the input data.

3.3.4.6 Engine

G-UNIV is powered by an 85hp Rotax 618 piston engine. FLIGHTLAB provides modelling options for an "ideal engine" (one which maintains a constant rotational speed and has no limit on power output), a "simple engine" (which models a simplified free turbine engine without thermodynamic effects) and turboshaft power plants.

In order to accurately model the throttle response, a custom piston engine component was created; however, data for the Rotax 618 throttle map was unavailable. There was also no flight test data for the trimmed throttle control position available.

As a compromise, data from the Rotax 914 engine (the 85hp engine used in the MT-03 autogyro), supplied in Ref. 74, was used to create a proposed throttle map, mirroring the

trend and progression seen in the 914 engine to create an approximate solution for the 618 engine model. The resulting throttle map for the 618 is shown by the green line in Figure 41. This throttle map was then tuned in-flight in the simulator to reduce the throttle sensitivity.

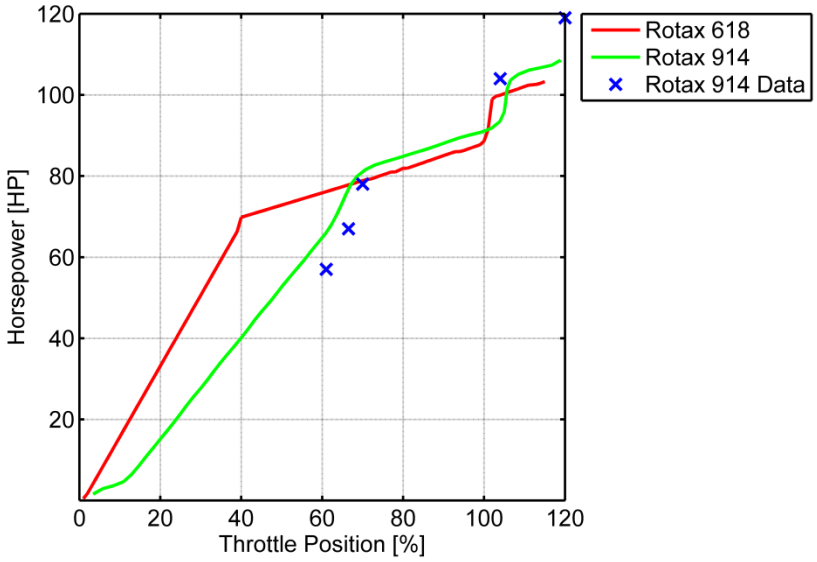

Figure 41: Rotax 618 throttle map

The component calculation logic runs as follows:

i. The throttle position ($throt_{actual}$) is used to obtain nominal engine power (P_{nom}) from the data presented Figure 41.

ii. The ambient temperature (T_{amb}), altitude (alt) and engine speed (Ω_{eng}) are read from the model.

iii. The International Standard Atmosphere (ISA) temperature (T_{ISA}) for the actual altitude is calculated from FLIGHTLAB-supplied look up tables.

iv. The difference from ISA conditions is established:

$$T_{diff} = T_{amb} - T_{ISA}$$

v. Look up maximum continuous power at the altitude in question from Table 15.

vi. Calculate a correction factor (CF) based on ISA conditions using throttle position:

$$CF = \frac{P_{\max amb}}{88.61}$$

where 88.61 is the engine horsepower at sea-level ISA conditions for 100% throttle setting.

vii. Calculate the corrected power (P_{act}) for the current throttle position:

$$P_{act} = CF \times P_{nom}$$

viii. Convert the available power into torque (T):

$$T = \frac{P_{act} \times 550}{\Omega_{eng}}$$

where the factor 550 represents the conversion between horsepower and ft.lbf.sec^{-1}.

The calculated torque is then passed to the propeller via the drivetrain component. FLIGHTLAB performs a torque balance between the engine and the propeller (with the new torque driving the propeller until it can no longer overcome the drag generated by the spinning blades) which results in a new calculated engine speed, which updates the propeller speed. Engine and propeller speed are linked by a fixed gearing ratio.

ALTITUDE [FT]	ISA TEMP (T_{ISA}) [°C]	TEMPERATURE DIFFERENCE TO ISA (T_{diff}) [°C]																
		-45	-40	-35	-30	-25	-20	-15	-10	-5	0	5	10	15	20	25	30	35
-2000	19	118	115	114	111	109.0	107.0	105.0	103.0	102.0	99.2	97.9	96.6	95.2	93.9	92.5	89.8	88.5
0	15	117	114	113	110	107.0	106.0	105.0	102.0	101.0	99.2	96.6	95.2	93.9	92.5	91.2	89.8	88.5
2000	11	117	114	111	109	107.0	105.0	103.0	102.0	99.2	97.9	96.6	93.9	92.5	91.2	89.8	88.5	87.2
4000	7	115	113	110	109	106.0	105.0	102.0	101.0	97.9	96.6	95.2	93.9	91.2	89.8	88.5	87.2	85.8
6000	3	114	111	110	107	105.0	103.0	101.0	99.2	97.9	95.2	93.9	92.5	91.2	88.5	87.2	85.8	0.0
8000	-1	113	110	109	106	103.0	102.0	99.2	97.9	96.6	93.9	92.5	91.2	89.8	88.5	85.8	84.5	0.0
10000	-5	111	110	107	105	103.0	101.0	99.2	96.6	95.2	92.5	91.2	89.8	88.5	87.2	84.5	0.0	0.0
12000	-9	110	109	106	103	102.0	99.2	96.6	95.2	93.9	91.2	89.8	88.5	87.2	85.8	0.0	0.0	0.0
14000	-13	109	106	103	102	99.2	97.9	95.2	93.9	91.2	89.8	88.5	87.2	84.5	0.0	0.0	0.0	0.0
16000	-17	107	105	102	101	97.9	96.6	93.9	92.5	89.8	88.5	87.2	85.8	0.0	0.0	0.0	0.0	0.0

Table 15: Rotax Engine performance (hp) for non-standard atmospheric conditions at maximum continuous power

3.3.4.7 Undercarriage

For the purposes of in-flight evaluation, modelling of the undercarriage was not strictly necessary, as the aerodynamic and inertial effects of the undercarriage were included in the modelling of the fuselage using the data from Ref. 46. However, in order to allow the

model to be flown in real-time and to interact with the ground model in the simulation environment, a simple undercarriage model was created.

This model consists of a two-stage spring-damper at each wheel location. The values of the spring and damper coefficients are set empirically to give a nominally stiff, but unverified ground contact response. This was considered acceptable as no manoeuvres requiring interaction with the ground were included within the scope of this study. The key modelling parameters for the main gear are shown in Table 16 and the properties of the nose gear are shown in Table 17.

Description	Value	Reference	Comment
Main gear location	[0.13 ±1.07 -0.14] m	Appendix A	
Rolling friction coefficients	[-0.1 -0.55]		Default FLIGHTLAB value
Braking friction coefficient	[-7 -3.5]		Default FLIGHTLAB value
Stiffness coefficients	[9680 1511] $lbf.ft^{-1}$		Default FLIGHTLAB value
Damping coefficients	[133 167] $lbf\text{-}ft.s^{-1}$		Default FLIGHTLAB value

Table 16: Main gear properties

Description	Value	Reference	Comment
Main gear location	[-1.62 0 -0.19] m	Appendix A	
Rolling friction coefficients	[-0.1 -0.55]		Default FLIGHTLAB value
Braking friction coefficient	[-7 -3.5]		Default FLIGHTLAB value
Stiffness coefficients	[9680 1511] $lbf.ft^{-1}$		Default FLIGHTLAB value
Damping coefficients	[133 167] $lbf\text{-}ft.s^{-1}$		Default FLIGHTLAB value

Table 17: Nose gear properties

3.3.4.8 Ancillary Services

The model of G-UNIV is equipped with a variety of ancillary services. These include a pre-rotator (which when engaged draws power from the engine to spin the rotor whilst the

autogyro is stationary to allow shorter take off runs), a rotor brake, a parking brake and wheel brakes. These services were included within the FLIGHTLAB model for use in the real-time simulation environment.

3.3.4.8.1 Pre-rotator

The pre-rotator mechanism is driven by a second 'phantom' instance of the Rotax engine – there are no mass or inertia properties associated with this engine, and thus it had no influence on the vehicle flight dynamics. This method of including the pre-rotator was selected as it was simpler and less computationally expensive than modelling a mechanical interlink between the rotor and the engine.

In the real time simulation environment, the pre-rotator was engaged by using the trigger switch on the centre stick, and the rotor speed was increased by opening the throttle.

3.3.4.8.2 Rotor Brake

The rotor brake was included to allow the pilot to reduce the rotor and vehicle speed whilst on the ground. This is a standard FLIGHTLAB component and was activated in the real-time simulation environment by depressing the hat switch on the centre stick to the right.

3.3.4.8.3 Wheel Brake

The wheel brake is included as a standard FLIGHTLAB feature as part of the landing gear component. When activated, the specified friction coefficients switch from the 'rolling' to 'braking' values shown in Table 16 and Table 17. The wheel brakes were activated by depressing the hat switch on the centre stick to the left.

3.3.4.8.4 Parking Brake

Once the vehicle has stopped, the parking brake could be activated so that the pilot does not have to continue to apply pressure to the wheel brake actuator. The park brake was activated by operating the two-position switch on the collective lever.

3.4 HELICOPTER MODELLING

3.4.1 G-UNIV Helicopter Model

In order to investigate the fundamental differences between the helicopter and the autogyro, and to address the research questions raised in Chapter 2, a model of a

helicopter was created in FLIGHTLAB. The methodology used for creating this model of a generic, conventional helicopter of comparable dimensions to G-UNIV is detailed below.

3.4.1.1 Geometry

The model of the helicopter was intended to be directly comparable to the model of the autogyro. This model has the same total mass as the model of the autogyro (355kg inclusive of pilot and fuel load), the same rotor geometry, and uses the same aerodynamic data for the fuselage, rotor and aerodynamic surfaces. The vertical tail surface was moved aft to be coincident with the tail rotor, maintaining its total surface area but removing the articulated portion which formed the rudder.

The remaining model geometry was defined by considering that of existing helicopters in the "light utility" class, such as the Robinson R22 [75], the Schweizer 300C [76] and the Bell 47 [77]. Whilst these helicopters weigh in excess of 355kg, and the helicopter model being created is of a fictional vehicle, it was considered a sensible design aim to achieve parity with existing aircraft designs. This method was also used in order to avoid any genuine handling qualities or stability deficiencies being negated during the model development phase, which could influence the subsequent comparison with the autogyro model.

3.4.1.2 Tail Rotor Sizing

The tail rotor is positioned such that it is outside of the main rotor radius, located 4.5m aft of the reference point (the reference point is located in the same position as that of the autogyro model).

In order to estimate an approximate size for the tail rotor area, the relationship between the tail rotor area and the main rotor area for a variety of existing light helicopters was established. The selected aircraft and their rotor properties are shown in Table 18.

Using the data in Table 18, it is possible to plot main rotor diameter against ratio of rotor areas (R/TR), as shown in Figure 42. Using Figure 42 and taking into account the low mass of the proposed helicopter model, an appropriate diameter for the tail rotor was selected; this is marked with a green triangle. The chosen tail rotor diameter is 1.28m.

Aircraft	Rotor Diameter (m)	Rotor Area [R] (m^2)	Tail Rotor Diameter (m)	Tail Rotor Area [TR] (m^2)	Ratio of Areas (R/TR)
Robinson R22	7.70	46.57	1.07	0.90	51.79
Lynx	12.80	128.68	2.36	4.37	29.42
AW109	11.00	95.03	2.03	3.24	29.36
Bell 47	11.32	100.64	1.87	2.75	36.64
Bell 204	14.63	168.10	1.78	2.49	67.55
Bell 407	10.66	89.25	1.56	1.91	46.69
Brantly B2	7.24	41.17	1.29	1.31	31.50
Enstrom 480	9.80	75.43	1.50	1.77	42.68
Schweizer 300C	8.05	50.92	1.27	1.27	40.07
FH-1100	10.79	91.44	1.83	2.63	34.76
MD500	8.10	51.53	1.40	1.54	33.47
Bo105	9.84	76.05	1.90	2.84	26.82
MI-1	14.30	160.61	2.50	4.91	32.72

Table 18: Tail and main rotor diameter properties for a variety of light helicopters

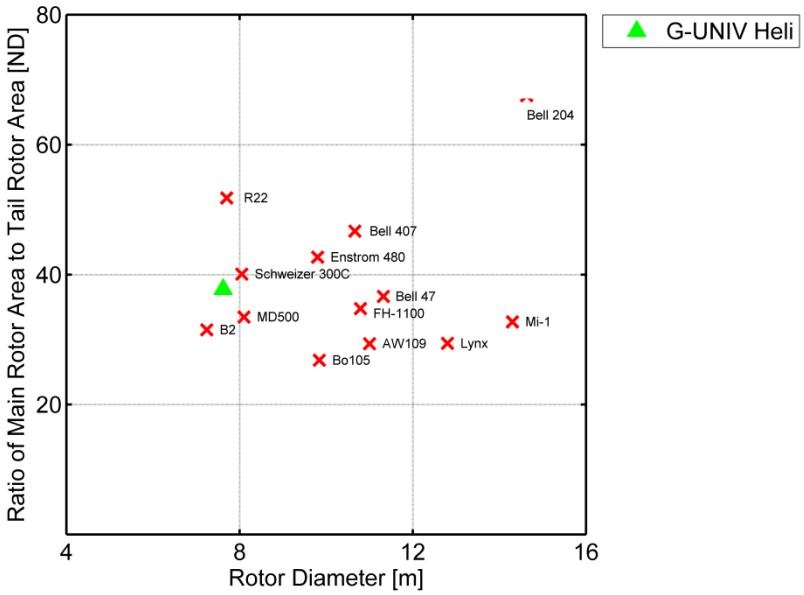

Figure 42: The relationship between main rotor and tail rotor sizing

3.4.1.3 Horizontal Tail Surface Sizing

A similar methodology was to that used when sizing the tail rotor was used to size the horizontal tail surface. A graph of the horizontal tail surface size against the main rotor area was plotted, and an appropriate area selected. This is shown in Figure 43. The raw data used for this is shown in Table 19.

Aircraft	Rotor Area [R] (m^2)	Horizontal Tail Surface Area (m^2)
Brantly B2	41.17	0.266
Robinson R22	46.57	0.1541
Schweizer 300C	50.92	0.1645
MD 500	51.53	0.4736
Bo105	76.05	0.6
Bell 407	89.25	1.034
FH-1100	91.44	0.564
Bell 47	100.64	1.3464
Lynx	128.68	0.63456
Mi-1	160.61	0.8304
Bell 204	168.10	1.8612

Table 19: Horizontal tail surface properties of various light helicopters

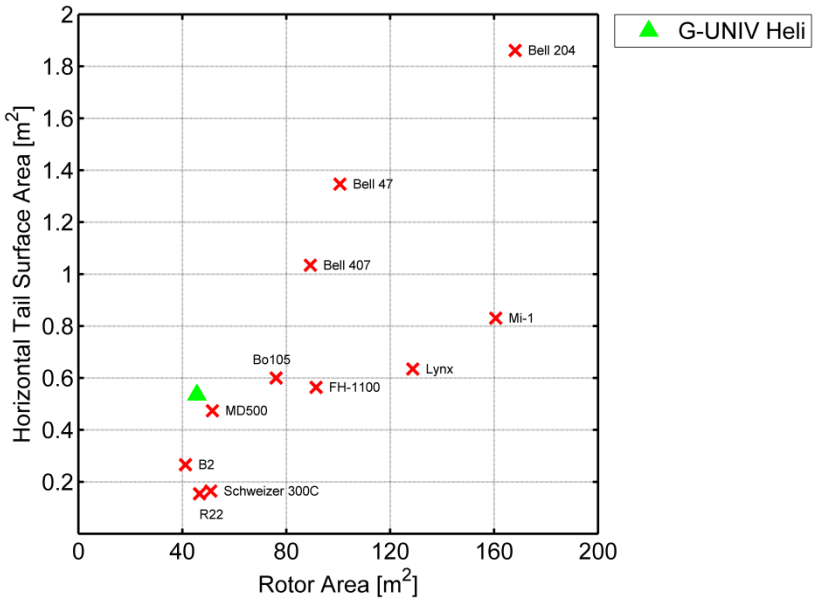

Figure 43: Horizontal tail surface and main rotor area relationship

3.4.1.4 Centre of Gravity Location

The longitudinal position of the centre of gravity, relative to the reference point shown in Figure 8, was approximated by estimating the mass and measuring the location of each of the components. Any remaining mass from the total was assumed to be linearly distributed along the horizontal axis. The formula used to evaluate the position of the centre of mass is:

$$\frac{\begin{bmatrix} (Mass\ of\ Pilot\ \times moment\ arm) \\ +\ (Mass\ of\ main\ rotor\ \times moment\ arm) \\ +\ (Mass\ of\ Engine\ and\ Fuel \times moment\ arm) \\ +\ (Mass\ of\ Horizontal\ Tail\ \times moment\ arm) \\ +\ (Mass\ of\ Tail\ Rotor\ \times moment\ arm) \end{bmatrix}}{Total\ mass\ of\ components} = Longitudinal\ C.G\ Position$$

The dressed mass of the pilot was assumed to be 95kg. The weight of the main rotor assembly is 17.24kg. The dry weight of the engine is 78kg [74], and 50 litres of fuel has a mass of 37.5kg (0.75 kg/litre). The mass of the tailplane was estimated by multiplying the area of the tailplane (0.356m^2) by the weight per square metre of sheet steel (15.7 kg/m^2) , totalling 5.59kg. The weight of the tail rotor is assumed to be equal to that of the

autogyro propeller at 3.63kg (they share an approximately equal diameter and the same aerofoil). The locations for all components are measured from Figure 44.

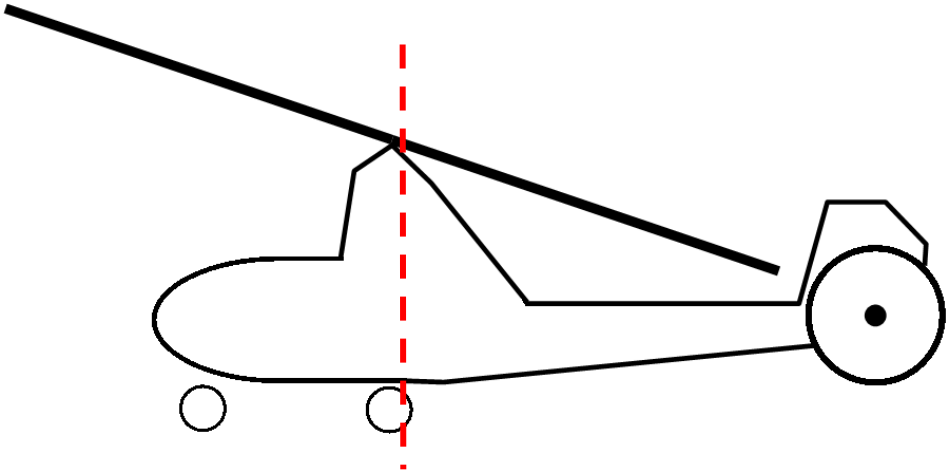

Figure 44: Scale drawing of helicopter based on G-UNIV autogyro with longitudinal centre of gravity position shown

Therefore, the longitudinal position of the centre of gravity evaluates to:

$$\frac{\left[(95 \times -0.75) + (0.038 \times 17.24) + \left(0.487 \times (78 + 37.5)\right) + (3.3 \times 5.59) + (4.5 \times 3.63)\right]}{(95 + 17.24 + 115.5 + 5.59 + 3.63)}$$

$$= \frac{20.44}{236.96} = \boldsymbol{0.086m}$$

This location is shown in Figure 44.

3.4.1.5 Engine Modelling

The G-UNIV helicopter model utilises the ideal engine model within FLIGHTLAB [61]; the engine provides sufficient power to ensure a constant rotor speed. The engine power is limited to 100hp, in line with the trend shown in Figure 45.

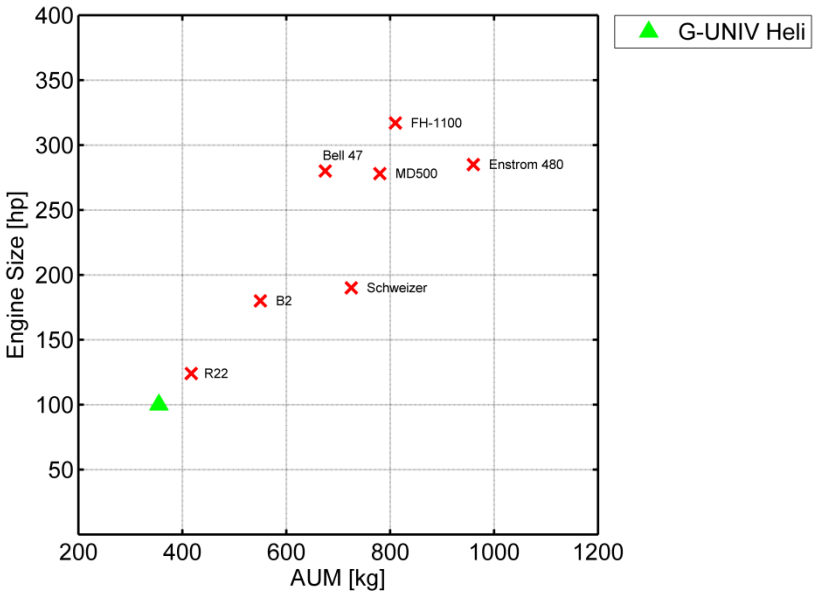

Figure 45: Engine horsepower ratings for various light weight helicopters

A comparison of the flight handling qualities of the helicopter and autogyro models is included in Chapters 6 and 7.

3.5 MODEL VALIDATION

The approach to validating the FLIGHTLAB model of the autogyro used four discrete but related tasks. This involved the comparison and matching between model and flight test of the following:

i. Longitudinal and lateral trim positions;
ii. Longitudinal and lateral dynamic responses in flight;
iii. Aerodynamic derivatives;
iv. Handling qualities from flight test.

3.5.1 Longitudinal and Lateral Trim Positions

Figure 46 shows a comparison between the trimmed control positions of the G-UNIV autogyro model and the flight test data provided by Glasgow University. In general, the model shows good agreement both in magnitude and the observed trend of each parameter with airspeed. Some parameters, for example throttle position/power setting and pedal position/rudder deflection were unavailable. Matching these parameters may

have improved the comparison between the two data sets; for example, the throttle setting (and thus the tail rotor torque) will affect the lateral shaft tilt angle.

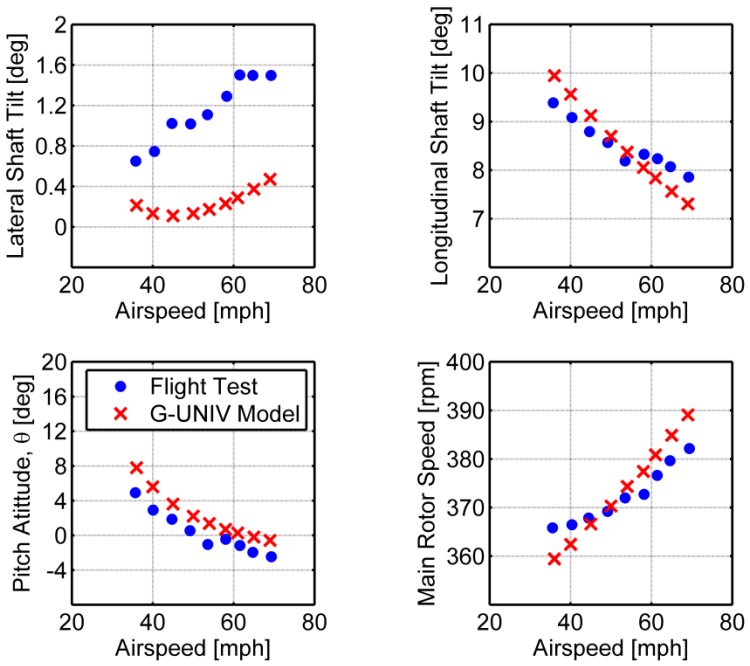

Figure 46: Trimmed control positions for G-UNIV FLIGHTLAB model compared to flight test values

The lateral shaft tilt shows a maximum offset error of approximately 1.2°, although the observed trend in the data is somewhat different to the flight test data. The longitudinal shaft tilt is generally better, showing a maximum offset error of around 0.5°, with the data showing a similar (though slightly steeper) linear trend to that of the flight test data.

The pitch attitude trend and magnitude are generally well predicted across the speed range, with an offset of approximately 2-3°.

The main rotor speed exhibits a linear trend across the speed range, rather than the slight curve observed in the flight test data. This could be attributed to the rotor inflow modelling, the sophistication of which was reduced in order to increase computational efficiency and reduce the amount of time the model takes to trim. The magnitude of the trimmed rotor speed is directly comparable to that of the flight test data, with a maximum error of approximately 7rpm.

3.5.2 Dynamic Response Validation

In order to validate the simulation model's dynamic response characteristics, flight test data, provided by Glasgow University, was used. The data is taken from a trial focussed on examining the longitudinal response of the G-UNIV aircraft, as described in Ref. 44.

This presented several challenges in terms of identifying appropriate manoeuvres to use for validation purposes. Ideally, open loop pulse or step inputs in each axis would be used to assess the dynamic response. However, due to the limited amount of data available, it was not possible to identify an appropriate manoeuvre for the yaw axis and an alternative method of tuning is described herein.

It was possible to identify appropriate manoeuvres for the pitch and roll axes, however both the pitch and roll response comparisons are somewhat skewed by the fact that the initial conditions could not be matched exactly. In the flight test data, the point at which the control inputs were initiated occurs when the aircraft is not in trim, often with considerable pitch or roll rates. It was not possible to accurately recreate these conditions when flying in real time in the simulator. The manoeuvres selected were intended to minimise this problem, however, they are far from ideal examples.

Ideally, more than one manoeuvre would be used to tune and validate the dynamic response. The on-axis response of the aircraft would be assessed using the first manoeuvre. It would then be possible to identify which aspects of the response required tuning (for example, rise time or amplitude). Appropriate tuning could then be applied until the aircraft response more closely resembled that of the flight test data. A second manoeuvre of a different type was then used to check that the tuning did not just provide a good response to the one initial manoeuvre selected. Due to the small number of manoeuvres available as previously discussed, this was not possible.

The dynamic response validation exercise was carried out 'online' in the HELIFLIGHT simulator, as described in 3.1.1. The perturbation from trim in lateral and longitudinal control and rudder deflection was extracted from the flight test data for the selected manoeuvres. An engineer pilot then flew the simulation model to the trim condition identified immediately before the selected inputs were made. Once at trim, control was taken away from the pilot and the extracted control perturbations were 'replayed'

through the model in real time. This resulted in direct replication of the control deflections during the flight test in the simulation environment. The response of the simulation model was recorded and compared to the flight test data.

3.5.2.1 Longitudinal Dynamic Response

Figure 47 shows the dynamic response of the simulation model to a longitudinal input, plotted as perturbation from the trim condition. It can be seen that the on-axis (q, ϑ), rotorspeed, airspeed and height responses provide excellent agreement to the flight test data; however, the off-axis responses in roll and yaw show generally poor agreement. This may be due in part to the difficulty in matching the start conditions in the simulator to those in the flight test data. The model is also sensitive to the start conditions in the simulator; any residual roll rate (for example) will proliferate through the simulation model's dynamic response, skewing the results when compared to the flight test data.

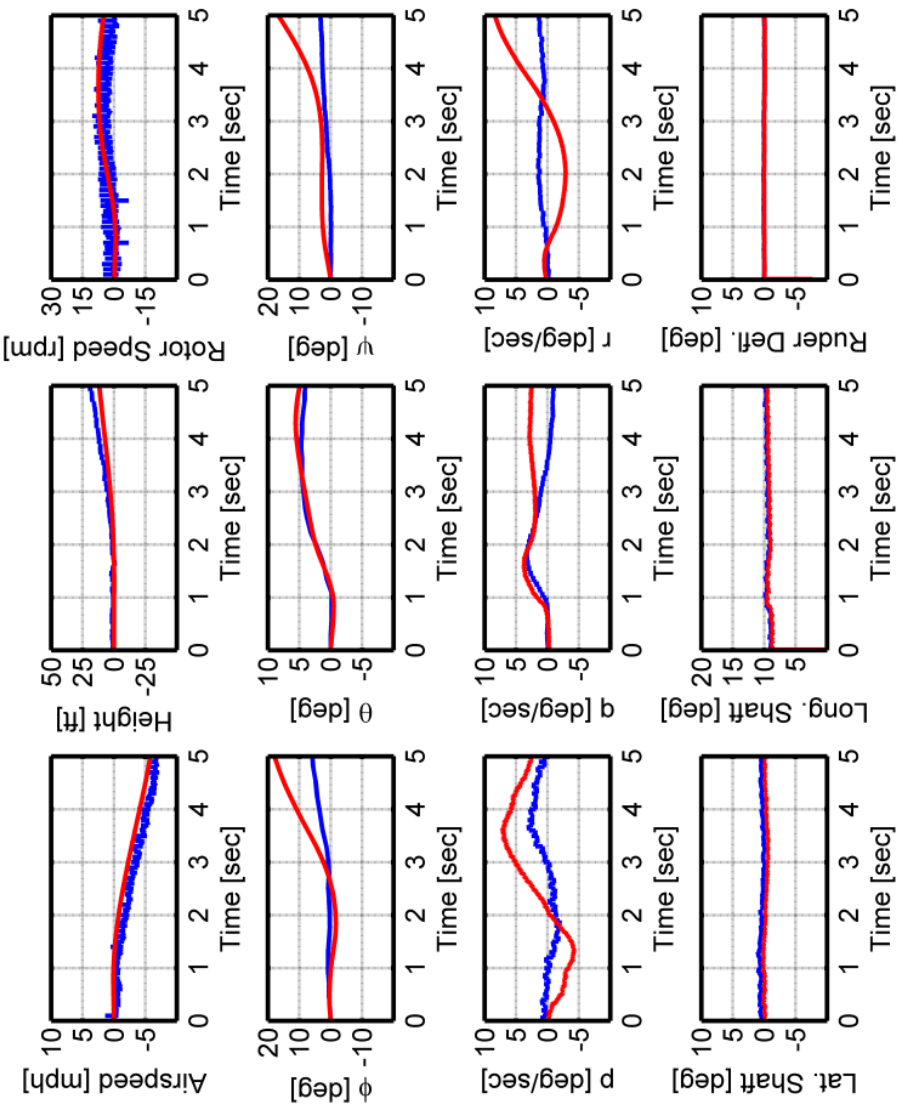

Figure 47: Longitudinal dynamic response validation with flight test data shown in blue and model dynamic response shown in red

3.5.2.2 Lateral Dynamic Response

The lateral dynamic response can be seen in Figure 48. Similarly to the longitudinal response, the on-axis response (p, φ) and the airspeed response show generally good agreement to the flight test data, with the longitudinal dynamics showing reasonable agreement in terms of direction and magnitude. In terms of correlation to the flight test date, the yaw response is poor.

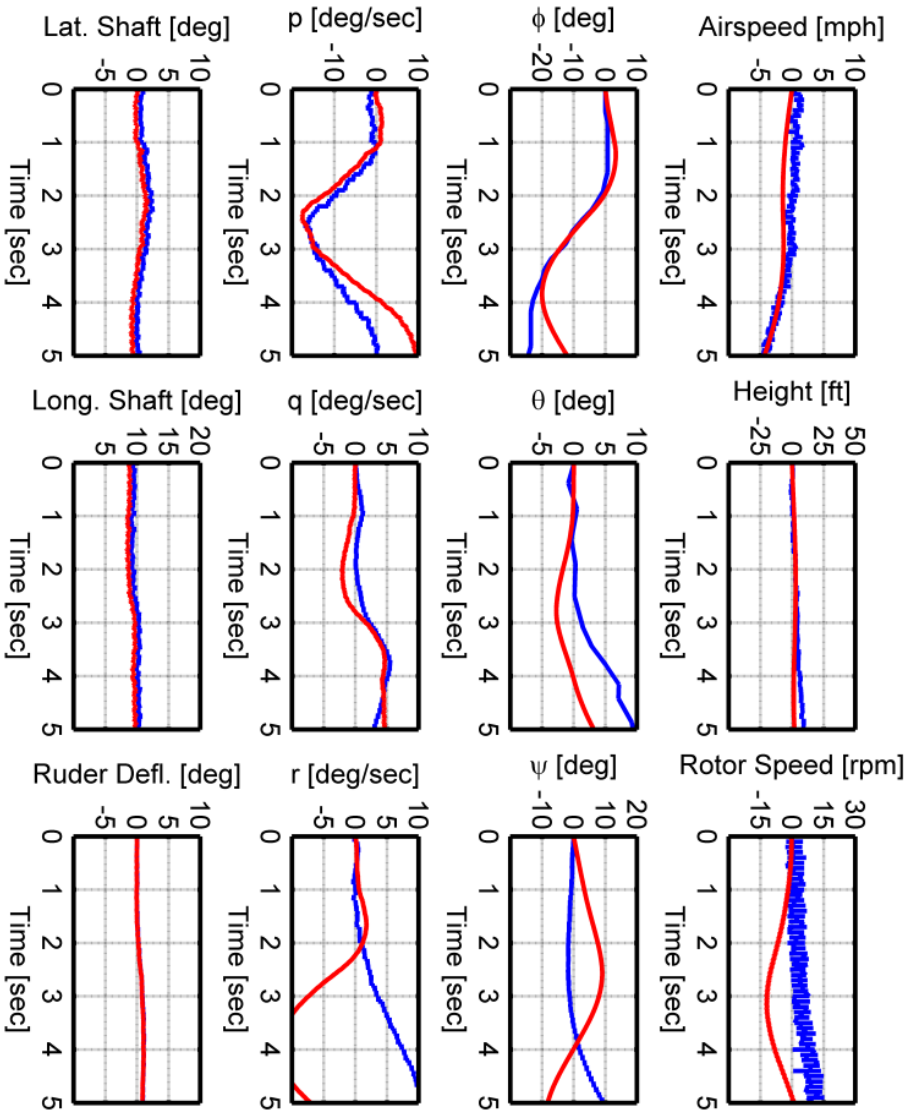

Figure 48: Lateral dynamic response validation with flight test data shown in blue and model dynamic response shown in red

3.5.2.3 Yaw Response

As no suitable manoeuvre could be identified within the flight test data for validating the yaw axis response, an alternative approach had to be adopted. A test pilot was asked to subjectively assess a range of rudder configurations. A variety of step and pulse inputs, and "turns on one control" (performing a turn using only the pedals in order to assess the

control power of the rudder surface) were performed and the most appropriate selected. This is a standard technique for assessing control power through piloted evaluation.

Although a highly experienced rotary-and-fixed-wing pilot, the test pilot was not an experienced autogyro pilot. Therefore, there remains scope for improvement in the fidelity of the yaw dynamics.

3.5.3 Aerodynamic Derivative Comparison

As part of the trial carried out in Ref. 7, the aerodynamic derivatives X_u, M_u, M_q, Z_w, M_w and $M_{\eta s}$ were estimated from flight test data. These estimated derivatives are shown in Figure 49 as blue lines, representing 95% confidence limits of the parameter estimation. The model derivatives (shown in red) are absolute values calculated by linearising the model in FLIGHTLAB [61].

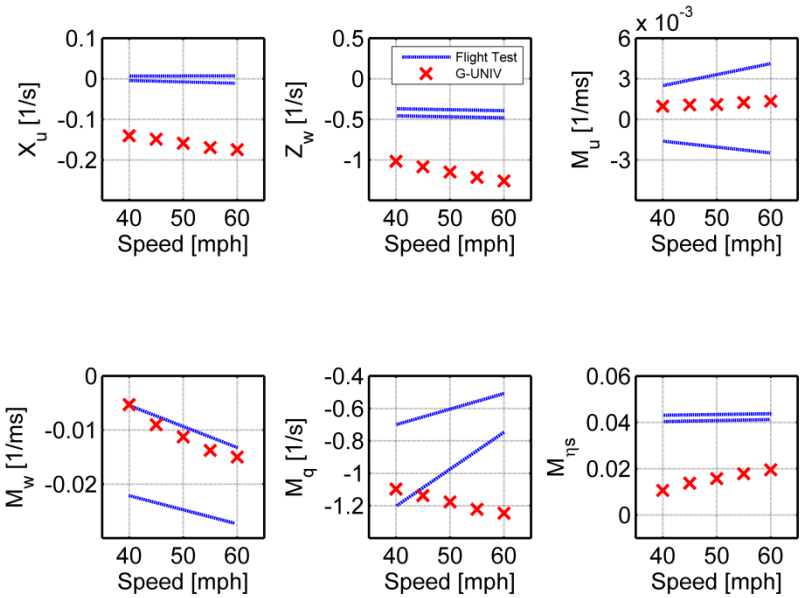

Figure 49: G-UNIV FLIGHTLAB model aerodynamic derivatives (red) compared to derivatives derived from flight test data (blue)

Figure 49 shows the model predicts both M_u (changing in pitch moment due to perturbation in forward velocity, sometimes referred to as speed stability) and M_w (heave damping) with reasonable agreement across the speed range.

X_u (drag damping), Z_w (normal force due to normal velocity), and $M_{\eta s}$ (moment due to longitudinal shaft perturbation) are less well predicted. The flight test data suggests that X_u, the drag damping derivative, is approximately equal to zero across the speed range, which would suggest there is almost no damping in the phugoid mode. The FLIGHTLAB model predicts a value between -0.1 and -0.2, implying there is damping present. $M_{\eta s}$, the longitudinal control sensitivity derivative, is also under-predicted by the model, suggesting that the model's response to control is somewhat less sensitive when compared to that of the real aircraft.

X_u is one of the key derivatives in prediction of the phugoid mode damping; the FLIGHTLAB model does not predict the value of X_U well. Figure 50 shows the individual component contributions which make up the total value of X_U. As part of the linearisation routines embedded within FLIGHTLAB, it is possible to extract the force and moment contributions to each individual derivative, from each individual model component, as an output parameter. It is possible to extract the forces acting on each component in the x, y and z directions (F_X, F_Y and F_Z) and as the location of the component relative to the centre of gravity is known, it is also possible to extract the corresponding contributions to the moments acting on the aircraft (M_X, M_Y and M_Z). The values of these contributions are normalised by the aircraft mass in the case of X_U.

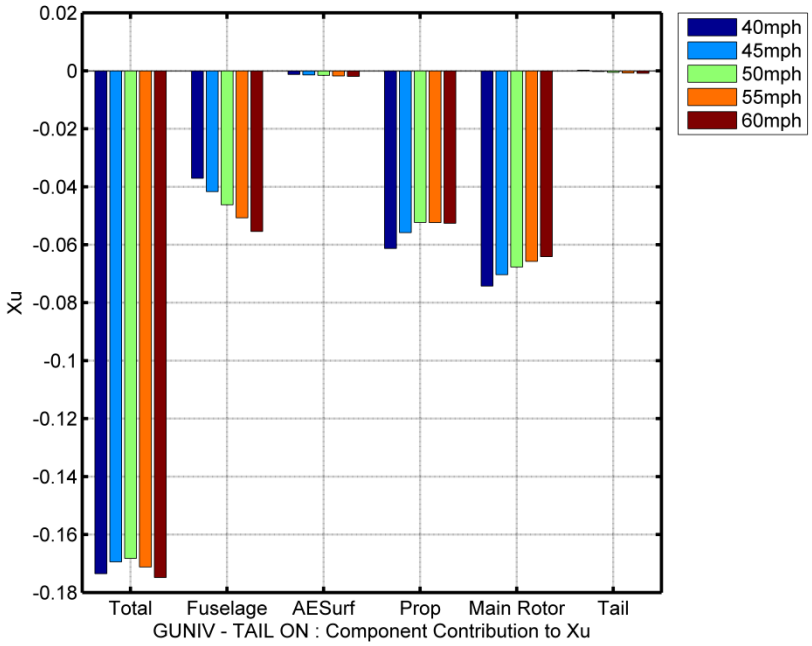

Figure 50: FLIGHTLAB-predicted contributions to X_U between 40 and 60mph

It can be seen that the main components which contribute to the total value of X_U are the fuselage, the main rotor and the propeller. These were three components were modelled using approximated data from alternative sources due to the unavailability of data from G-UNIV itself, resulting in the over-prediction of the drag damping. For example, the plan view of the G-UNIV compared to the VPM M14 shown in Figure 24 is much fatter than that of G-UNIV, thus the VPM M14 will have an increased profile drag compared to G-UNIV, although this was not taken in account in the modelling. As previously discussed, the NACA 8H12 used in the main rotor model is very sensitive to surface roughness, and as well as decreasing the amount of lift produced by the main rotor, if the surface roughness is increased compared to that taken from the wind tunnel data, the amount of drag produced by the rotor will be increased. The aerodynamic properties of the propeller also remain a complete unknown due to the custom nature of the aerofoil used. Although further artificial tuning of the fuselage aerodynamics may go some way to reducing the value of X_U, the only way to remedy these problems would be to perform a series of wind tunnel tests, similar to those described in [46], to characterise the G-UNIV fuselage aerodynamics and to characterise the aerodynamic properties of the actual G-UNIV rotor blades and propeller; this is an important area for further work to improve the model.

The pitch damping derivative, M_q, was tuned by varying the main rotor mass, as described in Section 3.3.4.1.2. This resulted in the magnitude of the model derivatives becoming comparable in magnitude to the values estimated from flight test, however the trend remains opposite, with the model derivatives becoming increasingly negative (restorative) as airspeed increases, whereas the flight test derivatives tend to become less negative as airspeed increases. This could be an artefact of the rigid blade model used in the simulation model.

3.5.4 Simulated Handling Qualities Flight Test for Validation

As a third method of validation, a programme of simulated handling qualities assessments, designed to replicate the tests performed by Bagiev and Thomson in Ref. 7, was carried out. Two manoeuvres from Ref. 7 were selected: the Slalom and the Acceleration-Deceleration. Inverse simulation was used to identify a range of course geometries to assess the flight envelope of the Montgomerie-Parsons autogyro. The results of replicating these tests are presented in the following sections.

3.5.4.1 Slalom

As previously stated, using inverse simulation techniques, Bagiev and Thomson modified the Slalom manoeuvre described in Ref. 7 to provide 5 courses of varying length and width (and thus aggressiveness) for the autogyro. The general geometry of the Slalom manoeuvre is shown in Figure 51 and the specific geometries of the courses used for testing are detailed in Table 20.

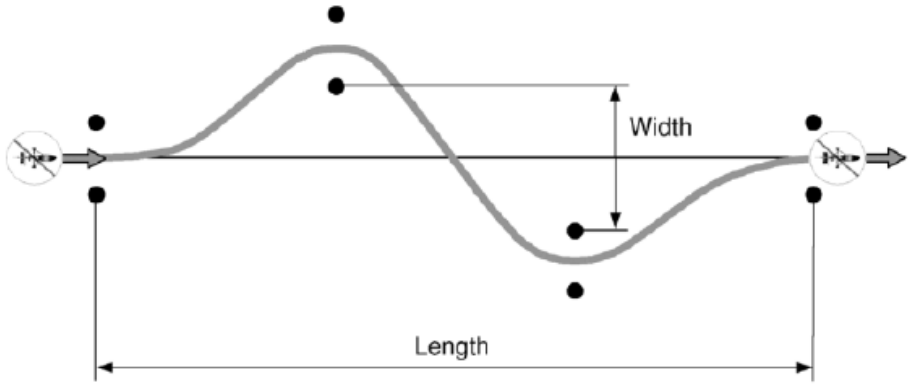

Figure 51: Slalom manoeuvre course layout [2]

Course Number	Length [m]	Width [m]	AR [ND]
1	400	30	0.067
2	300	30	0.1
3	225	30	0.13
4	300	60	0.2 (1)
5	150	30	0.2 (2)

Table 20: Slalom course geometries

In the simulation environment, the course is marked using a pair of 100ft high poles spaced 50ft apart. 100ft was chosen as this indicates to the pilot the height below which the manoeuvre must be completed. The appearance of the Slalom course in the simulation environment is shown in Figure 52. The pilot was allowed to perform a small number of familiarisation runs for each of the specified geometries and then 3 runs per geometry were performed, in a randomised order, to collect data.

Figure 52: Slalom course as presented to the pilot in the simulation environment

Ref. 2 specifies that the Slalom should be performed at a minimum airspeed of 60kts (≈70mph) in order to achieve desirable performance. It also specifies maintenance of an airspeed of 40kts or above as a boundary for adequate performance. Ref. 7 does not specify the limits for adequate performance, and as a result, creation of adequate criteria for the simulation trial was required. Bagiev and Thomson performed the Slalom at a range of airspeeds – 35, 50 and 70mph. The adequate performance criteria for each airspeed in the simulation trial was derived as 2/3 of the value of the desired performance criteria (in line with the relationship between the Ref. 2 values), as presented in Table 21.

It is worthy of note that the Montgomerie-Parsons aircraft manual states that the never-exceed speed (V_{NE}) of the autogyro is 70mph. It would therefore not be desirable to reach 70mph in regular operations. This is further reinforced by examination of Figure 8 in Ref. 7; the requirements of the test state that the manoeuvre should be initiated at 70mph, but the manoeuvre is actually initiated at approximately 67mph, and the pilot does not fly above this airspeed as is required of the manoeuvre.

	Maintain airspeed at or above:	Complete manoeuvre at or below reference height of:
Desirable criteria	(1) 70mph	100ft
	(2) 50mph	100ft
	(3) 35mph	100ft
Adequate criteria	(1) 46mph	100ft
	(2) 35mph	100ft
	(3) 22mph	100ft

Table 21: Desired and adequate performance requirements for Slalom manoeuvre

Each course geometry was flown 3 times at each of the 3 airspeeds of Table 2. The pilot was asked to rate all three runs on the Cooper-Harper Handling Qualities rating scale [54] and the Bedford Workload scale [78]. Although it is not standard practice (as it can mask poor HQRs and imposes a false linearity on the Cooper-Harper Scale), averaged HQRs are presented in order to allow comparison with the work performed in Ref. 7.

A comparison of the results for Slalom from both simulated and actual flight trials [7] are presented in Table 22. Level 1 HQRS are highlighted in green, Level 2 HQRs in yellow and Level 3 HQRS in orange. It can be seen that, as airspeed and AR (and thus the aggression required to complete the manoeuvre) increases, the HQRs assigned by the pilot degrade. It can also been seen that, broadly speaking, there is a good agreement between the overall handling qualities levels assigned in both the simulated and actual flight tests, which suggests the simulation model has comparable handling qualities to the G-UNIV aircraft. The HQRs are plotted for comparison in Figure 53.

Course	AR	Airspeed (mph)	Average HQR (Simulation)	Average HQR (Flight Test)
1	0.067	35	2	2
	0.067	50	2.3	2.5
	0.067	70	5.7	4.5
2	0.1	35	3	4
	0.1	50	4.3	4.5

	0.1	70	6.3	6
3	0.13	35	3.3	3.5
	0.13	50	5.7	5
	0.13	70	6.7	7
4	0.2 (1)	35	4	4.5
	0.2 (1)	50	5	6
	0.2 (1)	70	6	8
5	0.2 (2)	35	7.7	7
	0.2 (2)	50	8	8
	0.2 (2)	70	8.3	--

Table 22: A comparison of results from the Slalom manoeuvre between simulated flight trials and real flight trials

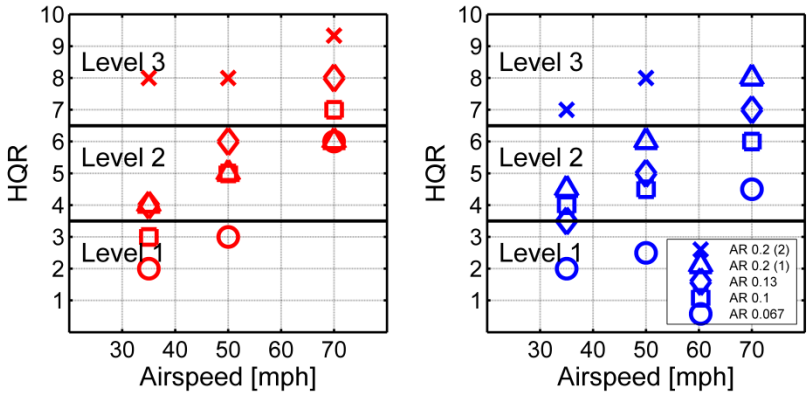

Figure 53: Comparison between simulated (red) and actual (blue) flight test HQRs for the Slalom manoeuvre

As was the case for the flight testing, when performing the Slalom task during the simulation trial, the pilot was unable to achieve 70mph. This affected the HQR the pilot was able to award when rating the aircraft on the Cooper-Harper scale, as desired performance (70mph and above) could not be achieved. This differs from the view created by HQRs awarded by the pilot who flew the manoeuvre in Ref. 7, shown in Figure 54. For example, for Slalom course 1 (AR 0.067) with a target airspeed of 70mph, the pilot gave an averaged HQR of 4.5. This would suggest that the aircraft was able to meet and maintain airspeed of 70mph or more throughout the manoeuvre.

The information contained within the aircraft manual and the performance demonstrated by the simulation model suggest that this is unlikely. This may have arisen due to the experience level of the pilot used for the flight trial described in Ref. 7. Whilst being an experienced autogyro pilot, he was not a trained test pilot. He was therefore unfamiliar with the use of rating scales and the process of evaluating an aircraft using a rating scale within the bounds of performance criteria.

Figure 55 shows the comparison of assigned HQRs from the simulated trial with the flight envelope predicted by the inverse simulation described in Ref. 7. All geometries that lie outside the predicted flight envelope were assigned HQRs in Level 3 (denoted by triangular markers); this is the same result as was observed in Ref. 7, as presented in Figure 55, suggesting that the simulation model has a comparable flight envelope to that of the real aircraft.

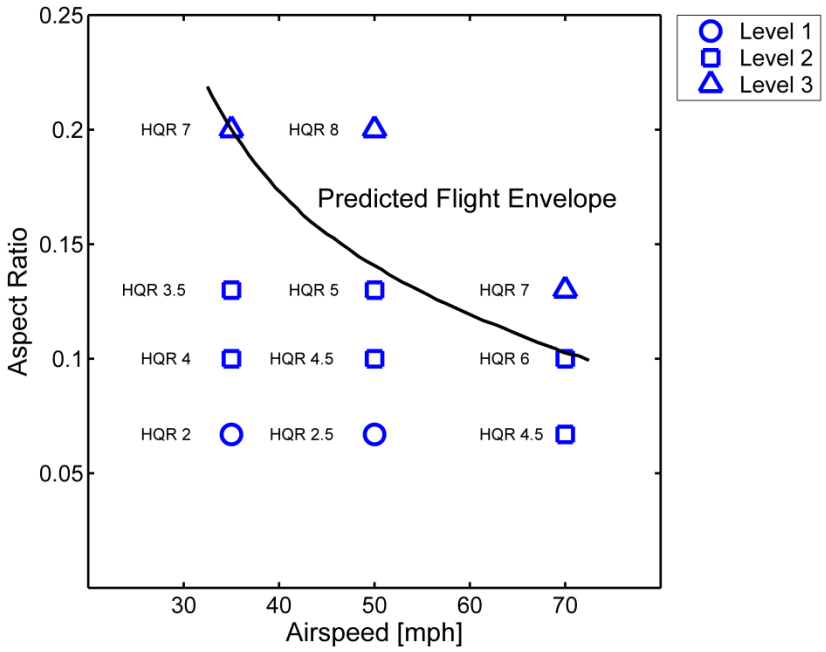

Figure 54: Predicted flight envelope for the Slalom manoeuvre compared to assigned HQRs from flight trial described in Ref. 7

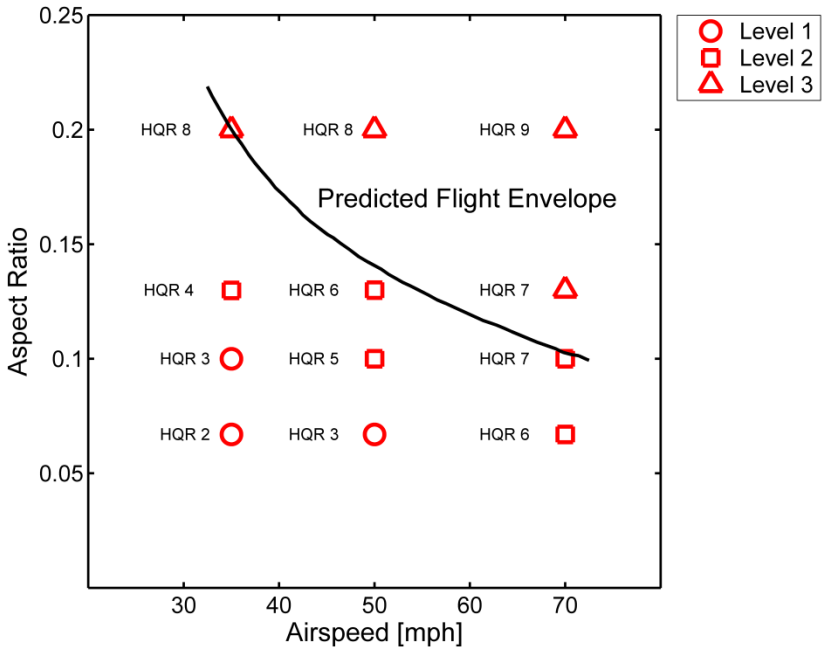

Figure 55: Predicted flight envelope for the Slalom manoeuvre compared to assigned HQRs from simulated flight trial

During the flight test described in Ref. 7, the pilot was unable to complete the course for the AR 0.2 (2) 70mph test point. However, it was possible for the pilot to complete the manoeuvre using the G-UNIV simulation model. A number of potential explanations for this are forthcoming. Firstly, the simulator provides a "safe" environment for the pilot. As such, he is able to fly the aircraft closer to its limits, and perhaps attempt manoeuvres which he would be uncomfortable or unwilling to perform in the real aircraft. It may also be a reflection of pilot skill and/or confidence. The pilot used in Ref. 7 was not a trained test pilot, and although highly experienced in flying this type of aircraft, may not have been practised in performing manoeuvres at such high levels of aggression. Thus, he may not have been able to approach the limits of the aircraft's performance envelope as would a test pilot.

Another key observation made during the Slalom flight test concerned the amount of sideslip being allowed to develop to complete the manoeuvre. In the flight test described in Ref. 7, the pilot is observed to be using "high angles of sideslip" to complete the Slalom manoeuvre. In comparison to this, during the simulated flight

test, the pilot used relatively small angles of sideslip (less than 5° in the simulated flight compared to over 30° at a peak for the original flight test for the AR 0.13 70mph case). The Slalom manoeuvre described in Ref. 7 does not prescribe a limit on the amount of sideslip permissible during the Slalom manoeuvre; however, the manoeuvre is typically flown using lateral stick as the primary control, with pedals used to co-ordinate turns. This strategy was employed by the pilot during the simulated flight test.

Whilst these differences in piloting technique and experience level do have an effect on the outcome of the ratings awarded, they were only shown to affect the extremes of the flight envelope, and therefore the majority of the ratings given are considered appropriate for comparison. Hence, it is possible to draw the conclusion that the simulation model and the real aircraft have comparable handling qualities.

3.5.4.2 Acceleration-Deceleration

As an autogyro cannot hover in the conventional sense, the Acceleration-Deceleration manoeuvre of Ref. 2 required some modification to make it suitable for this type of aircraft. The manoeuvre was therefore initiated at a specified airspeed (as opposed to the hover); the aircraft was then required to accelerate to a target airspeed before completing the manoeuvre by decelerating back to the initiation airspeed. In this way, the fundamental nature of the Acceleration-Deceleration manoeuvre was maintained, but made provision for aircraft with no hover capability. In order to assess the airspeed requirements, a range of initiation and target airspeeds were used, as detailed in Table 23.

Course	Initiation Airspeed (mph)	Target Airspeed (mph)
1	35	60
2	35	70
3	40	50
4	50	60
5	50	60
6	50	70

Table 23: Acceleration-Deceleration courses with airspeeds

Poles at the edges of a runway denote the Acceleration-Deceleration course, spaced at 500ft intervals, as shown in Figure 56.

Alongside the speed requirements, adequate and desired conditions for the altitude, position and heading were specified for the manoeuvre, as defined in Table 24.

	Desirable criteria	**Adequate criteria**
Maintain altitude below:	50ft	70ft
Maintain lateral track within:	±3m (10ft)	±6m (20ft)
Maintain heading within:	±10°	±20°

Table 24: Adequate and desired requirements for the Acceleration-Deceleration manoeuvre

Figure 56: The Acceleration-Deceleration course in the simulation environment

Ref. 2 also defines a requirement on pitch attitude for helicopter operations. As the autogyro mainly uses propeller thrust for rapid acceleration and deceleration, this

requirement was not considered appropriate and was removed for the purposes of the flight test.

The assigned handling qualities and workload ratings for the Acceleration-Deceleration manoeuvres are shown in Table 25.

Course	Airspeed Range (mph)	Average HQR (Simulation)	Average HQR (Flight Test)
1	35-60-35	4	2
2	35-70-35	4	2.5
3	40-50-40	4	1.5
4	40-60-40	4	2
5	50-60-50	2.3	2
6	50-70-50	2	4

Table 25: Simulation trial Acceleration-Deceleration results

A comparison of the assigned handling qualities for the Acceleration-Deceleration manoeuvre is presented in Figure 57. It can be seen that the assigned handling qualities for the Acceleration-Deceleration manoeuvre generally lie within different levels when the simulated flight test is compared to the original flight test. During the simulated flight trial, the test pilot commented on the presence of a lateral-directional cross coupling at the lower end of the speed range (40mph and below), resulting in moderate pilot compensation being required to stabilise the airspeed when returning to the initiation airspeed at the end of the manoeuvre. It was this compensation which resulted in the pilot assigning Level 2 handling qualities for these manoeuvres. This cross coupling became less problematic as forward airspeed increased, and thus the handling qualities rating improved to Level 1 for the manoeuvres flown at higher airspeeds. This may indicate a difference in the dynamic response of the simulation model but other factors are worthy of consideration (although these are only speculative).

The pilot used in the original flight tests had over 5000 hours of flying time on autogyros. The test pilot used for the simulated flight trials had approximately 2000 hours on fixed wing and 3000 hours on rotary wing aircraft. As was the case for the manoeuvres described previously in this Chapter, it may be that the autogyro pilot altered his piloting

technique (perhaps subconsciously) to mitigate the effects of this cross coupling present at lower airspeeds. Conversely, the simulator pilot had to make a conscious effort to achieve the same effect, which could have led to higher handling qualities ratings being awarded. A further possibility exists - the experienced autogyro pilot may have been more willing to tolerate deficiencies in the dynamic response of the aircraft because of this type familiarity than a pilot inexperienced on type, thus resulting in the pilot awarding better HQRs that perhaps would have been awarded without this familiarity.

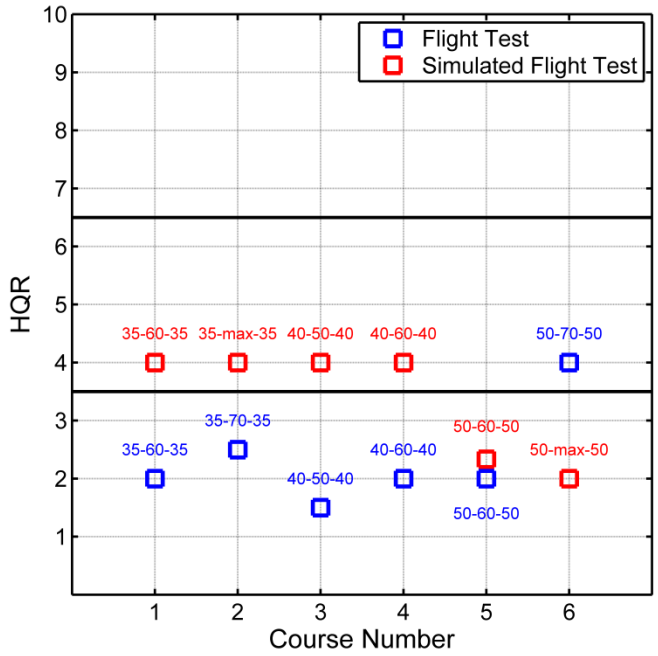

Figure 57: Comparison between averaged assigned HQRs for the Acceleration-Deceleration manoeuvre in simulated and actual flight tests

3.6 CONCLUSIONS

A model of the Montgomerie-Parsons autogyro designated 'G-UNIV' has been created using FLIGHTLAB. This model has been tuned using, and validated against, flight test data. Despite often considerable nature of the tuning required, the resulting model has been shown to exhibit trimmed control positions, dynamic responses and derivatives comparable to those of the real aircraft. The aircraft was also validated through simulated flight tests, and was found to exhibit similar handling qualities to that of the real aircraft.

In a similar manner, a model of a helicopter which is geometrically similar to the G-UNIV autogyro has also been created. Centre of gravity position and engine and horizontal stabiliser size were all estimated based on trends observed within the sizing of other light helicopters, and the sizing of the main and tail rotors were retained from the original G-UNIV model. As a hypothetical vehicle, it was not possible to validate this model against flight test data.

Chapter 4

EVALUATION OF EXISTING CAA RECOMMENDATIONS

After a series of 5 fatal autogyro accidents between 1989 and 1991, the Civil Aviation Authority (CAA) commissioned a programme of research into both the airworthiness and aerodynamic characteristics of light autogyros. The results of this programme of research were published in CAA Report 2009/02 [4].

Paper 2009/02 [4] presented 4 main findings/recommendations:

1. It is recommended that the vertical location of the centre of gravity (c.g.) should lie within a ± 2 inch envelope of the propeller thrust line.

This recommendation was included in the revision of CAP 643 British Civil Aviation Requirements Section T: Light Gyroplanes [5] (referred to as BCAR Section T), the CAA's autogyro airworthiness and design standard.

2. Horizontal tailplanes are largely ineffective in improving the long term pitch dynamic stability (phugoid mode).

3. Extreme manoeuvring can lead to excessive rotor teeter angles during certain phases of flight, potentially resulting in the rotor blades striking the prop or empennage.

A recommendation to ensure satisfactory control margin and rotor clearance up to 1.1 V_{NE} was included in the revision of Ref. 5 as a result of this recommendation.

4. The chordwise centre of gravity of the rotor blades should always lie at or ahead of the 25% chord position to prevent rotor blade instability.

Paper 2009/02 serves as an illustration of the growing body of knowledge surrounding autogyros; however, it concludes that "*there remains little indication that rigorous scientific or engineering investigation of airworthiness has occurred*" [4] due to the limited number of configurations used in the research.

Where possible these recommendations were addressed through use of the autogyro model described in Chapter 3. The results of this investigation and the development of related ideas are discussed in this Chapter.

4.1 VERTICAL CENTRE OF GRAVITY POSITIONING

The first recommendation from Ref. 4 states that the centre of gravity of the aircraft should be located vertically within an envelope described by ±2 inches of the propeller thrust line to ensure long-term pitch stability is achieved. In order to scrutinise this recommendation, five versions of the model were created, with the c.g. located at ±4 inches, ±2inches and coincident with the propeller thrust line. The nominal aircraft c.g. position is located 1.49 inches (3.8cm) below the prop thrust line.

The G-UNIV simulation model developed in Chapter 3 is a non-linear model, which enables high fidelity, real-time dynamic manoeuvring to be undertaken. However, for the purposes of stability analysis, FLIGHTLAB allows for the generation of bespoke, reduced-order linear simulation models for a given flight condition. This linearisation process, described in Ref. 62, uses an extension to the classical longitudinal equations of motion that includes rotor speed as a degree of freedom. This extension was required to enable the rotor acceleration to be driven to zero by the linearisation process, to account for the fact that the autogyro's main rotor speed is not governed, thus ensuring that the model was appropriately trimmed. The process was repeated for each of the five c.g. positions across a speed range of 30 – 70mph in 5mph increments, and the resulting eigenvalues are presented in Figure 58.

Figure 58 shows the progression of the phugoid mode eigenvalues derived from the linearised models across the S-plane for variations in both c.g. position and airspeed. All eigenvalues corresponding to oscillatory modes exist in complex conjugate pairs, but for clarity only the positive imaginary half of the scale is shown. For all configurations, the eigenvalues are seen to migrate from the right-hand half plane (the unstable region) to the left-hand half plane (the stable region) as airspeed increases. It should be noted that the model was unable to achieve trimmed flight at 35mph for the +2 and +4 inch c.g. positions, hence the corresponding lines on Figure 58 begin at 40mph.

Figure 59 shows the behaviour of the phugoid mode eigenvalues at the lower end of the speed range, in 1mph increments between 35 and 50mph.

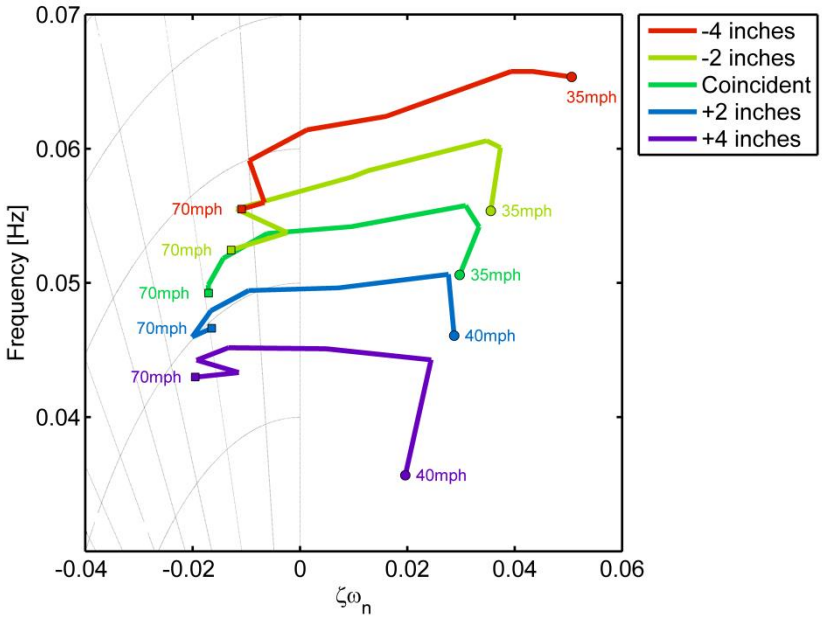

Figure 58: Phugoid mode Eigenvalues for G-UNIV with varying vertical centre of gravity positions relative to the propeller thrustline

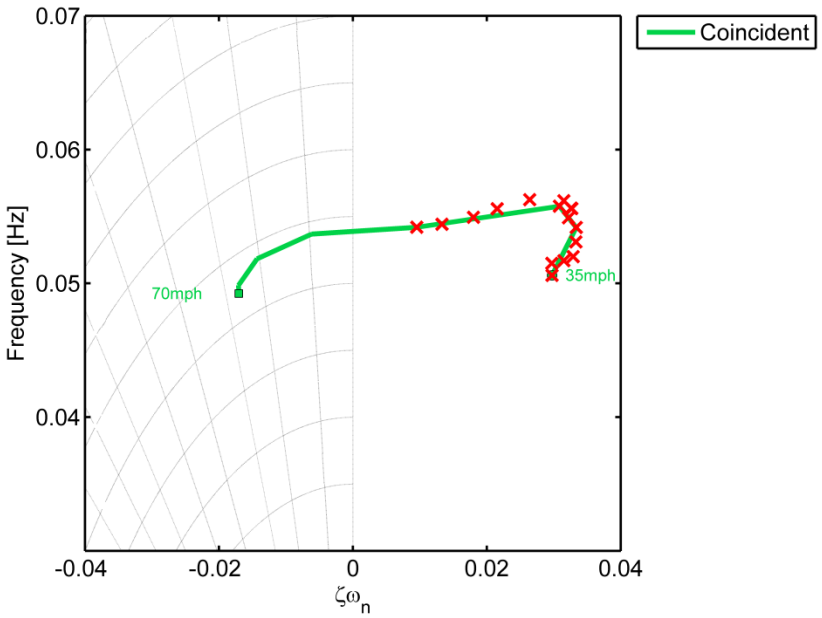

Figure 59: Phugoid mode Eigenvalues for G-UNIV with coincident propeller and vertical centre of gravity position showing Eigenvalues derived in 1mph increments

The recommendation in Ref. 4 states that the vertical position of the centre of gravity should lie within a ±2 inch envelope of the propeller thrustline as "a sensible design aim to achieve pitch dynamic stability". Figure 58 clearly illustrates that it is the increasing airspeed which forces the phugoid mode eigenvalues into the stable region, not the position of the vertical centre of gravity relative to the thrustline (for this aircraft). This is due to the increase in tailplane effectiveness with increasing airspeed. As an example, the phugoid mode becomes stable between 50 and 55 mph for the aircraft with the c.g. located at the +4 inch position; moving the c.g. to the position where it is coincident with the propeller thrustline, thus complying with the ±2 inch envelope recommendation, results in no change to the point at which the phugoid becomes stable.

Figure 58 also shows that varying the location of the vertical position of the c.g. altered the frequency of the phugoid mode oscillation. For the lowest common speed (40mph), this varied from 0.035Hz to 0.066Hz, corresponding to a difference in phugoid period of 13.4 seconds; this represents a significant change in long period aircraft response. This may have implications for the handling qualities of the aircraft, and its degree of compliance to the relevant airworthiness requirements.

BCAR Section T [5], the Civil Aviation Authority's airworthiness requirements for autogyros, places compliance limits on the time which oscillations must damp to one half amplitude based on their period as follows:

"Longitudinal, lateral or directional oscillations with controls fixed or free and following a single disturbance in smooth air, should at least meet the following criteria:

- *a) Any oscillation having a period of less than 5 seconds should damp to one-half amplitude in not more than one cycle. There should be no tendency for undamped small amplitude oscillations to persist.*
- *b) Any oscillation having a period between 5 and 10 seconds should damp to one half amplitude in not more than two cycles. There should be no tendency for undamped small oscillations to persist.*
- *c) Any oscillation having a period between 10 and 20 seconds should be damped, and in no circumstances should an oscillation having a period*

greater than 20 seconds achieve more than double amplitude in less than 20 seconds."

These limits are shown in Figure 60, overlaid with the phugoid mode eigenvalues. The aircraft is compliant with the BCAR Section T requirements if these values lie to the left hand side of the bold black line. It can be seen that all configurations which meet the previously recommended ±2 inch envelope recommendation do not meet the BCAR Section T requirements below 55mph, whilst the configuration with the centre of gravity located 4inches above the thrustline meets the requirement for all airspeeds.

The analysis presented in this Section does not entirely contradict the recommendation for the positioning of the thrustline relative to the vertical position of the centre of gravity made in Ref. 4. However, it should be noted that it is in direct opposition to the results of the weight and balance survey of single-seat aircraft carried out by the CAA [79]. As part of this survey, 5 aircraft were tested. Only one of these 5 was found to conform to the handling requirements detailed within BCAR Section T; the aircraft that had been modified such that its centre of gravity was positioned within ±2 inches of the propeller thrustline. However, Figure 60 shows that despite modification in order to meet the ±2 inch criterion, this configuration of aircraft (G-UNIV) does not meet the BCAR Section T requirements. This suggests that the ±2 inch recommendation for the position of the centre of gravity may be overly restrictive, preventing the aircraft from achieving compliance with this BCAR Section T requirement. It may also be the case that the recommendations made in Ref. 79, whilst valid for the aircraft tested, are not appropriate for read-across to other types of autogyro. For example, Figure 60 shows that positioning the centre of gravity 4 inches above the propeller thrustline would allow the aircraft to become compliant with BCAR Section T across its entire flight envelope.

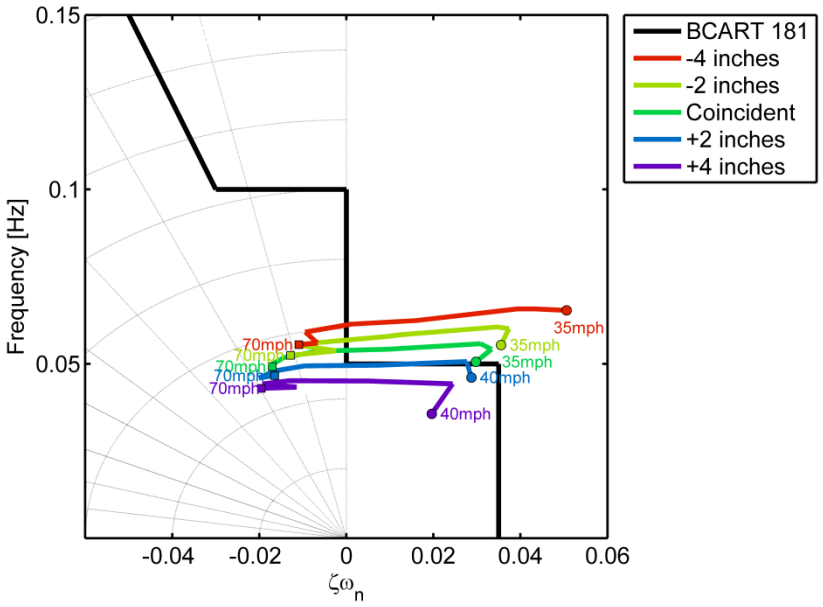

Figure 60: Phugoid mode Eigenvalues for G-UNIV with varying vertical centre of gravity positions relative to the propeller thrustline, overlaid with BCAR Section T requirements

4.1.1 Aerodynamic derivatives and vertical centre of gravity positioning

Ref. 50 states that the dominant effect of changing the vertical position of the centre of gravity is on the heave damping derivative M_w; a key derivative in the characterisation of both the short period and phugoid modes. M_q and M_u also play a key role in the stability characteristics of the phugoid mode. Xu (drag damping) also plays an important role in characterising the frequency of the phugoid mode.

As part of the linearisation process, FLIGHTLAB populates tables of all applicable aerodynamic derivatives; these were recorded for each variation in c.g. position and airspeed. Figure 61 illustrates the effect of moving the vertical centre of gravity relative to the propeller thrustline on the resulting value of M_w (which had not been characterised by Ref. 50). Similarly, Figure 62 and Figure 63 show the results for M_q and M_u.

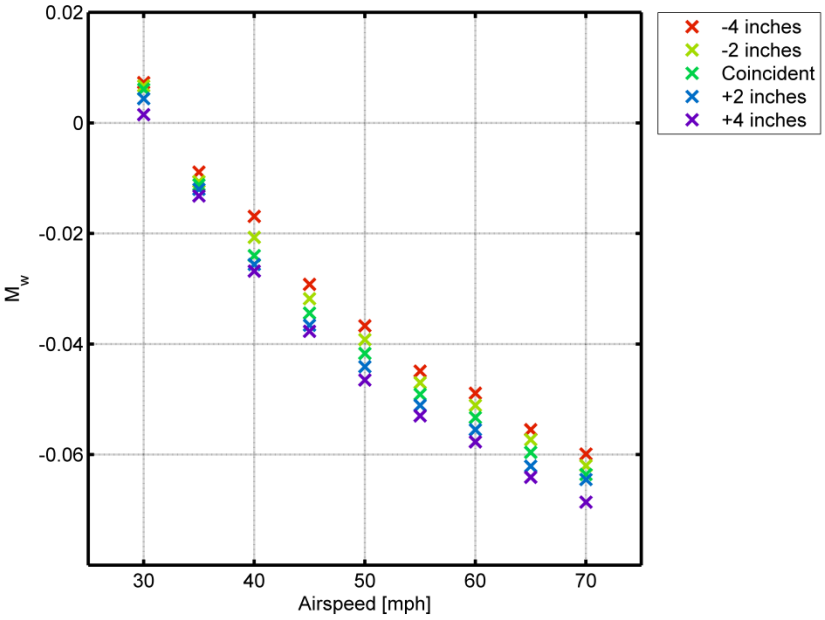

Figure 61: Variation of M_w with vertical centre of gravity position

Figure 61 shows that moving the vertical position of the c.g. has a clear effect on each of the derivatives. Specifically, positive vertical displacement of the c.g. was shown to cause a reduction in $M_{w,}$ becoming more pronounced with airspeed.

Figure 62 shows the vairation of M_q with vertical centre of gravity position and with airspeed. M_q is seen to become increasingly negative as the position of the centre of gravity moves downwards, effectively reducing the pitch damping, which will lead to a reduction in the frequency of the phugoid mode, as seen in Figure 60. M_q has the largest magnitude of all three derivatives being considered and is therefore the most dominant in defining the behaviour of the phugoid mode.

Figure 63 shows the variation of M_u, the pitching moment due to change in speed. As expected, the values for theconfiguration in which the vertical centre of gravity is coincident with the propeller thrustline, and thus the moment arm is reduced to zero, are approximately zero. As the c.g. moves above or below the propeller thrustline, the value of M_u becomes correspondingly negative or positive, the magnitude of the ±4inch configuration values of M_u being approximately double those of the corresponding

±2inch configuration. As is usual for a fixed wing aircraft, the values of M_u are small compared to those of the other derivatives due to the low speeds being considered.

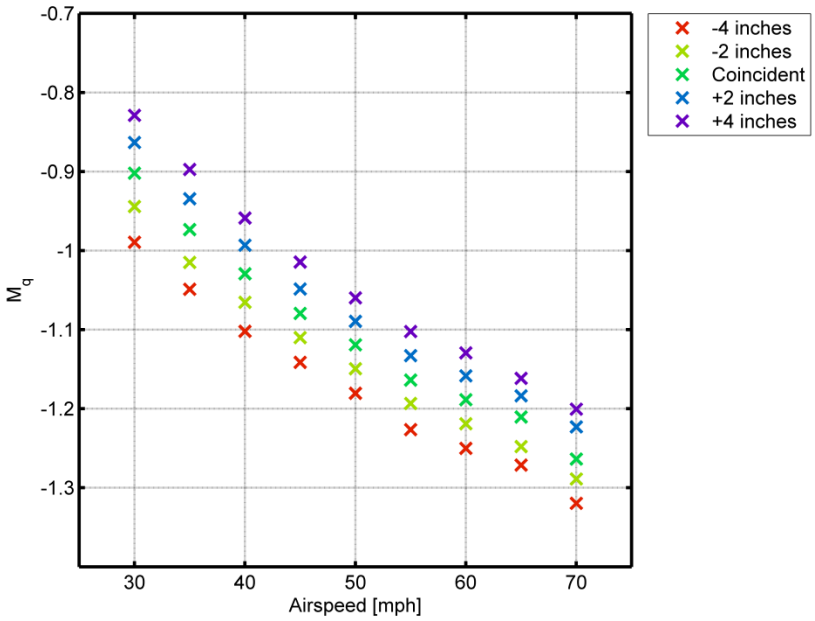

Figure 62: Variation of M_q with vertical centre of gravity position

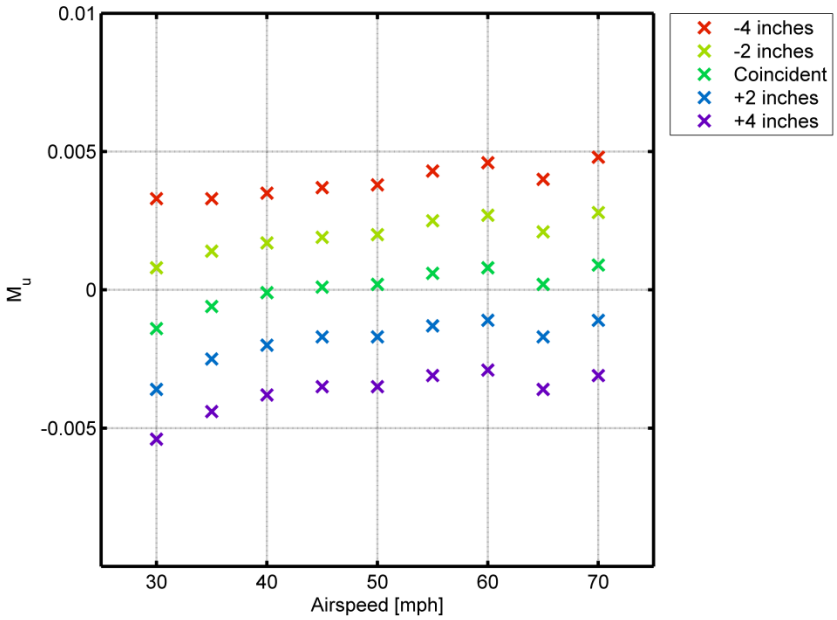

Figure 63: Variation of M_u with vertical centre of gravity position

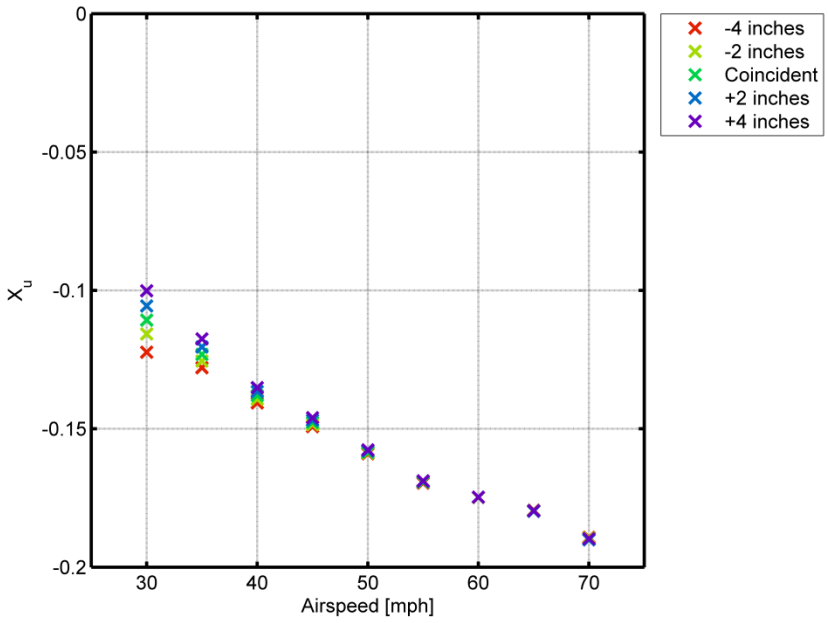

Figure 64: Variation of Xu with vertical centre of gravity position

Figure 64 shows the variation of X_U (also referred to as drag damping) with speed for the 5 vertical centre of gravity positions. It can be seen that the effect of the vertical position of the centre of gravity has the most effect on the value of X_U at the lower end of the speed range.

The effect of this variation in the magnitude of X_U can be seen in Figure 60; the phugoid mode eigenvalues at the lower end of the speed range show a much wider variation in frequency, with the -4 inch configuration having the highest frequency and the largest value of X_U and the +4 inch configuration having the lowest frequency and the smallest value of X_U at 35mph. As airspeed increases, the values of X_U begin to converge; this is again reflected in Figure 60, with the value of the phugoid mode frequency converging over a smaller range at the higher end of the speed range (70mph).

4.2 TAILPLANE EFFECTIVENESS

The requirement for a horizontal stabiliser is an issue of some debate within the autogyro community. Before the publication of CAA Paper 2009/02, *"The Aerodynamics of Gyroplanes"* [4], there was little published research into the effectiveness of the autogyro

tailplane or its effect on the handling qualities and the longitudinal dynamic stability characteristics of the aircraft (specifically, the phugoid mode). Much of the experience and knowledge accumulated on this subject comes anecdotally from autogyro pilots and/or aircraft homebuilders, and as such does not have the support of "rigorous and objective analysis" [4].

In order to assess tailplane effectiveness, a separate model of the G-UNIV autogyro was created with the horizontal tail surface removed. The geometry of the vertical fin and rudder assembly remain the same. In reality, removal of the tailplane would also necessitate removal of the winglets; however, in order to isolate the effect of the removal of the tailplane, the aerodynamic modelling of the winglets remain.

4.2.1 Trimmed Flight Control Positions

Figure 65 shows a comparison of the trimmed control positions for both 'tail on' and 'tail off' aircraft configurations. It can be seen that removal of the tailplane results in a considerable change in both the magnitude and trend of the longitudinal shaft tilt (and thus the longitudinal stick position). With the tailplane attached, as airspeed increases the longitudinal shaft tilt reduces linearly, providing the pilot with predictable tactile cues (as there is a direct relationship between longitudinal shaft tilt and longitudinal stick position). With the tailplane removed, the longitudinal shaft tilt is seen to initially decrease, reaching a minimum value at 45mph before beginning to increasing again as airspeed continues to increase. This no longer provides the predictable tactile cues that were apparent for the 'tail on' configuration, which may lead to an increased pilot workload due to increased complexity in required control strategy and unpredictable handling, potentially presenting a safety risk.

For the 'tail off' configuration, the longitudinal shaft tilt displays a trend analogous to the drag curve of the aircraft. This is due to the fact that the rotor speed and thus the amount of lift and drag generated by the main rotor, increases with the square airspeed due to the increased mass of air passing through the rotor.

Similarly for the 'tail on' configuration, the magnitude of the force in the vertical direction produced by the tailplane increases with the square of airspeed (as shown in Figure 32), but due to the reducing pitch attitude the direction of this forces changes as airspeed

increases, becoming negative at 50mph. At speeds below 50mph, where the tail is contributing a positive force I the vertical direction, the longitudinal shaft tilt increases to reduce the lift force being generated by the main rotor. At speeds above 50mph, where the tail is opposing the action of the main rotor lift, the main rotor shaft tilt reduces to compensate. This results in the linear decrease in longitudinal shaft tilt shown in Figure 65.

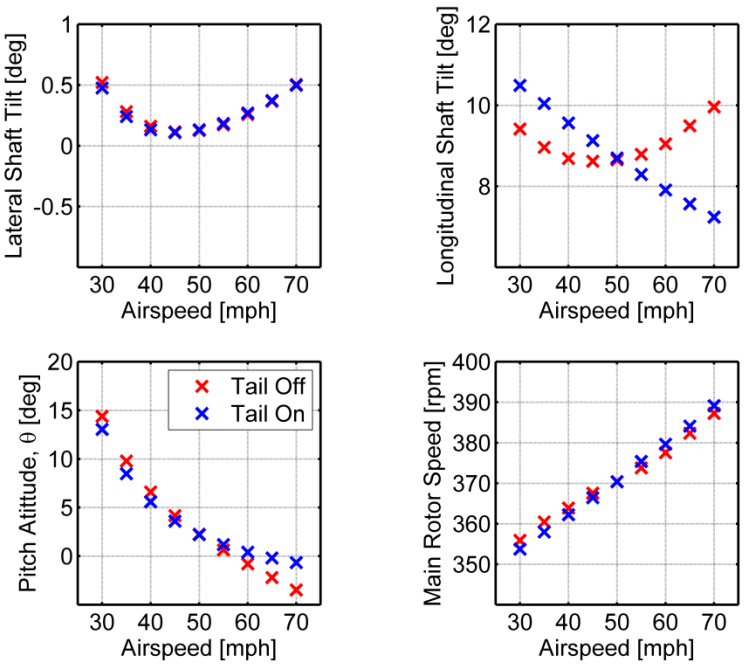

Figure 65: A comparison of trimmed flight control positions for 'tail on' and 'tail off' configuration

Removal of the tailplane, for this configuration, can be seen to have a considerable effect on the trimmed flight control positions, in direct contrast to the recommendations made in Ref. 4 which states that "trim is insignificantly affected by the tailplane".

4.2.2 The Phugoid Mode

Similar to the analysis described in Section 4, both 'tail on' and 'tail off' models were trimmed and linearised from 35 to 70mph. The phugoid mode eigenvalues are shown in Figure 66 for both configurations.

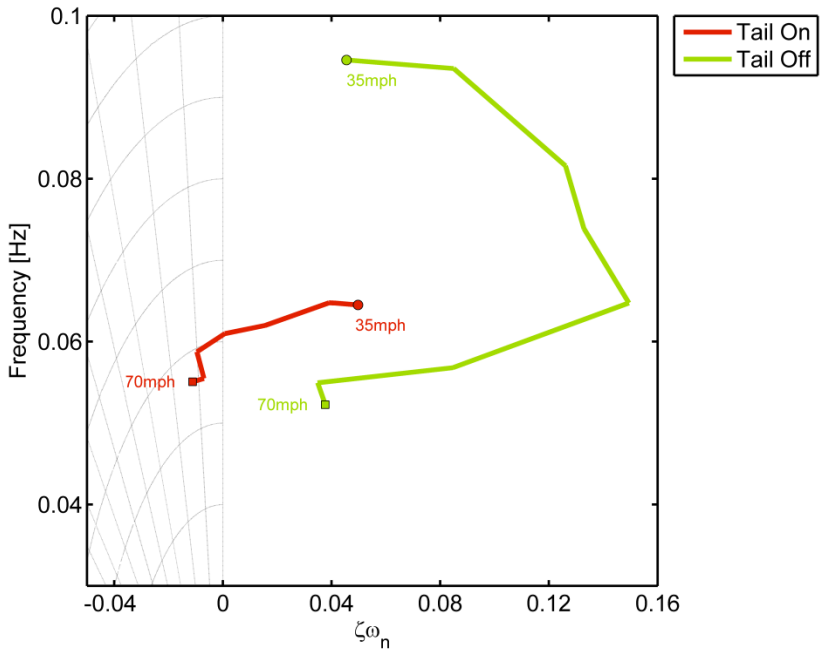

Figure 66: Comparison of phugoid mode eigenvalues for autogyros configured both with and without a horizontal tailplane

Figure 66 illustrates that removing the tailplane has a dramatic effect on the characteristsics of the phugiod mode for an aircraft of this configuration. At low airspeed the frequency of the phugoid mode is considerably increased. Removal of the tailplane also results in the phugoid mode characteristics varying in a much less predictable manner as airspeed increases; unpredictabiltiy in the phugoid mode may result in handling qualities deficiencies in flight. These results contradict the findings presented in Ref. 4, which show that "the phugoid mode is negligibly affected by the presence of a tailplane at low to medium speeds".

In order to assess the impact of the precence of the tailplane on B CAR T compliance, these eigenvalues were plotted against the phugoid mode requirements in Figure 67.

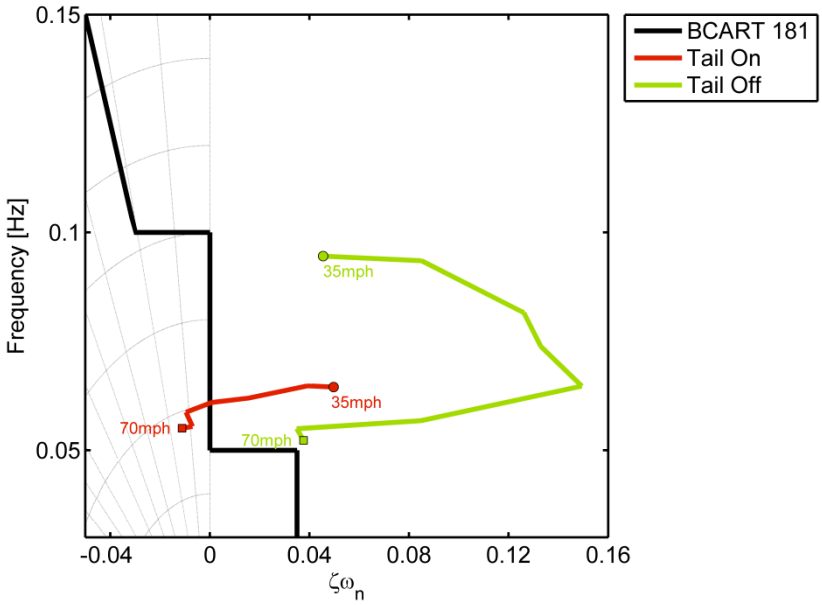

Figure 67: Comparison of phugoid mode eigenvalues for autogyro configured both with and without a horizontal tailplane, overlaid with BCAR Section T requirements

Figure 67 shows that, in the absence of the tailplane, the phugoid remains non-compliant across the range of airspeeds tested. Conversely, with the tailplane, the phugiod mode moves into the compliance region as airspeed increases above 50mph. The degree to which this contradicts the findings of Ref. 4 depends upon the precise definition of "low to medium speeds"; no further details were available to investigate this further.

4.2.3 The Short Period

Figure 68 shows a comparison between the short period and phugoid modes for the tail on and tail off aircraft configurations. It can be seen that removal of the tailplane results in significant changes to the characteristics of the short period mode; without a tailplane the short period mode becomes non-oscillatory. This supports the findings of Ref. 4, and is investigated in further detail in the subsequent Sections.

Despite the differences in the short period dynamic characteristics, Figure 68 shows that both configurations of aircraft are compliant with the requirements of BCAR Section T. Despite this, the fundamental change in the characteristics of the short period with and without a tailplane will result in the pilot experiencing a difference in the handling of the

aircraft, which may result in handling qualities deficiencies. This is discussed further as part of the piloted evaluation reported in Chapter 6.

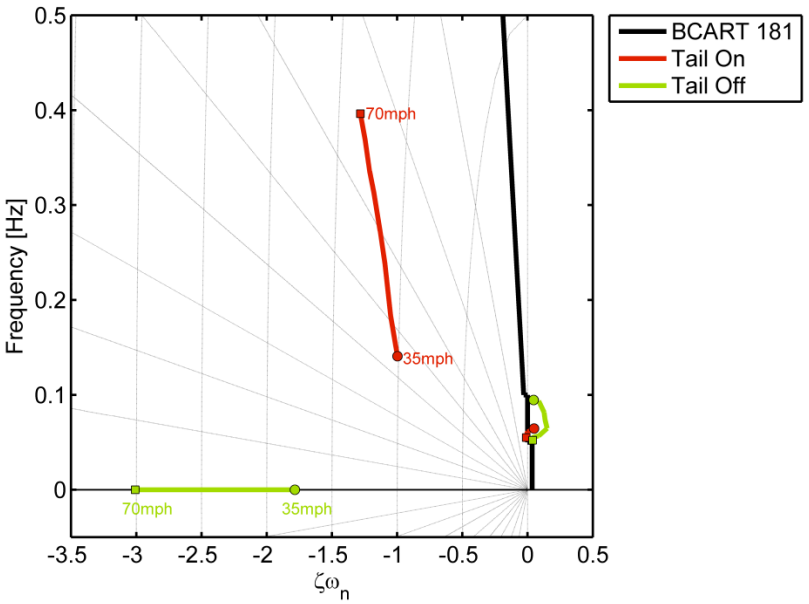

Figure 68: A comparison of the short period modes for both the tail on and tail off configurations, overlaid with BCAR Section T requirements

4.2.4 *Aerodynamic Derivatives*

Figure 69 shows the change in the values of the longitudinal stability derivatives which are key to the characterisation of the phugoid mode as airspeed increases for both the 'tail on' and 'tail off' configurations. It can be observed that, for this particular aircraft, that the removal of the tailplane results in significant differences in both the values of the derivatives and the manner in which they vary as airspeed increases. As X_U is dominated by contributions from the fuselage, main rotor and the propeller it is not considered here.

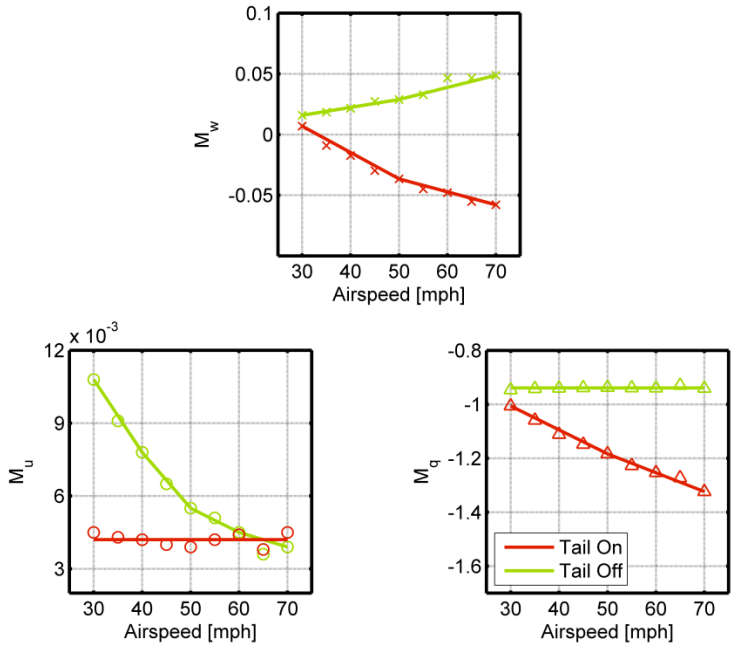

Figure 69: Comparison of the variation of aerodynamic derivatives key to phugoid stability with airspeed for both tail on and tail off configurations

4.2.4.1 *M_w – Heave Damping*

With the tailplane attached, Figure 69 shows that M_w becomes increasingly negative (stabilising) as airspeed, and thus tailplane effectiveness, increases. An opposite trend is observed for the configuration without a tailplane; M_w becomes increasingly positive (destabilising) as airspeed increases.

Figure 70 and Figure 71 show the individual component contributions which make up the total value of the aerodynamic derivative. As part of the linearisation routines embedded within FLIGHTLAB, it is possible to extract the force and moment contributions to each

individual derivative, from each individual component, as an output parameter. It is possible to extract the forces acting on each component in the x, y and z directions (F_X, F_Y and F_Z) and as the location of the component relative to the centre of gravity is known, it is also possible to extract the corresponding contributions to the moments acting on the aircraft (M_X, M_Y and M_Z). The values of these contributions are normalised by the pitch moment of inertia (as they are all pitch derivatives being considered in this case).

Contributions from the fuselage, propeller, main rotor and horizontal tail surface are considered. The major column labelled 'AESurf' represents the contribution from the remaining aerodynamic surfaces; in this case the rudder, vertical fin and winglets. The sum of the contributions from these components when added together gives the total value of the derivative under consideration.

The first column shows the absolute value of the derivative, in this case M_w. This is derived from the linearised model of the aircraft. The aircraft model was linearised in 5mph increments from 30 to 70mph. The minor columns within each component contribution represent each of these airspeeds, with dark blue representing 30mph, through to dark red representing 70mph.

It can be seen in Figure 70 that the tailplane provides a large restorative contribution to the overall value of M_w for the 'tail on' configuration. It is also the largest contribution by magnitude, dominating the resulting value of the derivative.

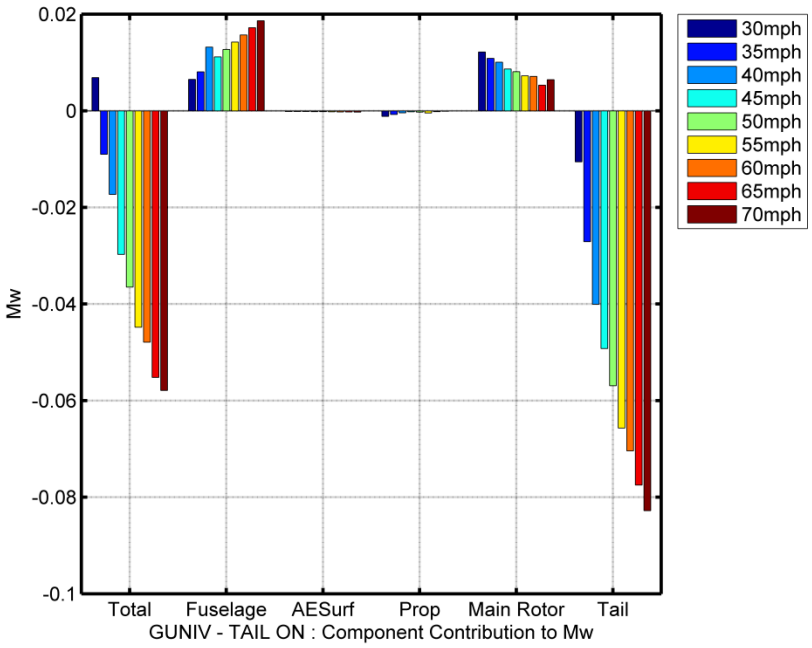

Figure 70: Component contributions to M_w for tail on configuration

Comparing the characteristics of the contributions to M_w shown in Figure 70 to those for the 'tail off' configuration shown in Figure 71, there are substantial differences. Across the airspeed range, the value of M_w is positive (destabilising) for the 'tail off' configuration, becoming increasingly large with airspeed, and in the absence of the increasingly large restorative contribution from the tailplane the contributions from the fuselage and main rotor dominate the derivative.

There is also a fundamental difference in the trend within the contribution from the main rotor between the two aircraft configurations; for both configurations the contribution remains positive (destabilising) across the airspeed range, however, for the 'tail on' configuration the contribution from the main rotor decreases linearly as airspeed increases, but for the 'tail off' configuration the contribution is to increase as airspeed increases. This is related to the differing trimmed longitudinal shaft tilt position shown in Figure 65, with the magnitude of the contribution from the main rotor following the trend within the trimmed longitudinal shaft tilt position (and thus the main rotor incidence).

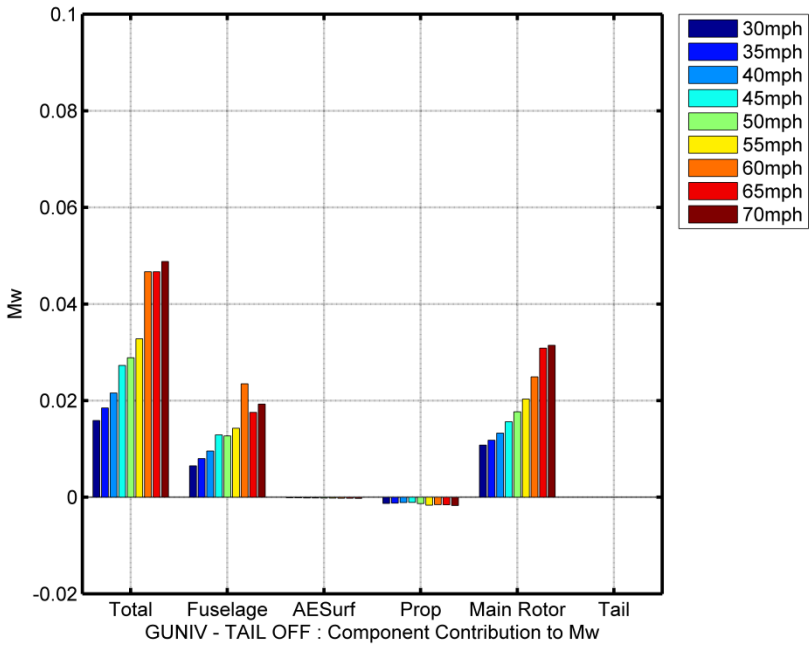

Figure 71: Component contributions to M_w for tail off configuration

4.2.4.2 M_q – Pitch Damping

With the tailplane attached, Figure 69 shows that M_q becomes increasingly negative (stabilising) as airspeed, and thus tailplane effectiveness, increases. For the 'tail off' configuration, the value of M_q remains approximately constant across the airspeed range. Figure 72 and Figure 73 show the component contribution to the overall value of M_q.

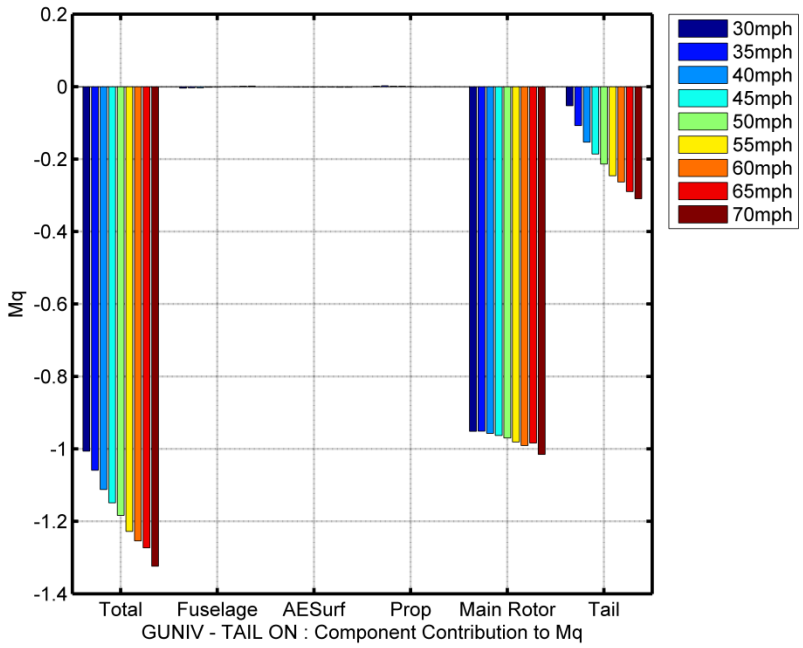

Figure 72: Component contributions to M_q for tail on configuration

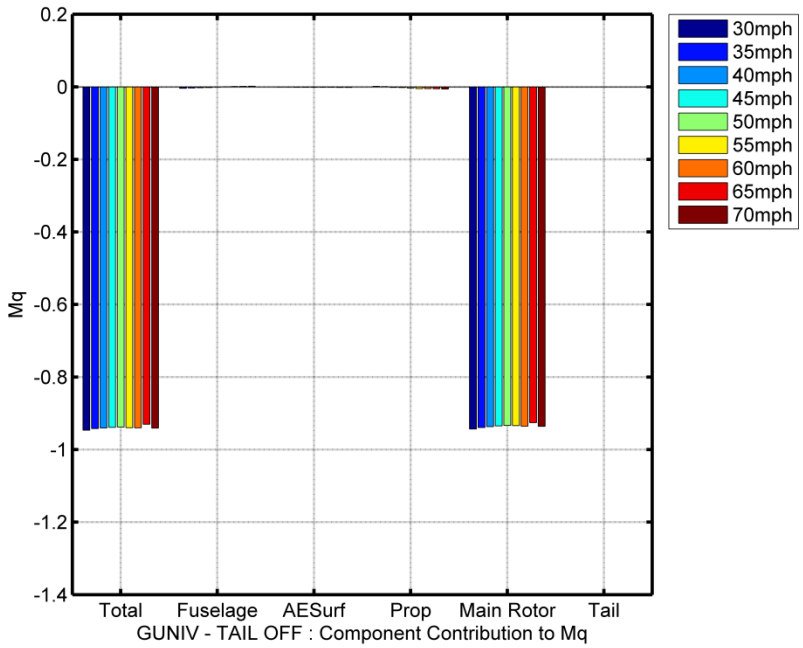

Figure 73: Component contributions to M_q for tail off configuration

It can be seen that for both aircraft configurations, M_q is dominated by the negative (stabilising) contribution from the main rotor. As shown in Chapter 3, the magnitude of this derivative is determined by the mass of the main rotor blades, hence it is approximately constant (to within the tolerance of the linearisation) with increasing airspeed. Addition of the tailplane results in M_q becoming increasingly negative with airspeed because the tailplane generates more lift and thus a greater moment as airspeed increases, adding a further restoring (stabilising) contribution to the total value of M_q.

4.2.4.3 M_u – Speed Stability

With tailplane attached, Figure 69 shows that M_u remains approximately constant as airspeed increases. For the 'tail off' aircraft configuration, M_u is seen to decrease with airspeed. The component contributions to M_u for both aircraft configurations are shown in Figure 74 and Figure 75.

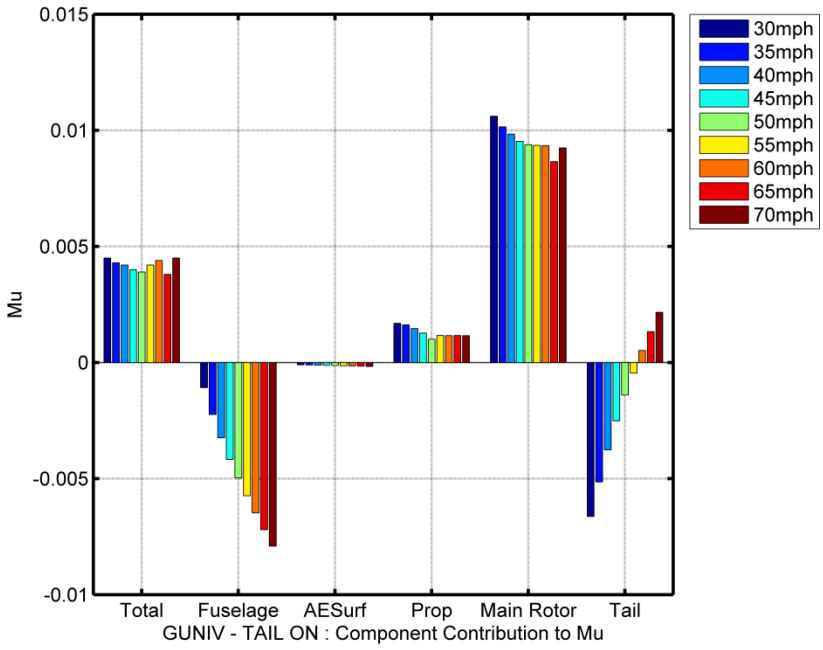

Figure 74: Component contributions to M_u for tail on configuration

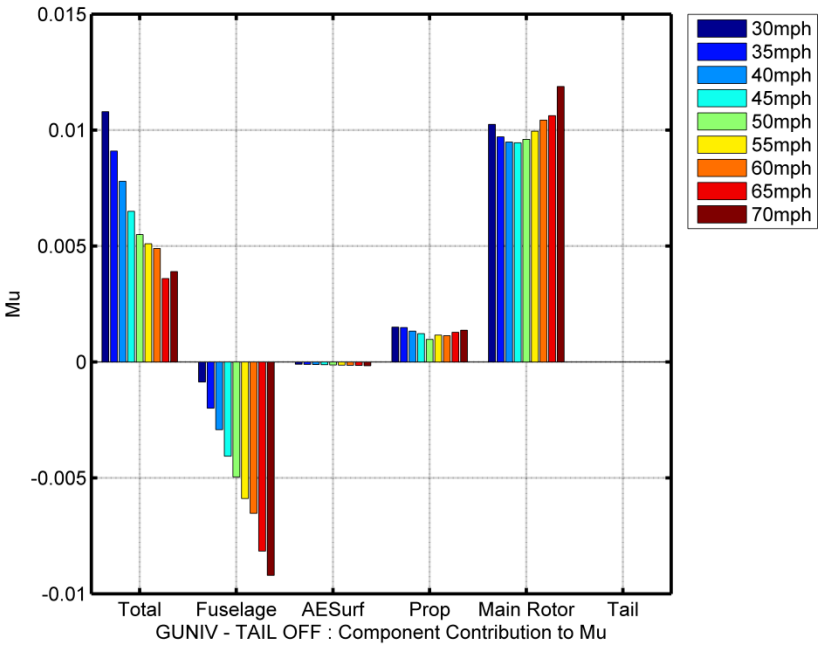

Figure 75: Component contributions to M_u for tail off configuration

For the 'tail on' configuration, it can be seen that the tail provides a stabilising (negative) contribution to the overall derivative at speeds up to 55mph, and a destabilising contribution from 60 to 70mph. This corresponds to the point at which the trimmed flight pitch attitude, ϑ, and thus the tailplane incidence, becomes negative and the tail begins to generate lift in the opposite direction (due to it being a flat plate of zero camber).

For both configurations, the contribution from the main rotor is destabilising, remaining positive throughout the airspeed range considered. However, for the 'tail on' configuration, the contribution decreases with airspeed, while for the 'tail off' configuration the contribution is seen to be decrease up to 45mph and then increase between 50 and 70mph. This is analogous to the trimmed flight trimmed longitudinal shaft tilt position, and thus rotor incidence, shown in Figure 65.

It is worthy of note that the magnitude of M_u is considerably smaller than that of M_q and M_w, and is "very nearly independent of velocity, or Mach number; thus the derivative M_u is often assumed to be negligibly small for those flight conditions." [80],

hence it does not have as large a role to play in determining the overall characteristics of the phugoid mode as M_q and M_w.

4.2.5 Assigned Handling Qualities: Acceleration-Deceleration

In order to assess the impact of removing the tailplane on the handling qualities of the aircraft, the Acceleration-Deceleration manoeuvre described in Chapter 3 was flown both with and without the tailplane. The pilot rated the handling qualities of the aircraft in both configurations using the Cooper Harper scale, and the results are shown in Figure 76. It should be noted that, unlike the results reported in Chapter 3, the handling qualities ratings presented in Figure 76 are plotted directly, rather than averaged.

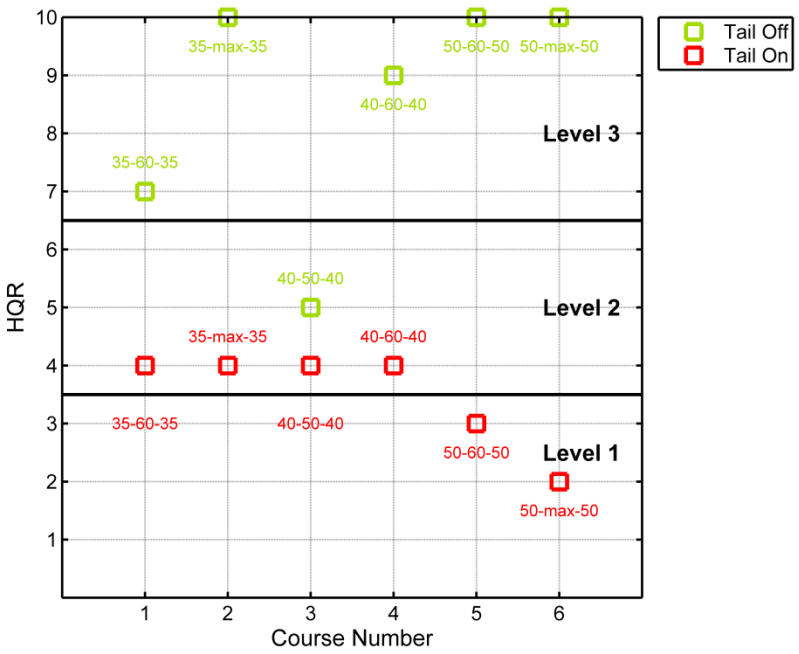

Figure 76: A comparison of handling qualities ratings for the Acceleration-Deceleration manoeuvre

Figure 76 illustrates that for the 'tail off' configuration, the handling qualities of the aircraft become significantly degraded compared to those of the 'tail on' aircraft; all ratings moving into Level 3, with the exception of the test point flown on course 3 which remains in Level 2.

This degradation in handling qualities can be attributed to the presence of a divergent phugoid mode which was not observed in the 'tail on' aircraft configuration; the pilot reported that this phugoid mode was very easy to excite, particularly at airspeeds above 50mph, and was "almost impossible" to supress. The existence of this mode is supported by Figure 66, which shows the 'tail off' phugoid mode as unstable throughout the flight envelope.

The test point carried out on course 3 is the test point which required the least aggressive change in airspeed, with the manoeuvre being initiated at 40mph, accelerating to 50mph. It is the only test point to remain inside Level 2, receiving an HQR 5. The pilot reported a distinct change in the handling qualities of the aircraft at around 45mph, with the aircraft becoming exhibiting a "wallow" in the pitch axis and the stick beginning to migrate aft as airspeed continued to increase.

The presence of this positive stick curve slope, and the fact that the direction of the stick-curve slope reverses as airspeed increases above 45mph for the 'tail off' aircraft configuration (as shown in Figure 65) indicates further undesirable handling characteristics. The presence of this positive stick-curve slope is both counter-intuitive and causes the phugoid oscillation to become problematic; as airspeed increases, pushing forward on the stick in order to prevent the aircraft climbing generates a nose down pitching moment. This nose down attitude will cause the airspeed to increase. As airspeed increases, the aircraft will produce a nose up pitching moment, which will in turn cause the airspeed to decrease. This change in aircraft attitude manifests itself as a phugoid oscillation, and as the eigenvalues of the phugoid mode are unstable in the 'tail off' configuration, the oscillation will continue to increase in amplitude until control is lost without pilot intervention.

For the test points carried out on course numbers 5 and 6 the pilot observed a 'cliff edge' in the handling qualities. The term 'cliff edge' is used to describe a sudden and unanticipated change in the handling characteristics of the aircraft. Course 5 and 6 require the manoeuvre to be initiated at 50mph, above the 45mph point at which the stick curve slope becomes positive. Beyond this point, the pilot observed that his control inputs were driving the phugoid mode, and the time to double amplitude of the phugoid oscillation was very short.

For both test points at course 5 and 6, an HQR 10 was awarded as the pilot was unable to complete the manoeuvre. It is also worthy of note that the simulator provides a 'sterile', safe environment in which to attempt to complete these tasks; it is unlikely that in the real world the pilot would attempt any of the test points, as the likely result is loss of the aircraft.

4.3 EXCESSIVE TEETER ANGLES

The occurrence of excessive teeter angles under extreme manoeuvring may result in the main rotor striking the propeller and/or tail assembly. For G-UNIV, propeller strike will occur when the total rotor angle relative to the longitudinal axis of the aircraft exceeds 29°, and tail strike will occur at 36.5° (assuming the blades are rigid, as they are in the FLIGHTLAB model). These angles were ascertained thorough measurement of the scale drawing provided in Appendix A. The total rotor angle relative to the longitudinal axis of the aircraft is given by adding the rotor teeter angle to the longitudinal shaft tilt. These angles are illustrated in Figure 77.

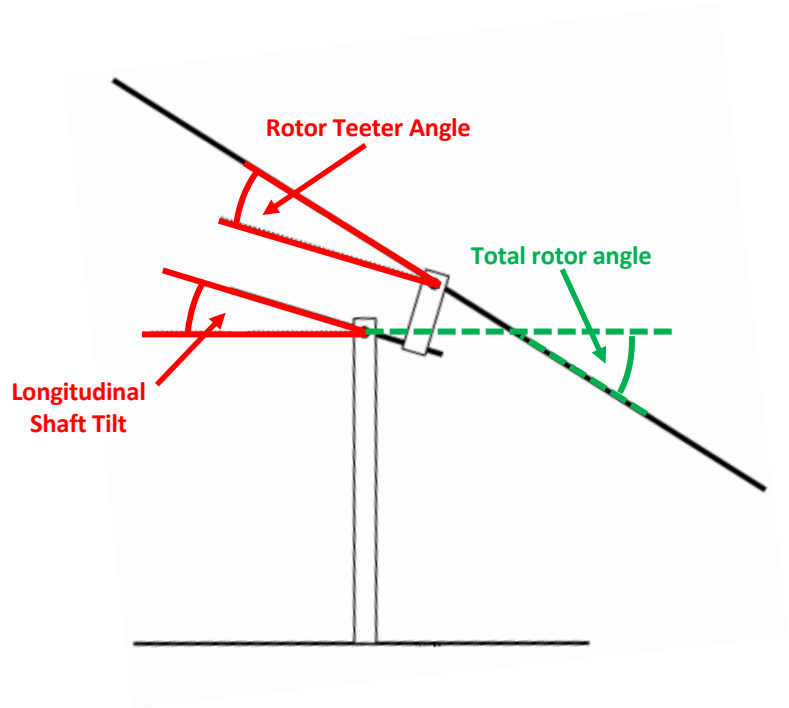

Figure 77: Schematic of rotor hub geometry, showing rotor teeter angle and longitudinal shaft tilt

In order to assess the likelihood of the main rotor striking the empennage in flight, the model was trimmed in 5mph speed increments across the flight envelope and a maximum amplitude aft step input of 4 seconds duration was applied in the longitudinal axis. The red line shown in Figure 78 represents the 29° limit at which the main rotor will strike the propeller.

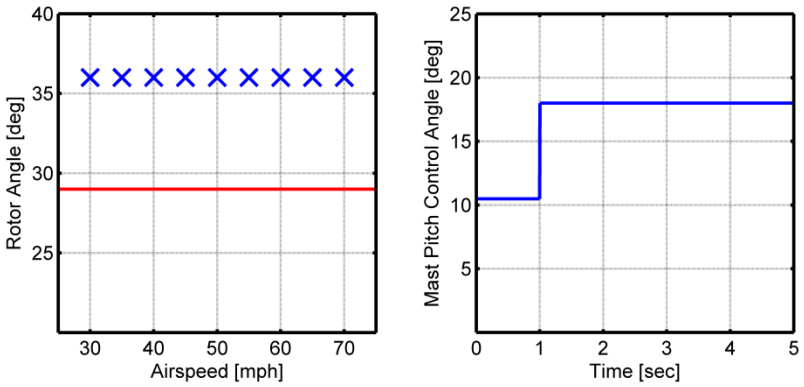

Figure 78: Main rotor angle response (left) to a 4 sec duration step input (right), with red line representing the angle at which propeller strike will occur

Figure 78 clearly shows that the main rotor is able to strike the propeller at all airspeeds within the flight envelope. The longitudinal shaft tilt of the main rotor mast is limited in both the aircraft and the model to 18°. The maximum total rotor angle observed during the simulated high aggression longitudinal input is approximately 36°; this means that teeter angles of approximately 18° were observed under this simulated manoeuvre.

During ground checks it was observed that the strike plate (which is intended to prevent excessive teeter angles occurring) was ineffectual (Ref. 4, Paragraph 11.3.1), allowing the main rotor to be teetered through the plane of the propeller until the tip touched the ground. In this extreme position, 2cm of clearance between the under surface of the main rotor and the strike plate remained; the strike plate which is intended to limit teetering is ineffective. The minimum teeter angle required to cause propeller strike was measured to be 11.1° [4]. Under manoeuvre loads, the model develops teeter angles of approximately 18°, illustrating that it is possible to exceed the 11.1° limit, resulting in a potentially catastrophic propeller strike.

The analyses described in this section have demonstrated that it is possible for the rotor to pass through the plane of the propeller, and that the existing solution (rotor strike plate) is not effective in providing mitigation. On this basis, recommendation 3 of Ref. 4 relating to excessive teeter angles is supported by the findings of this study.

4.4 CHORD-WISE BLADE CENTRE OF GRAVITY

The FLIGHTLAB autogyro model utilises a rigid blade model, and as such is not able to analyse the effect of moving the chord-wise blade centre of gravity. The effect of moving the chord-wise blade centre of gravity is discussed at length in Ref. 66 and Ref. 4. The fact remains that "the technical ability of the gyroplane community and the test and analysis facilities available to them may severely compromise or inhibit the collection of meaningful, or even correct data with which to demonstrate compliance" [4] and as result this recommendation does little to enhance safety or airworthiness for the autogyro community.

4.5 CONCLUSIONS

The FLIGHTLAB model described in Chapter 3 has been used to investigate and analyse the three of the four recommendations presented in Ref. 4. The conclusions of these investigations are presented below.

"1) It is recommended that the vertical location of the centre of gravity (c.g.) should lie within a ± 2 inch envelope of the propeller thrust line."

It has been shown that, for this aircraft configuration, the recommendation to limit the location of the vertical centre of gravity to the propeller thrustline to within a ±2 inch envelope may be overly restrictive, and that compliance with the BCAR Section T requirements can only be achieved across the entire flight envelope by locating the centre of gravity 4 inches above the propeller thrustline. To apply this recommendation to autogyro design generally may prove to be too much of a "one-size fits all" solution; whilst it may have to the ability to ensure that some autogyro designs become compliant with BCAR Section T requirements, it also has the potential to force configurations which are demonstrably compliant outside the ±2 inch thrustline envelope into the non-compliance region, as demonstrated by Figure 60. These investigations have, however, shown that the vertical positioning of the centre of gravity relative to the propeller thrustline is important in determining the frequency of the phugoid mode, in support of

findings in Ref. 4. It is therefore recommended that further investigation is warranted into the applicability of this reference across a range of types in the autogyro class.

"2) Horizontal tailplanes are largely ineffective in improving the long term pitch dynamic stability (phugoid mode)."

The removal of the tailplane was shown to result in a pronounced change in the both the longitudinal trim characteristics and the properties of the phugoid mode eigenvalues with airspeed for this aircraft. With a tailplane, the phugoid mode displayed a linear, predictable progression with airspeed; removing the tailplane results in the frequency of the phugoid mode changing unpredictably with airspeed increases. The longitudinal trim characteristics of the aircraft also displayed considerable differences between the two configurations. With tailplane attached the longitudinal shaft tilt, and thus the longitudinal stick position, decreases linearly with airspeed; without the tailplane the longitudinal stick position is seen to initially decrease with airspeed, but begins to increase again with airspeed beyond 45mph. The tailplane has also been shown to be important in shaping the key derivatives which determine the characteristics of the phugoid and short period modes, M_q, M_u and M_w.

Removal of the tailplane was also shown to have severe consequences for the handling qualities of the aircraft, with most HQRs moving from Level 2 into Level 3 for the Acceleration-Deceleration manoeuvre when compared to the 'tail on' configuration, with some test points being abandoned due to the fact that the 'tail off' aircraft configuration was uncontrollable. The presence of a divergent phugoid which was very easy to excite and almost impossible to supress was observed, with the pilot commenting that in the real world, the consequences of trying to complete the Acceleration-Deceleration manoeuvre in the 'tail off' configuration would likely be the loss of the aircraft.

These findings are in direct opposition to recommendation 2 of Ref. 4.

"3) Extreme manoeuvring can lead to excessive rotor teeter angles during certain phases of flight, potentially resulting in the rotor blades striking the prop or empennage."

It has been demonstrated that it is possible, during high aggression manoeuvres, for the main rotor teeter angle to exceed the safe limit and strike the propeller and/or tail assembly. This supports the recommendation presented in Ref. 4, and it should be

further noted that the existing strike plate design is not providing effective mitigation against this issue.

"4) The chordwise centre of gravity of the rotor blades should always lie at or ahead of the 25% chord position to prevent rotor blade instability."

Due to the use of a rigid blade model for the main rotor, it was not possible to investigate this recommendation, and as such it is not possible to comment on the validity or applicability of this recommendation. This could be achieved through further development of the G-UNIV simulation model.

Chapter 5

A COMPARISON OF PREDICTED HANDLING QUALITIES FOR AUTOGYRO AND HELICOPTER

Aircraft safety can be related to the ease and precision with which a pilot can fly the aircraft. These attributes can be enhanced by pilot training and by endowing the aircraft with intrinsically good handling qualities through design. As discussed in Chapter 2, autogyros have a considerably poorer safety record than other types of aircraft in the same sub-category. One potential explanation for this would be for control of the aircraft to require a skill level than are beyond the capabilities of the pilot (perhaps due to insufficient training) or in situations in which handling qualities are degraded; for example, in poor visibility or in the presence of atmospheric disturbance.

Handling qualities can be quantified in two ways; predicted and assigned. Predicted handling qualities involve quantitative metrics such as performance, agility and stability, while assigned handling qualities refers to qualitative assessment of the aircraft by pilots when flying role-representative manoeuvres to a prescribed set of performance parameters, often assessed using the Cooper-Harper Handling Qualities Rating Scale [54]. In order to isolate handling characteristics of interest, these manoeuvres are often divided into simplified mission tasks elements (MTEs). For military rotorcraft, requirements for both predicted and assigned handling qualities and MTE course descriptions can be found in ADS-33 [2]. Handling qualities are classified as Levels 1, 2 or 3; and aircraft which display 'Level 1' handling qualities are considered fit for purpose within their specified operational flight envelope.

There are currently no standards or specifications by which autogyro handling qualities can be quantified. However, one of the key research questions raised in Chapter 2 is whether an existing rotary wing specification such as ADS-33 can be used to assess autogyro handling qualities; and if not, what new criteria are required to ensure future autogyro designs feature Level 1 handling qualities, and by implication, are safe to fly. In order to begin addressing this subject, a comparison of predicted handling qualities was

undertaken for both the autogyro and a generic helicopter of equivalent geometry and mass.

Using the FLIGHTLAB models of both the autogyro and helicopter defined in Chapter 3, the work described within this Chapter explored the existing predicted handling qualities requirements defined in ADS-33, along with other criteria such as pilot attack, to compare the predicted handling qualities of both platforms. This Chapter also sought to draw conclusions upon the applicability of the ADS-33 specification to the assessment of autogyro handling qualities.

5.1 DEFINITIONS

5.1.1 Speed Regimes

For each of the metrics described, ADS-33 specifies requirements for 'Hover and Low Speed' and 'Forward Flight'. 'Hover and Low Speed' requirements are applicable to manoeuvres carried out from hover (0kts airspeed) up to 45kts, and 'Forward Flight' covers manoeuvres at 45kts and above. The autogyro community typically uses miles per hour (mph) to quantify forward airspeed. As such, in the following analyses, 'Hover and Low Speed' are used herein to refer to airspeeds up to 50mph, and 'Forward Flight' applies to airspeeds of 50mph and above (45kts is equivalent to 51.8mph).

Consideration of 50mph test points in both the 'Low Speed' and 'Forward Flight' categories also allows for consideration of whether the 45kts cut-off point between 'Low Speed' and 'Forward Flight' is appropriate and applicable to the autogyro.

5.1.2 The Dynamo Construct

The dynamo construct, shown in Figure 79, divides the dynamic manoeuvre envelope into four regions on the frequency-amplitude chart. These four regions correlate with the predicted handling qualities metrics defined in ADS-33 (bandwidth, mid-term response to controls, quickness, cross coupling and control power), addressing both stability (in the low/medium amplitude region) and agility criteria (in the moderate/large amplitude, low/medium frequency region). It also provides a theoretical basis for illustration of the relationship between the different criteria analysed herein.

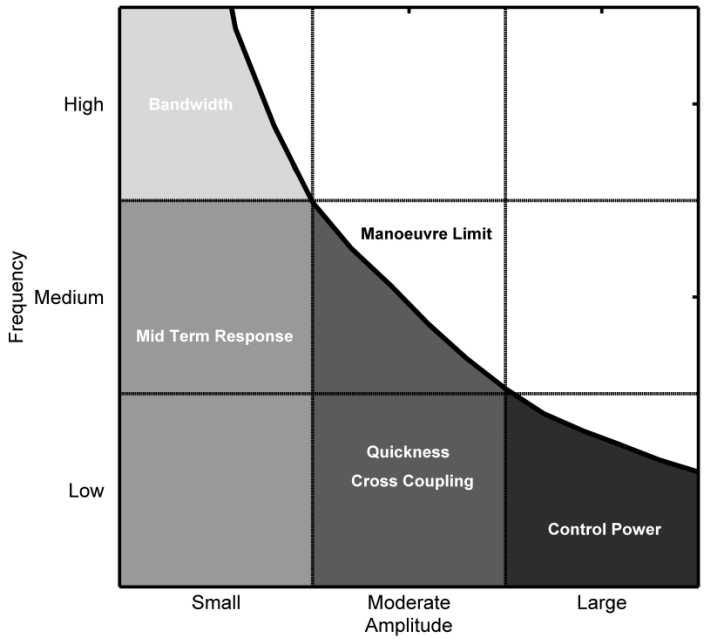

Figure 79: The Dynamo Construct

ADS-33 also provides criteria to assess inter-axis couplings for conventional rotorcraft, such as pitch due to roll, roll due to pitch and yaw due to collective. The latter is not applicable to the autogyro, due to the absence of a collective; this is an example of where the requirements specified in ADS-33 are not applicable to the autogyro.

There may also be a requirement to develop new criteria for the autogyro for deficiencies which are not identified within either the traditional dynamo construct or the inter-axis coupling criteria. For example, the roll due to power coupling, caused by the increasing torque from the propeller which is present in the autogyro model, has been reported as

"objectionable" by test pilots (Section 5.4). The overall handling of the autogyro model would benefit from reduction in this cross-coupling, but ADS-33 does not provide a metric by which is possible to quantify the extent to which it would be desirable to reduce this cross coupling. A methodology for developing such a metric is discussed in Section 5.7.

5.1.3 The Usable Cue Environment

The availability of appropriate visual cues can have a significant effect on the ability of the pilot to complete tasks within the specified performance criteria. These can be broadly divided into translational and attitude cues, each of which ADS-33 requires the assessing pilot to rate on a scale of one to five. These ratings are then used to establish the overall Usable Cue Environment (UCE) level on a scale of one to three, as shown in Figure 80.

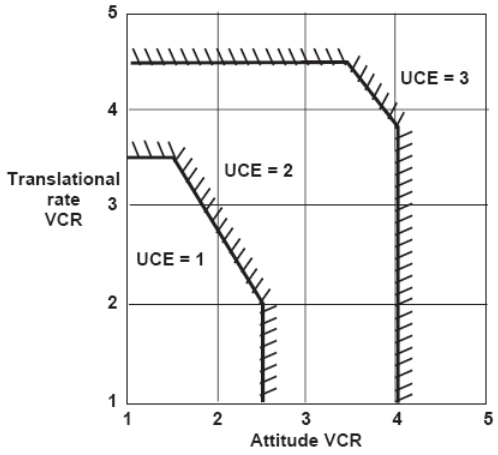

Figure 80: Useable Cue Environment Chart [2]

Although the autogyro would not typically be expected to operate in a degraded UCE, the criteria are included in the analysis presented in this Chapter for completeness.

5.1.4 Pilot Attention Levels

ASDS-33 makes provision for the fact that pilots are not always able to focus the entirety of their attention on the primary handling task. For example, the reduced pilot workload capacity which results from attention being drawn to secondary tasks such as navigation or radio operations could be problematic if there is not an adequate safety margin. Similarly, provision is also made for tasks to which the pilot would be expected to apply full attention such as target acquisition and tracking. Whilst it is not anticipated that

autogyro will regularly be flown in the target acquisition and tracking role, the divided attention operations criteria are relevant to single pilot operation. The target acquisition criteria are included for completeness.

5.2 BANDWIDTH

5.2.1 Introduction

The closed-loop system consisting of the pilot and aircraft will gradually diminish in stability as pilot gain (the magnitude of and how rapidly control inputs are applied) or disturbing frequency rises. The point at which instability occurs is known as the crossover frequency, and the bandwidth frequency corresponds to a lower value which provides adequate safety margin. This is usually defined as the highest frequency at which the pilot can double their gain (referred to as the gain bandwidth) or allow a 135° phase lag between the control input and aircraft response (referred to as the phase bandwidth) without causing instability; the higher the bandwidth, the larger the margin of safety.

Bandwidth can also be related to pilot workload and aircraft handling. Whilst the assessment of workload relies heavily upon subjective pilot opinion, it is usually found that as bandwidth increases, pilot workload decreases [59]. With lower workload, the 'ease and precision' with which a pilot can fly an aircraft is increased, and thus the handling qualities are perceptibly improved. Deficiencies in the frequency domain response of the aircraft can lead to situations in which the pilot drives the aircraft into an undesired oscillation whilst attempting to compensate; this is known as a pilot-induced oscillation (PIO). Gain bandwidth can be a good indicator of how susceptible to PIO an aircraft is; low gain margin indicates that a small change in pilot gain can result in a large reduction in phase margin, causing the crossover frequency to be suddenly reached and PIO to occur.

ADS-33 specifies bandwidth performance criteria for pitch, roll and yaw axes in both the low speed and forward flight regimes. Yaw bandwidth is not assessed for the autogyro due to the difference in response type between the helicopter model with a tail rotor and the autogyro model's rudder; the pedals in the autogyro relate to command of sideslip, whereas the helicopter pedals generate a yaw rate response.

Bandwidth is calculated by applying a frequency sweep to the aircraft to the axis of input, typically ranging from 0.05Hz to 3Hz in magnitude. Spectral analysis of the output is then carried out to identify the phase lag between the input and output over the range of frequencies applied. The magnitude of the input used is typically around 5% of the full control range. From the aircraft response, the frequency at which the phase lag equals 135° (providing at phase margin of 45° over the neutral stability frequency), and thus the phase bandwidth, can be determined.

Phase delay is calculated as:

$$\tau_p = \frac{\Delta\Phi 2\omega_{180}}{57.3(2\omega_{180})}$$

where ω_{180} is the neutral stability frequency and $\Delta\Phi 2\ \omega_{180}$ is the phase lag change between the neutral stability frequency and twice the neutral stability point (the point at which the phase lag is 180°).

The gain bandwidth can be determined as the point at which the magnitude of the aircraft response is 6dB greater than the response at where the phase lag is 180°. The overall aircraft bandwidth is the lowest of the gain and phase bandwidths.

Figure 81 and Figure 82 show the typical range of input frequencies used, the aircraft responses and the bode plots generated through spectral analysis.

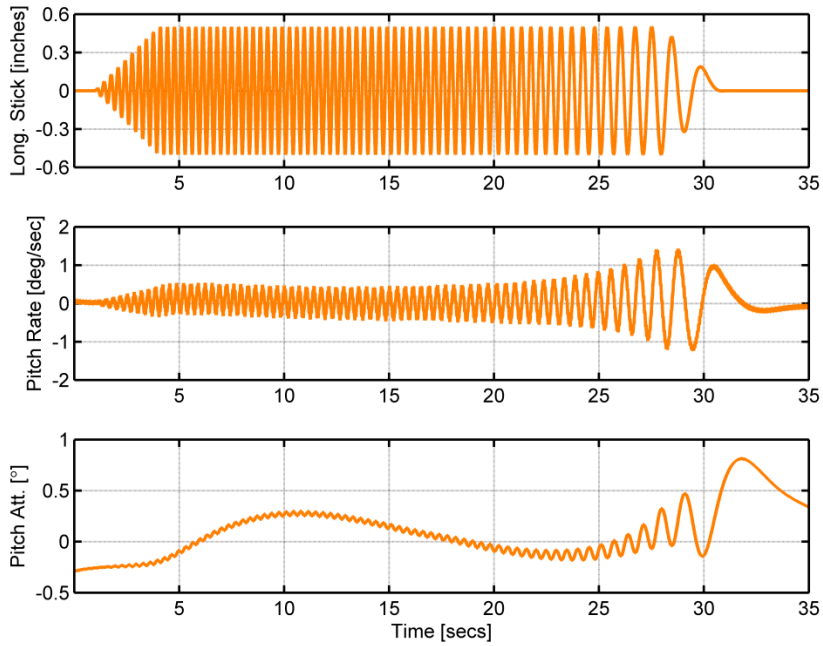

Figure 81: Typical input and aircraft response to input used in bandwidth analysis (response shown is for pitch bandwidth inputs at 50mph)

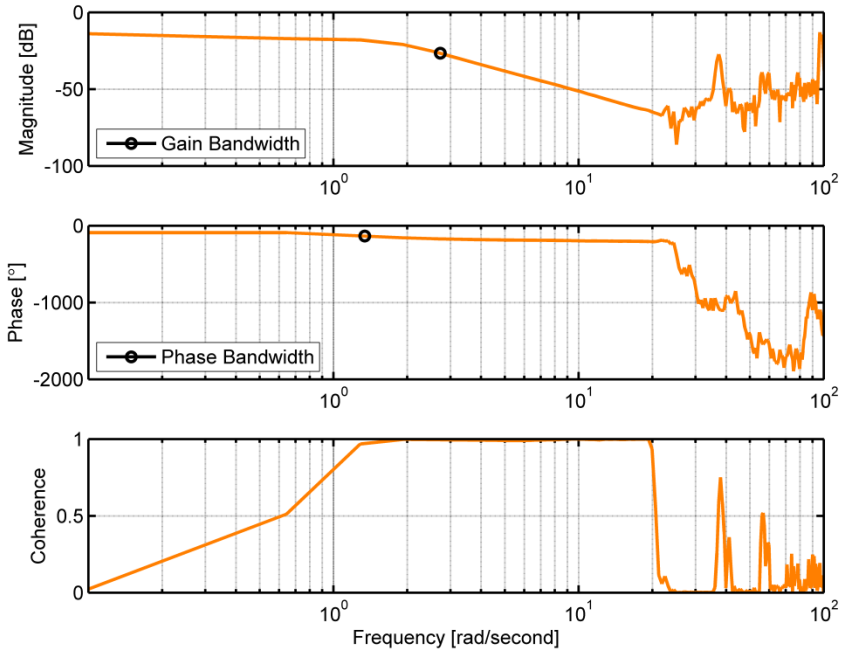

Figure 82: Gain and Phase pitch bandwidth calculation results shown for autogyro at 50mph

5.2.2 Pitch Bandwidth Assessment

ADS-33 specifies bandwidth criteria for 3 flight regimes: target acquisition and tracking, all other MTEs in Useable Cue Environment (UCE) 1, and all other MTEs in UCE > 1 and/or divided attention operations (as defined in Section 5.1). The bandwidth analysis method described in Section 5.2.1 was repeated for both the helicopter and autogyro models for a number of flight conditions; the findings are presented in the following Sections.

5.2.2.1 Low Speed Flight Pitch Bandwidth

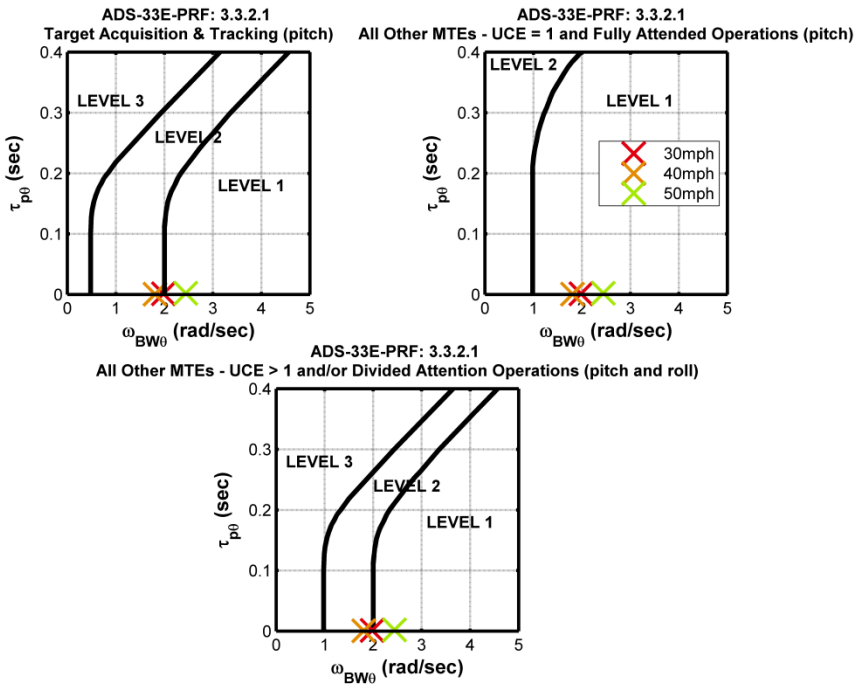

Figure 83: Low speed pitch bandwidth calculations for G-UNIV autogyro

Figure 83 shows the bandwidth characteristics of the autogyro model in the low speed flight regime. For UCE = 1 and fully attended operations, the autogyro displays consistently Level 1 characteristics against the ADS-33 criteria. For both target acquisition and track and UCE > 1/divided attention operations (the more demanding, higher workload tasks), the aircraft performance falls into Level 2 for the 30 and 40 mph cases, remaining in Level 1 for the 50 mph case. These Level 2 ratings suggest that the pilot may experience significant difficulty when applying small amplitude, high frequency corrective control inputs in the pitch axis, without causing the aircraft to become unstable.

Figure 83 shows that the value of the phase delay, $\tau_{p\theta}$, remains consistent across the speed range. The phase delay is a parameter which describes the aircraft response above the bandwidth frequency. If the phase delay is low, the phase lag does not increase significantly with the input frequency beyond the bandwidth frequency. This suggests that, for these test conditions, the amount of phase lag which occurs above the bandwidth frequency remains approximately the same, suggesting there is not a sudden discontinuity in phase lag characteristics, which may result in further controllability issues (aside from the inevitable instability), as input frequency increases.

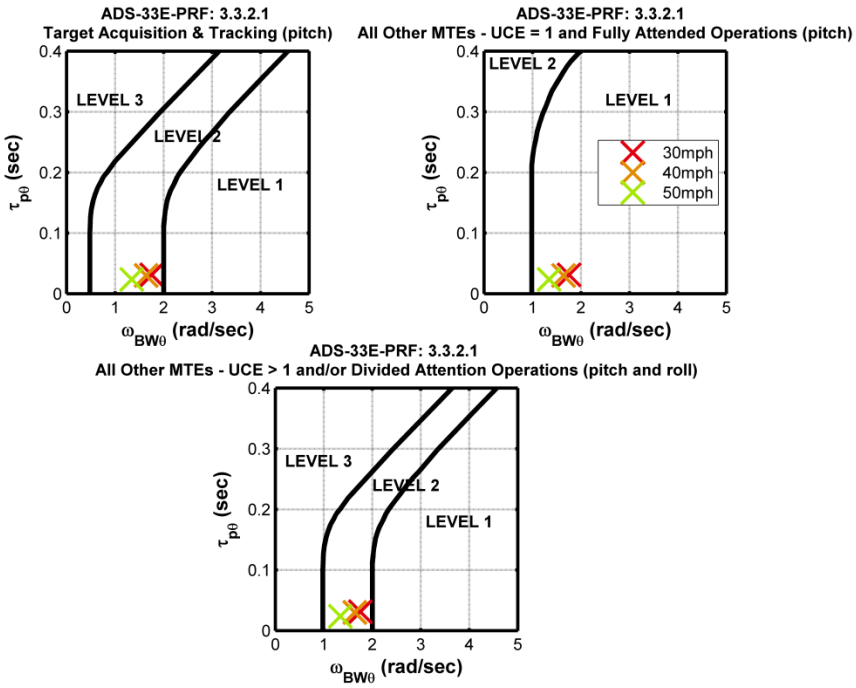

Figure 84: Low speed pitch bandwidth calculations for helicopter

Figure 84 shows the bandwidth results for the helicopter model in the low speed regime. Similarly to the results for the autogyro model shown in Figure 83, the helicopter model exhibits Level 1 handling qualities for UCE = 1 and fully attended operations, with UCE > 1 and divided attention operations and target acquisition and tracking tasks achieving Level 2 handling qualities. The phase delay shows a slight increase for the helicopter model, however this is not of sufficient magnitude to have any significant consequences for the overall handling qualities level predicted.

It is not unexpected that the autogyro and helicopter models display similar pitch bandwidth characteristics, as they are of roughly equivalent geometry and employ the same teetering rotor system. Additionally, neither model employs a stability augmentation system, which can have a significant effect on the low-speed handling qualities of a small rotorcraft [59].

5.2.2.2 Forward Flight Pitch Bandwidth

Figure 85 and Figure 86 show the forward flight pitch bandwidth characteristics for the autogyro and helicopter models respectively.

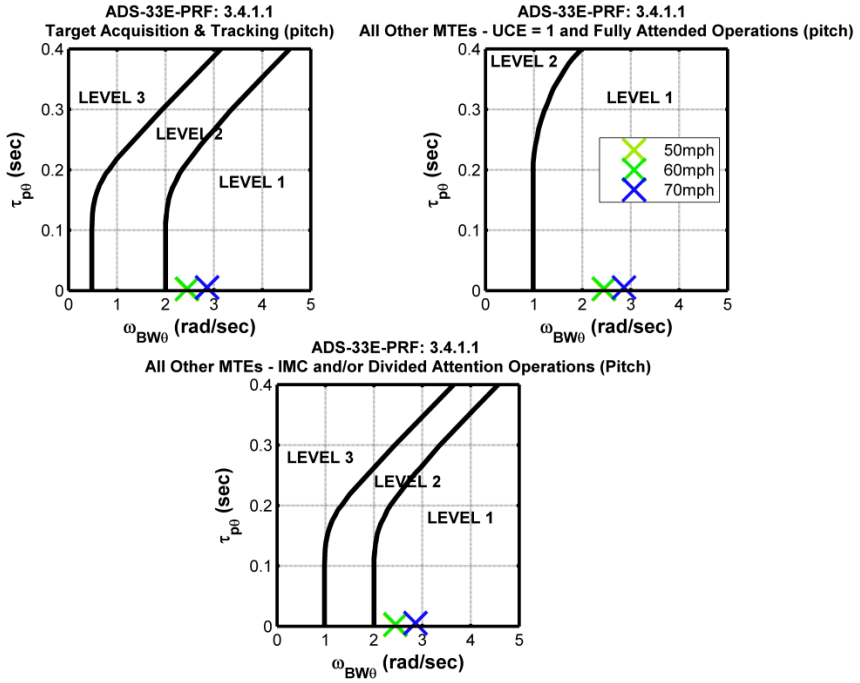

Figure 85: Forward flight pitch bandwidth for autogyro

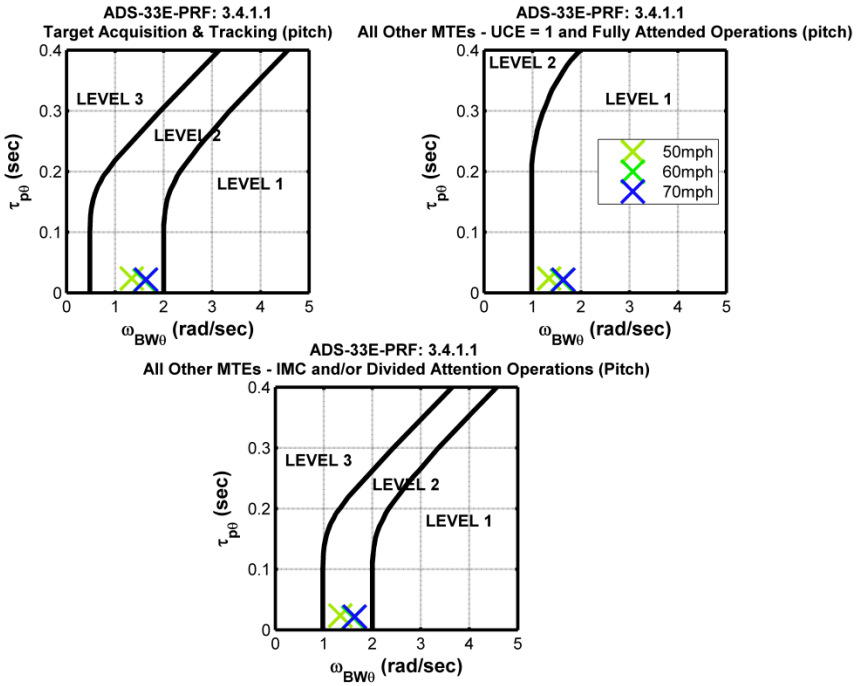

Figure 86: Forward flight pitch bandwidth for helicopter

For all criteria in the forward flight regime, Figure 85 and Figure 86 show that both the helicopter and the autogyro display Level 1 predicted handling qualities. The phase delay values for both autogyro and helicopter are comparable to those displayed in the low speed regime, suggesting there is not a sudden change in the bandwidth characteristics of either aircraft as airspeed increases.

5.2.3 Roll Bandwidth

As for the pitch bandwidth requirements, ADS-33 provides three sets of criteria for roll bandwidth. The process described in Section 5.2.1 was repeated for the roll axis of both aircraft models, and the findings are presented in this Section.

5.2.3.1 Low Speed Flight Roll Bandwidth

Figure 87 shows the roll bandwidth characteristics of the autogyro in the low speed flight regime.

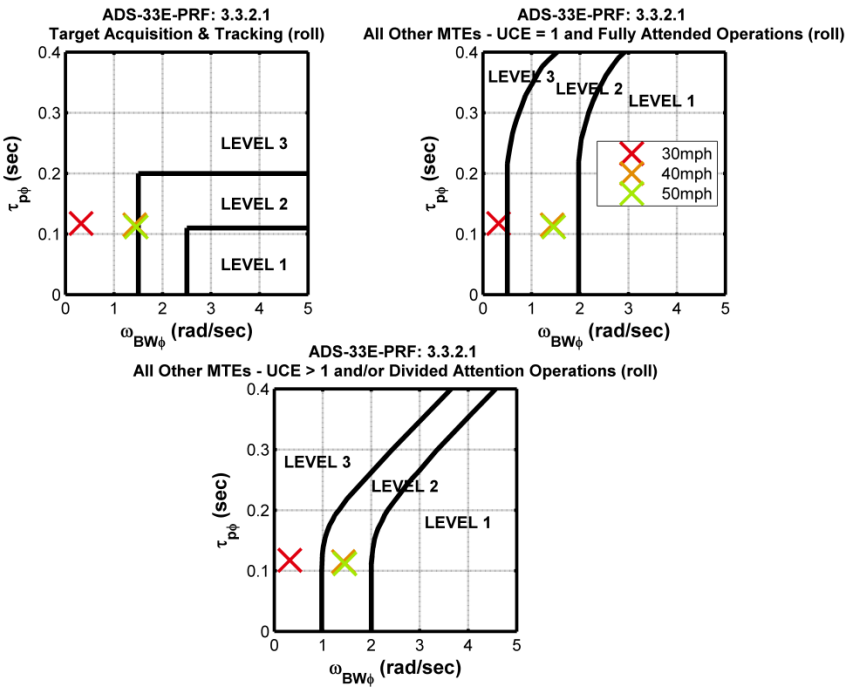

Figure 87: Low speed roll bandwidth for autogyro

Figure 87 shows that at 30mph the autogyro displays Level 3 handling qualities against all ADS-33 roll bandwidth criteria. For the target acquisition and tracking task, the aircraft handling qualities remain in Level 3 for all airspeeds; for all other tasks, the aircraft handling qualities migrate into Level 2 as airspeed increases. This result indicates a serious deficiency in the roll axis, suggesting that under aggressive manoeuvring (such as that required during tracking tasks) the pilot of the aircraft will be unable to achieve the level of precision required to complete the task successfully and potentially without triggering instability in the roll axis. This is likely due to the low levels of roll damping present in the autogyro at low speed (as illustrated by the high roll quickness values shown in Section 5.4.2.1).

Figure 87 also shows that the phase delay values for all three test points in the low speed regime are significantly increased when compared to those in the pitch axis. This suggests that the phase delay will increase considerably above the bandwidth frequency. This will result in unrecoverable roll axis divergence when control inputs above the bandwidth frequency are applied. Upon triggering aircraft instability above the bandwidth frequency, a pilot's reaction may be to apply further inputs to try to regain

control of the aircraft. If the phase delay increases considerably above the bandwidth frequency, these inputs are likely to result in the aircraft becoming more unstable; this may lead to loss of the aircraft through loss of control.

The considerable increase in the phase delay values between the roll and pitch axes also suggests the aircraft handling qualities are not well harmonised. It is undesirable to have the characteristics of one axis be substantially different to those in another axis, as this can result in excessive amounts of pilot attention being diverted into one axis, creating a potentially dangerous situation where there is not enough remaining capacity to maintain control of the aircraft.

The results for the low speed roll bandwidth for the helicopter model are shown in Figure 88. The helicopter exhibits Level 2 predicted handling qualities for all tasks except the target acquisition and tracking task at 40 and 50mph, where the predicted handling qualities ratings are in Level 3. Comparing these results to those of the autogyro, shown in Figure 87, show that the helicopter has a reduced phase delay compared to the autogyro. The values of phase delay are also similar to those of the helicopter in the pitch axis, suggesting the helicopter handling characteristics are better harmonised than those of the autogyro.

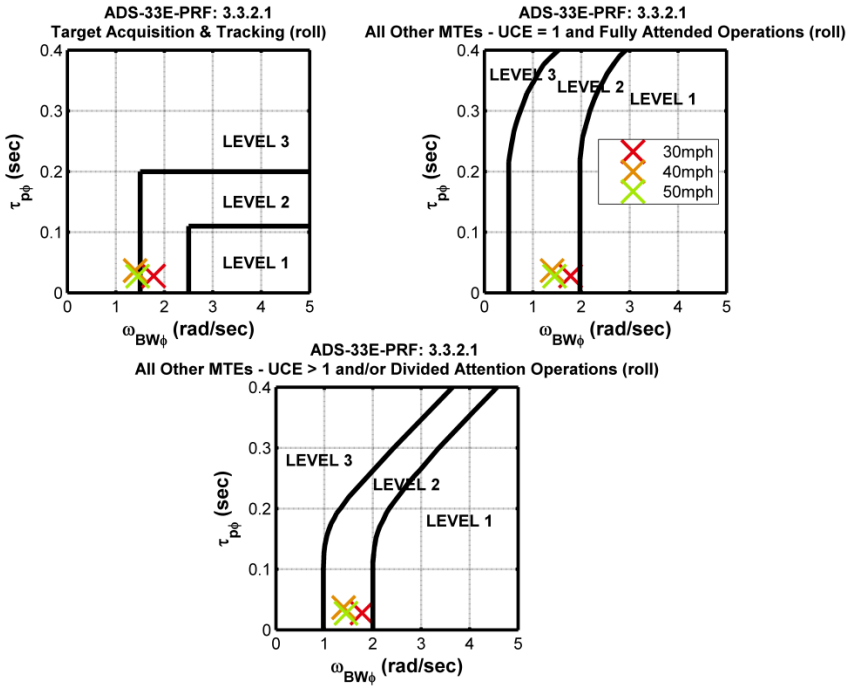

Figure 88: Low speed roll bandwidth for helicopter

5.2.3.2 Forward Flight Roll Bandwidth

Figure 89 and Figure 90 show the forward flight roll bandwidth results for autogyro and helicopter respectively.

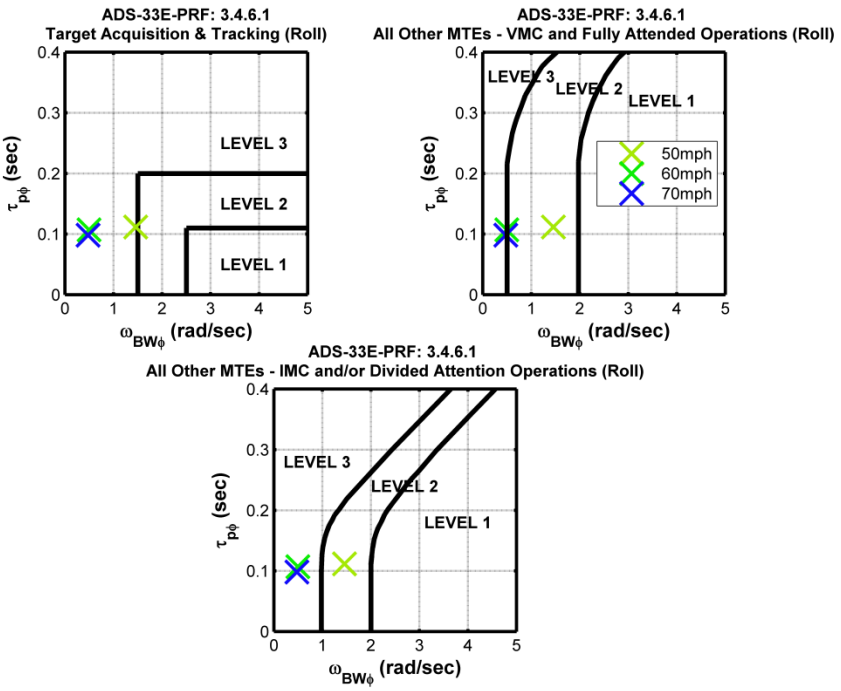

Figure 89: Forward flight roll bandwidth for autogyro

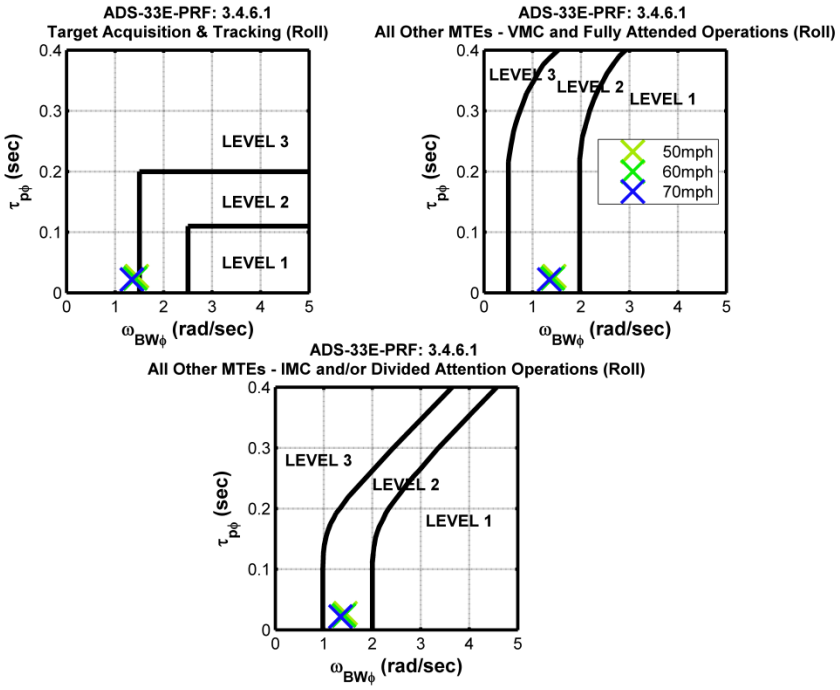

Figure 90: Forward flight roll bandwidth for helicopter

For the autogyro, all test points above 50mph exhibit Level 3 predicted handling qualities. For the helicopter model, all test points remain in Level 2, except those for target

acquisition and tracking, which remain just inside Level 3. For both autogyro and helicopter, the value of phase delay remain similar to those in the low speed regime, with the autogyro's phase delay characteristics being significantly different to those in the pitch axis at equivalent test points. This further supports the assertion that the handling qualities of the autogyro are not well harmonised in the pitch and roll axes.

5.2.4 Bandwidth Conclusions

Overall, the analyses presented in this Section have demonstrated that it is possible to make predictions about autogyro handling qualities through use of the ADS-33 bandwidth criteria. Bandwidth is an inherent characteristic of an aircraft, and the criteria presented in ADS-33 are based upon the consequence and likelihood that control inputs will be applied at above the bandwidth frequency, triggering aircraft instability. As bandwidth frequency increases, the likelihood of reaching the bandwidth frequency decreases as it is not physically possible for the pilot to apply control inputs at such a high rate. Conversely, as bandwidth frequency decreases, the pilot is more likely and more able to apply control inputs at the bandwidth frequency, resulting in a higher predicted handling qualities Level being assigned. On this basis, the predicted autogyro handling qualities discussed in this Section appear to be reasonable and valid. However, in order to determine the degree of applicability of the ADS-33 criteria to autogyros, the findings of this Section were validated during the piloted evaluation presented in Chapter 6.

5.3 MID-TERM RESPONSE TO CONTROLS

ADS-33 specifies requirements on the aircraft response to small amplitude inputs up to the bandwidth frequency. These boundaries specify the limits of acceptable mid-term pitch characteristics in terms of frequency and damping. As the autogyro has a rate response type, any oscillatory modes following an abrupt control input should have an effective damping ratio of at least $\zeta = 0.35$ in order to achieve Level 1 handling qualities. Those oscillatory modes with a natural frequency (ω_n) of less than 0.5 rad.s^{-1} should have an effective damping ratio of at least $\zeta = 0.19$. Unstable modes (or those with low damping ratios) require significant pilot attention and workload to suppress in order to prevent loss of control. These results are generated by linearising the simulation model (featuring the nine rigid body states, p, q, r, φ, ϑ, ψ and Ω, the rotor speed degree of freedom for the autogyro model only) and extracting the eigenvalues from the state matrix. The eigenvalues are then plotted on the s-plane along with the

requirements on damping ratio and natural frequency. The results are shown in Figure 91 and Figure 92 for the autogyro and the helicopter respectively (note only the phugoid and short period modes are shown).

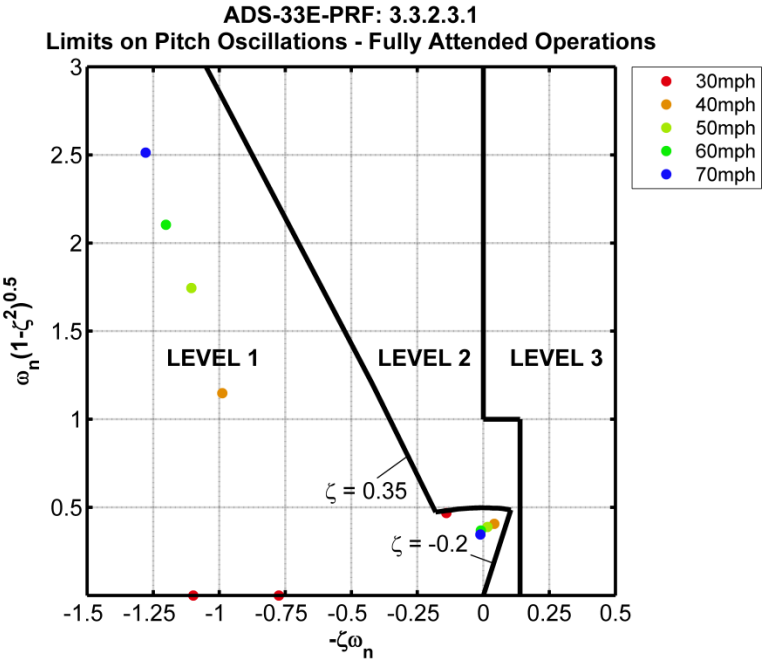

Figure 91: ADS-33 requirements for mid-term response to controls (autogyro)

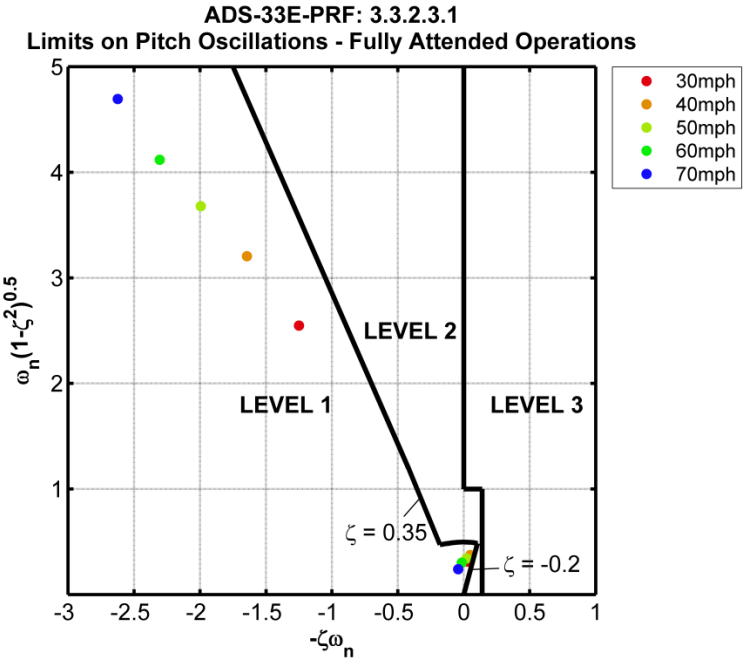

Figure 92: ADS-33 requirements for mid-term response to controls (helicopter)

The phugoid (points gathered near to the origin) and short period (points in the upper left quadrant of the S-plane) modes are shown to achieve Level 1 predicted handling qualities ratings for both the autogyro and the helicopter model. Both aircraft types possess marginally stable phugoid modes, which increase in stability as airspeed increases. The phugoid modes of the two aircraft also share a comparable damped frequency. The short period mode for the autogyro is non-oscillatory at 30mph, whereas the helicopter has an oscillatory short period at all airspeeds. The damped frequency of the helicopter's short period mode is also increased compared to that of the autogyro model; this could be attributed to the increased pitch damping due to the horizontal tail surface present in the autogyro. It may also be due to the relatively further aft position of the helicopter model's longitudinal centre of gravity position relative to the main rotor in the helicopter, which results in a larger pitching moment from the main rotor being present due to the increased length of the moment arm.

As for the bandwidth criteria, this Section has shown that it is possible to use the ADS-33 criteria to predict autogyro handling qualities of the mid-term response to controls. The modes present in the autogyro's dynamic motion are the same as those present in the helicopter (with the exception of the addition of the rotorspeed degree of freedom), and

therefore will manifest themselves in the same way as those modes present in the helicopter; their characteristics are dependent on their location on the S-plane, and are not aircraft-type-specific. On this basis, if a phugoid mode with a damped frequency of 0.35 is considered acceptable in a helicopter, there is no reason to consider it unacceptable in an autogyro. These findings were validated though use of piloted simulation, as discussed in Chapter 6.

The requirements laid out in the CAA's airworthiness requirements for autogyros, BCAR Section T [5], were discussed in Chapter 4. These requirements place limits on the time in which oscillations must damp to half amplitude, based on their period. Converting these requirements to the frequency domain and plotting them alongside the ADS-33 requirements for mid-term response to controls, as shown in Figure 93, illustrates that it is possible to be compliant with the BCAR Section T requirements while sill achieving Level 3 predicted handling qualities (indicated by the shaded area in Figure 93). If the ADS-33 requirements are considered to be applicable to the autogyro, this may suggest that the requirements presented in BCAR Section T are not stringent enough and allow vehicles with significant handling qualities to be declared airworthy.

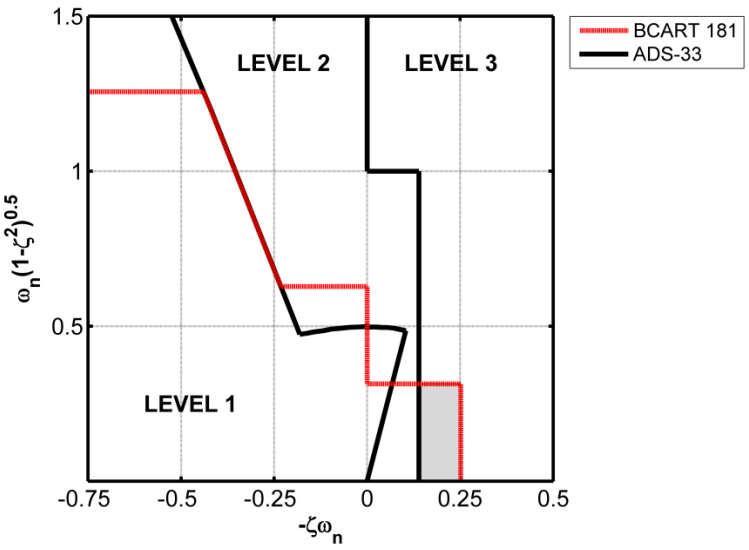

Figure 93: ADS-33 and BCAR Section T 181 autogyro response requirements

5.4 QUICKNESS

Quickness is a measure of the inherent manoeuvre agility of an aircraft [59]. If the value of the quickness parameter is too high, a pilot may describe the aircraft as being oversensitive or twitchy; if the quickness is too low, the pilot may experience a sluggish response and struggle to achieve tracking tasks. Quickness can be evaluated in all three axes, and occupies the 'moderate amplitude' section of the dynamo construct (from 5 to 30° attitude change in the pitch axis and from 10 to 60° in the roll and yaw axes).

As these analyses were carried out offline (i.e. without a pilot in the loop), it is possible to assess the entire range of attitude changes in all axes using maximum aggression inputs without any safety implications. It is unlikely that, in flight, a pilot would be able to generate the ideal inputs used within this analysis, and as such the data presented here represents a maximal estimation of aircraft performance, and the quickness achieved in-flight may be reduced.

5.4.1 Pitch Quickness

Pitch quickness is defined as "the ratio of peak pitch rate to change in pitch attitude" [2]:

$$\boldsymbol{Q_{pitch}} = \frac{\boldsymbol{q_{pk}}}{\boldsymbol{\Delta\theta_{pk}}}$$

where q_{pk} is the peak value of pitch rate achieved, and $\Delta\vartheta_{pk}$ is the change in pitch attitude.

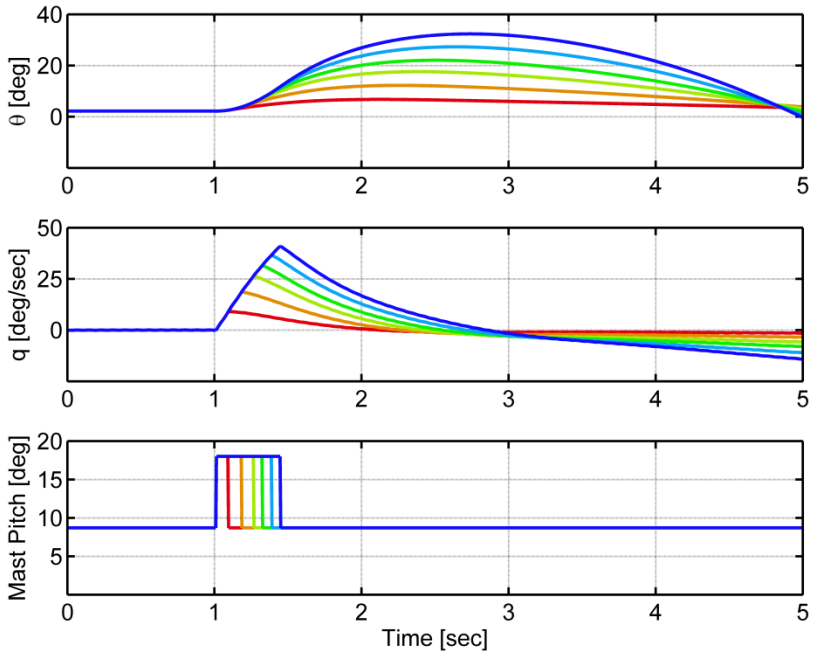

Figure 94: Pitch quickness control input and aircraft response at 50mph for targeted attitude changes from 5° to 30°

ADS-33 states that "the required attitude changes shall be made as rapidly as possible from one steady attitude to another without significant reversals in the sign of the cockpit control input relative to the trim position". As such, a maximum amplitude pulse input in the longitudinal control with insignificant rise time was used to generate the required aircraft response, as shown in Figure 94. The duration of the pulse input was modified in order to achieve a range of attitude changes in accordance with the requirements of ADS-33, which states that "the attitude changes required for compliance with this requirement shall vary from 5° in pitch to the limits of the Operational Flight Envelope or 30° in pitch, whichever is less." Attitude changes in increments of approximately 5° were targeted, from 5° to 30°.

As for the bandwidth requirements ADS-33 specifies quickness requirements for both target acquisition and tracking tasks, with any manoeuvres outside this definition being classified as 'All Other MTEs'. As it is unlikely that the autogyro type aircraft will be used in the target acquisition and tracking role, both the helicopter and autogyro are only assessed against the requirements for 'All Other MTEs' within this Section.

5.4.1.1 Low Speed Flight Pitch Quickness

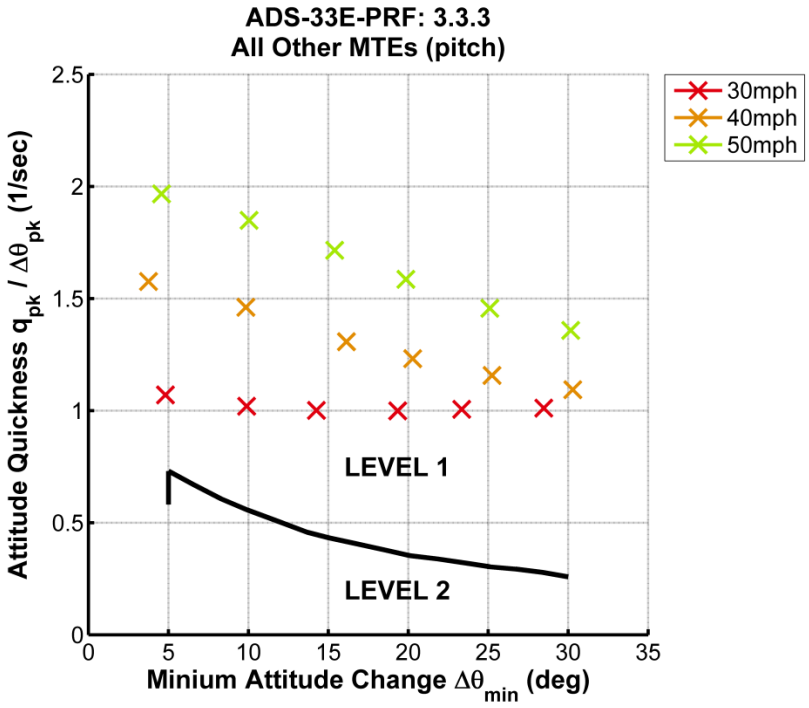

Figure 95: Estimation of autogyro low speed pitch quickness

Figure 95 shows the predicted pitch quickness of the autogyro model in the low speed flight regime. For all test points, the autogyro displays predicted Level 1 handling qualities. Figure 96 shows the predicted pitch quickness for the helicopter model; again, all points test points possess Level 1 predicted handling qualities (disregarding the test point which falls below the 5° minimum pitch angle change at 30mph).

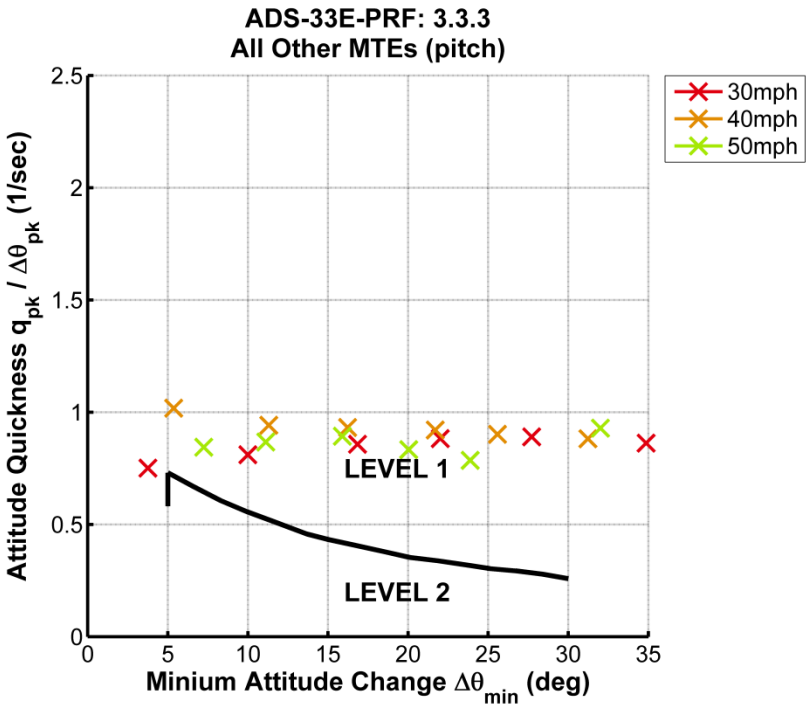

Figure 96: Estimation of helicopter low speed pitch quickness

Figure 95 and Figure 96 do illustrate several considerable differences between the autogyro and helicopter model. Primarily, the helicopter displays a relatively constant value of quickness across the 30 – 50mph airspeed range, with all test points achieving a quickness value of between 0.8 and 1sec^{-1}. This will endow the aircraft with consistent handling qualities over what is quite a small range of airspeeds. The autogyro however, displays significant differences in the values of quickness achieved, varying both with airspeed and with change in pitch attitude. The magnitude of the quickness values is also much greater for the autogyro than the helicopter, suggesting the autogyro possesses a large amount of inherent agility. This is discussed further in Section 5.6.1, along with its effect on cross coupling.

As airspeed increases, the smaller attitude changes display a greater variance in quickness than those at larger attitude changes. This suggests that under close manoeuvring the pilot may experience difficulties controlling the aircraft to the required level of precision as the handling qualities of the aircraft are not consistent; the aircraft will be perceptibly 'twitchier' at 50 mph than at 30 mph due to its increased quickness.

This variation in handling qualities will increase pilot workload and has the potential to affect the controllability of the aircraft.

Generally, the ADS-33 requirements on pitch quickness do reflect the autogyro's pitch quickness characteristics; pilots reported high levels of agility in the pitch axis during simulated test flights, which is supported by the fact that the autogyro falls within the Level 1 predicted handling qualities region of the chart. As the criteria described in ADS-33 are intended to be used to analyse rotorcraft of any size it follows that the criteria are appropriate for the autogyro. However, ADS-33 does not stipulate an upper bound for the acceptable level of quickness possessed by an aircraft. For this particular autogyro model, the high level of quickness may pose handling issues – too much agility may be as bad as not enough in certain flight conditions.

The delineation between Level 1 and Level 2 predicted handling qualities also needs to be investigated, as the current position may not be appropriate. This could be done through further flight testing, and a methodology for doing this is described later in this Chapter, though it is beyond the scope of this Thesis to carry out the required flight testing.

It should be noted that there are no pitch quickness criteria for the forward flight regime defined in ADS-33.

5.4.2 Roll Quickness

Roll quickness is defined as "the ratio of peak roll rate to change in roll attitude" [2]:

$$\boldsymbol{Q_{roll} = \frac{p_{pk}}{\Delta \phi_{pk}}}$$

Similarly to the inputs used to evaluate pitch quickness, a maximum amplitude pulse input in the lateral cyclic was used to generate the required roll attitude changes. An example of the responses generated is shown in Figure 97. ADS-33 states that "the attitude changes required for compliance with this requirement shall vary from 10° in roll to the limits of the Operational Flight Envelope or 60° in roll, whichever is less". As such, attitude changes in increments of 10°, from 10° to 60°, were targeted.

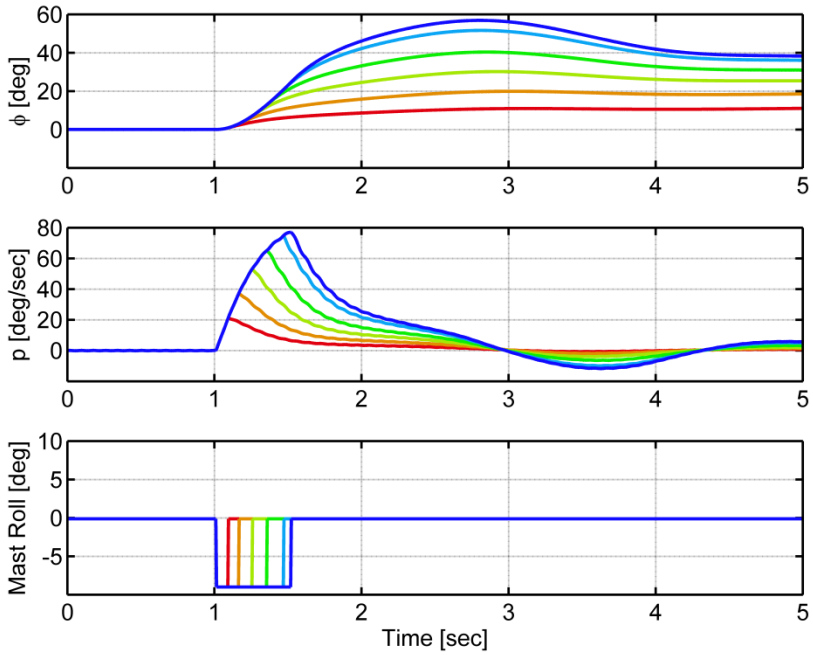

Figure 97: Roll quickness control input and aircraft response at 50mph for targeted attitude changes from 10° to 60° (autogyro)

A slight oscillation in the roll rate response can also be observed in Figure 97, which increases in amplitude as the target attitude change increases. This is due to the large fin and rudder assembly generating a large side force in roll, which in turn excites the Dutch roll mode (a coupled oscillation in roll and yaw). The amount of side force increases with attitude change, which manifests itself as the increasing amplitude observed.

5.4.2.1 Low Speed Flight Roll Quickness

Figure 98 shows the roll axis quickness for the autogyro model in the low speed flight regime. Comparison with the ADS-33 boundaries demonstrates that the aircraft falls within Level 1 for all conditions with the exception of the smallest attitude change at 30mph. Furthermore, the majority of the points are well above the level 1/2 boundary, indicating that the aircraft features extremely high levels of quickness in the roll axis. This can be attributed to the relatively small size of this aircraft (and hence low roll inertia) combined with the high roll control power described is Section 5.5.2. The autogyro model also does not possess large horizontal surfaces to provide roll damping

It should also be noted that the trend of decreasing roll quickness with increasing attitude change shown for all points above 30° conforms to that which would typically be expected for a conventional rotorcraft (as shown in Figure 99).

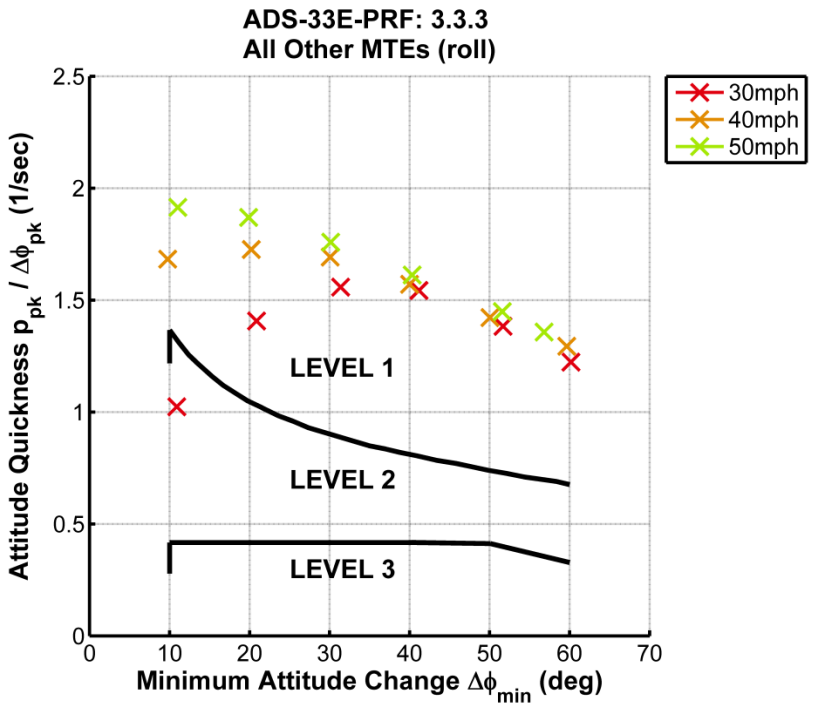

Figure 98: Estimation of autogyro low speed roll quickness

Figure 99 shows that the roll quickness values for the helicopter model fall entirely within Level 1, indicating a high level of agility in this axis. In contrast to the autogyro values shown in Figure 98, Figure 99 shows that the helicopter roll quickness values are independent of airspeed; a similar trend to that displayed in the pitch axis. This has significant implications in terms of piloted handing qualities, as it demonstrates that the helicopter would be more predictable in terms of roll response during dynamic manoeuvres in which airspeed varies. In compensating for the inconsistency of the roll axis response with variation in airspeed, for the autogyro pilot will experience a higher level of handling workload. For aggressive, high workload tasks, this is likely to reduce the level of attainable manoeuvre precision; when operating in the proximity of the ground or other obstacles, this could be safety-critical.

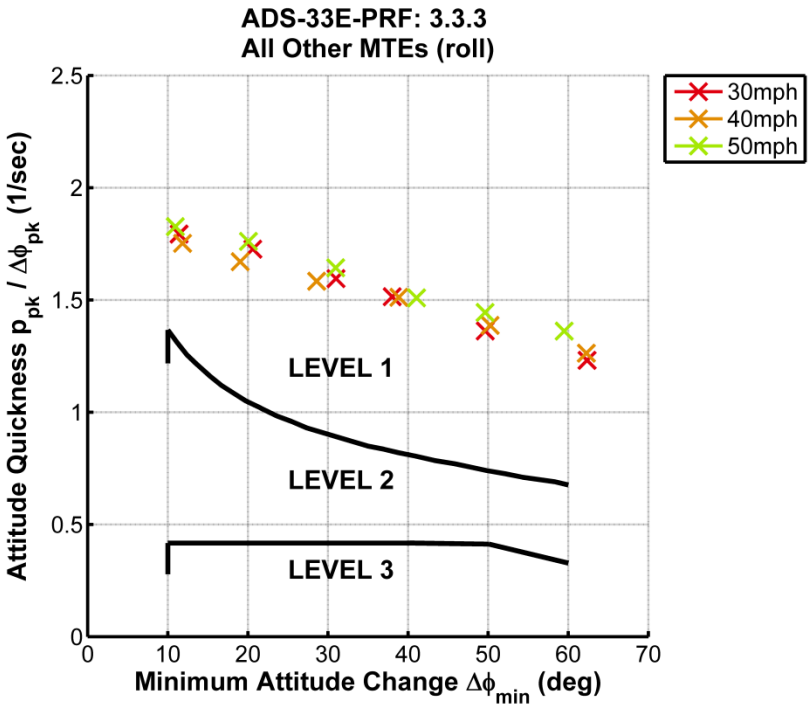

Figure 99: Estimation of helicopter low speed roll quickness

5.4.2.2 Forward Flight Roll Quickness

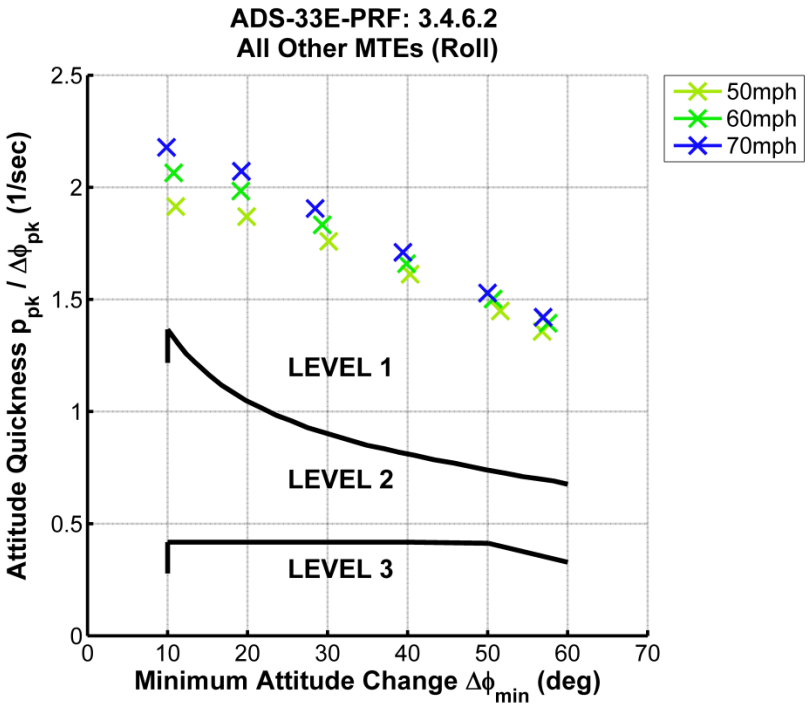

Figure 100: Estimation of autogyro forward flight roll quickness

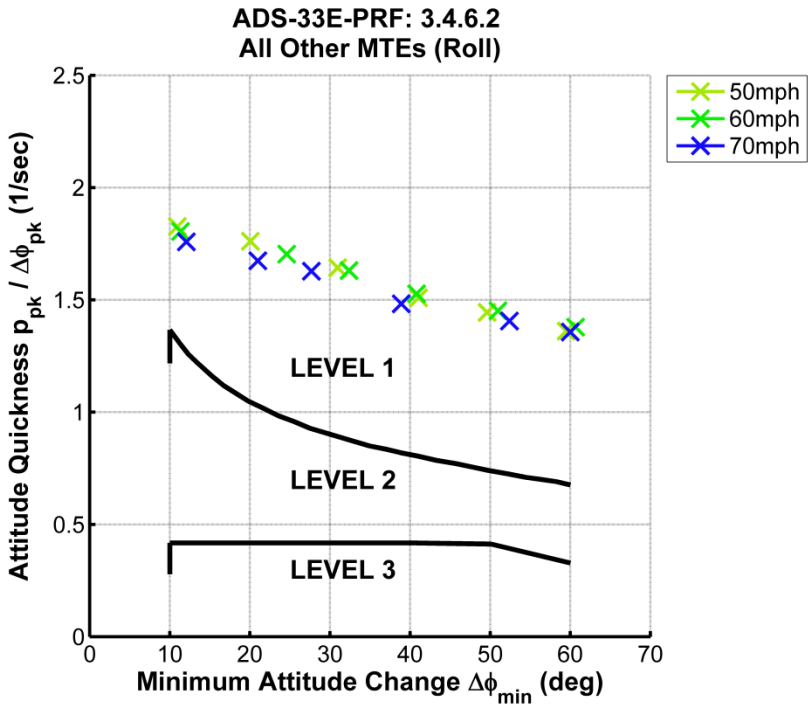

Figure 101: Estimation of helicopter forward flight roll quickness

Figure 100 and Figure 101 show the estimated roll quickness in the forward flight regime for the autogyro and helicopter respectively. Similarly to those test points in the low speed regime, the autogyro continues to display a variation in the quickness values predicted as airspeed and attitude change increase, though the variance is smaller at the higher airspeeds. The helicopter model continues to display roll quickness values consistent with those in the low speed regime. All test points for both the helicopter and autogyro lie in Level 1.

As for the pitch quickness evaluation, the use of the roll quickness parameter has highlighted some potential deficiencies in the autogyro's handling qualities which could prove safety critical. Again, whilst the location of the separation between Level 1/2 and Level 2/3 handling qualities cannot be commented upon, the results are consistent with piloted evaluation, which reported "extreme levels" of roll agility. A method for development of autogyro specific roll quickness limits is described in Section 5.5.2 of this Chapter.

5.4.3 Yaw Quickness

Yaw quickness is defined as "the ratio of peak yaw rate to change in yaw attitude" [2]:

$$Q_{yaw} = \frac{r_{pk}}{\Delta\psi_{pk}}$$

Similarly to the inputs used to evaluate yaw quickness, a maximum amplitude step input in the pedal input is used to generate the required yaw attitude changes. An example of the responses generated is shown in Figure 102. Attitude changes in increments of 10°, from 10° to 60°, were targeted.

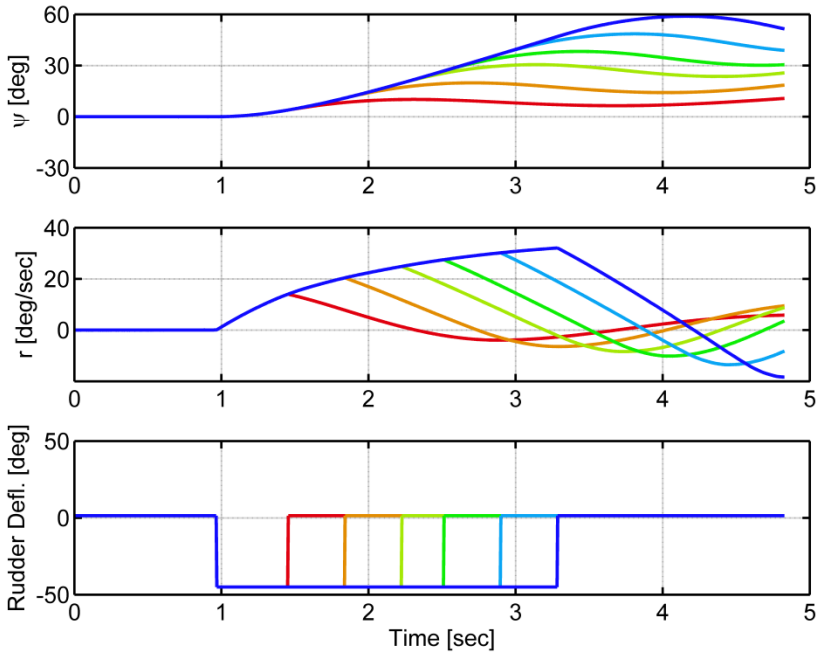

Figure 102: Yaw quickness control input and aircraft response at 50mph for targeted attitude changes from 10° to 60° (autogyro)

It should be noted that, as for pitch quickness, there are no forward flight criteria for yaw quickness.

5.4.3.1 Low Speed Yaw Quickness

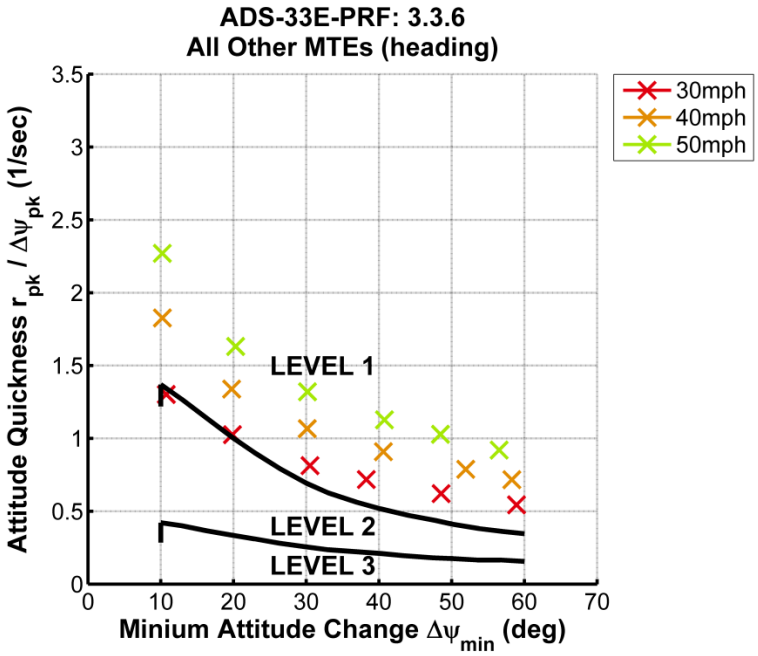

Figure 103: Estimation of autogyro low speed yaw quickness

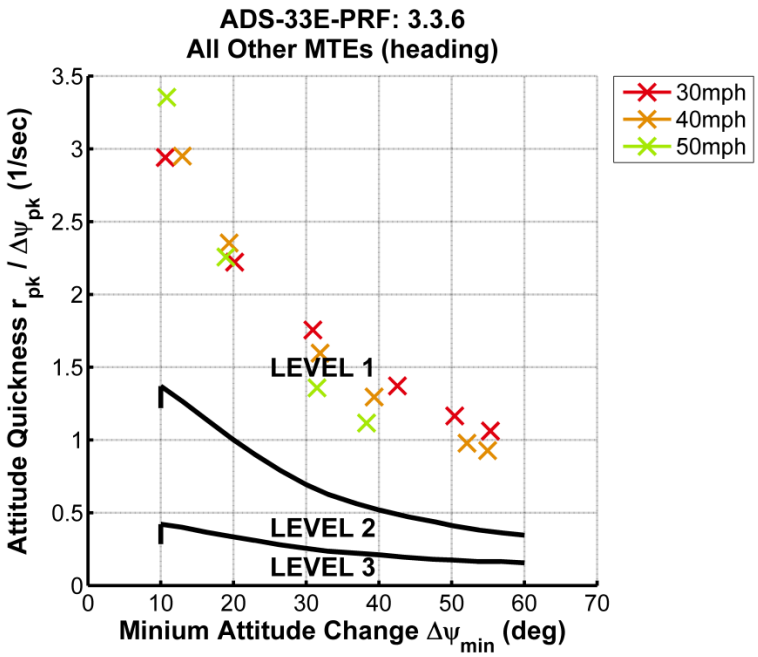

Figure 104: Estimation of helicopter low speed yaw quickness

Figure 103 and Figure 104 show the yaw quickness for the autogyro and helicopter respectively. As for the pitch and roll axes, the yaw axis shows significant differences in the quickness values for a given yaw attitude change throughout the airspeed range for the autogyro. The quickness in the yaw axis for the autogyro is seen to increase with airspeed; this is likely due to the increased rudder effectiveness as airspeed increases.

All test points are in Level 1 for both autogyro and helicopter, except for the lowest attitude change at 30mph for the autogyro, which was just inside Level 2. As for the pitch and roll axes, during simulated flight trials pilots reported high levels of quickness in the yaw axis, which is reflected in the Level 1 predicted handling qualities.

The analyses discussed in this Section have shown that, for quickness in all three axes, it was possible to make predictions regarding the handling qualities of the autogyro using the ADS-33 criteria. Furthermore, evaluation of the quickness parameter has highlighted potential deficiencies in the handling qualities of the autogyro and some key differences from those of the helicopter. Further work and further flight testing with a variety of different autogyro types, in both the simulated environment and in real-world flight test, would be required to determine whether the existing ADS-33 Level 1/2 and Level 2/3 boundaries are applicable to the autogyro. As for the bandwidth and mid-term response to controls criteria, the existing quickness requirements may prove to be applicable, however a mechanism by which the magnitude and effect of the excessive quickness reported in all axes during flight tests can be quantified would be desirable.

5.5 CONTROL POWER

Control power is the performance metric for large amplitude manoeuvres; it is the maximum achievable angular rate in any given axis (for rate-response types). The control power is evaluated by applying a maximum amplitude control input in the axis concerned, and holding it until the steady state response has developed. ADS-33 prescribes three aggression levels for control power, with Level 1, 2 and 3 performance requirements associated with ‘limited manoeuvring’, ‘moderate manoeuvring’ and ‘aggressive manoeuvring’ tasks. Both the autogyro and helicopter models were assessed against all three aggression levels for completeness; however it is unlikely that in their role as sports-utility aircraft they would ever be required to perform ‘aggressive manoeuvring’ which is typically associated with tasks such as air-to-air combat.

ADS-33 specifies requirements for heave axis control power; this is not evaluated here as it is not applicable to the autogyro aircraft.

5.5.1 Pitch Control Power

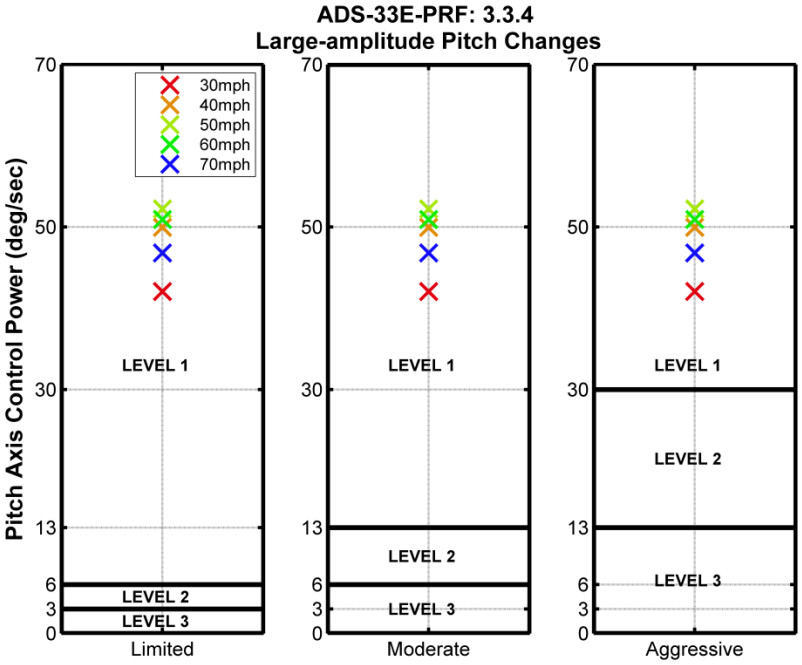

Figure 105: Pitch control power for autogyro

The pitch control power for both autogyro and helicopter models are shown in Figure 105 and Figure 106 respectively, with both aircraft easily achieving Level 1 handling qualities at all tests points, against all criteria. This is to be expected as both aircraft have relatively low mass and low pitch inertias; the high control power is also responsible for the large values of quickness observed in Section 5.4. Similarly to the requirements for quickness, ADS-33 does not specify upper limits on control power; and in the case of this aircraft that may be detrimental to the overall handling qualities, and thus safety of this aircraft type.

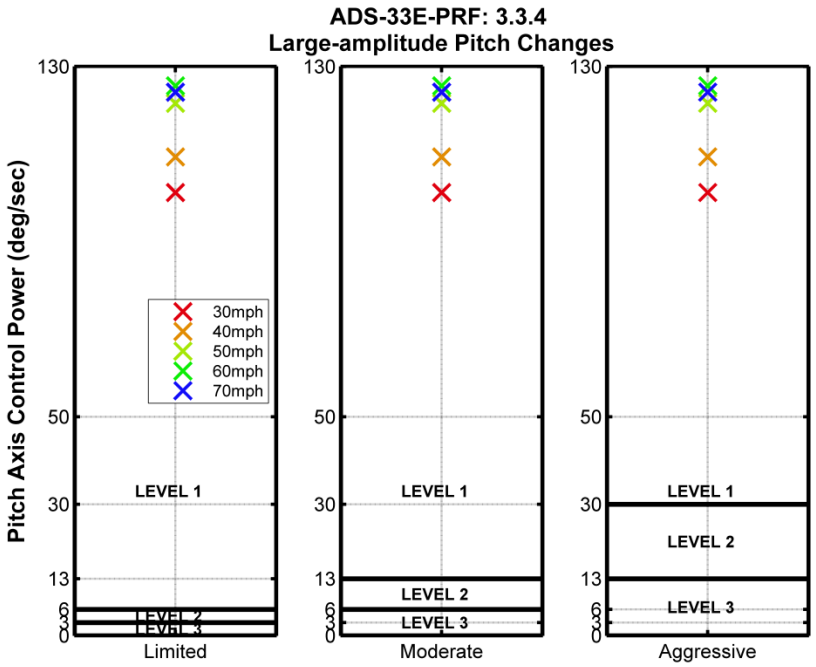

Figure 106: Pitch control power for helicopter

5.5.2 Roll Control Power

The roll control power for autogyro and helicopter are shown in Figure 107 and Figure 108. As for pitch control power, all test points for roll control power proved to be well inside Level 1 for all aggressions. Low roll inertia, coupled with a lack of significant horizontal surfaces to provide roll damping and a strong (though anecdotally reported) torque-to-roll couple each play a part in allowing the aircraft to generate this high control power.

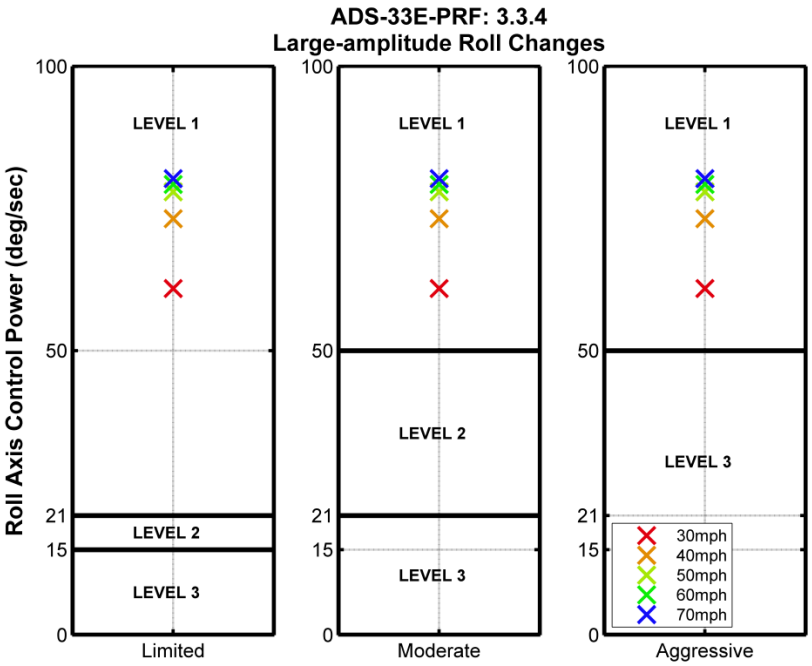

Figure 107: Roll Control Power for Autogyro

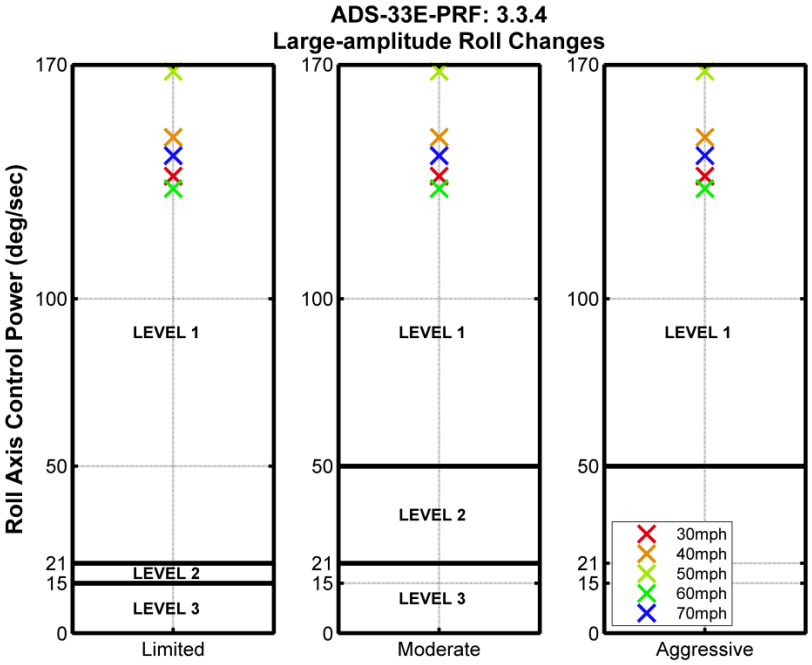

Figure 108: Roll Control Power for Helicopter

5.5.3 *Yaw Control Power*

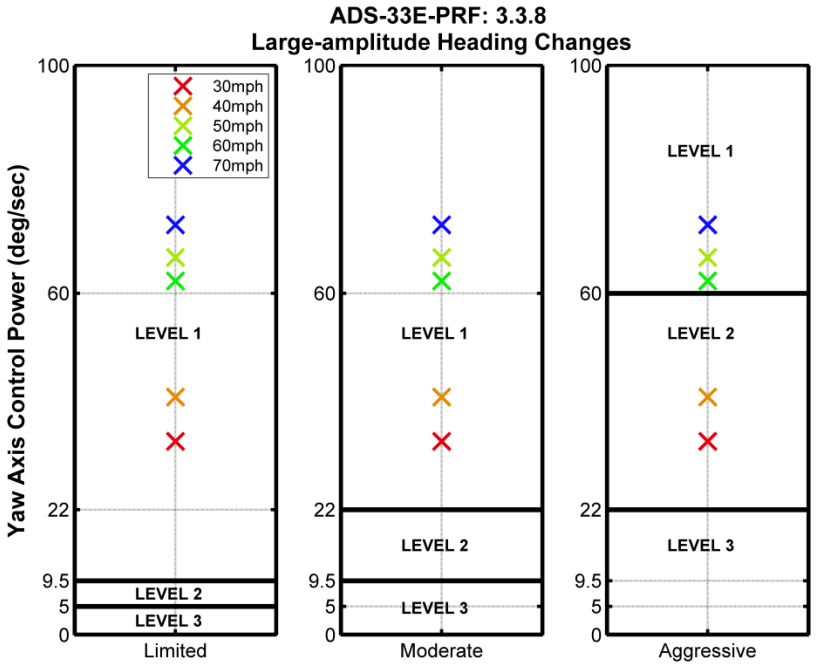

Figure 109: Yaw Control Power for Autogyro

The yaw axis is the axis in which significant differences between the autogyro and helicopter models are evident. Results for the autogyro model are shown in Figure 109. For limited and moderate manoeuvring, all test points are in Level 1. For aggressive manoeuvring, the higher speed test points (50, 60 and 70mph) achieve Level 1, with the 30 and 40mph test points achieving Level 2 predicted handling qualities. Generally, as airspeed increases, the control power in the yaw axis also increases. This is due to the increased effectiveness of the rudder at increased airspeeds (the force generated by the rudder being directly proportional the square of the velocity of the air passing over it). This will result in the pilot having to reduce the magnitude of control inputs applied to the rudder pedals as airspeed increases in order to generate the same change in heading in the same amount of time. This variance in handling performance with airspeed will increase pilot workload.

Conversely to this, Figure 110 shows that the yaw control power for the helicopter model decreases with increasing airspeed; as forward airspeed increases, so does yaw stability, resulting in a reduction in yaw control power.

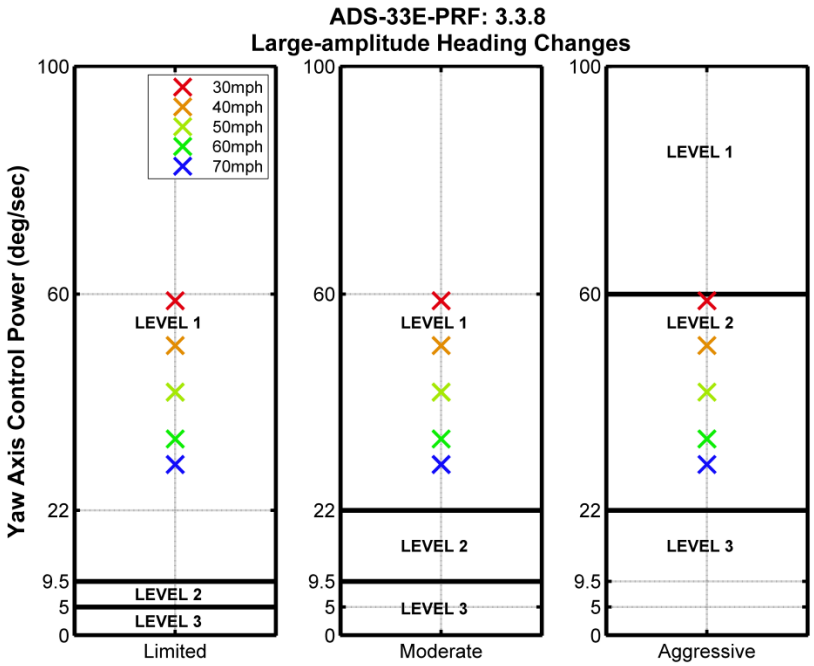

Figure 110: Yaw Control Power for helicopter

The increased control power at high airspeeds in yaw, and the generally high control power in all axes is a potential source of deficiency in the autogyro, and under rapid manoeuvring, one which may become safety critical. This issue is discussed further in the context of the piloted evaluation described in Chapter 6.

5.6 CROSS COUPLING

Satisfactory handling qualities in the on-axis response criteria previously described in this Chapter are not enough to guarantee overall good flying qualities for any type of aircraft. Helicopters are characterised by the nature of their complex inter-axis couplings; applying a response in any given axis will generate a response in one or more of the other axes. ADS-33 defines its cross coupling criteria as "the ratio of peak off-axis attitude response from trim within 4 seconds to the desired (on-axis) attitude response from trim at 4 seconds, following an abrupt lateral or longitudinal cockpit control step input, shall not exceed ±0.25 for Level 1 or ±0.60 for Level 2. Heading shall be maintained essentially constant." These values are constant across the airspeed envelope. The pitch due to roll and roll due to pitch criteria are defined as:

$$\boldsymbol{Pitch\ due\ to\ Roll} = \frac{\Delta\boldsymbol{\theta_{pk}}}{\Delta\boldsymbol{\phi_4}}$$

or

$$\textbf{\textit{Roll due to Pitch}} = \frac{\Delta \boldsymbol{\phi_{pk}}}{\Delta \boldsymbol{\theta_4}}$$

where $\Delta\vartheta_{pk}$ and $\Delta\varphi_{pk}$ the peak change in pitch or roll attitude and $\Delta\vartheta_4$ and $\Delta\varphi_4$ are the change in the off-axis attitudes 4 seconds after the control input has been applied.

In order to maintain the requirement for the heading to be maintained "essentially constant", responses to control inputs were extracted from the model with the heading states 'locked out', which artificially drives the dynamic response in the yaw axis to zero, such that heading is maintained.

Figure 111 shows an example of the dynamic response from a longitudinal input designed to generate the required response to evaluate cross coupling. A 1 inch step input is used, limited to 1 second in duration in order to allow the response to develop.

ADS-33 also specifies limits on the yaw due to collective cross coupling commonly found in helicopters. This is not analysed here as the autogyro does not experience this cross coupling.

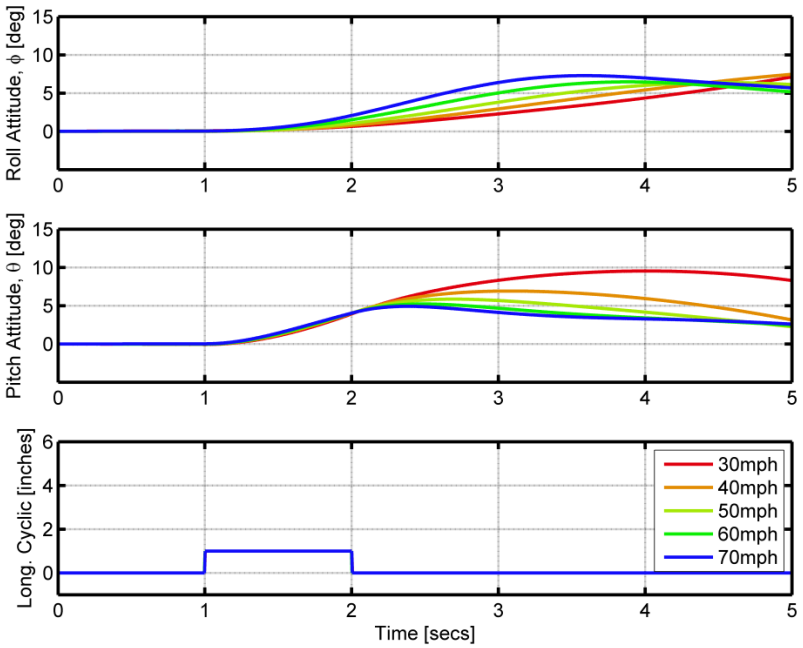

Figure 111: Example output for roll due to pitch cross coupling calculation

5.6.1 Roll due to Pitch and Pitch due to Roll

The roll due to pitch and pitch due to roll couplings for autogyro and helicopter models are evaluated in Figure 112 and Figure 113; it can be clearly seen that the autogyro displays significantly larger cross couplings in both the pitch and roll axes than the geometrically equivalent helicopter. This can be attributed in part to the high quickness of the autogyro in both axes compared to the helicopter.

Both the pitch due to roll and roll due to pitch cross couplings arise due to gyroscopic precession. When a rotor is disturbed by an externally acting force (for example the application of roll or pitch control) the advancing blade will experience an increase in lift due to the higher relative velocity it experiences compared to that of the retreating blade. Because of this, the rotor blade experiences a sinusoidally varying force, oscillating about the normal plane at its natural frequency, which is dependent upon the blade mass and the centrifugal force acting upon the blade. This frequency is near identical to the rotational frequency of the rotor. As a result of this, when an external force tries to tilt the plane of the rotor, this sinusoidal force on each blade is driving the blade at its natural resonant frequency. At resonance, the driving force and the velocity are in phase, and the amplitude of the response is 90° out of phase. This is how the roll due to pitch and pitch due to roll couplings arise; application of control in the pitch axis will cause a response in the roll axis, and vice versa.

For all test points, the autogyro has roll due to pitch ratings in Level 3, with the magnitude of the coupling increasing with airspeed. The pitch due to roll ratings begin in Level 3 at 30mph, moving through Level 2 as airspeed increases, and into Level 1 and 70mph.

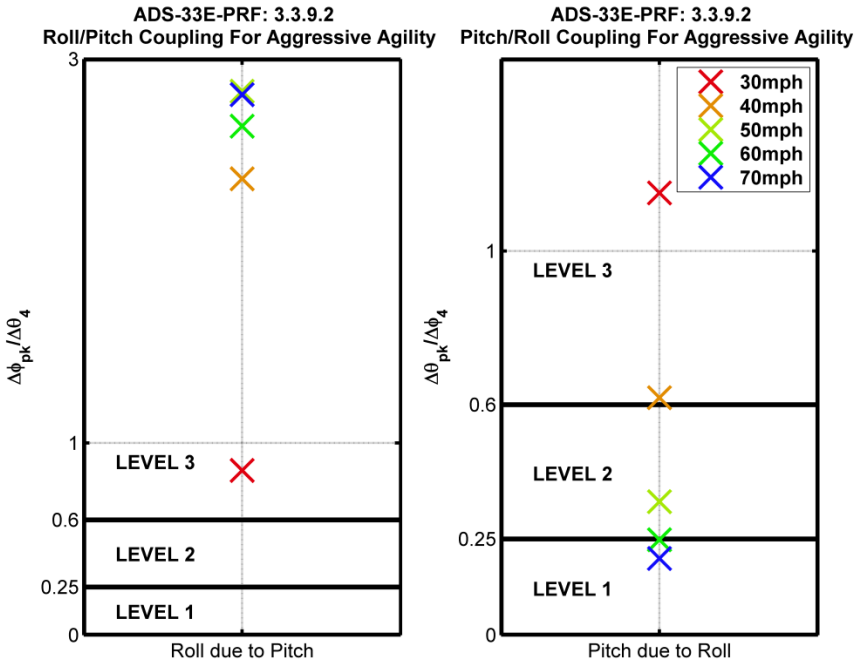

Figure 112: Roll due to Pitch and Pitch due to Roll cross coupling evaluation for autogyro

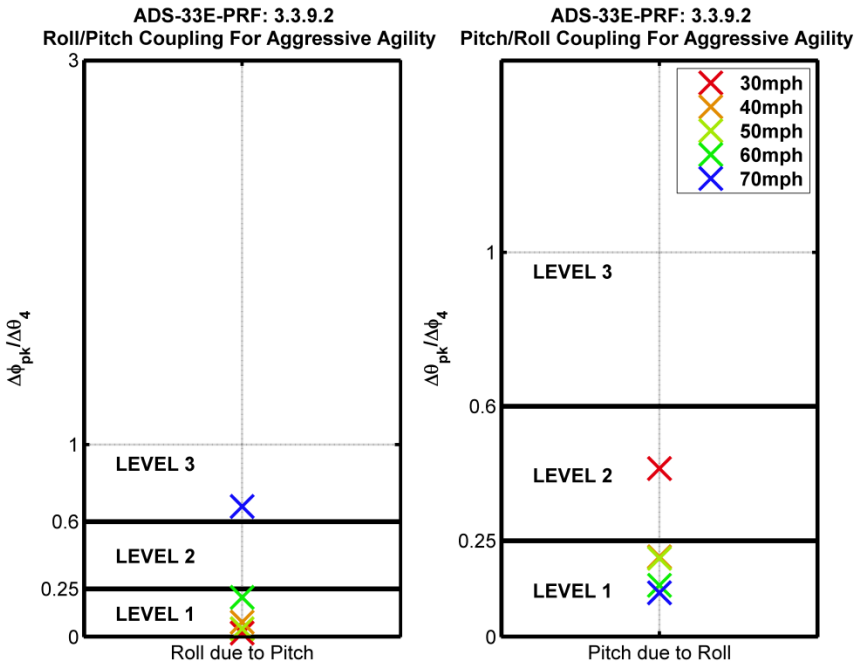

Figure 113: Roll due to Pitch and Pitch due to Roll cross coupling evaluation for helicopter

The helicopter model displays similar trends, as shown in Figure 113, though its cross-couplings are of markedly smaller magnitude than those of the autogyro. The helicopter roll due to pitch coupling is in Level 1 for all test points up to 60mph, though the magnitude of the cross coupling does increase with airspeed. At 70mph, the roll due to pitch coupling moves into Level 3.

Similarly to the autogyro, the pitch due to roll cross coupling is seen to decrease with airspeed, but the magnitude of the coupling is reduced when compared to that of the autogyro. At 30mph, the pitch due to roll cross coupling lies in Level 2, moving into Level 1 at 40mph and continuing to reduce up to 70mph.

The difference in magnitude of the roll to pitch and pitch to roll couplings may be attributed to the difference in the on-axis criteria characteristics of the two aircraft. The autogyro's low roll damping and low roll inertia, coupled with high pitch quickness and control power will result in high roll due to pitch coupling. Similarly, the autogyro's limited pitch damping and very high roll control power will result in large pitch due to roll coupling.

The autogyro also features direct mechanical control, with the longitudinal and lateral controls being directly linked to the rotorhead. This eliminates the delays introduced by the addition of electromechanical or hydraulic actuators used in the more complex helicopter system (modelled in FLIGHTLAB by first order transfer functions), which would result in additional phase delay between the application of the force and the reaction, moving the oscillating frequency of the rotor away from the resonant frequency and reducing the magnitude of the resultant blade displacement that causes the cross couplings. This mechanical control coupled with low axial inertias and high control power also accounts for the high levels of quickness observed.

One of the main differences between the autogyro and the helicopter is the control used to command the speed of the aircraft. In an autogyro, the airspeed is controlled by the throttle, and decoupled from the main rotor; in a helicopter, cyclic pitch of the main rotor is used to select airspeed. Therefore, large roll due to pitch couplings are undesirable in a helicopter as they would impact on the pilot's ability to control the flight path and ultimately the airspeed of the aircraft. The large roll due to pitch coupling experienced

by the autogyro will have a more considerable impact on the pilot's ability to control the rate of climb and descent of the aircraft. Due to the fact that the effect of these cross couplings will affect each of these different aircraft types in different ways, it is unlikely that, for example, the amount roll due to pitch coupling that is considered acceptable in a helicopter would be considered acceptable for an autogyro, and thus the ADS-33 requirements may not be applicable to the autogyro in this case.

Further flight testing with a range of different aircraft models would be required to ascertain what level of cross coupling would be acceptable for the autogyro. The simulation model used to analyse the existing criteria in this Chapter would be an ideal candidate for this task as, for example, it can be easily reconfigured with increased roll inertia or a larger horizontal tailplane in order to vary the roll damping and thus the roll due to pitch. A simple control system to eliminate cross couplings could also be implemented. A variety of configurations with differing levels of cross coupling would then be assessed using the Cooper Harper scale during piloted MTEs, and the resulting assigned handling qualities used to derive the Level 1/2 and Level 2/3 boundaries (a similar methodology to that described in Section 5.7 for derivation of roll quickness criteria).

5.7 DEVELOPMENT OF HANDLING QUALITIES REQUIREMENTS FOR AUTOGYROS

In "*Handling Qualities Assessment of an Autogiro"* [7], Bagiev and Thomson demonstrate the definition of handling qualities criteria for both the roll quickness and pilot attack parameters. The definition of the criteria for Level 1, Level 2 and Level 3 boundaries for these criteria were based on flight test data gathered using the G-UNIV aircraft. Bagiev and Thomson conclude that the test data gathered was "insufficient to determine proper handling qualities levels". The use of only one aircraft type and a single pilot (who was not a formally trained test pilot) also placed limitations on the validity of any conclusions generated from the data gathered during these flight tests.

It is the intention of this Section to use data gathered during simulated flight trials, using the simulation model described in Chapter 3, to analyse the recommendations made in Ref. 4 and to comment upon their validity. Where appropriate, recommendations were modified or added based on these findings.

5.7.1 Roll Quickness

Ref. 7 uses flight test data recorded during the Slalom manoeuvre, as defined in Chapter 3, to establish Level 1/2 and Level 2/3 boundaries for the prediction of roll quickness. Each test point recorded during the manoeuvre is associated with an HQR, awarded based on ratings derived using the Cooper-Harper handling qualities scale [54]. Bagiev and Thomson used these ratings to create boundaries similar to those found in ADS-33 [2], such that points which had HQRs 1 to 3 lay within the Level 1, points with HQRs 4 to 6 lay within Level 2 and those with HQR 7 to 10 lay within Level 3. These proposed levels for roll quickness are shown in Figure 114, plotted alongside the existing boundaries from ADS-33 and the 70 deg.sec^{-1} manoeuvre limit.

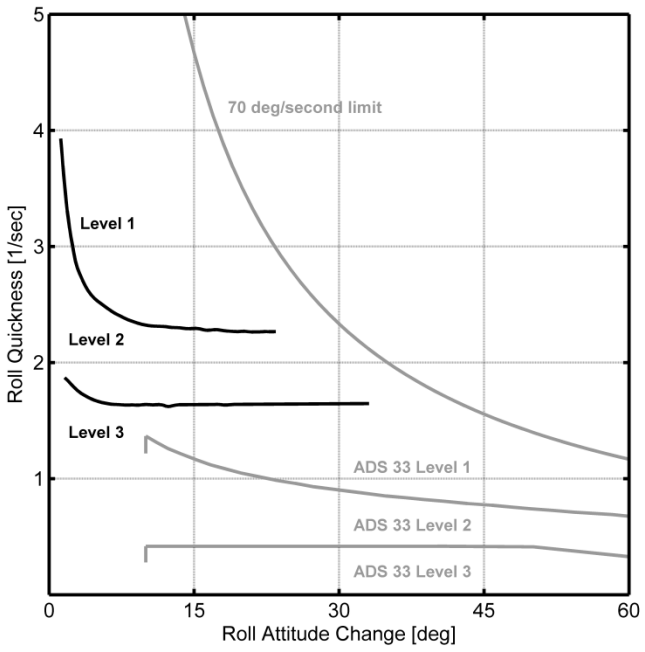

Figure 114: Proposed roll quickness limits for autogyro from Ref. 7

These boundaries represent a first attempt at defining 'ADS-33 style' handling qualities requirements for the autogyro, with some caveats. In the flight test described in Ref. 7, the pilot is observed to be using "high angles of sideslip" in order to generate the lateral velocity required to complete the slalom manoeuvre. ADS-33 [2] does not prescribe a limit on the amount of sideslip permissible during the slalom manoeuvre; however, the manoeuvre is typically flown (in a helicopter) using lateral stick as the primary control,

with pedals used to co-ordinate turns. As a result of this piloting strategy, the maximum roll attitude change for the autogyro flight test data does not exceed 10°.

Quickness is a parameter which relates to what ADS-33 describes as "moderate amplitude attitude changes", stating that "the attitude changes required for compliance with this requirement (quickness) shall vary from 10° in roll to the limit of the Operational Flight Envelope or 60° in roll, whichever is less". The data set used to generate the suggested boundaries in Ref. 7 does not meet this requirement, and therefore is not appropriate for use in this context. The proposed boundaries are also based on a limited amount of data, flown using only one pilot, with Ref. 7 stating that "the availability of more data using different pilots and aircraft would of course confirm the positioning of these boundaries."

In order to further develop these boundaries, this process was repeated with data gathered from simulated flight tests using the slalom manoeuvre described in Chapter 3 (3.5.4.1). These flight tests use a range of course geometries and airspeeds to vary the aggression level required to complete the manoeuvre. Each run was rated using the Cooper-Harper scale [54]. This series of flight tests was carried out using a qualified test pilot, and the conventional piloting technique of using roll attitude change to generate the required lateral velocities to complete the slalom course. The results of these flight tests are shown in Figure 115, Figure 116 and Figure 117, with each Figure individually representing a given HQR Level for clarity. Test points with attitude changes less than 10° have been included for completeness, and in order to provide data against which to compare the proposed limits from Ref. 7.

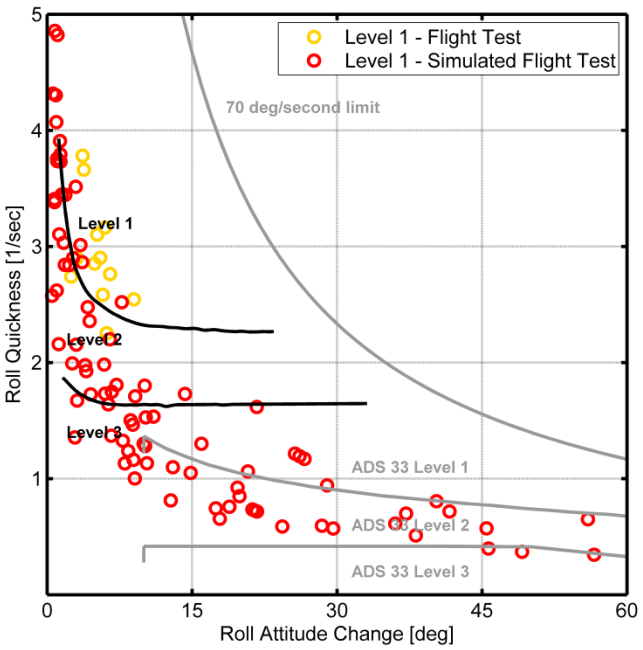

Figure 115: Autogyro roll quickness evaluated for both flight test and simulated slalom manoeuvre – Level 1 test points only

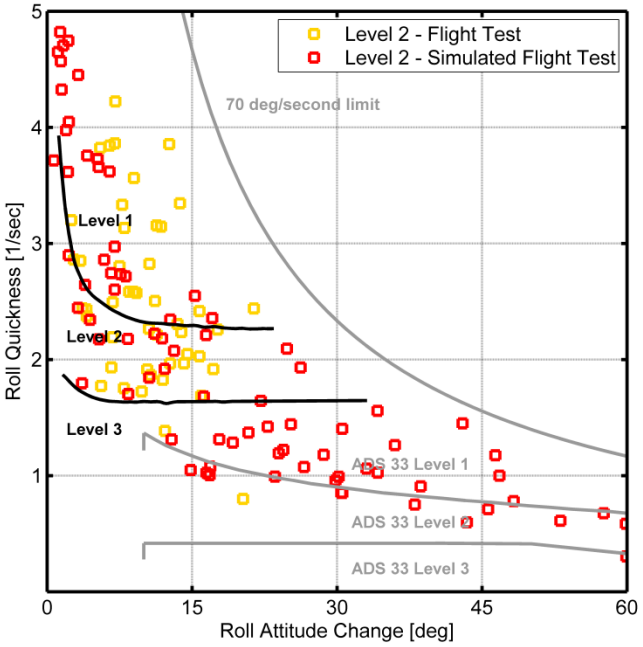

Figure 116: Autogyro roll quickness evaluated for both flight test and simulated slalom manoeuvre – Level 2 test points only

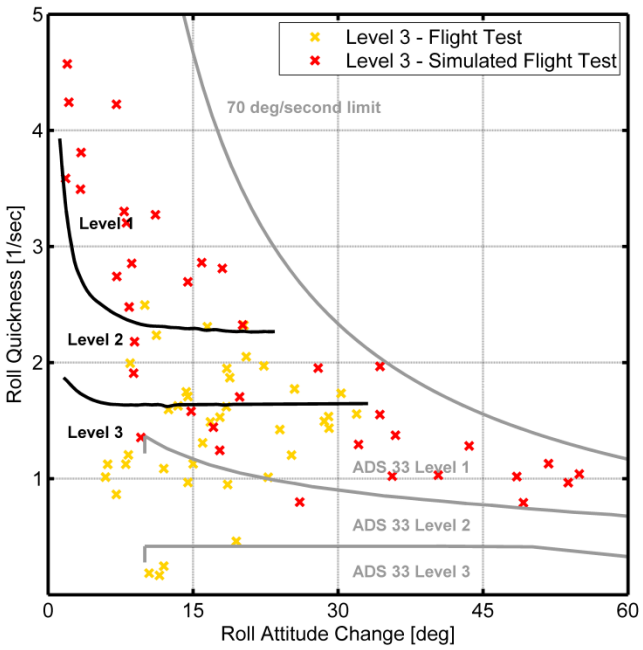

Figure 117: Autogyro roll quickness evaluated for both flight test and simulated slalom manoeuvre – Level 3 test points only

Figure 115 - Figure 117 illustrate that the data from the simulated flight test does not show a strong agreement with either the boundaries proposed in Ref. 7 or the extant boundaries from ADS-33 [2].

It can be seen that the trend within the data is reversed relative to that shown in the data from the original flight trial; as the HQR ratings increase (moving from Level 1 to Level 3), the quickness also increases. This is shown in Figure 118. Re-plotting the calculated quickness parameters from the simulation trial, without those test points which fall below the 10° roll attitude change threshold, it can clearly be seen that the majority of the Level 2 test points have higher quickness compared to those test points with associated Level 1 HQRs, and those with Level 3 HQRs generally have a higher quickness than those with Level 1 or 2 HQRs. This is in direct opposition to what was expected from feedback during the simulated flight test programme; pilots described the aircraft as being "nimble" in roll and possessing "high levels of agility" – suggesting that, fundamentally, the autogyro has a high level of roll quickness. Considering the aircraft

geometry supports this; the fuselage is narrow, and there are no large horizontal surfaces to generate large amounts of roll damping which would decrease roll quickness.

Utilising the methodology described in Ref. 7, proposed handling qualities levels have been created from the data. These levels are shown in Figure 119 and Figure 120.

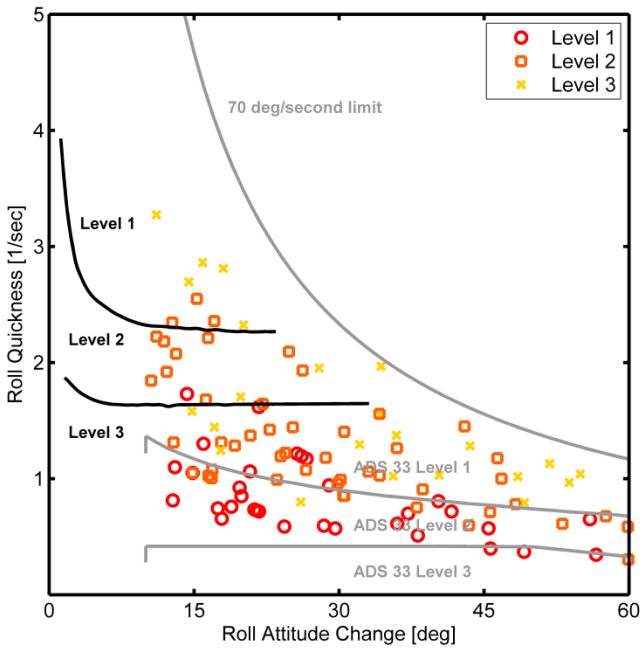

Figure 118: Roll quickness parameter for the slalom manoeuvre, plotted against both limits proposed in Ref. 7 and limits from ADS-33 [2]

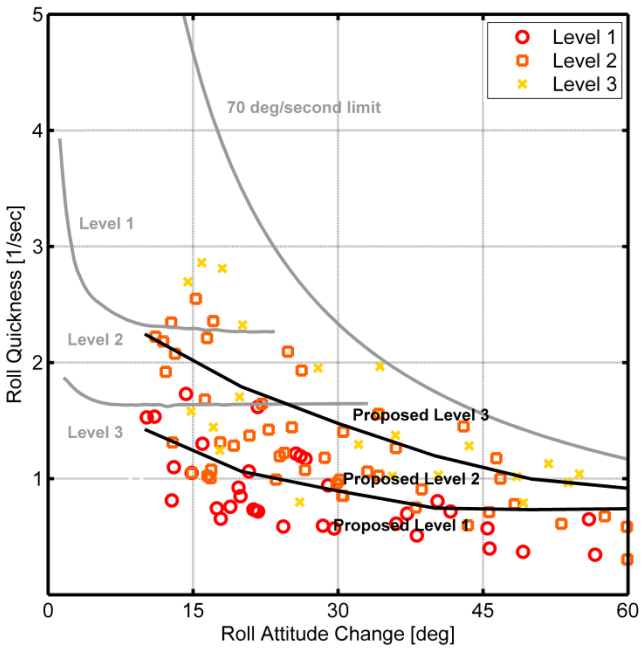

Figure 119: Proposed roll quickness limits based on simulated flight test data (with data)

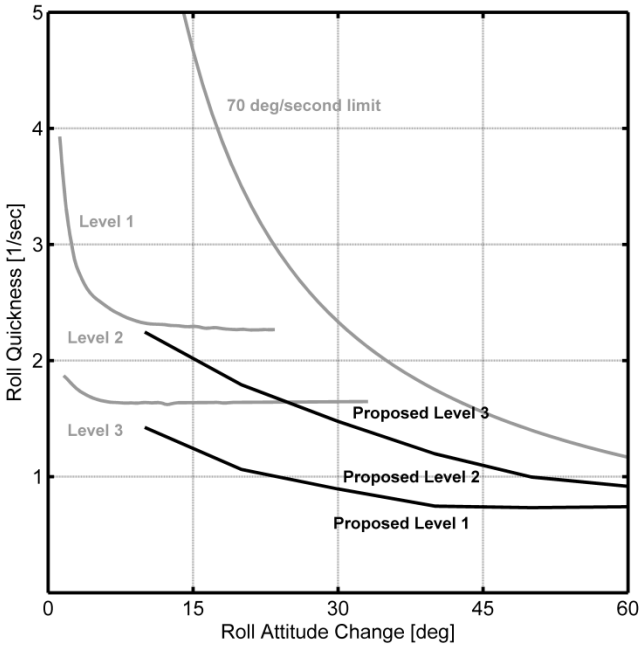

Figure 120: Proposed roll quickness limits based on simulated flight test data (without data)

This reversal in trend has occurred for a several reasons. The data presented in Figure 118 and Figure 119 is gathered from manoeuvres flown at a variety of airspeeds (35, 50 and 70mph) and across a variety of course geometries. This means that that the level of aggression required to complete the slalom manoeuvre is varied for each test point; those carried out at higher airspeeds and those on lower aspect ratio courses (i.e. short and wide courses) will require larger and more rapid control inputs to successfully generate the bank angles, and thus the lateral velocity, required to complete the course. This is illustrated in Figure 121; the control inputs used, and the resulting bank angles generated, for the higher aspect ratio (AR = 0.067) course are markedly smaller than those used for the lower aspect ratio course (AR = 0.2). The rate at which the control inputs are applied is also reduced, as there is no need for the pilot to be more aggressive in order to complete the course to within the desired criteria. ADS-33 states that the "required attitude changes shall be made as rapidly as possible from one steady attitude to another"; for the higher aspect ratio course (AR = 0.067), the method of applying control inputs clearly does not meet this requirement. As a result, this more gentle application of control does not generate a true measure of the aircraft roll quickness, as the maximum possible roll rate is not generated.

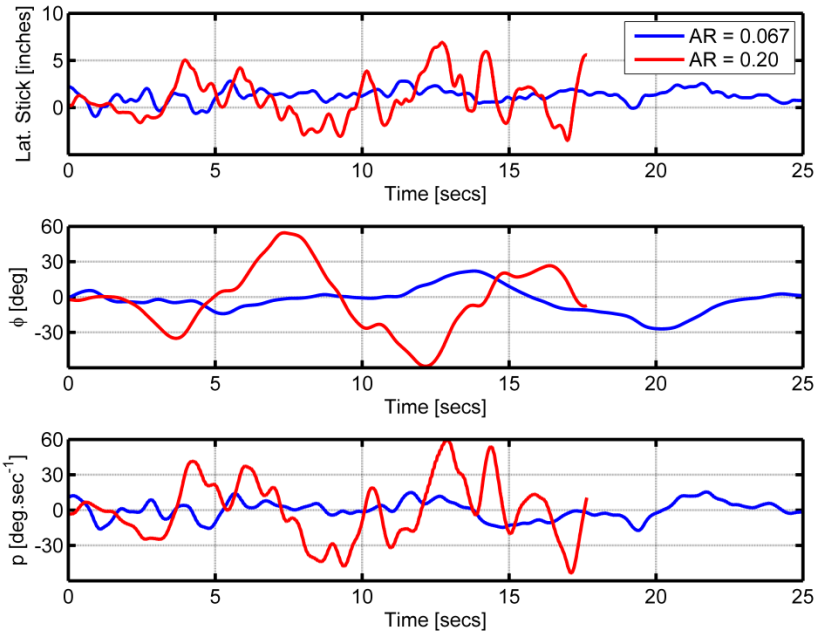

Figure 121: Sample control trace from 2 slalom manoeuvres of different aspect ratio, performed at 35mph

This becomes problematic; at the lower end of the speed range, and for the higher aspect ratio courses, the pilot is easily able to achieve desired performance for the slalom manoeuvre utilising this gentle control strategy and thus awards Level 1 handling qualities to runs during which a true measure of the aircraft quickness has not been recorded. As airspeed increases, and course aspect ratio decreases, the pilot finds completing the task to within the desired criteria impossible, and as a result is forced to award Level 2 and Level 3 HQRs. These more challenging test points do more accurately reflect the true value of the roll quickness, due to the more aggressive pilot strategy required to complete the course but are associated with poorer handling qualities, which result in the reversal of the ordering of the handling qualities levels observed in Figure 119 and Figure 120.

For each combination of airspeed and course aspect ratio, the pilot also awarded a workload rating using the Bedford Workload Scale. As the airspeed increases and/or aspect ratio of the course decreases, and thus the magnitude and rate of control inputs increases, the pilot workload also perceptibly increases. This is illustrated in Figure 122. The increasing workload generated by this increased control activity makes it more difficult for the pilot to complete the manoeuvre to within in the desired and adequate criteria, increasing pilot compensation; this causes the HQRs awarded to increase, further contributing to the reversal in the ordering of the handling qualities levels observed in Figure 119 and Figure 120.

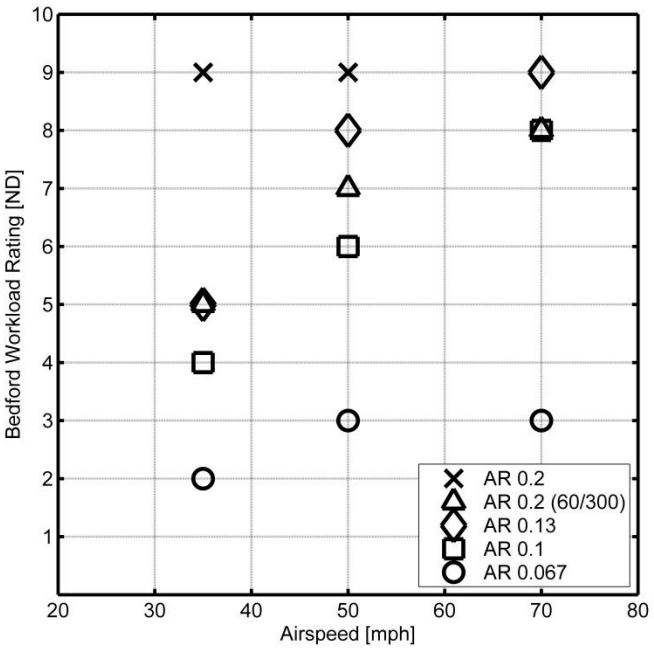

Figure 122: Pilot workload ratings for all slalom manoeuvres

Ref. 7 states that "the availability of more data using different pilots and aircraft would of course confirm the positioning of these boundaries." Whilst the investigations presented here represent the contribution of more data, and data flown using a different pilot, the conclusions drawn are still based only upon the analysis of one aircraft type. However, it is possible to comment upon the validity of the method used to generate these results.

ADS-33 specifies only a single geometry for the slalom course. In the investigation presented here, a variety of course geometries are used and, as discussed, this has implications for the resulting handling qualities and the derivation of the boundaries between Levels. As quickness is an innate quality of a given aircraft, defined by the aircraft geometry, the first step in defining the requirements for roll quickness should be to identify a course geometry which will force pilots to use a control strategy which will generate results that reflect the true quickness of the aircraft.

This could be achieved through inverse simulation as demonstrated in Ref. 58, allowing the slalom manoeuvre to be completed without manoeuvre limits of the rotorhead being

reached, remaining within the input frequency range of a human pilot and within safe bank angle limits.

5.7.2 Pilot Attack

Pilot attack is an objective metric used to assess pilot workload. It should be noted that, although it is not part of ADS-33, this parameter was selected for autogyro handling qualities evaluation by Ref. 7. Therefore, it is considered in this Section for the purposes of comparison. For the lateral axis, it is defined as the ratio between the peak value of the rate of change of lateral stick displacement and the corresponding net stick displacement (Ref. 59):

$$\boldsymbol{Pilot\ Attack} = \frac{\dot{\boldsymbol{\eta}}_{\boldsymbol{peak}}}{\Delta \boldsymbol{\eta}}$$

The pilot attack metric was developed by Padfield et al. [60] and it is hypothesised that workload levels can be defined as a function of the change in net stick displacement.

Ref. 7 also demonstrates a similar type of analysis for the pilot attack parameter to that carried out for quickness; the resulting proposed levels are shown in Figure 123. For the purpose of these results, 100% of stick travel is defined as moving from full displacement to the left to full displacement to the right.

As for the evaluation of roll quickness, data from simulated flight trials of the slalom manoeuvre was used to evaluate the pilot attack parameter in the lateral axis. The results of this evaluation are shown in Figure 124 to Figure 126, plotted against the proposed levels from Ref. 7 and the original data from the real-world flight test used to define the proposed level boundaries. It should be noted that there are no workload levels defined for the pilot attack chart for helicopters.

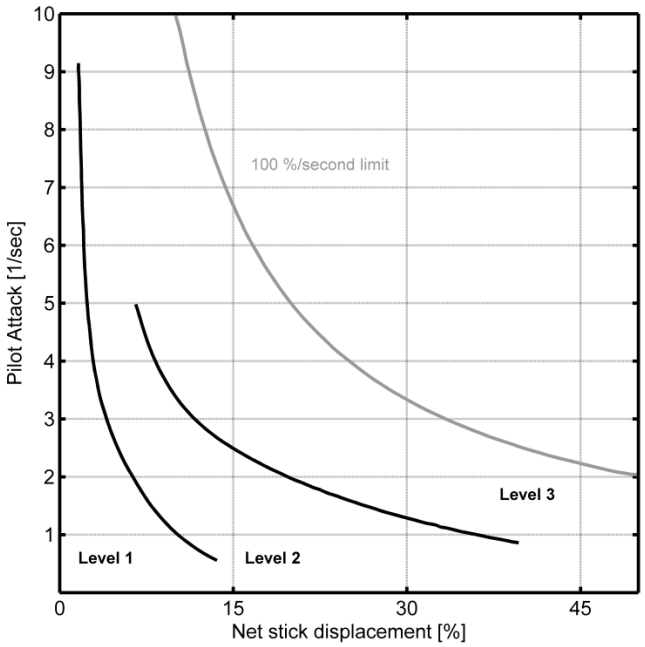

Figure 123: Proposed handling qualities levels for Pilot Attack from Ref. 7

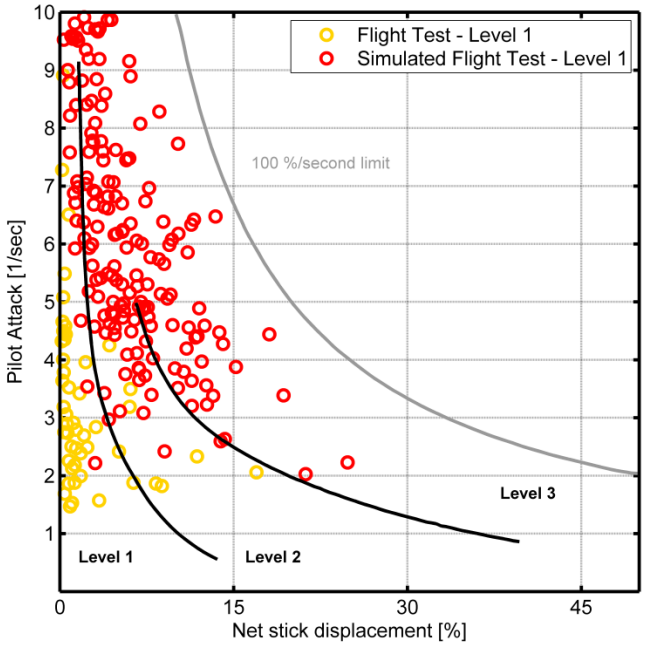

Figure 124: Autogyro pilot attack parameter evaluated for both flight test and simulated slalom manoeuvre – Level 1 test points only

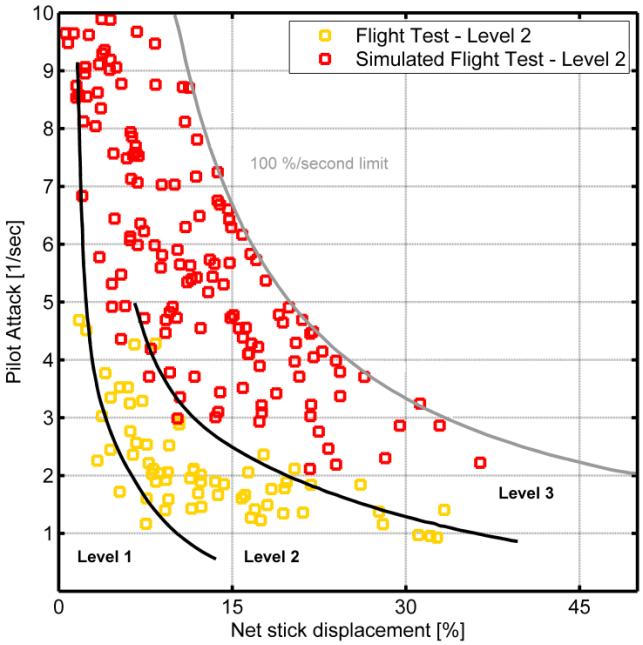

Figure 125: Autogyro pilot attack parameter evaluated for both flight test and simulated slalom manoeuvre – Level 2 test points only

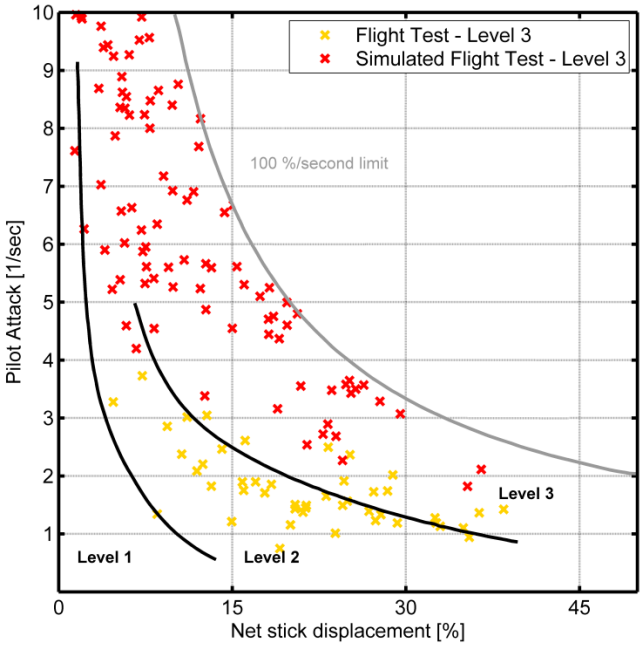

Figure 126: Autogyro pilot attack parameter evaluated for both flight test and simulated slalom manoeuvre – Level 3 test points only

As per the results for roll quickness, the simulated flight test results for pilot attack do not agree well with the levels for pilot attack proposed in Ref. 7. This may be due to differences between the control feel in the simulator and that of the real aircraft. The real aircraft employs a simple mechanical link between the rotor and the cyclic controller, which will result in considerable stick forces in flight. This will limit the rate at which the pilot can move the cyclic control. In the simulator, the stick forces will be considerably lower; it is not possible to quantify to what extent as the stick forces in the real aircraft are unknown.

The non-standard technique used to fly the original slalom manoeuvre will also affect the results; using excessive sideslip to complete the course will mean that the pilot does not use the fully capability of the lateral cyclic, reducing the net stick displacement values associated with a given HQR.

Using the simulated flight test data presented in Figure 124 to Figure 126 is possible to re-draw and propose new autogyro handling qualities levels for pilot attack, as illustrated in Figure 127.

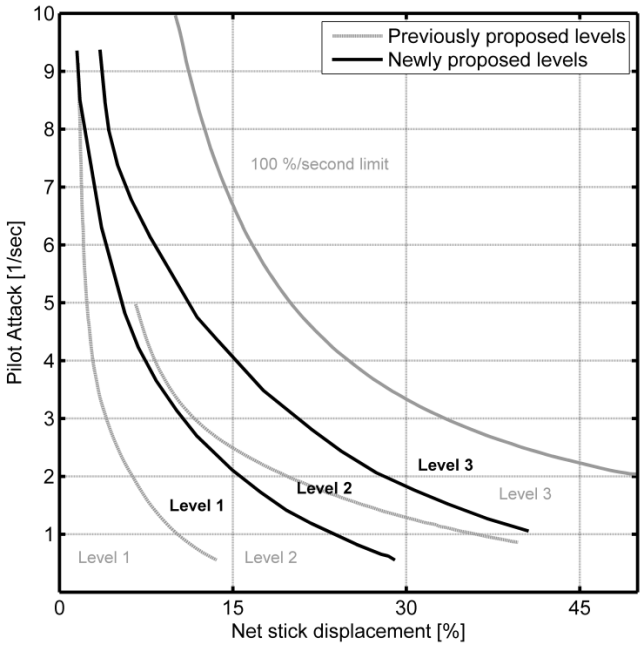

Figure 127: Proposed handling qualities levels for pilot attack manoeuvre

5.7.3 Roll due to Power Cross Coupling

During simulated flight trials, it has been reported by pilots that there is a strong power to roll coupling present in the autogyro model. The presence of this coupling is not unexpected; the autogyro is not equipped with an anti-torque system, so there is nothing to counter the torque reaction generate by the propeller. This, coupled with low roll inertia due to the aircraft's low mass and low roll damping due to the absence of large horizontal surfaces (wings or a large tailplane), would result in a considerable amount of roll developing if an abrupt increase in power were to be applied. There are currently no prescribed predicted handling qualities levels to quantify the acceptable magnitude of this power to roll cross coupling, and it is beyond the scope of a single PhD Thesis to quantify such a parameter; the number of different autogyro configurations, test conditions and pilots required to would require a significant research effort to draw definitive conclusions.

However, the autogyro model used herein to explore the existing criteria would be a very useful tool in taking the first steps towards providing predicted handling qualities Levels for this cross-coupling. The process of defining the Levels would be similar to that described in Section 5.7 of this Chapter; defining an MTE featuring an abrupt speed change and assigning handling qualities ratings to the manoeuvre at a range of different conditions across the flight test envelope would allow Level 1/2 and 2/3 boundaries to be identified. The ability of the model to be rapidly altered to increase or decrease the roll damping (and thus increase of decrease the magnitude of the power to roll cross coupling) would allow for this process to be repeated, identifying the acceptable magnitude of this cross coupling and the appropriate location of the Level 1/2 and 2/3 boundaries.

5.8 CONCLUSIONS

A complete analysis of the predicted handling qualities metrics defined in ADS-33 [2] has been carried out. This in itself is a significant novelty as it is the first time an analysis of this type has been carried out in its entirety. The existing criteria have been considered in the light of their applicability to autogyro-type aircraft and development of autogyro-specific handling qualities has been considered. Alongside this, the autogyro model has also been compared to a geometrically equivalent helicopter model in order to identify any key differences in predicted handling qualities between the two configurations.

The use of the existing ADS-33 criteria has highlighted some potential areas of concern in the autogyro's handling qualities. For example, the autogyro displays extremely strong pitch due to roll and roll due to pitch cross couplings, both in terms of absolute magnitude of the couplings and relative to the geometrically equivalent helicopter. The autogyro also displays very high quickness and control power in the pitch and roll axes; although this lead to the aircraft achieving Level 1 predicted handling qualities, it is likely that the excessive control power and quickness will cause issues during closely controlled flight. These areas are discussed further following the piloted evaluation presented in Chapter 6.

In terms of the suitability of the predicted handling qualities requirements specified in ADS-33 and their applicability to the autogyro, the conclusion to be drawn is less clear. Criteria in the high frequency and low amplitude sector of the dynamo construct (the bandwidth and mid-term response criteria) were considered likely to be appropriate for analysis of the autogyro. In the case of the bandwidth criteria, this was based upon the fact that the consequence and likelihood that control inputs will be applied at or above the bandwidth frequency, triggering aircraft instability, are not specific to aircraft type. In the case of the mid-term response criteria, the ability of the pilot to maintain control over the natural modes of the aircraft is also a fundamental requirement, and is unlikely to vary significantly between rotary-wing vehicle types.

The ADS-33 criteria for parameters such as quickness, control power and cross coupling may also be applicable to autogyros, but may require redefinition of the Level 1/2 and 2/3 boundaries; this could account for the reduced inertia of the autogyro compared to the helicopters which were used in the development of ADS-33. The lack of any upper limit of acceptability on the quickness and control power criteria is also an issue; excessive amounts of quickness or control power may cause as many handling deficiencies as a lack a of quickness or control power.

Comparing the autogyro to a geometrically equivalent helicopter also highlighted some interesting differences in the predicted handling qualities. For example, the helicopter tends to display an approximately constant value of quickness in all three axes, whereas the autogyro tended to display increasing quickness as the airspeed increased. This variation in quickness will lead to increased pilot workload and may play a role in a

safety-critical situation. The autogyro also tended to have higher values of all parameters assessed; the values of quickness and control power are much larger than those of the helicopter model and the magnitude of the cross couplings experienced by the autogyro are larger than those experienced by the helicopter. This superfluity of agility and heavily coupled response may be indicative of significant handling qualities deficiencies of the autogyro.

It has also been demonstrated that there remains scope for further development of autogyro specific handling qualities ratings for parameters such as quickness and pilot attack. Using the method described in Ref. 7, boundaries for the Level 1/2 and Level 2/3 handling qualities were generated. Further work is required to firmly establish these boundaries; assessment against other autogyro type vehicles and the definition of a singular Slalom course geometry to be used to derive handling qualities ratings is required, as this was shown to have an effect on the location of the predicted boundaries.

The themes developed in this Chapter are further discussed in Chapter 6, where both ADS-33 and non-ADS-33 MTEs are used to generate assigned handling qualities ratings.

Chapter 6

A COMPARISON OF ASSIGNED HANDLING QUALITIES FOR AUTOGYRO AND HELICOPTER

Chapter 5 utilised the predicted handling qualities metrics defined within ADS-33 to generate a set of predicted handling qualities for both the autogyro and helicopter models. Developing this theme, it is the intention of Chapter 6 to generate a set of assigned handling qualities ratings for both models, using real-time piloted simulation and role representative mission task elements (MTEs). This is intended to highlight any deficiencies with the flight dynamics and handling qualities of both the autogyro and helicopter, as well as to highlight the differences between the two vehicle types.

ADS-33 [2] defines 23 distinct MTEs, intended to cover all aspects of helicopter operations and performance in all axes. Each MTE is bounded by a strict definition of the test course, and the performance parameters within which the aircraft must complete the test course. The performance parameters are divided into two tiers; “desired performance” and “adequate performance”. Assigned handling qualities are generated by qualitatively rating the achieved performance of the aircraft while undertaking these MTEs using the Cooper-Harper handling qualities rating scale, as shown in Figure 128. Desired performance requirements are more stringent than those defined in the adequate performance requirements. Typically, aircraft which meet the desired performance requirements will be awarded HQRs from 1 to 3 and are considered to not require improvement. Those which meet the adequate criteria, whilst maintaining an appropriate level of pilot workload, will receive HQRs between 4 and 6 and will require improvement before the aircraft is considered safe to release into service. Those aircraft in which it is not possible to meet the adequate criteria will receive HQRs between 7 and 9 and are considered unsafe to operate. Those aircraft which receive an HQR of 10 are not controllable.

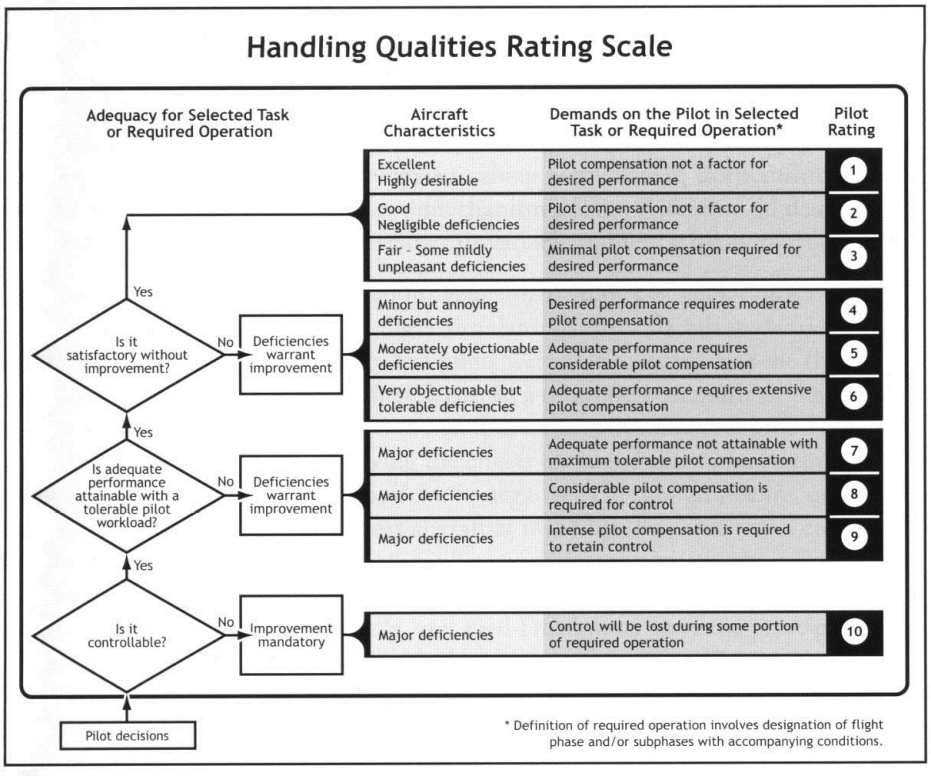

Figure 128: The Cooper-Harper Handling Qualities Rating Scale [54]

As stated in Chapter 5, there is no standard by which autogyro handling qualities can be quantified, and there are no autogyro-specific MTEs; however, the work carried out in Refs. 7, 9 and 10 indicated that ADS-33 style MTEs may provide a good platform from which to develop autogyro-specific MTEs. It is the intention of this Chapter to continue addressing the research question posed in Chapter 5; can an existing rotary wing specification such as ADS-33 be used to assess autogyro handling qualities, and if not, what new criteria are required to ensure future autogyro designs exhibit Level 1 handling qualities?

This Chapter will assess both the autogyro and helicopter models against 2 ADS-33 MTEs (Slalom, Acceleration-Deceleration) and 2 non-ADS-33 MTEs (the Roll Step and Heave Hop). The results from these qualitative assessments will then be used to draw conclusions on the validity of the MTEs and their applicability to the autogyro, and to suggest modifications or improvements to create autogyro specific MTEs. The results will also be used to consider if the predicted handling qualities ratings generated in Chapter 5

are valid and to identify to what degree the existing predictive criteria highlight the aircraft deficiencies experienced in flight.

Finally, the autogyro model will be assessed with a simple roll rate feedback loop implemented. Chapter 5's assessment of the predicted handling qualities of the autogyro indicated strong roll due to pitch and pitch due to roll cross couplings present in the autogyro; the intention of implementing a simple roll rate feedback loop is to attempt to quantify the improvement in handling qualities of the autogyro with reduced levels of cross coupling.

6.1 METHODOLOGY

The trials reported in this Chapter were carried out using 3 qualified test pilots (graduates of the Empire Test Pilots' School). In order to guarantee consistency across each trial, and every pilot, a repeatable and methodical process was employed. Due to financial constraints, it was not possible to ensure that each test pilot flew all test points across all 4 MTEs; the details of which pilot flew which manoeuvre are shown in Table 26, noting that Pilot B flew the Heave Hop manoeuvre with the roll controller implemented in the autogyro model (denoted by (A)) and Pilot C flew the autogyro in its un-augmented state.

	Slalom		**Accel-Decel**		**Roll Step**		**Heave Hop**	
	Gyro	Heli	Gyro	Heli	Gyro	Heli	Gyro	Heli
Pilot A		**X**		**X**		**X**		**X**
Pilot B	**X**		**X**				**X (A)**	
Pilot C					**X**		**X**	

Table 26: Pilot trials matrix for autogyro and helicopter

Pilots were permitted to fly each test point a maximum of three times. This ensured that the pilots gained sufficient familiarity with the aircraft response to push the aircraft to the safe limit of its performance, whilst preventing significant pilot learning which may result in the inherent deficiencies of the aircraft being masked by modification of the piloting technique. This approach also allowed for the pilot to ensure that the level of performance achieved during each MTE was as high as possible, and that a tolerable level of workload was maintained throughout.

Taking an incremental approach to the testing also mirrors the methodology which would be applied in a real-world testing situation, and allows any 'cliff-edges' to be identified. A cliff edge refers to a situation in which a small change in control strategy results in a large change in aircraft response. Cliff edges typically occur as aggression levels increase, and can be problematic for pilots due to their unpredictable and often violent nature. The existence of handling qualities cliff edges is investigated in this Chapter by varying the MTE performance targets or the geometry of the MTEs (such as the target airspeed or gate spacing) where appropriate.

After each manoeuvre was completed, the pilot was asked to award both aircraft types an HQR using the Cooper-Harper scale (as shown in Figure 128) and to assess the task workload using the Bedford Workload rating scale, shown in Figure 129. Both scales follow a hierarchical decision tree format, with the user being guided through a 10-point nonlinear rating scale, each point of which is associated with a descriptor of the handling qualities or workload level respectively. Both scales provide a quick method of rating the performance in and the difficulty of executing the MTE, but do not provide diagnostic capability which can be used to identify the cause of any deficiencies. The order in which the test points are carried out is randomised to further prevent pilot learning (and thus artificial masking of the true HQRs), and to avoid automatic trending within the HQRs/BWRs awarded (the pilot automatically increasing the HQR to reflect increasing task difficulty when no change in task execution accuracy or aggression level has occurred).

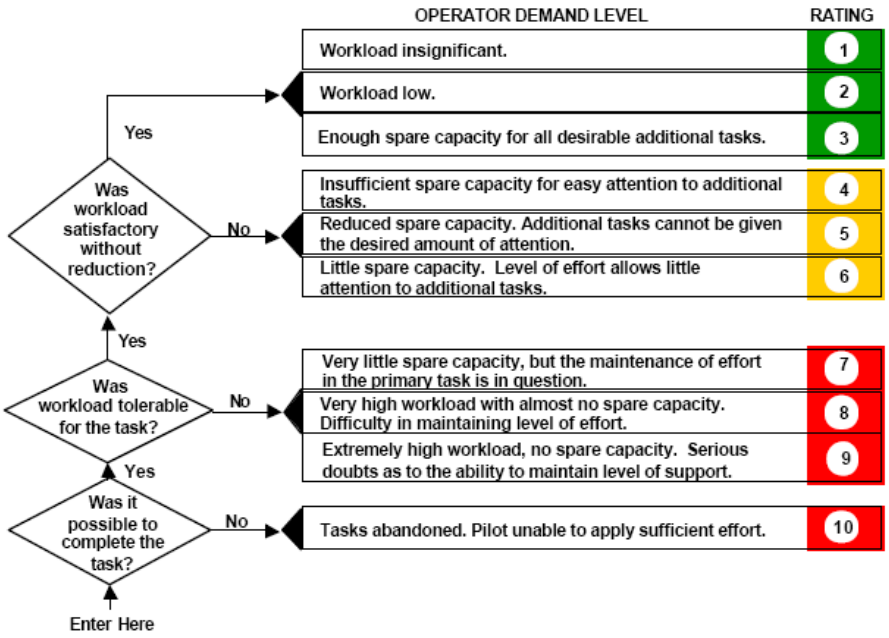

Figure 129: The Bedford Workload Rating Scale

Test points were occasionally repeated to ensure that the pilots were not being affected by external factors, such as fatigue, and to ensure consistency across the ratings being applied, implying that the true performance of the aircraft was being observed.

Comprehensive briefing pre-trial (both via written communication in the week leading up to the trial, and oral communication directly prior to the trial commencing), and de-briefing post-trial was carried out in order to assure both pilot and test engineer were fully prepared and that all pertinent points on aircraft performance were recorded. Post-manoeuvre de-briefs were also carried out, the pilot pausing after completion of each test point to describe the driving factors behind each rating awarded; for example if control in a particular axis or available control power was the main factor in awarding a poor HQR, this methodology would allow for this to be captured.

6.2 SLALOM

The Slalom manoeuvre is defined in ADS-33. It is designed to assess the ability of an aircraft to manoeuvre aggressively in the forward flight regime with respect to objects on the ground. It is also intended to test the ease of turn co-ordination in moderately aggressive flight, and to detect any objectionable inter-axis couplings. As demonstrated in Chapter 5, the poor predicted handling qualities ratings for the inter-axis couplings

suggest that the autogyro may struggle in this regard, however its high roll quickness and control power should allow for aggressive manoeuvring.

In order to determine if there are any 'cliff edges' present in the handling qualities of both the autogyro and helicopter models, the aggression level of the Slalom manoeuvre was varied by increasing the airspeed and the aspect ratio of the course geometry, details of which are contained in Section 6.2.2.

6.2.1 Manoeuvre Description

The manoeuvre described herein differs from that in ADS-33 in that the course geometry and airspeeds analysed are varied; the Slalom prescribed within ADS-33 is flown with a single geometry and airspeed in a good visual environment (GVE). The airspeed and course lengths used for this simulated Slalom manoeuvre are prescribed in Table 27. As test points will be varied, the airspeeds and distances between turns will change. The following manoeuvre description applies to the first test point in the test matrix (Table 28).

The manoeuvre should be initiated in level un-accelerated flight at airspeed of 35 mph, lined up with the centreline of the test course. The pilot shall perform one smooth turn to left and one smooth turn to right at 150m intervals. The turns shall be at least 15 m from the centreline, with a maximum lateral error of 15 m. The manoeuvre is to be accomplished below the reference altitude of 30m (100ft). The manoeuvre should be completed on the centreline, in coordinated straight and level flight. Airspeed should be maintained at or above the indicated airspeed for each manoeuvre.

6.2.2 Course Geometries

A schematic of the Slalom course is shown in Figure 130, and the pilot view of the simulated Slalom course is shown in Figure 131. The definitions of the geometries of the 5 Slalom courses are detailed in Table 27. In the simulation environment, the course is marked using a pair of 100ft high poles spaced 50ft apart. 100ft was chosen as this indicates to the pilot the height below which the manoeuvre must be completed.

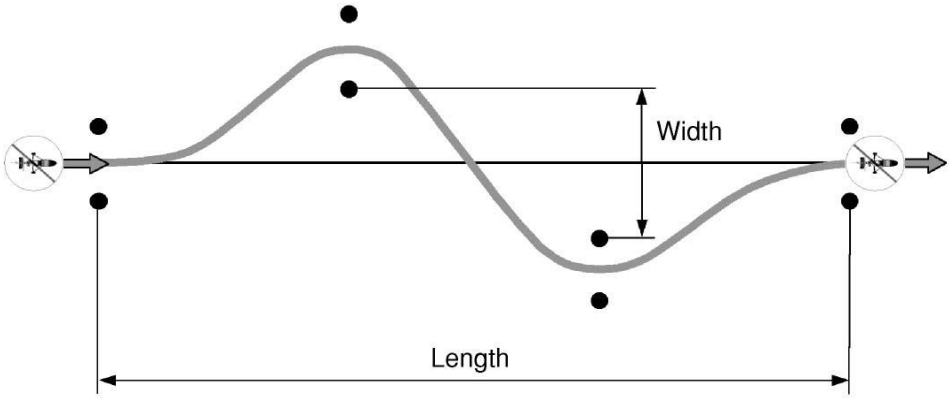

Figure 130: Slalom course schematic [2]

Figure 131: Pilot view of simulated Slalom course

Course Number	Length (m)	Width (m)	Aspect Ratio
1	450	30	0.067
2	300	30	0.10
3	225	30	0.13
4	300	60	0.20 (1)
5	150	30	0.20 (2)

Table 27: Slalom course geometries

6.2.3 Test Matrix

Table 28 shows the combinations of airspeeds and course geometries which will be investigated. Those test points shaded grey are outside the flight envelope predicted by Ref. 7; as this flight test programme is to be carried out in the simulated environment it is possible to investigate test points at and beyond the limits of the flight envelope in relative safety.

Run Number	Course Number	Airspeed (mph)
1	1	35
2	1	50
3	1	70
4	2	35
5	2	50
6	2	70
7	3	35
8	3	50
9	3	70
10	4	35
11	4	50
12	4	70
13	5	35
14	5	50
15	5	70

Table 28: Slalom course test matrix

6.2.4 Performance Requirements

Table 29 shows the desired and adequate performance targets for the Slalom manoeuvre for both the helicopter and autogyro models. These performance targets are derived from ADS-33 [2].

	DESIRED	ADEQUATE
Height	< 100ft	< 100ft
Speed	±5 mph	±10 mph
Track	±15ft	±30ft
Yaw angle	±10deg	±15deg

Table 29: Performance requirements for Slalom manoeuvre

6.2.5 Results

The results of the Slalom manoeuvre are presented in Table 30 and Figure 132. For clarity, in Table 30, Level 1 HQRs are coloured green, Level 2 HQRs are coloured yellow and Level 3 HQRs are coloured orange in order to allow a visual comparison to be made between autogyro and helicopter.

Run Number	Course Number	Airspeed (mph)	Autogyro HQRs	Helicopter HQRs
1	1 (AR 0.067)	35	2	2
2	1 (AR 0.067)	50	3	3
3	1 (AR 0.067)	70	7	5
4	2 (AR 0.1)	35	3	4
5	2 (AR 0.1)	50	5	5
6	2 (AR 0.1)	70	7	7
7	3 (AR 0.13)	35	4	4
8	3 (AR 0.13)	50	6	6
9	3 (AR 0.13)	70	8	9
10	4 (AR 0.2(1))	35	4	4
11	4 (AR 0.2(1))	50	6	6
12	4 (AR 0.2(1))	70	6	7
13	5 (AR 0.2(2))	35	10	7
14	5 (AR 0.2(2))	50	9	10
15	5 (AR 0.2(2))	70	10	-

Table 30: Slalom manoeuvre HQRs for autogyro and helicopter

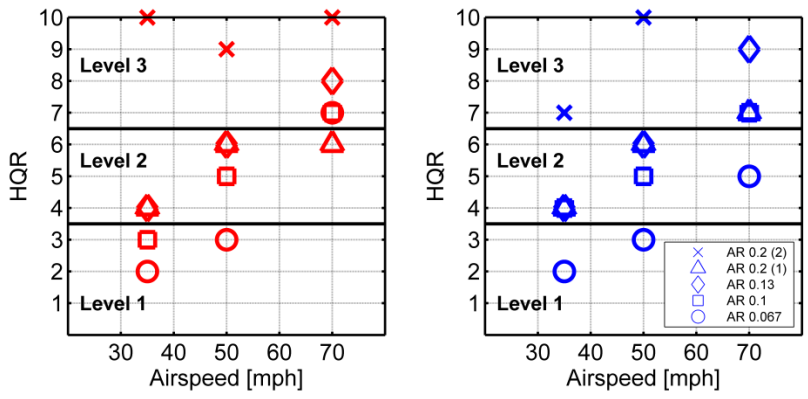

Figure 132: A comparison of assigned handling qualities of the autogyro (red) and helicopter (blue) models for the Slalom manoeuvre

Similar trends can be observed within the data for both the autogyro and helicopter models. As airspeed increases for a given course geometry, the handling qualities ratings degrade, as shown in Figure 132. Similarly, as the aspect ratio of the course decreases (i.e. the course becoming wider and the longitudinal separation of gates decreases), the handling qualities ratings also degrade for a given airspeed. Generally, for each test point the handling qualities of the autogyro and helicopter lie within the same Level, the exceptions to this being runs number 3, 4 and 12 as shown in Table 30.

One of the main issues encountered by the autogyro when trying to complete the Slalom MTE was the lack of sufficient roll control power to generate the lateral velocities required to successfully complete the course. Whilst Chapter 5's predicted handling qualities illustrated high levels of both roll quickness and control power, which would suggest that the autogyro model would have good performance on the more aggressive Slalom course geometries (those which are flown at high speed or are wide, with the gates spaced closely together), the aircraft struggled to meet the desired and adequate performance targets. The large pitch due to roll cross coupling present is largely responsible for this.

As an example, Figure 133 shows the recorded flight path data for the Slalom manoeuvre (with adequate limits shown in red and desirable limits shown in green), overlaid with the flight data from the trail with the autogyro flying Course 1 at 70mph. Whilst this course geometry is not of low aspect ratio, the high velocity requires the pilot to be aggressive to complete the course successfully. The pilot is seen to be using very high bank angles, which leads to a reduction in speed and an unstoppable pitch down motion due to the presence of the pitch due to roll cross-couple. As such, adequate performance could not be achieved in terms of airspeed maintenance and the manoeuvre was awarded an HQR 7.

The same manoeuvre was also flown using the helicopter model, the results of which are shown in Figure 134. Chapter 5 illustrated that, though still strongly cross coupled in pitch and roll, the helicopter has a comparatively smaller pitch due to roll cross coupling. This results in an improvement in comparative performance between the helicopter and autogyro; Figure 134 shows that both airspeed maintenance and yaw attitude

performance are improved, and now lie within the adequate region, when compared to those shown in Figure 133. As a result, this test point was awarded an HQR 5.

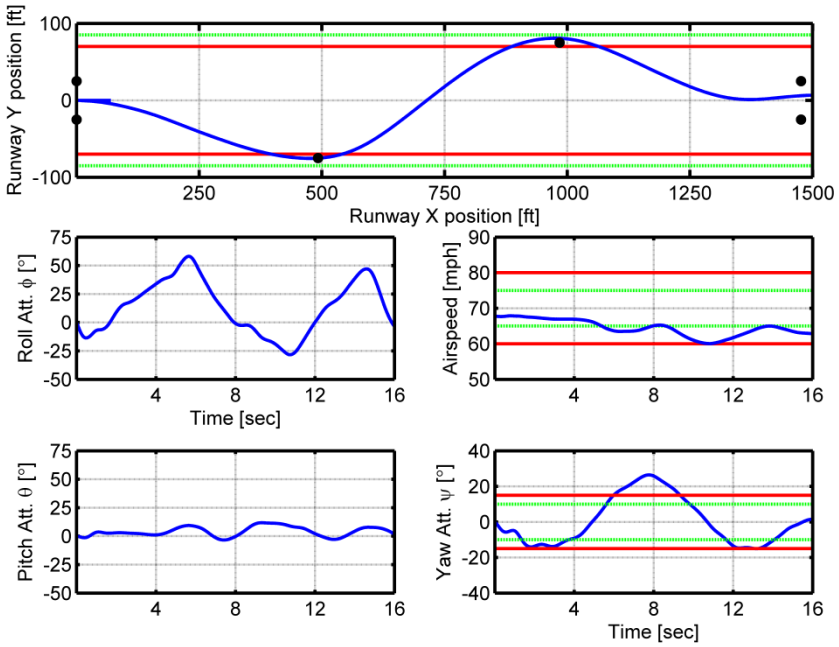

Figure 133: Flight test data for autogyro model flying Slalom manoeuvre on Course 1 at 70mph

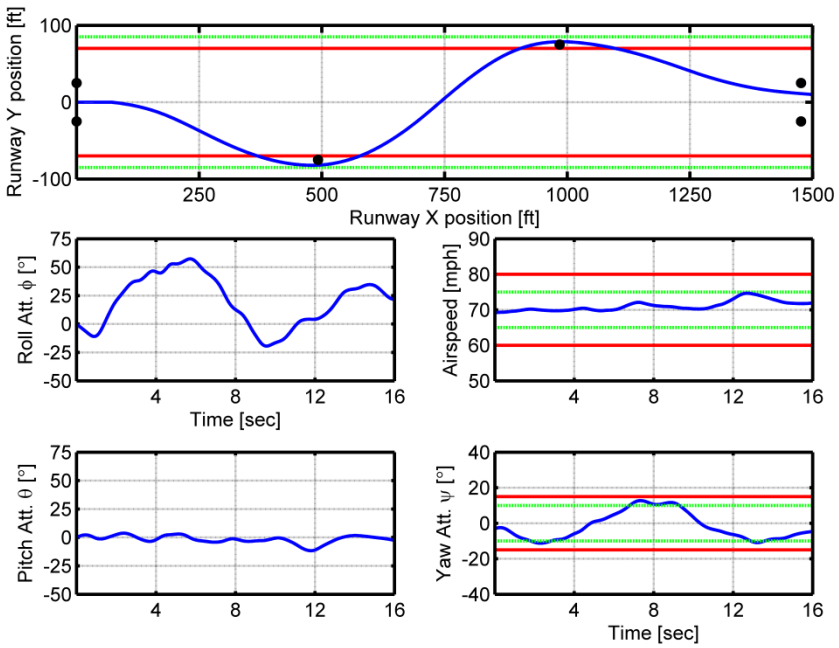

Figure 134: Flight test data for helicopter model flying Slalom manoeuvre on Course 1 at 70mph

The Slalom manoeuvre is intended "to detect any objectionable inter-axis couplings" when applied to analysing the helicopter; applied to the autogyro it has similar utility. It is also intended to test the ease of turn co-ordination and assess the ability of the aircraft manoeuvre aggressively. During the simulated flight trial, the pilot did not highlight any issues with turn co-ordination, and flew as aggressively as required to complete the course; it is therefore not possible to draw a firm conclusion about whether or not the Slalom manoeuvre highlights these deficiencies in the autogyro – it may be the case that these deficiencies are absent, or that the manoeuvre does not highlight them.

6.3 ACCELERATION-DECELERATION

The Acceleration-Deceleration MTE is defined in ADS-33 [2]. The Acceleration-Deceleration is intended to check the pitch axis handling qualities during aggressive manoeuvring near the limits of aircraft performance and highlight any undesirable inter-axis couplings in the later-directional and longitudinal axes. The manoeuvre is also intended to check for harmony between the pitch and heave axis and to check that there is adequate rotor response and no overly complex power requirements during aggressive manoeuvring.

6.3.1 Manoeuvre Description

As an autogyro cannot hover in the conventional sense, the Acceleration-Deceleration manoeuvre of Ref. 2 required some modification to make it suitable for this class of vehicle. The manoeuvre is initiated at a specified airspeed (as opposed to in the hover); the aircraft then accelerates to the target airspeed before completing the manoeuvre by decelerating back to the initiation airspeed. In order to vary the aggression level of the manoeuvre to investigate the presence of cliff edges, a number of combinations of initiation and target airspeeds were used, as detailed in Section 6.3.4. The following manoeuvre description relates to the first test point in the test matrix for the autogyro model.

From level un-accelerated flight at an airspeed of 35mph, the pilot will rapidly increase power to approximately maximum, and maintain altitude constant during the acceleration to an airspeed of 60mph. Upon reaching the target airspeed, the pilot will initiate an aggressive deceleration, reducing the power and holding altitude constant. The manoeuvre should be completed at the initial airspeed of 35mph.

For the helicopter model, the manoeuvre is performed slightly differently due to use of pitch attitude to increase airspeed (rather than the engine power setting, as for the autogyro). For consistency, the manoeuvre is still initiated from a target airspeed, with the pilot aggressively pitching nose-down to accelerate the aircraft to the target airspeed. Upon reaching the target airspeed, the pilot will initiate a deceleration to the initiation airspeed by aggressively pulling back on the longitudinal cyclic. The maximum nose-down attitude should occur immediately after initiating the manoeuvre, and the peak nose-up attitude should occur just before returning to the initiation airspeed during the deceleration phase; altitude should be held constant throughout.

6.3.2 Course Geometry

A schematic of the Slalom course is shown in Figure 135; poles at the edges of a runway denote the Acceleration-Deceleration course, spaced at 500ft intervals as shown in Figure 136. The distance between the red bands is 50ft, and the height of the green band is 20ft.

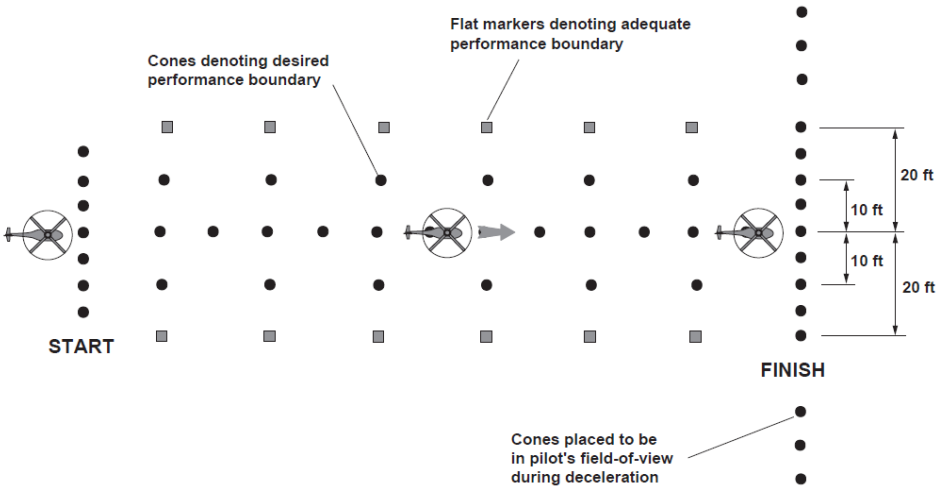

Figure 135: Acceleration-Deceleration course geometry [2]

Figure 136: Pilot view of simulated Acceleration-Deceleration course

6.3.3 Performance Requirements

The performance requirements for the Acceleration-Deceleration manoeuvre are shown in Table 31.

	DESIRED	ADEQUATE
Maintain altitude below:	50ft	70ft
Maintain lateral track within:	±3m (10ft)	±6m (20ft)
Maintain heading within:	±10°	±20°

Table 31: Performance requirements for Acceleration-Deceleration manoeuvre

As the autogyro does not use nose up pitch attitude in deceleration, the pitch attitude is not specified for this variation of the task as it is in the original task definition [2]. The pitch attitude requirement is also removed for the helicopter.

6.3.4 Test Matrix

Table 32 shows the speed ranges at which the manoeuvres will be performed. For example, run 1 will be initiated at 35mph, accelerating to 60mph before decelerating back to 35 mph.

Run Number	Target Airspeeds (mph)
1	35-60-35
2	35-max-35 (35-70-35 for helicopter)
3	40-50-40
4	40-60-40
5	50-60-50
6	50-max-50 (50-70-50 for helicopter)

Table 32: Test matrix for Acceleration-Deceleration manoeuvre

6.3.5 Results

The results of the Acceleration-Deceleration are shown in Table 33 and Figure 137. As for the Slalom manoeuvre, the autogyro and helicopter display broadly similar Level 2 handling qualities ratings, with the autogyro showing a slight improvement in handling qualities on Course 5 and 6, with HQRs moving into Level 1.

Course	Airspeed Range (mph)	Autogyro HQRs	Helicopter HQRs
1	35-60-35	4	4
2	35-max-35	4	4
3	40-50-40	4	4
4	40-60-40	4	4
5	50-60-50	3	4
6	50-max-50	2	4

Table 33: Acceleration-Deceleration manoeuvre HQRs for autogyro and helicopter

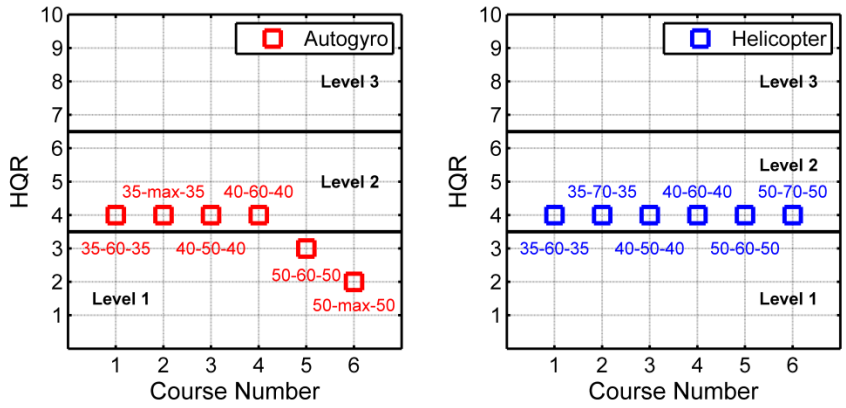

Figure 137: A comparison of assigned handling qualities of the autogyro (red) and helicopter (blue) models for the Acceleration-Deceleration manoeuvre

Figure 138 and Figure 139 show the flight test data for the autogyro and helicopter respectively, flying the Acceleration-Deceleration manoeuvre on Course 6. For this test point the autogyro was awarded an HQR 2 and the helicopter was awarded an HQR 4.

The autogyro was able to achieve desired performance within all three parameters as defined in Table 31. Lateral position tracking was generally good, with the pilot only having to use relatively small roll attitude corrections in order to maintain lateral position, and the pilot was able to maintain yaw attitude and complete the manoeuvre below 50ft.

For both the autogyro and the helicopter models, pilots reported that control in the lateral axis was the area which required most attention, and a high portion of their capacity was applied in order to maintain control. The helicopter was described as "twitchy and skittish" in roll and pilots reported poor roll damping in the autogyro model. Figure 137 shows that as the test points target airspeed increases, the autogyro HQR decreases. The comparatively smaller change in airspeed between the initiation airspeed and the target airspeed compared to the previous test points resulted in this improvement in HQR, requiring the pilot to be less aggressive, thus decreasing the magnitude of the cross couplings triggered in the aircraft, and allowing more spare capacity to deal with the other deficiencies present in the autogyro, thus allowing the course to be completed within the desired criteria.

The helicopter was unable to maintain height below the desired target height of 50ft, as shown in Figure 139. This was primarily due to the pilot not having enough spare capacity to monitor the height while attempting to maintain lateral position and simultaneously counter the roll due to pitch cross coupling that the aircraft was experiencing.

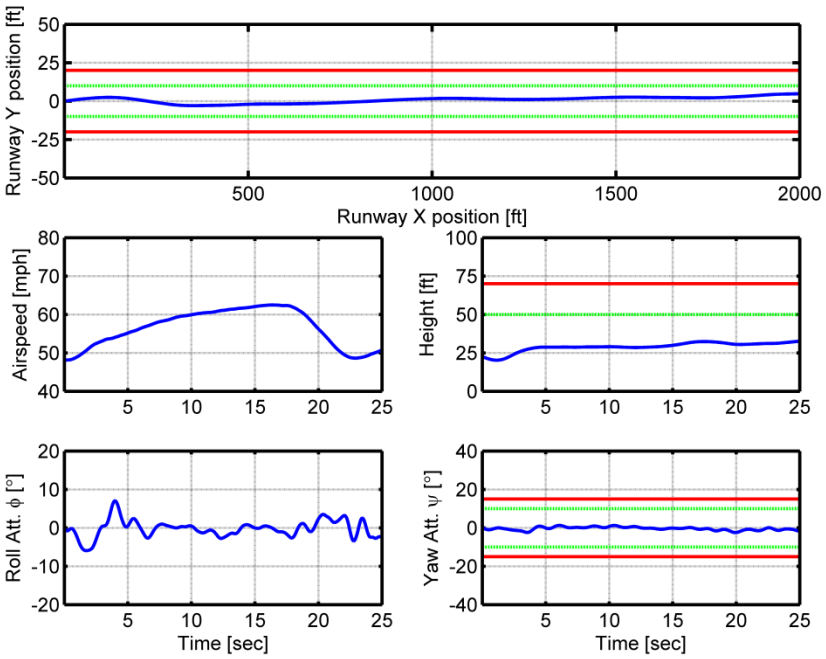

Figure 138: Flight test data for autogyro model flying Acceleration-Deceleration manoeuvre on Course 6 (50-max-50, HQR 2)

The test point shown in Figure 138 requires the pilot to accelerate the autogyro from 50mph to the maximum speed of the aircraft; approximately 63mph (as, due to insufficient engine power, the autogyro is unable to reach 70mph). One of the intentions of the Acceleration-Deceleration manoeuvre is to "highlight any undesirable inter-axis couplings in the later-directional and longitudinal axes". As the autogyro mainly uses the throttle setting (as opposed to pitch attitude) to accelerate or decelerate, this manoeuvre will not reveal the extent of the roll due to pitch cross coupling present in the autogyro as intended. The profile of both the longitudinal stick and the pitch attitude used during the manoeuvre can be seen in Figure 140; the maximum pitch attitude reached is around -6° during the deceleration phase of the manoeuvre, in contrast to the helicopter, which used over 30° of nose up pitch attitude during the same phase.

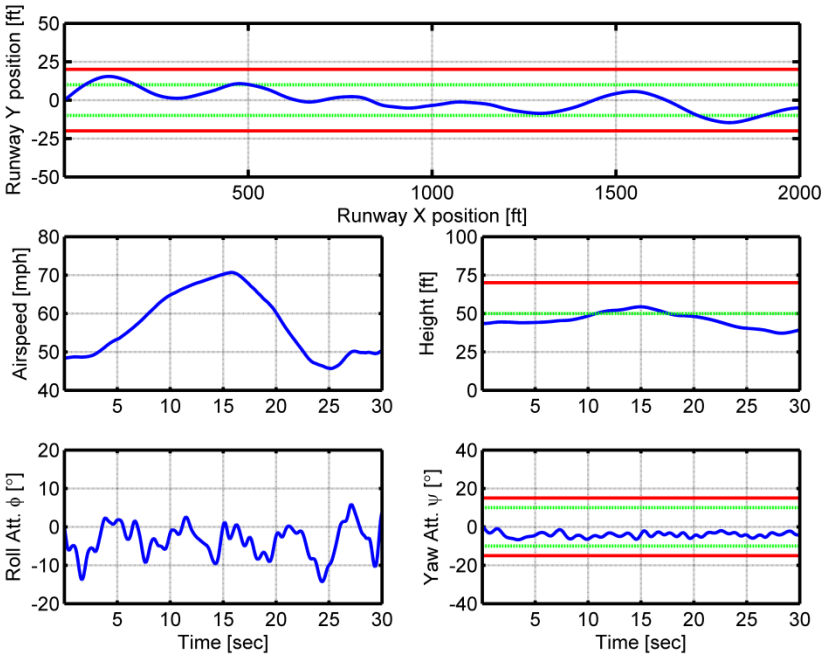

Figure 139: Flight test data for helicopter model flying Acceleration-Deceleration manoeuvre on Course 6 (50-max-50, HQR 4)

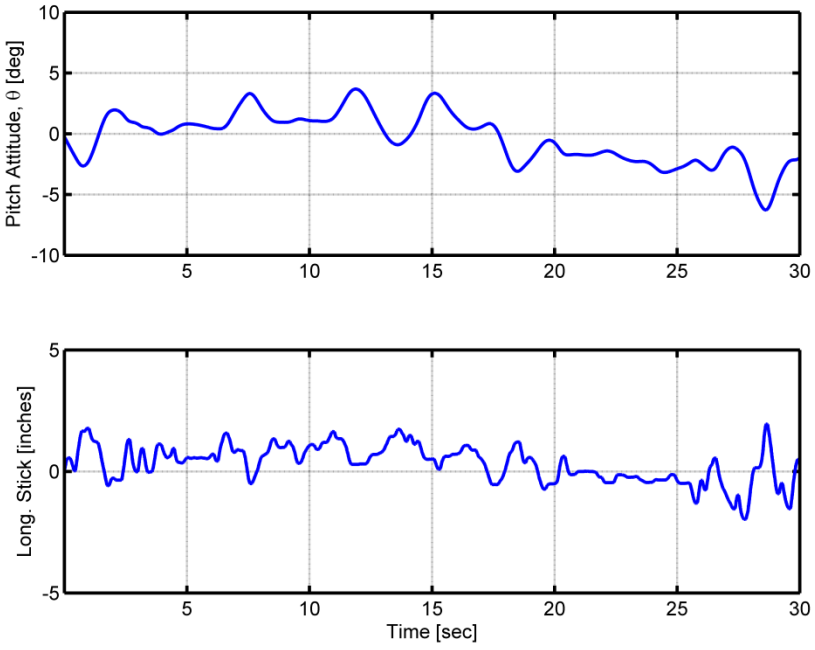

Figure 140: Pitch attitude and longitudinal stick inputs for autogyro flying Acceleration-Deceleration manoeuvre on Course 6 (50-max-50, HQR 2)

As a result of this requirement to use large pitch attitudes, the helicopter experienced greater roll due to pitch cross coupling (predicted in Chapter 5 to lie within Level 3 at 70mph) and could not maintain lateral position within the desired criteria. This also further explains the improvement of the HQR rating for the autogyro at high speeds. As airspeed increases the cross coupling becomes more pronounced for both aircraft types, however, as the autogyro is not using pitch attitude to decelerate, the over-riding effect is the increase in longitudinal stability from the increased effectiveness of the tailplane as airspeed increases. An increase in the longitudinal stability of the aircraft results in a reduction of workload in the longitudinal axis, creating extra capacity for the pilot which can then be used to more tightly control the lateral position of the aircraft or the height, allowing the aircraft to achieve desired performance against the criteria in Table 31 and improving the subsequent HQR awarded. As a result of this, it can be concluded that the Acceleration-Deceleration may not be a suitable manoeuvre for assessing the autogyro roll due to pitch cross coupling. It is, however, useful in highlighting the differences between the autogyro and helicopter, highlighting the effects of their use of differing control inceptors to complete the same manoeuvre.

6.4 HEAVE HOP

The Heave Hop manoeuvre is a non-ADS-33 manoeuvre, initially developed for the assessment of tilt rotors [81]. The intention of the manoeuvre is to check the ability to achieve a positive load factor, generated in a moderately aggressive manner from trimmed flight, to maintain this positive load factor for a few seconds, before transiting to a negative steady load factor and to recover to level flight quickly. The whole task should be accomplished with minimum deviations in airspeed, roll angle and heading. The manoeuvre will also reveal any undesirable cross couplings.

6.4.1 Manoeuvre Description

In order to detect the presence of any cliff edges in the handling qualities of both aircraft, and to fully explore the flight envelope, the level of aggression used during the manoeuvre is varied by changing the target airspeed at which the manoeuvre is completed and the spacing between the pull-up and push-down stages of the manoeuvre. The following manoeuvre descriptions refer to run number 1 and run number 4 defined in the test matrix given in Section 6.4.4.

The first manoeuvre requires the pilot to climb to a height of 200ft over a distance of 1000ft. The pilot will initiate the manoeuvre at a stabilised airspeed of 35mph, lined up with the centre line of the test course, and pass beneath the first set of white poles. The pilot will then pull up in order to pass over the first set of black poles. Maintaining altitude, the aircraft shall pass over the second pair of white poles before commencing a descent to pass beneath the second pair of black poles.

The second manoeuvre requires that the pilot initiate the manoeuvre at a stabilised airspeed of 35mph and pass beneath the first set of white poles. The pilot will then commence pull up in order to pass over the first set of black poles, immediately descending to pass beneath the second pair of white poles before again commencing a climb to pass over the second pair of black poles.

6.4.2 Course Geometry

A schematic of the Heave Hop course is shown in Figure 141. The course consists of 4 sets of alternately coloured black and white poles spaced at 1000ft intervals within a V-shaped valley, with a 60ft horizontal gap through which the aircraft is able to pass.

6.4.3 Performance Requirements

	DESIRED	**ADEQUATE**
Height	+20ft at top of pull up -20ft at bottom of transition down	+30ft at top of pull up -30ft at bottom of transition down
Speed	±5 mph	±10 mph
Bank angle	±5deg	±10deg
Track	±15ft	±30ft
Yaw angle	±10deg	±15deg

Table 34: Performance Requirements for Heave Hop manoeuvre [81]

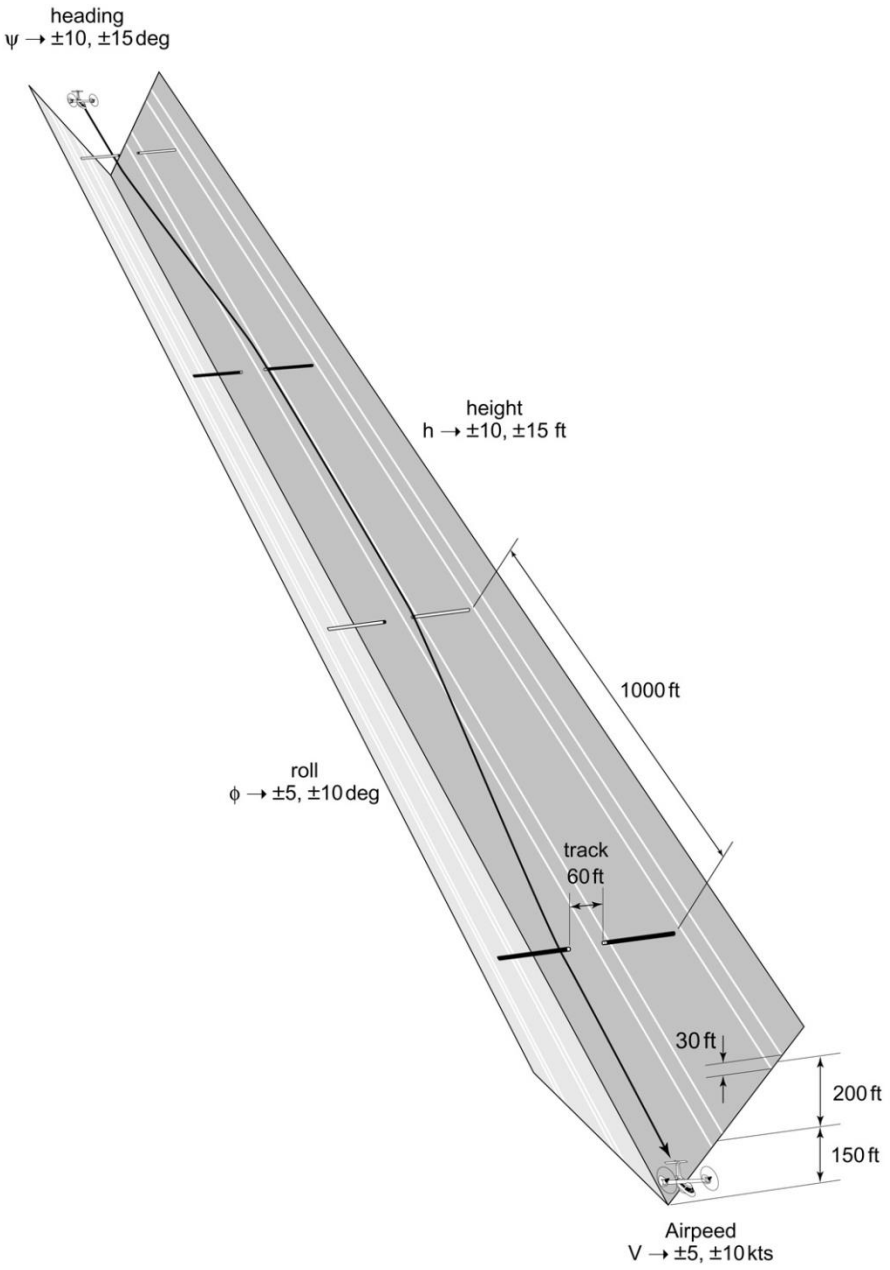

Figure 141: Heave Hop course geometry [81]

6.4.4 Test Matrix

Table 35 shows the test matrix for the Heave Hop manoeuvre for both helicopter and autogyro.

Run Number	Course Number	Airspeed (mph)
1	1	35
2	1	50
3	1	70
4	2	35
5	2	50
6	2	70

Table 35: Heave Hop test matrix

6.4.5 Results

The results of the Heave Hop manoeuvre are shown in Table 36 and Figure 142.

Course	Airspeed Range (mph)	Autogyro HQRs	Helicopter HQRs
1	35	8	3
	50	8	5
	70	7	8
2	35	8	5
	50	9	6
	70	9	7

Table 36: Heave Hop manoeuvre HQRs for autogyro and helicopter

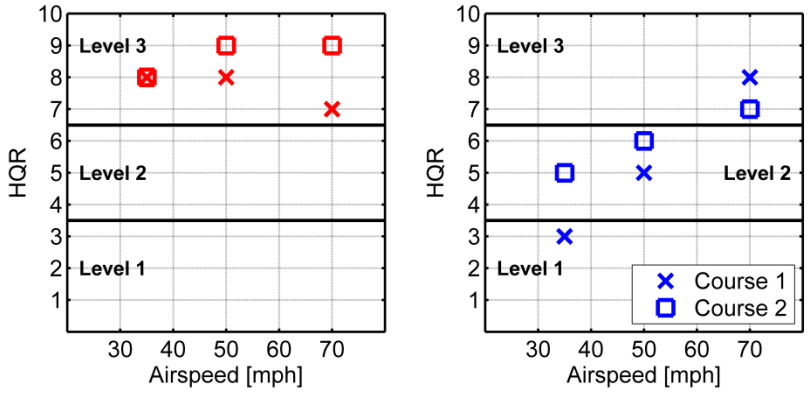

Figure 142: A comparison of assigned handling qualities of the autogyro (red) and helicopter (blue) models for the Heave Hop manoeuvre

Figure 142 illustrates that the autogyro has significantly poorer handling qualities than the helicopter at low and medium airspeeds during the Heave Hop manoeuvre, with HQRs remaining in Level 3 throughout, compared to the helicopter's HQRs which degrade with airspeed. This can be attributed to a number of factors.

Taking the test point at 35mph on Course 1 as an example (as this is the test point which has the greatest difference in HQRs between the two aircraft types), it can be seen that the autogyro was unable to meet the adequate performance criteria for the any of the criteria except the lateral positioning requirements; this is illustrated in Figure 143.

The pilot was unsuccessful in attempts to meet the required climb performance, failing to reach adequate height to pass over the second gate. Airspeed also varied more than 10mph, and the roll attitude varied between ±15°. This inability to climb quickly can be attributed to the simple fact that the engine in the autogyro is not powerful enough to generate the required climb rate. The pilot also noted the presence of a roll due to throttle coupling; upon abruptly opening the throttle to commence the ascent at around the 2.5 second mark, the aircraft rolled to the left. Upon attempting to correct this roll, the pilot also triggered the pitch due to roll cross coupling present in the aircraft. Managing and correcting these cross-couples, whilst attempting to maintain lateral position used all available pilot capacity and generated excessive pilot workload, resulting in the exceedance of the adequate limitations in all but the lateral position of the aircraft, and thus was awarded an HQR 8.

In contrast, at the same test condition, the helicopter was awarded an HQR 3. In the absence of a throttle, the helicopter uses collective pitch in order to climb to reach the second pair of poles, and there is no roll due to throttle coupling. The helicopter does still experience some changes in roll attitude as the pilot attempts to maintain lateral position, but as the pitch due to roll cross coupling present in the helicopter is significantly smaller than that of the autogyro (as illustrated in Chapter 5), the pilot has sufficient capacity to counter the pitch due to roll coupling which occurs as the pilot works to maintain lateral position. As a consequence of this lower workload, the pilot then has capacity to focus on maintenance of speed and other parameters, and is able to target and achieve a flight profile which is within the desired limits of the course for all requirements, as shown in Figure 144.

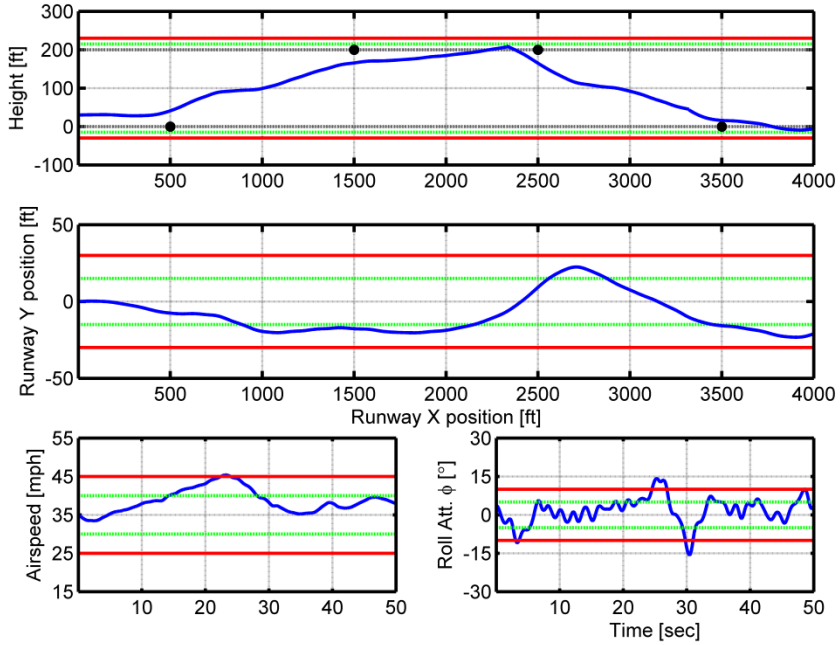

Figure 143: Flight test data for autogyro model flying Heave Hop manoeuvre on Course 1 (35mph, HQR 8)

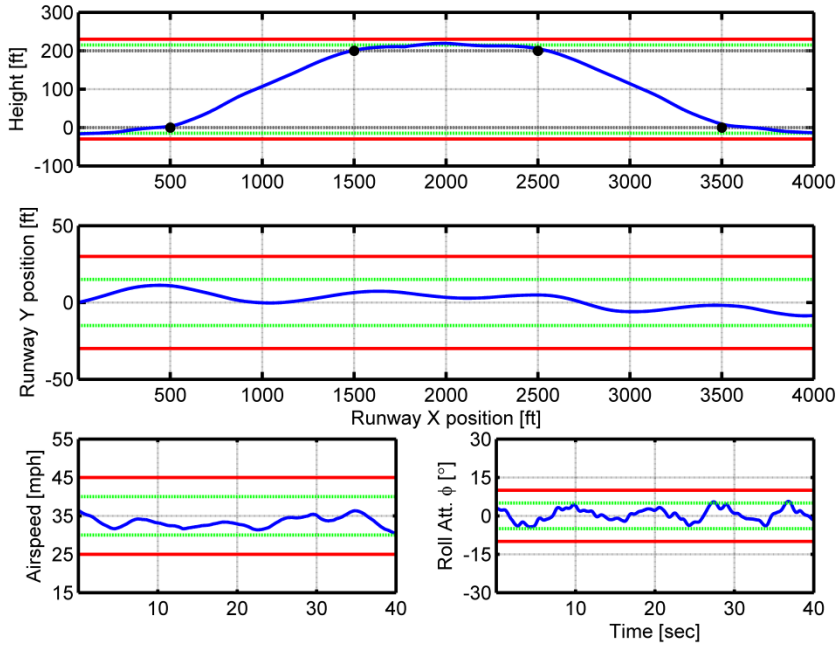

Figure 144: Flight test data for helicopter model flying Heave Hop manoeuvre on Course 1 (35mph, HQR 3)

Another fundamental difference between the helicopter and the autogyro is the difference in rotor governing. The helicopter is equipped with a main rotor governor, which maintains the rotor at a constant speed; the main rotor speed of the autogyro is ungoverned, and therefore is free to vary depending upon the rotor loading.

Figure 145 shows an example of the variation in rotor speed for the autogyro at 50mph on Course 1 (the least aggressive course). It can be clearly seen that as the pilot commences the pull up manoeuvre by opening the throttle at the 2 second mark, the rotor speed surges from 400 to 425rpm, before dipping to around 390 rpm as the pilot reduces the power setting to attempt to counter the large roll due to throttle cross coupling and stabilise the climb. The throttle is then held open at around 60%, as the climb is completed and the pilot transitions between the two upper poles. To initiate the descent, the pilot fully closes the throttle at around 20 seconds. As the aircraft descends, the rotor speed decays further, to approximately 370rpm. The rotor speed again surges to around 425rpm as the pilot again increases the throttle setting to arrest the descent and stabilise the aircraft after passing through the final low gate.

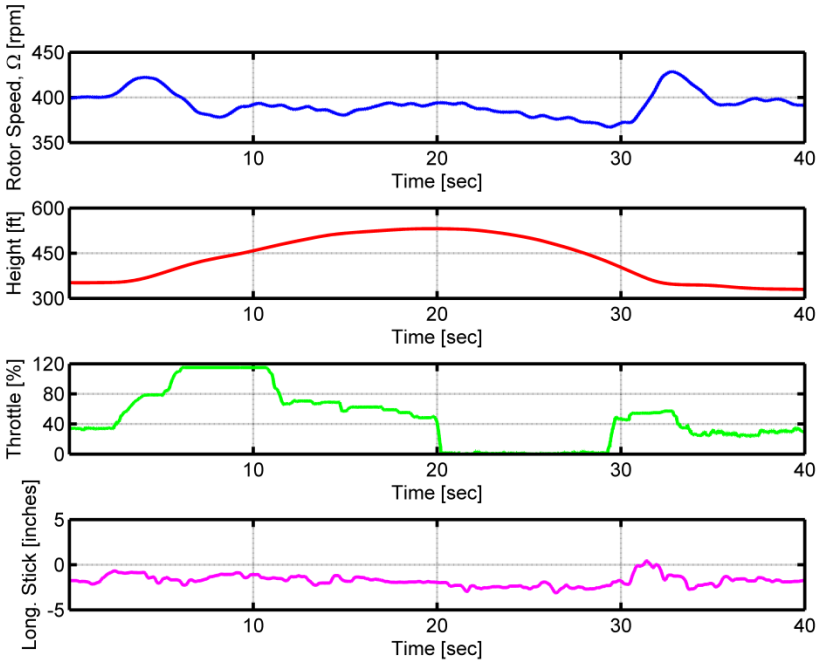

Figure 145: Example of rotorspeed variation during Heave Hop manoeuvre on Course 1 (50mph, HQR 8)

These changes in rotor speed correspond to changes in the loading of the main rotor disc. Upon initiating the pull up, the pilot aggressively increases the throttle in order to climb, generating positive 'g' and increasing the rotor inflow, increasing the disc loading. This causes the rotor to speed up, generating more thrust. This will cause the aircraft to climb; however, it will also increase the control power of the main rotor, meaning that the control sensitivity will be perceptibly increased. If the pull up is significantly aggressive, this sudden increase in control power combined with the roll due to throttle cross coupling present in the autogyro may result in a potential catastrophic loss of control. Whilst this has not been seen amongst flight test data gathered in the course of this study, this may prove to be an avenue of further work, as the simulator provides a safe environment in which to perform these type of extreme manoeuvres.

The opposite happens as the pilot closes the throttle and begins to descend. The aircraft enters a low 'g' flight regime (i.e. $0g < g < 1g$), the rotor is unloaded and the rotor speed decreases. This can be similarly problematic; entering a low 'g' condition will reduce the available control power, resulting in potential handling issues. In the Heave Hop manoeuvre for example, large deviations in roll attitude are observed in Figure 143 (for the 35mph test point) at around the 30 second mark, the time which corresponds to the initiation of the descent. It is likely these deviations were caused by a combination of the presence of the cross couplings already discussed, which the pilot is then unable to successfully counter due to the reduction in the available control power under low 'g' conditions.

In extreme cases, it is possible to enter 0g or negative 'g' conditions; this would result in the complete unloading of the rotor and irreversible loss of control of the aircraft.

Complete unloading of the rotor can also result in the aircraft experiencing a "bunt over" (sometimes referred to as "power push over", or PPO). This will only occur when the engine thrustline is above the vertical position of the c.g. As the main rotor is unloaded, the thrust available (and therefore also the control power available) and the drag (due to the decrease in rotor speed) will both rapidly reduce. With the reduction in thrust, the restoring moment of the main rotor also decreases, allowing the moment generated by the prop and engine to become dominant. If the thrustline is above the centre of gravity, this will force the nose of the aircraft downwards, into an unrecoverable flight condition.

This can occur almost instantaneously if the initiation of the 0g condition is sudden. Again, this has not been seen during the flight test data gathered in the course of this study; however it may be an appropriate target for future flight trials to demonstrate this.

Finally, unloading the rotor can lead to blade instability and flapping. As demonstrated in Chapter 4, it is very possible that this autogyro model will experience a tail or propeller strike; an occurrence which is made more likely under low 'g' conditions.

With the addition of the rotor speed governor, the helicopter does not experience these problems in conventional flight.

In the development of autogyro-specific handling qualities, requirements for control of rotor speed will be of considerable importance. The control of rotor speed during autogyro flight is critical to safety, and as the fundamental mechanical nature of the autogyro's main rotor may allow rotor speed to decrease to zero under negative load factor, it will be critical to establish both at what point the rotor speed loss becomes intolerable, and in what conditions intolerable rotor speed loss occurs. In the same way that ADS-33 [2] provides generic manoeuvre limits which can be applied to all military helicopters, any requirements on rotorspeed control developed for the autogyro should be generic and applicable to all autogyro types.

The Heave Hop manoeuvre would provide a basis to begin developing specific requirements for rotorspeed control for the autogyro, as the manoeuvre has been shown to excite the variation in rotorspeed which is under consideration. In the simulation environment it is also possible to easily modify the Heave Hop course geometry (varying the distance between gates, for example) to provoke more extreme losses in rotorspeed, as was done for the slalom manoeuvre described in Section 6.2.1.

Similarly to the slalom manoeuvre, inverse simulation could be used to determine a selection of course geometries which would generate varying amounts of change in the load factor acting on the main rotor, and thus result in varying degrees of rotor speed loss. Flying these course geometries and assigning HQRs using the Cooper-Harper scale would allow the level of handling difficulties induced by the loss of rotor speed to be established, and Level 1/2 and Level 2/3 boundaries to be established using the same

technique described in Chapter 5 for determining Quickness requirements for the autogyro.

The use of the Heave Hop manoeuvre to assess both the autogyro and helicopter models also highlighted a further fundamental difference between the two aircraft types. The helicopter is able to vary and control the load factor acting on the main rotor through collective control – something which is entirely absent in the autogyro. The addition of collective control allows the helicopter to safely perform manoeuvres in autorotation, such as landing after engine failure, as it gives the pilot the ability to control the amount of energy stored in the main rotor and the ability to control when this energy is released. Addition of collective control to the autogyro would prove difficult; it would require the installation of a further control inceptor and would add to the mechanical complexity of the autogyro, a vehicle which is attractive due to its simplistic design. It is possible to implement such a design in the simulation environment, modifying the model to be fitted with an articulated rotor linked to the collective controller in the simulator, to investigate if such a system would confer any benefits on autogyro-type vehicles.

6.5 HEAVE HOP WITH ROLL CONTROLLER

As identified during several of the manoeuvres discussed in this Chapter, the autogyro experiences severe cross couplings as a result of its poor roll damping and large amounts of control power. In order to assess the impact of this deficiency and to understand the level of improvement that could be achieved, a simple roll rate proportional feedback loop was implemented in the autogyro model, as shown in Figure 146.

The development of this controller is not intended to be a holistic assessment of the improvements that a control system can provide for the autogyro; it is intended to illustrate the potential of such an application and generate impetus for further work.

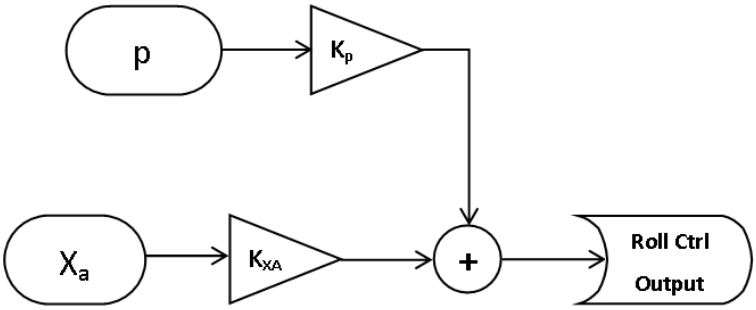

Figure 146: Proportional feedback on roll axis

The value of K_{XA} converts the magnitude of the stick input in inches to degrees of lateral shaft tilt. It is a constant value. The value of the gain K_p was varied, using -5, -10 and -20 deg/deg.sec^{-1}. To evaluate the effect and effectiveness of this simple controller in reducing the workload generated by the presence of the cross couplings in the autogyro, the Heave Hop manoeuvre was selected. It was chosen as it is the manoeuvre in which the autogyro showed the most significant difference to the equivalent helicopter model, and was the manoeuvre in which the presence of inherent cross couplings in the autogyro were made most apparent, and were the most problematic.

The Heave Hop manoeuvre was re-flown in the three configurations with varying roll rate gain values, with the pilot rating the manoeuvre using the Cooper Harper handling qualities rating scale as before. Only the 1st course geometry was used (passing over/under each pole, maintaining altitude and descending between the second/third poles). The results are shown in Figure 147.

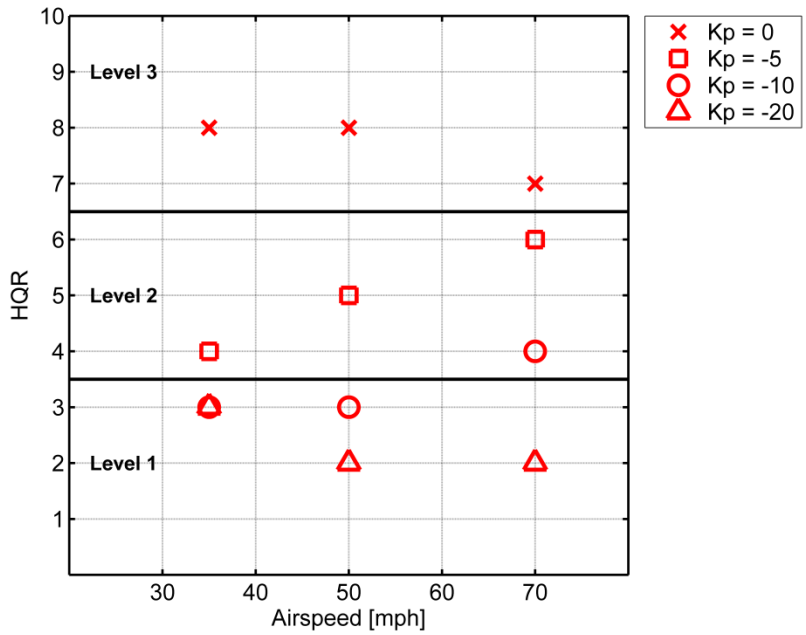

Figure 147: Assigned handling qualities of the autogyro model for the Heave Hop manoeuvre with varying K_p feedback

Figure 147 clearly illustrates that the higher the gain, the greater the improvement in the HQR awarded, with test points for the un-augmented aircraft being in Level 3, moving through Level 2 and into Level 1 as the magnitude of K_p, and thus the authority of the controller, is increased.

The improvement in handling qualities can be attributed to the fact that the roll controller effectively eliminates the roll due to throttle and roll due to pitch cross couplings in the autogyro by applying a deflection to the roll control in order to counter any developing roll rate; this effectively increases the roll damping of the autogyro. This reduction in roll due to pitch cross coupling with the addition of roll rate feedback is shown in Figure 148, which shows that for the highest gain values, the roll due to pitch cross coupling will be just inside Level 2 according to the predictive handling qualities assessment method in ADS-33E.

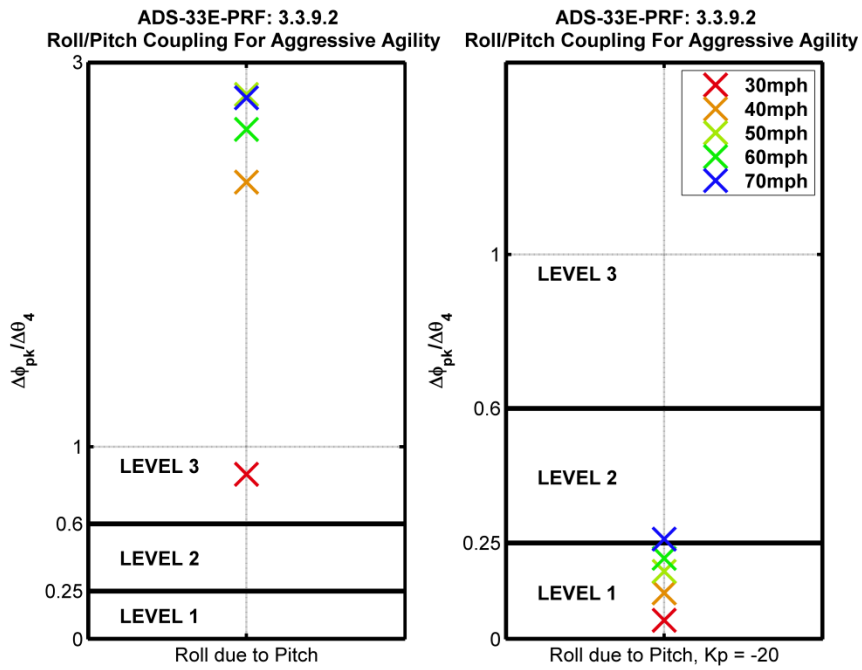

Figure 148: Comparison of roll due to pitch cross coupling for autogyro for un-augmented and augmented models

The controller with the highest authority (i.e. the largest gain value) achieves the best HQRs for this particular manoeuvre due to the fact that it feeds back the highest proportion of the roll rate; aggressively damping it out before it has time to initiate the roll cross couplings present in the model. As a result, both the magnitude and frequency of control inputs in the roll axis are reduced. This is illustrated in Figure 149.

Whilst the controller provides varying degrees of improvement for the Heave Hop manoeuvre, depending on the magnitude of the gain selected, there will be a trade-off between improving the roll cross coupling characteristics and the decreasing the roll agility. The higher the magnitude of the feedback gain applied to the roll axis, the smaller the roll due to pitch cross coupling, but the higher the increase in the roll damping. If the roll damping becomes too large, the aircraft will feel sluggish in roll; an undesirable characteristic. In order to identify the optimal value of K_p the controller must be assessed against the predicted handling qualities metrics demonstrated in Chapter 5 (quickness, control power etc.), and against MTEs which focus on the roll axis handling qualities (such as the Slalom or the Roll Step) in order to create a holistic view of what effect the varying controller configurations have on the performance of the autogyro.

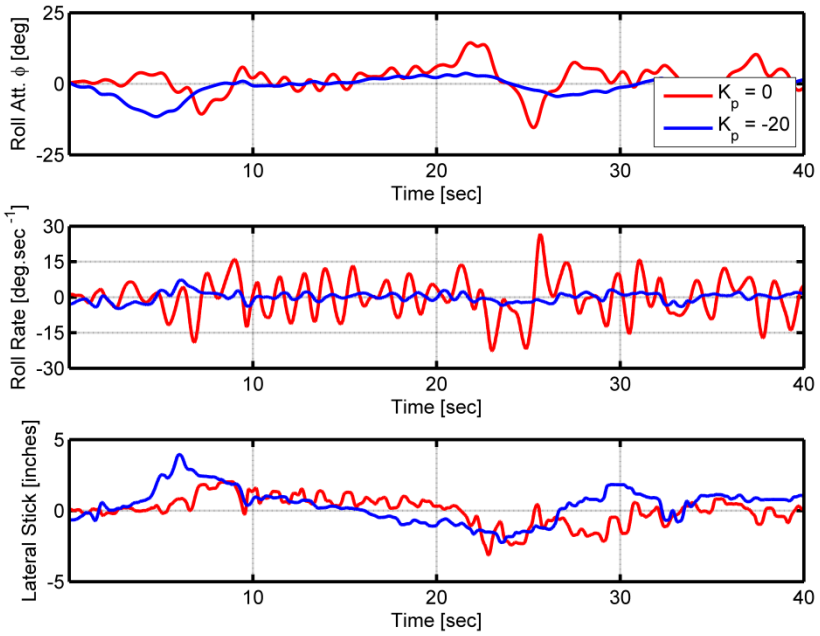

Figure 149: A comparison of roll rate, attitude and lateral control input for the Heave Hope manoeuvre at 70mph with varying K_p feedback (K_p = 0, HQR 7, K_p = -20, HQR 2)

Another disadvantage of implementing a controller in a real-world autogyro would be the cost and complexity of such a system. One of the attractions of the autogyro as a platform, in comparison to the aeroplane or conventional helicopter, is its mechanical simplicity. This makes repair and maintenance much cheaper and easier, keeping costs down. Increasing the roll damping to reduce cross couplings in the autogyro could be achieved through changes to the design of the autogyro, for example increasing the horizontal tail size, which would maintain the simplicity of the vehicle. A study of the practicalities of this is beyond the scope of this Thesis, but would prove an interesting field for further work.

6.6 ROLL STEP

The Roll Step manoeuvre is a forward flight manoeuvre intended to assess the roll axis bandwidth, quickness and control power. It is not defined in ADS-33, having been developed for the assessment of tilt rotor aircraft [82]. The Roll Step is used to check the aircraft's ability to manoeuvre in forward flight with respect to the ground level and to assess turn co-ordination in moderately aggressive flight. This manoeuvre will also reveal the presence of any objectionable inter-axis couplings between roll and the remaining

axes. The Roll Step will be completed at 3 airspeeds in order to assess the aircraft in low, medium and high speed flight conditions.

6.6.1 Manoeuvre Description

The pilot should initiate the manoeuvre at steady airspeed 30mph aligned with the left hand side of the runway at a height of 50ft. The aircraft shall pass through the first 4 gates before initiating a turn to the right to cross the runway and align with the right hand side of the runway before the sixth gate (completing the reposition from one side of the runway to the other in 1000ft). The aircraft will then pass through the sixth gate, tracking the right hand edge of the runway. After passing through the third tenth gate, the pilot will initiate a turn to re-cross the runway and pass through the twelfth and final gate, realigned with the left hand side of the runway. This is Course 1. Course 2 requires the aircraft to complete the lateral reposition across the runway within 500ft, between the fourth and fifth gates.

6.6.2 Course Geometry

The course geometry for the Roll Step is shown in Figure 150. The test course consists of a 200ft wide runway which is flanked by a series of gates 500ft apart (only the primary gates are shown in Figure 150).

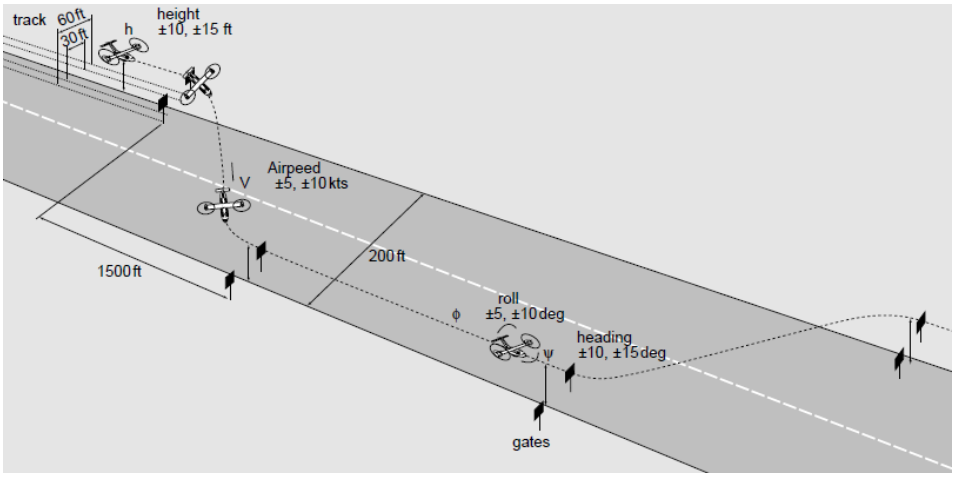

Figure 150: The Roll Step course geometry [82]

6.6.3 Performance Requirements

	DESIRED	ADEQUATE
Height	±10ft	±15ft

Speed	±5 mph	±10 mph
Track	±15ft	±30ft
Yaw angle	±10deg	±15deg

Table 37: Performance requirements for the Roll Step manoeuvre

6.6.4 Test Matrix

Course Number	Target Airspeed (mph)
1	35
	50
	70
2	35
	50
	70

Table 38: Roll Step test matrix

6.6.5 Results

The results of the Roll Step manoeuvre are shown in Table 39 and Figure 151.

Course	Airspeed Range (mph)	Autogyro HQRs	Helicopter HQRs
1	35	7	2
	50	7	2
	70	7	3
2	35	8	2
	50	9	3
	70	9	3

Table 39: Roll Step manoeuvre HQRs for autogyro and helicopter

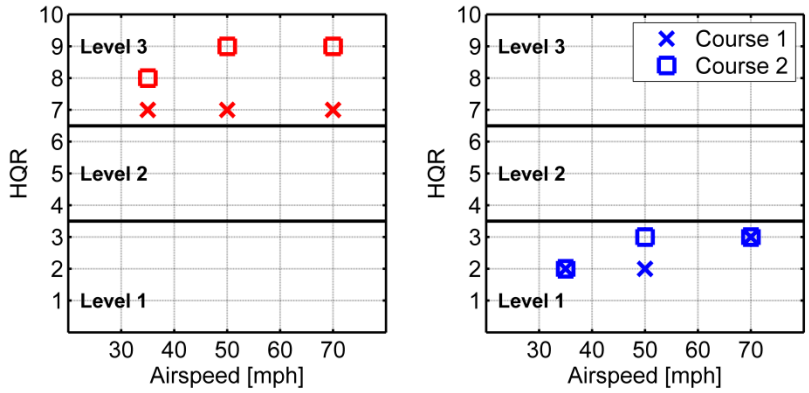

Figure 151: A comparison of assigned handling qualities of the autogyro (red) and helicopter (blue) models for the Roll Step manoeuvre

For all test points, Figure 151 shows that the handling qualities of the autogyro lie within Level 3, and all test points for the helicopter lie within Level 1.

Similarly to the Acceleration-Deceleration manoeuvre, the pilot struggled to maintain lateral position within the adequate boundaries when flying the autogyro. This is shown in Figure 152 (note that only the first cross-runway transition is shown in order to highlight the detail of runway position keeping; for all other parameters, the whole manoeuvre is illustrated).

One of the objectives of the Roll Step manoeuvre is to reveal the presence of any objectionable inter-axis couplings. Piloting the autogyro, the pilot again highlighted the undesirable nature of the pitch due to roll cross coupling; upon initiating the crossing of the runway at around the 3 second mark in Figure 153, the autogyro pitch attitude also increases. The pilot is then forced to counter this cross coupling, diverting workload from maintaining lateral position into control of the aircraft. As a result of this high workload, the autogyro is awarded an HQR 7 for the 35mph test point on Course 1. This issue persisted throughout the test points, becoming an increasingly prominent driver of pilot workload as the airspeed increased and the time for the pilot to make corrective inputs decreased. In contrast, the reduced pitch due to roll cross coupling of the helicopter compared to that of the autogyro allows the pilot to focus attention and effort on maintaining airspeed and altitude, as well as lateral position. This results in a much more

tightly controlled flight path, and allows all parameters to be achieved within the desired criteria for the same test point, resulting in the manoeuvre being awarded an HQR 2.

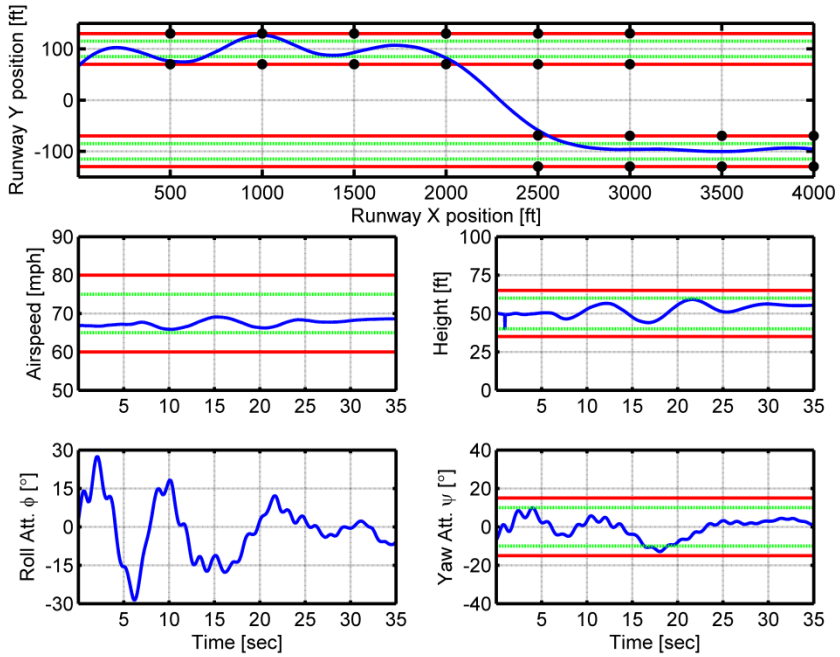

Figure 152: Flight test data for autogyro model flying Roll Step manoeuvre on Course 1 (70mph, HQR 7)

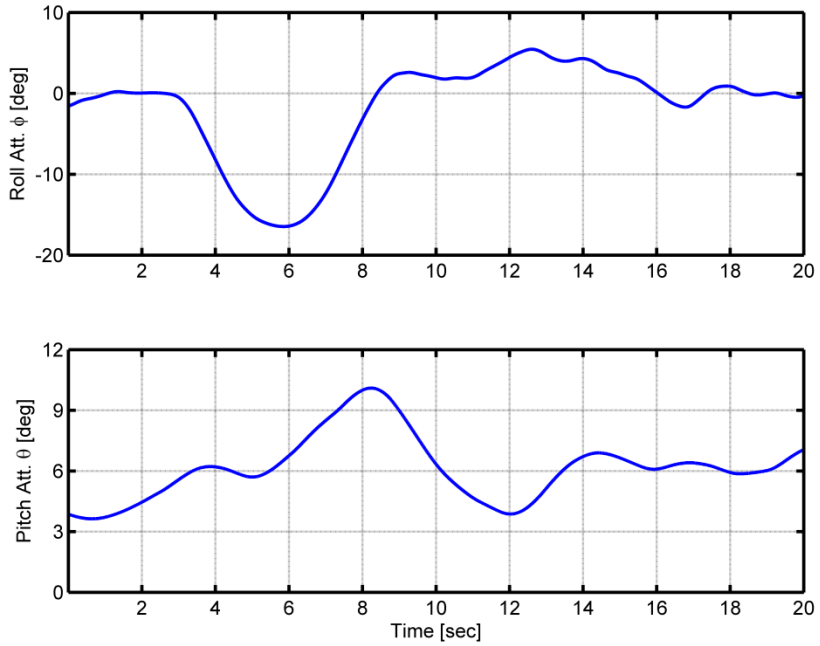

Figure 153: Example of autogyro pitch due to roll cross coupling during the Roll Step manoeuvre (Course 1, 35mph, HQR 7)

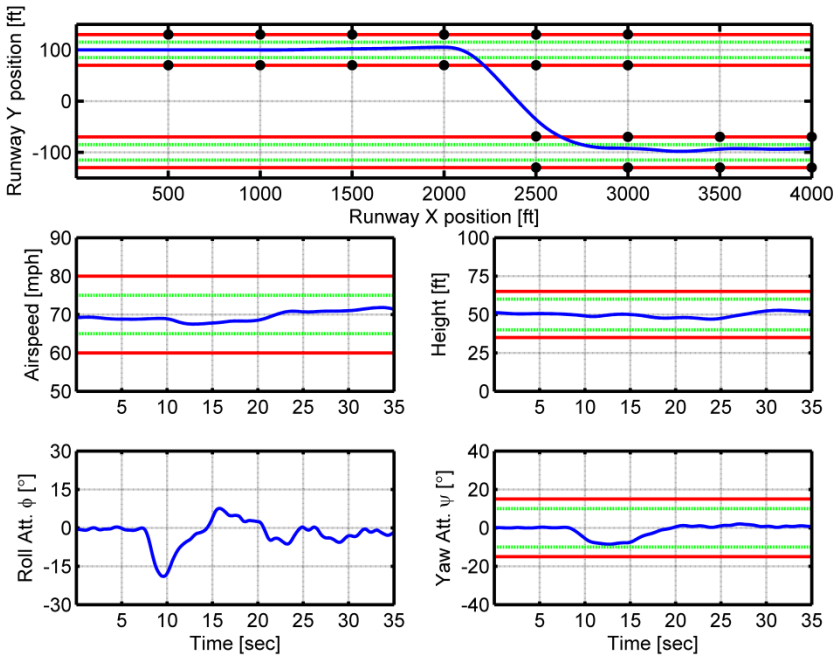

Figure 154: Flight test data for helicopter model flying Roll Step manoeuvre on Course 1 (70mph, HQR 2)

Similarly to the Slalom, the Roll Step manoeuvre highlights the presence of objectionable inter-axis couplings, and therefore can be applied to the autogyro. As for the Slalom, no deficiencies in the turn co-ordination were highlighted, so it is not possible to say if the Roll Step highlights these deficiencies in the autogyro.

6.7 CONCLUSIONS

An analysis of the assigned handling qualities of the autogyro and helicopter has been carried out, utilising both ADS-33 [2] and non-ADS-33 MTEs. This builds upon the work carried out in Ref. 7, and presents analysis of two new MTEs (the Heave Hop and the Roll Step), against which the autogyro has previously not been assessed. All 4 MTEs have been considered in terms of their applicability to the autogyro, and modifications have been made where appropriate. The results of the assessment of the assigned handling qualities have also been considered in the light of the predicted handling qualities assessment carried out in Chapter 5, in order to verify that the predicted handling qualities metrics do indeed highlight the same deficiencies as observed during flight test. Finally the results of the assigned handling qualities for both autogyro and helicopter to identify if any of the manoeuvres in particular highlight the fundamental differences between the autogyro and helicopter which may be responsible for the autogyro's considerably worse accident rate.

Broadly similar performance and trends in result were identified for the autogyro and helicopter in the Slalom manoeuvre. The presence of the pitch due to roll cross coupling in both autogyro and helicopter was identified as the driving factor behind this; the helicopter achieving slightly improved performance at the same test condition due to the reduced magnitude of its pitch due to roll cross coupling as predicted in Chapter 5, and as a result being awarded a lower HQR for the example test point. The Slalom manoeuvre is intended "to detect any objectionable inter-axis couplings" when applied to analysing the helicopter; it has shown that it has similar utility when applied to the autogyro.

The Acceleration-Deceleration manoeuvre was also used to assess both autogyro and helicopter. As the autogyro cannot hover, the manoeuvre was modified such that it was initiated at a target initiation airspeed, rather than from hover, before the pilot accelerated to the target airspeed before decelerating back to the initiation airspeed to complete the manoeuvre. For consistency, the helicopter was assessed using the same

methodology. Again, helicopter and autogyro displayed broadly similar performance characteristics. The Acceleration-Deceleration also highlighted a fundamental difference between the autogyro and helicopter. The helicopter uses pitch attitude to accelerate and decelerate, meaning that the Acceleration-Deceleration manoeuvre is a good way to demonstrate the presence of any roll due to pitch cross coupling. The autogyro uses throttle setting to accelerate, not pitch attitude, so the Acceleration-Deceleration manoeuvre is not able to as clearly highlight the presence of any undesirable roll due to pitch couplings and should not be used to assess this characteristic of the autogyro.

The Heave Hop manoeuvre is a non-ADS-33 manoeuvre which was initially developed for the assessment of tilt rotors [81]; the autogyro has not been assessed against this manoeuvre before. This manoeuvre was chosen for the assessment of the autogyro as it is intended to assess the aircraft's performance under both high and low g conditions. This is an important factor in autogyro performance, as entering high or low g conditions may cause the main rotor to speed up or slow down due to changes in the rotor loading. This can lead to a change in the handling qualities of the aircraft due to the reduction in control power available when rotor speed decreases. The autogyro was shown to have significantly poorer handling qualities than the helicopter across all test points. This was attributed to two main factors; the variation in rotorspeed which only occurs in the autogyro, and the roll due to throttle cross coupling present only in the autogyro model. Both of these issues presented the pilot with an increased workload while flying the autogyro compared to the helicopter. As a consequence of this increase workload, the pilot then has less capacity to focus on maintenance of speed and other parameters while piloting the autogyro, leading to the desirable and adequate performance limits being exceeded.

A simple roll rate proportional feedback controller was installed within the autogyro model in order to assess the impact of the presence of the cross couplings experienced by the autogyro, and to establish the extent to which a simplistic controller could improve the autogyro performance in the Heave Hop manoeuvre. The development of the controller was not intended to be a holistic assessment of the improvements that a control system can provide for the autogyro; it was intended to illustrate the potential of such an application and generate impetus for further work. The controller gains were

varied across a range of values in order to assess the impact of increasing the controller authority.

It was clearly shown that the higher the magnitude of the gain, the more significant the improvement in handling qualities; the elimination of the roll due to pitch and roll due to throttle cross couplings provided by the simple controller enabled the autogyro to achieve Level 1 HQRs at the highest gain value.

As a result of assessing the autogyro against the Heave Hop manoeuvre, two clear paths for further work have emerged. The acceptable extent of the roll due to throttle cross coupling must be quantified for the autogyro. Development of an ADS-33 style cross coupling chart would be a good way to do this, dividing the autogyro performance in to Levels 1 to 3 based on assigned handling qualities ratings and defining the upper limits of each Level. This could be achieved through development of an MTE which more effectively isolates the throttle response of the aircraft, for example using an MTE that involves aggressively accelerating the aircraft at test points throughout the flight envelope, and measuring the roll response due to the throttle positioning. The amount of roll attitude generated could then be compared to the awarded HQR and handling qualities Levels could be established, much in the same manner as the development of quickness requirements illustrated in Chapter 5.

Secondly, the holistic design and assessment of a feedback controller for the autogyro in all axes could prove to be an interesting development of the simple roll axis controller described herein; this simple controller has shown it is capable of improving the handling qualities in the roll axis and it may be that the application of a simple control system in all axes will provide the autogyro with the 'ease and precision' of handling required to make the autogyro a safer aircraft to fly.

Finally, the autogyro and helicopter were assessed against the Roll Step manoeuvre. Again, this manoeuvre was designed to be used in the assessment of tilt rotor type aircraft, and the autogyro has not been assessed against it before. The Roll Step intends to check the aircraft's ability to manoeuvre in forward flight with respect to ground level, to check roll and heave axis co-ordination and to assess turn co-ordination in moderately aggressive flight. The Roll Step will also reveal the presence of any objectionable inter-

axis couplings between roll and the remaining axes. For both the autogyro and helicopter, the Roll Step highlighted the presence of the pitch due to roll cross coupling predicted by the analysis performed in Chapter 5.

Chapter 7

CONCLUSIONS

Chapters 3 to 6 describe the development of a simulation model of an autogyro and its use in the derivation and assessment of the model's handling qualities against ADS-33 [2]. Consideration was also given to the recommendations made in CAA Report 2009 [4] in Chapter 4. The conclusions from each of these lines of investigation were illustrated individually within their respective Chapters; it is the intention of this final chapter to draw together the overall conclusions with respect to the research questions posed in Chapter 2 to create and overview of what has been achieved, and to illustrate potential avenues for development of the research undertaken.

7.1 RESEARCH CONCLUSIONS

7.1.1 Modelling and Simulation of an Autogyro

In order to begin assessing the research questions highlighted in Chapter 2, a simulation model of an autogyro had to be created. The G-UNIV research autogyro, owned by Glasgow University was chosen as the aircraft upon which the model would be based for a number of reasons; a full set of the inertial and geometric data required to create the model was available, there was a small amount of flight test available to use in validating the model and the real aircraft had been used in piloted handling qualities assessment, meaning there were baseline handling qualities ratings to compare those of the completed model against. Chapter 3 describes the creation and validation of this autogyro model, and the creation of a geometrically similar helicopter model which was also used during the analysis presented in this Thesis.

The autogyro model was validated using three methods; a comparison of the model's dynamic response with dynamic responses presented in the flight test data was performed, the derivatives of the model were compared to those estimated in flight and the handling qualities of the model compared to those of the real aircraft.

The autogyro model was shown to exhibit trimmed control positions, dynamic responses and derivatives comparable to those of the real aircraft. The autogyro model also displayed broadly similar handling qualities ratings to that of the real aircraft.

As it is a purely hypothetical vehicle, it was not possible to validate the helicopter model in the same way.

7.1.2 Evaluation of the existing recommendations in CAA Report 2009/02 [4]

Paper 2009/02 [4] represents the culmination of the most significant body of work surrounding the autogyro in recent years.

The final report presented 4 main findings/recommendations:

1. It is recommended that the vertical location of the centre of gravity (c.g.) should lie within a ± 2 inch envelope of the propeller thrust line.

2. Horizontal tailplanes are largely ineffective in improving the long term pitch dynamic stability (phugoid mode).

3. Extreme manoeuvring can lead to excessive rotor teeter angles during certain phases of flight, potentially resulting in the rotor blades striking the prop or empennage.

4. The chordwise centre of gravity of the rotor blades should always lie at or ahead of the 25% chord position to prevent rotor blade instability.

The recommendations made in Ref. 4 were based on a limited number of configurations of autogyro; one of the intentions of Chapter 4 was to expand upon the number of configurations used in establishing these recommendations. The autogyro model created in Chapter 3 was used to evaluate the four recommendations.

The research questions in Chapter 2 asked "how valid are the 4 findings and recommendations made in CAA Paper 2009 [4]?" The answer to this question varies depending upon the recommendation being considered.

The first recommendation suggests that the position of the vertical position of the centre of gravity should lie within a vertical envelope of ±2 inches from the propeller thrustline. The results of Chapter 4 suggest this may be overly restrictive; BCAR Section T compliance could be achieved with the centre of gravity outside this envelope. Whilst this is a sensible design aim (intended to reduce the moment generated by the engine

and propeller), to apply a 'one size fits all' solution has the potential to force configurations which are demonstrably compliant outside of the ±2 inch thrustline envelope into the non-compliance region. These investigations have also shown that the vertical positioning of the centre of gravity relative to the propeller thrustline is important in determining the frequency of the phugoid mode, in support of findings of Ref. 4.

The second recommendation relates to tailplane effectiveness. Ref. 4 concluded that the presence of a tailplane made no difference to the characteristics of either the longitudinal trim characteristics of the aircraft, or the characteristics of the phugoid mode. However, in direct contrast to this, the work of Chapter 4 illustrated that a pronounced change in both of these characteristics occurred in the autogyro model. With a tailplane, the phugoid mode variation was linear and predictable with airspeed; removing the tailplane results in the frequency of the phugoid mode changing unpredictably as airspeed increases. With tailplane attached the longitudinal shaft tilt, and thus the longitudinal stick position, decreased linearly with airspeed; without the tailplane the longitudinal trim stick position is seen to initially decrease with airspeed, but begins to increase again with airspeed beyond 45mph. The tailplane has also been shown to be important in shaping the key derivatives which determine the characteristics of the phugoid and short period modes, M_q, M_u and M_w.

Removing the tailplane also had consequences for the handling qualities of the autogyro model during piloted simulation. Without the tail, the aircraft displays a divergent phugoid, which was described by the pilot as being 'very easy to excite' and 'almost impossible to supress'.

These findings are in direct contradiction to those of Ref. 4. This is another research path which requires further work.

Chapter 4 also showed that under extreme manoeuvring it is possible for the main rotor blades to strike the prop and empennage. This directly supports the findings of Ref. 4.

The final recommendation of Ref. 4 was not assessed; the autogyro model uses a rigid blade model and thus it is not possible to assess the impact of changing the chordwise centre of gravity of the blade.

7.1.3 Autogyro Handling Qualities

One of the research questions posed in Chapter 2 asked if existing rotary wing specifications, such as ADS-33 [2], could be used to assess the handling qualities of the autogyro. A full analysis of the predictive metrics defined in ADS-33 was carried out, alongside an analysis of a select number of MTEs from both ADS-33 and other sources.

Chapter 5 presented a comprehensive analysis of the predictive handling qualities metrics prescribed in ADS-33. Whilst this analysis did highlight areas of possible handling deficiencies (such as strong pitch due to roll and roll due to pitch cross couplings and large amounts of quickness and control power in all axes), the conclusions available to be drawn are less clear. Criteria in the low amplitude, high frequency sector of the dynamo construct, such as bandwidth were considered to be applicable to the autogyro in their prescribed form due to the fact that consequence of and likelihood that control inputs will be applied at or above the bandwidth frequency, triggering aircraft instability, is not specific to aircraft type. In the case of the mid-term response criteria, the ability of the pilot to maintain control over the natural modes of the aircraft is also a fundamental requirement, and is unlikely to vary significantly between rotary-wing vehicle types.

The methodology used for assessing parameters such as quickness, control power and cross coupling were shown to be applicable to the autogyro, however there remains scope to re-address the positioning of the Level 1/2 and Level 2/3 boundaries in order to account for the reduced inertia of the autogyro when compared to the helicopters the specification was originally designed for. The lack of an upper limit to the acceptable levels of quickness and control power was also identified as an issue; excessive quickness and control power may causes as much of a handling deficiency as insufficient quickness and control power.

When comparing the predictions for the autogyro and helicopter, another key difference between the two vehicle types was identified. In general the helicopter model has well harmonised handling qualities; for example, the helicopter tends to display an approximately constant value of quickness in all three axes, whereas the autogyro tended to display increasing quickness as the airspeed increased. To add to this, the autogyro generally has higher values and a more pronounced response for all the metrics analysed; this superfluity of agility and heavily coupled response was shown to be indicative of

significant handling qualities deficiencies of the autogyro; the application of existing predictive handling qualities metrics was able to indicate predictively the areas which were demonstrated to be undesirable during the simulated piloted flight trials described in Chapter 6.

The assigned handling qualities of both the autogyro and the helicopter were explored using piloted simulation, as reported in Chapter 6. Both aircraft types were assessed against 2 ADS-33 manoeuvres (the Slalom and the Acceleration-Deceleration) and 2 manoeuvres initially developed for tilt rotors (the Heave Hop and the Roll Step).

In the Slalom manoeuvre, the autogyro and helicopter achieved broadly similar performance and handling qualities ratings, with the helicopter achieving slightly improved performance due to its comparatively smaller pitch due to roll cross-couple. The Slalom manoeuvre is intended to reveal any objectionable cross-couplings when used to assess helicopters; it has been shown it has similar utility when applied to the autogyro. It also reveals the extent of the cross couplings predicted in Chapter 5, rating worse than the helicopter which was predicted to experience a pitch due to roll cross coupling of lesser magnitude, and can therefore be said to be applicable to the autogyro.

Analysis of the Acceleration-Deceleration manoeuvre demonstrated that not all existing MTEs can be applied directly to the autogyro; as the autogyro cannot hover, the Acceleration-Deceleration had to be modified to be initiated from a specified airspeed before completing the rest of the manoeuvre. Another of the research questions of Chapter 2 refers to establishing the fundamental differences between the autogyro and the helicopter, and the Acceleration-Deceleration highlights one of them. The helicopter uses pitch attitude to accelerate and decelerate, meaning that the Acceleration-Deceleration manoeuvre is a good way to demonstrate the presence of any roll due to pitch cross coupling in such vehicles. The autogyro uses throttle setting to accelerate, not pitch attitude, so the Acceleration-Deceleration manoeuvre is not able to as clearly highlight the presence of any undesirable roll due to pitch couplings and therefore cannot be used to assess this characteristic of the autogyro. The Acceleration-Deceleration also highlighted the presence of a roll due to throttle cross coupling in the autogyro which is not present in the helicopter.

The Heave Hop manoeuvre also highlighted another of the fundamental differences between the autogyro and the helicopter. The helicopter has a rotor governor, meaning that the rotor speed is maintained constant, irrespective of the manoeuvre being undertaken. As the autogyro rotor operates in the autorotative regime, the rotor is ungoverned, and thus the speed is free to vary. During the Heave Hop, this lead to a change in the handling qualities of the aircraft due to the reduction in control power available when rotor speed decreases, for example. This causes the handling qualities to become unpredictable, increasing the pilot workload to intolerable levels. This is reflected in the autogyro's significantly poorer HQRs when compared to the helicopter.

Finally, the autogyro was assessed using the Roll Step manoeuvre. For both the autogyro and helicopter, the Roll Step highlighted the presence of the pitch due to roll cross coupling predicted by the analysis performed in Chapter 5, and is therefore considered useful in the assessing this aspect of the performance of the autogyro.

7.2 PROPOSALS FOR FURTHER WORK

One of the main outputs of this Thesis is the creation and documentation of a simulation model of an autogyro. Unlike the model described in Ref. 6, the model is not subject to commercial restriction and is able to successfully find a mathematical solution to establish the trimmed control positions to achieve trimmed flight in the offline environment; previous iterations of the model described in Ref. 6 were not able to achieve this.

As a result of the development of this model, there exists a functional tool upon the use of which further work can be based. The nature of the model allows for rapid prototyping of any autogyro configuration or geometry, which can then be analysed in the real-time or offline simulation environment provided by FLIGHTLAB.

7.2.1 Further work based upon CAA Report 2009/02 findings

The work of Chapter 4 concluded that the ±2 inch vertical envelope relative to the propeller thrustline within which the centre of gravity should lie may prove overly restrictive. Therefore, further analysis is required, using different configurations. The autogyro model developed in the course of this project would provide an ideal platform

to do this; it is easily reconfigured to represent different vehicles, the use of the built in linearisation tool can be easily used to reproduce the work carried out within Chapter 4.

The second recommendation, which states that tailplanes are largely ineffective in improving the longitudinal dynamics, could also be investigated in a similar manner; reconfiguring the model to represent different autogyros, performing the required analysis to replicate the work performed in Chapter 4 and then removing the tail and repeating the analyses in order to compare the results.

The third and final recommendation in Ref. 4 analysed in Chapter 4 relates to the tail striking the prop and empennage under extreme manoeuvring. Chapter 4 also highlighted that Ref. 4 found the strike plate, designed to prevent the rotor coming into contact with the propeller or empennage, is ineffective. The design of an effective strike plate which could be fitted to the autogyro would provide an improvement in the airworthiness of the autogyro and is a potential avenue for further work.

The 4th recommendation in Chapter 4, relating to blade aeroelastic effects, was not assessed as the blade model used in the autogyro model describe in this Thesis is a rigid blade model. FLIGHTLAB does provide the option to model the blade as an aeroelastic rotor; modification of the model to include an aeroelastic rotor is an obvious path for further work. It may also prove interesting to repeat the analysis of recommendations 1 to 3 with an aeroelastic blade model to assess the impact, if any, upon the results.

7.2.2 Handling Qualities

The final research question in Chapter 2 asks "If existing specifications such as ADS-33 are not applicable to the autogyro, new metrics to assess the handling qualities of the autogyro must be developed. What are the requirements of these metrics and what methodology should be used to develop them?"

Chapter 5 explored the application of the existing predicted handling qualities metrics from ADS-33. There remains scope for further work surrounding the definition and positioning of the Level 1/2 and Level 2/3 boundaries for all the predicted handling qualities metrics when applied to the autogyro. A method for doing this was presented in Chapter 5, using assigned handling qualities ratings from an appropriate MTE to define the location of the Level 1/2 and Level 2/3 boundaries; for example, using the assigned

handling qualities ratings from the Slalom MTE to define the roll quickness limits. In order for these Levels to be firmly defined, different configurations of autogyro need to be assessed in the same manner. It would be possible to assess many different autogyro combinations using the autogyro model created within this Thesis as a baseline.

During the course of the assigned handling qualities assessment of the autogyro, the presence of a roll due to throttle cross coupling was identified. The development of a predictive handling qualities metric for this cross coupling, in the same style as those in ADS-33 for the pitch due to roll and roll due to pitch cross couplings, would be a suitable avenue to progress the work described in this Thesis. The same method of quantifying the locations of the Level 1/2 and Level 2/3 boundaries as that suggested above could be used.

In general, Chapter 6 demonstrated that the MTEs chosen highlight the deficiencies they are intended to identify (save for the Acceleration-Deceleration), though before these manoeuvres can be deemed "suitable" for assessment of the autogyro, further work is required to assess different types of autogyro in different configurations to allow firm conclusions to be drawn. Attention should also be paid to the definition of the adequate and desired tolerances imposed upon the autogyro in the MTE definition; at present, the tolerances used were the standard tolerances from the original manoeuvre definitions, which may prove to be too stringent or too lax for the autogyro.

Chapter 6 demonstrated the implementation of a simple roll rate feedback loop. This feedback loop illustrated the potential for improving the handling qualities of the autogyro using feedback control to eliminate cross couplings, moving the handling qualities of the autogyro from Level 3 in its un-augmented state, to Level 1 when the largest amount of feedback was applied during assessment using the Heave Hop manoeuvre. The feedback implemented was only applied to one axis, and the level of improvement only assessed against one manoeuvre. A natural progression of this work would be to expand the control system design into other axes, and the carry out a holistic assessment of the autogyro against several other MTEs and predicted handling qualities metrics to assess the extent of the improvement that is possible over the un-augmented aircraft. Other types of feedback control could also be investigated, such as integral or derivative control.

7.3 WILL THE AUTOGYRO EVER BE TRULY DOMESTICATED?

This Thesis represents a step on the road towards domesticating the autogyro. Through identification of the deficiencies present in the autogyro, it is possible to implement solutions which remedy these deficiencies and make the autogyro safer and more airworthy. Improvement of the base level handling qualities, through new design and modification of existing design, will also improve the autogyro's airworthiness; in order to achieve this, the development of an autogyro specific handling qualities specification is an important step. In this Thesis, steps have been taken to begin developing such a specification, drawing from and adapting an existing specification, and many of the suggestions for further work represent the next steps in bringing this goal to fruition. Only when a strict set of guidelines for what is considered 'domestication' exist can designers and engineers begin working towards creating the domesticated autogyro.

REFERENCES

1. http://www.caa.co.uk/docs/56/UK%20reg%20cofa%20and%20weight%20group%20010110.pdf
2. Anon., “Handling Qualities Requirements for Military Rotorcraft” *Aeronautical Design Standard ADS-33*, US Army Aviation and Troop Command (2000)
3. Leishman, J. Gordon. "Development of the autogiro: a technical perspective." *Journal of Aircraft* 41.4 (2004): 765-781.
4. Anon., “CAA Paper 2009/02: The Aerodynamics of Gyroplanes” *Civil Aviation Authority Report* (2010)
5. Anon. “CAP643: British Civil Airworthiness Requirements Section T Light Gyroplanes”, *Civil Aviation Authority Report* (2005)
6. Jump, M., Kendrick, S., Perfect, P., Padfield, G.D, Ridgway, G.R., **“**Rapid Prototyping and Validation of an Autogyro Simulation Model” *Proceedings of CEAS Air and Space Conference* (2009)
7. Bagiev, Marat, and Douglas G. Thomson. "Handling Qualities Assessment of an Autogiro", *Journal of the American Helicopter Society* 55.3 (2010): 32003-1
8. Padfield, G.D, “The Tau of Flight Control”, *The Aeronautical Journal,* (2011): 115-1171
9. Houston, S.S, Thomson, D.G., Spathopoulos, V.M., "Experiments in Autogyro Airworthiness for Improved Handling Qualities", *Proceedings of 57th Annual Forum of the American Helicopter Society* (2001)
10. Bagiev, Marat, and Douglas G. Thomson. "Handling Qualities Evaluation of an Autogiro Against the Existing Rotorcraft Criteria." *Journal of Aircraft* 46.1 (2009): 168-174
11. Anon, *Degree of Doctor in Philosophy. Notes for Guidance of Examiners*, [cited 25/07/14]. Available from http://www.liv.ac.uk/media/livacuk/studentadministration/research/documents/Thesis,Preparation,Guidelines.pdf
12. de la Cierva, Juan, and Rose, D., "Wings of Tomorrow: The Story of the Autogiro." *New York: Brewer, Warren, Putnam* (1931).

13. Glauert, H., "A General Theory of the Autogyro" *Aeronautical Research Council, Reports and Memoranda* 1111 (1926)
14. la Cierva, J., “A Letter to RAeS with Comments on the Paper Presented by H. Glauert on 20 January 1927,” *Journal of the Royal Aeronautical Society*, Vol. 31, No. 198 (1927): pp. 505, 50
15. Lock, C. N. H. "Further development of autogyro theory." *Aeronautical Research Council, Reports and Memoranda 1127* (1927)
16. Wheatley, John B. "The aerodynamic analysis of the gyroplane rotating-wing system." *NACA TN 492* (1934)
17. Glauert, H., "Lift and Torque of an Autogyro on the Ground" *Aeronautical Research Council, Reports and Memoranda* 1131 (1927)
18. Lock, C. N. H., and Townend, H. C. H.. “Wind tunnel experiments on a model autogyro at small angles of incidence” *Aeronautical Research Council, Reports and Memoranda 1154* (1928)
19. Glauert, H. and Lock, C. N. H., “A summary of the experimental and theoretical investigations of the characteristics of an autogyro”, *Aeronautical Research Council, Reports and Memoranda 1162* (1928)
20. Wheatly, J.B., ”Lift and Drag Characteristics and Gliding Performance of an Autogiro as Determined in Flight", *NACA TR 434* (1932)
21. Wheatly, J.B., ”Wing Pressure Distribution and Rotor-blade Motion of an Autogiro as Determined in Flight", *NACA TR 475* (1933)
22. Wheatly, J.B., Bioletti, C., "Wind Tunnel Tests of a 10-foot-Diameter Gyroplane Rotor", *NACA TR 536* (1935)
23. Wheatley, John B. “An Aerodynamic analysis of the autogiro rotor with a comparison between calculated and experimental results” *NACA TR 487* (1935)
24. Wheatly, J.B., Hood, M.J., "Full-Scale Wind Tunnel Tests of a PCA-2 Autogiro Rotor", *NACA TR 515* (1935)
25. Wheatly, J.B., “A Study of Autogiro Rotor Blade Oscillations in the Plane of the Rotor Disk", *NACA TN 58,* (1936)
26. Wheatly, J.B., Bioletti, C., "Analysis and Model Tests of Autogiro Jump Take-off", *NACA TN 582* (1936)

27. Wheatly, J.B., “An Analytical and Experimental Study of the Effect of Period Blade Twist on the Thrust, Torque, and Flapping Motion of an Autogyo Rotor", *NACA TR 591* (1937)
28. Wheatly, J.B., "An Analysis of the Factors that Determine the Periodic Twist of an Autogiro Rotor Blade, with a Comparison of Predicted and measured Results", *NACA TR 600* (1937)
29. Bailey, F.J. Jr., “A Study of the Torque Equilibrium of an Autogiro Rotor”, *NACA TR 623* (1937)
30. Bailey, F.J. Jr., Gustafon, F.B., “Observations in flight of the region of stalled flow over the blades of an autogiro rotor”, *NACA TN 741* (1939)
31. Breguet, L., “The Gyroplane – Its Principles and its Possibilities”, *NACA Technical Memorandum 816* (1937)
32. Schrenk, M., “Static Longitudinal Stability and Longitudinal Control of Autogiro Rotors”, *NACA Technical Memorandum 879* (1938)
33. Anon, *Sikorsky R-4*, [cited 25/07/14]. Available from http://en.wikipedia.org/wiki/Sikorsky_R-4
34. Anon., “CAP701: Aviation Safety Review 1990 - 1999” *Civil Aviation Authority Report* (2000)
35. Anon., “CAP735: Aviation Safety Review 1992 - 2001” *Civil Aviation Authority Report* (2002)
36. Anon., “CAP763: Aviation Safety Review 2005” *Civil Aviation Authority Report* (2006)
37. Anon., “CAP780: Aviation Safety Review 2008” *Civil Aviation Authority Report* (2008)
38. Bennett, James AJ., "The Era of the Autogiro'." *Journal of the Royal Aeronautical Society* 65 (1961): 649-60.
39. Wallis, K.H., “Design and Construction of a low—cost Autogyro Aircraft and Detailed Prospects for Future Application”, *The Aeronautical Journal* 67 (1963): 111 – 118
40. Schad, J.L., "Small Autogyro Performance", *Journal of the American Helicopter Society* 10 (1965)
41. Nicholls, J.M., “Ultralight autogiro fatalities in South Australia”, *Medical Journal of Australia* 149 (1988)

42. Anon, "Airworthiness Review of Air Command Gyroplanes", *Air Accidents Investigation Branch Report* (1991)

43. Houston, S. S., "Longitudinal Stability of Gyroplanes", *The Aeronautical Journal* 100 No. 991 (1996): pp. 1-6

44. Houston, S. S. "Identification of autogyro longitudinal stability and control characteristics." *Journal of Guidance, Control, and Dynamics* 21.3 (1998): 391-399

45. Houston, S. S. "Identification of gyroplane lateral/directional stability and control characteristics from flight test." *Proceedings of the Institution of Mechanical Engineers, Part G: Journal of Aerospace Engineering* 212.4 (1998): 271-285

46. Coton, F. N., and L. Smrcek. "Aerodynamic characteristics of a gyroplane configuration." *Journal of aircraft* 35.2 (1998): 274-279

47. Houston, S. S. "Validation of a rotorcraft mathematical model for autogyro simulation." *Journal of Aircraft* 37.3 (2000): 403-409

48. Houston, S. S. "Analysis of rotorcraft flight dynamics in autorotation." *Journal of guidance, control, and dynamics* 25.1 (2002): 33-39

49. Spathopoulos , V. M. "An *Investigation of the Flight Dynamic Characteristics of Gyroplanes by Use of Flight Tests*" *The Aeronautical Journal* 108 No. 1088 (2004) pp 531-535

50. Houston, S.S, Thomson, D.G., Spathopoulos, V.M., "Experiments in Autogyro Airworthiness for Improved Handling Qualities", *Proceedings of 57th Annual Forum of the American Helicopter Society* (2001)

51. Bagiev, Marat, and Douglas G. Thomson. "Handling Qualities Evaluation of an Autogiro Against the Existing Rotorcraft Criteria." *Journal of Aircraft* 46.1 (2009): 168-174

52. Anon., "V/STOL Handling-Qualities Criteria", *AGARD Report R-577-70* (1970)

53. Anon., "Flying Qualities of Piloted Aircraft", *Department of Defence Handbook MIL-HDBK-1797* (1997)

54. Cooper, G. E., and Harper, R. P., "The Use of Pilot Rating in the Evaluation of Aircraft Handling Qualities" *NASA TN D-5153* (1969)

55. Mitchell, David G., et al. "Evolution, revolution, and challenges of handling qualities", *Journal of guidance, control, and dynamics* 27.1 (2004): 12-28

56. Anon., "Military Specification: Helicopter Flying And Ground Handling Qualities", *Department of Defence Handbook MIL-8501A* (1961)

57. Hess, R. A., Wang, S.H., and Gao, C., "Generalized technique for inverse simulation applied to aircraft manoeuvres", *Journal of Guidance, Control, and Dynamics* 14.5 (1991): 920-926

58. Rutherford, S., and D. G. Thomson. "Improved methodology for inverse simulation" *Aeronautical Journal* 100.993 (1996): 79-86

59. Padfield, Gareth D., *Helicopter flight dynamics,* Wiley-Blackwell, 2008

60. Padfield, G. D., et al. "Where Does the workload go when pilots attack manoeuvres? An analysis of results from flying qualities theory and experiment." *20th European Rotorcraft Forum, Amsterdam, Netherlands* (1994)

61. DuVal, Ronald W. "Areal-time multi-body dynamics architecture for rotorcraft simulation" *The Challenge of Realistic Rotorcraft Simulation: Proceedings*. Vol. 1. (2001)

62. G.D. Padfield and M. D. White, "Flight Simulation in Academia: HELIFLIGHT in its First Year of Operation", *The Aeronautical Journal*, Royal Aeronautical Society, Vol. 107, No. 1075, pp. 529-538, (September 2003)

63. White, MD, Perfect, P, Padfield, GD, Gubbels, AW, and Berryman, AC, "Acceptance Testing and Commissioning of a Flight Simulator for Rotorcraft Simulation Fidelity Research" *Proceedings of the IMechE, Part G: Journal of Aerospace Engineering* (March 2012)

64. Bickerstaffe, I.H. "Portrait of Landscape", *Proceedings of IMAGE Conference* (1998) Scottsdale, Arizona.

65. Anon, *FLIGHTLAB Theory Manual (Vol. One)* (March 2004) Advanced Rotorcraft Technology: Mountain View, California

66. Trchalík, Josef. "Aeroelastic modelling of gyroplane rotors." *PhD diss*., University of Glasgow (2009)

67. Trchalík J., Gillies E. A., Thomson D. G., "Aeroelastic Behaviour of a Gyroplane Rotor in Axial Descent and Forward Flight" *32nd European Rotorcraft Forum***,** Maastricht, the Netherlands (September 2006)

68. Schaefer, R.F. and H.A. Smith, "Aerodynmic characteristics of the NACA 8-H-12 airfoil section at six Reynolds numbers from 1.8 x 10^6 to 11.0 x 10^6" *NACA TN*

1998 (December 1949) Langley Aeronautical Laboratory, Langley Air Force Base, Va., USA.

69. Anon, [cited 25/07/14]. Available from http://www.ivoprop.com/ultralightmodel.htm
70. Anon, [cited 25/07/14]. Available from http://aerospace.illinois.edu/m-selig/ads/coord_database.html#C
71. Peters, D.A. and C. He, "Finite state induced flow models part II: Three dimensional rotor disk*" Journal of Aircraft*" (1995) 32(2).
72. Abbott, I.H. and A.E.V. Doenhoff, "Theory of Wing Sections including a summary of airfoil data" *Dover Publications Inc.* (1959) New York
73. McCormick, B.W., "Aerodynamics, Aeronautics and Flight Mechanics". *John Wiley & Sons Inc.* (1995) New York
74. Anon., "Operators manual for Rotax engine type 914 series" *BRP-Rotax GmbH & Co. KG* (2006)
75. Robinson R-22 [cited 25/07/14], available from http://www.the-blueprints.com/vectordrawings/show/5411/robinson_r22/
76. Schwiezer 300 C [cited 25/07/14] available from http://www.helistart.com/helicopters/Schweizer/300C
77. Bell 47 [cited 25/07/14] available from http://www.bigscaleheli.com/joomla/index.php?option=com_content&view=article&id=53&Itemid=111
78. Roscoe, A.H. and G.A. Ellis, "A Subjective Rating Scale for Assessing Pilot Workload in Flight: A Decade of Practical Use" *Royal Aircraft Establishment* TR 90019. (1990)
79. Talbot, N., White, W.F.R., "Montgomerie Bensen Autogyro Stability Investigation", *CAA Internal Report Ref. 9/50/5/C66/1* Issue 3 (Nov. 2005)
80. Cook, Michael V. "Flight dynamics principles: a linear systems approach to aircraft stability and control" *Butterworth-Heinemann* (2012)
81. Padfield, Gareth D., Victoria Brookes, and Michael A. Meyer. "Progress in Civil Tilt-Rotor Handling Qualities." *Journal of the American Helicopter Society* 51.1 (2006): 80-91.

82. Meyer, Michael A., and Gareth D. Padfield. "First steps in the development of handling qualities criteria for a civil tilt rotor." *Journal of the American Helicopter Society* 50.1 (2005): 33-45.

APPENDICES

Appendix A – G-UNIV DATA SHEET

Airframe reference point is taken as the intersection of the projection of the mast centreline and the keel centreline with the x-body axis aligned with the keel. The rotor rotates in an anti-clockwise direction when viewed from above. The following represents the default data set used in the simulations presented in this report.

Gross Mass	355 kg
Moments of Inertia	
I_{xx}	72.96 kg m^2
I_{yy}	297.21 kg m^2
I_{zz}	224.25 kg m^2
I_{xz}	0 kg m^2
Co-ordinates (in metres) for:	
Nominal Centre of Mass	(0.199, 0, -0.757)
Hub Plate Pivot Point	(-0.038, 0, -1.968)
Propeller Hub	(-0.91, 0, -0.795)
Fuselage C.P.	(1.626, 0, -0.48)
Tailplane C.P.	(-1.02, 0, -0.057)
Fin C.P.	(-1.0, 0, -0.268)
End Plate C.P.	(-1.09, ±0.45, -0.063)
Rudder C.P.	(-1.633, 0, -0.392)
Rotor Blade Parameters:	
Radius	3.81 m
Chord	0.97 m
Mass	17.255 kg
Flapping Inertia	83.492 kg m^2
Lift Curve Slope	5.75 /rad
Shaft Length	0.137 m
Shaft Offset	0.025 m
Fuselage Data:	
Side Area	0.798 m^2
Plan Area	0.916 m^2
Frontal Area	0.448 m^2

Tailplane Data:	
Area	0.356 m^2
Lift curve Slope	3.5 /rad
Setting Angle	0°
Fin Data:	
Area	0.281 m^2
Lift curve Slope	3.5 /rad
Setting Angle	0°
Endplate Data:	
Area	0.107 m^2
Lift curve Slope	3.5 /rad
Setting Angle	0°
Rudder Data:	
Area	0.368 m^2
Lift curve Slope	3.5 /rad
Propellor Data:	
Blade Radius	0.787 m
Blade Chord	0.09 m
Blade Twist	0°
Orientation of thrust line	1.0°
C.G. normal distance from thrust line	0.018m (below)

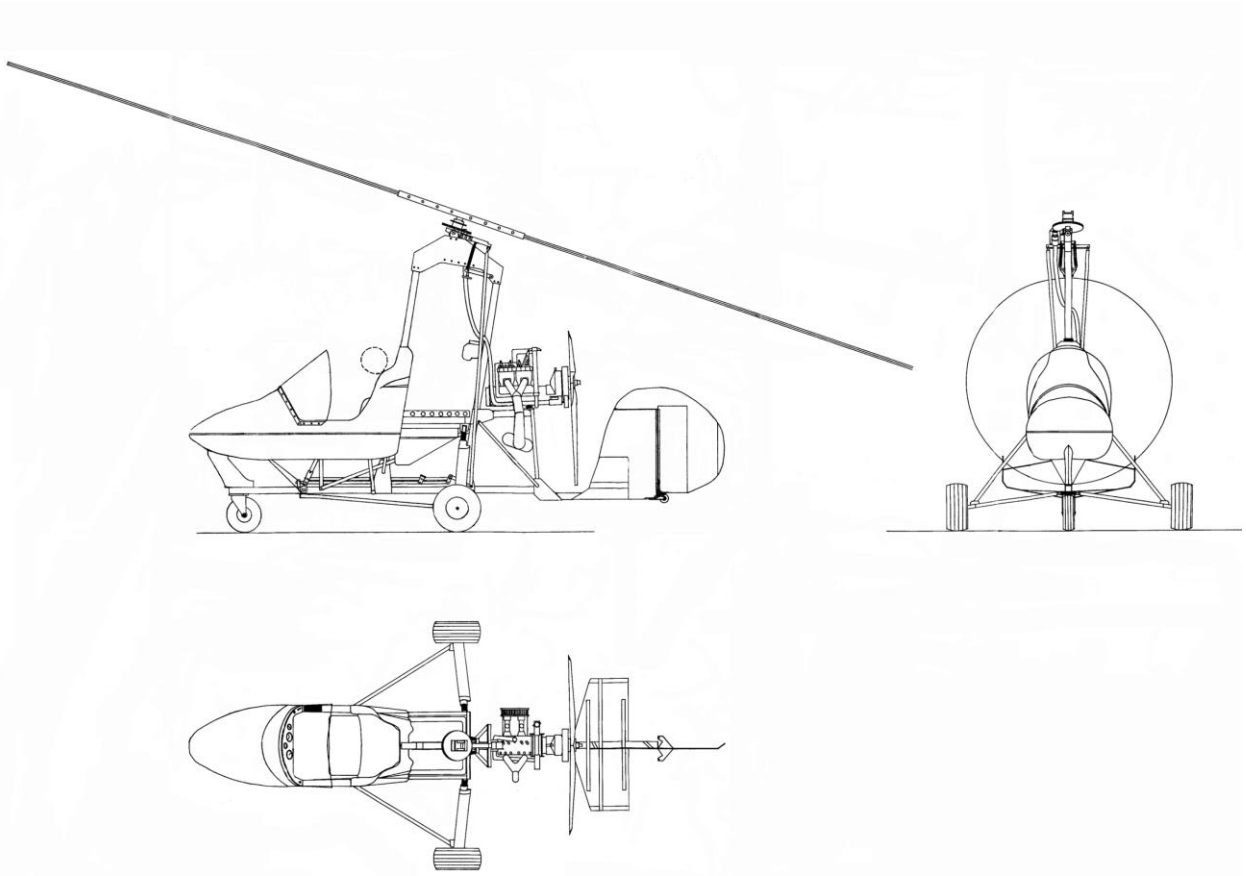

Figure A2.2: The Montgomerie-Parsons Two-Place Gyroplane

Appendix B – Published Papers

Robinson, S., and M. Jump. "Progress in the Development of Handling Qualities Critical Design Guidelines for an Autogyro." American Helicopter Society 67th Annual Forum. 2011.